The identification of novel strategies for the prevention and treatment of breast cancer in *BRCA1*-mutation carriers

Emma Nolan

A thesis submitted in total fulfilment of the
requirements of the degree of

Doctor of Philosophy

March 2017

The Walter and Eliza Hall Institute of Medical Research
Department of Medical Biology
The University of Melbourne

Abstract

Women who harbour germline mutations in the tumour suppressor gene *BRCA1* have a high lifetime risk of developing early onset basal-like breast tumours that carry a poor prognosis. Beyond prophylactic mastectomy, there are currently few options available to *BRCA1*-mutation carriers to minimise their risk and thus the identification of an effective prevention strategy remains a 'holy grail' for the field. Given deregulated progesterone signalling has been implicated in *BRCA1*-associated oncogenesis, this thesis has explored the role of the progesterone target gene *RANKL* in the preneoplastic phase. Breast tissue from *BRCA1*-mutation carriers was found to harbour an expanded subset of RANKL-responsive $RANK^+$ luminal progenitor cells that are highly proliferative, have grossly defective DNA repair mechanisms and exhibit a molecular signature closely aligned with that of basal-like breast tumours. These findings suggest that $RANK^+$ progenitors are a key target population for transformation in *BRCA1*-mutation carriers. Inhibition of RANKL via the monoclonal antibody denosumab in human breast organoids derived from *BRCA1*-mutant tissue attenuated progesterone-induced proliferation, while proliferation was markedly reduced in breast biopsies from *BRCA1*-mutation carriers who were treated with denosumab. Furthermore, RANKL inhibition in a *Brca1*-deficient mouse model significantly curtailed mammary tumorigenesis. Together these findings implicate RANKL blockade as a compelling strategy for the prevention of breast cancer in *BRCA1*-mutation carriers.

This work also examined novel therapeutic targets for the treatment of *BRCA1*-mutated breast tumours. A remarkable improvement in tumour response was observed when conventional chemotherapy was supplemented with either a RANKL inhibitor or dual immune checkpoint blockade, providing a rationale for clinical studies to examine these therapeutic targets in *BRCA1*-mutated breast cancer. Collectively, the work presented in this thesis provides key insights into the molecular mechanisms governing tumour initiation and progression in *BRCA1*-mutation carriers and has significant implications for the prevention and treatment of breast cancer in high risk women.

Declaration

This is to certify that:

1. This thesis comprises only my original work, except where indicated in the Preface
2. Due acknowledgement has been made in text to all other material presented
3. This thesis is less than 100,000 words in length, exclusive of figures, tables and bibliographies

Emma Elizabeth Nolan
The Walter and Eliza Hall Institute of Medical Research
Department of Medical Biology
The University of Melbourne
Parkville, Victoria, 3052
Australia

Preface

In accordance with the regulations of The University of Melbourne, the author's contribution to each Chapter was as follows:

Chapter 3 95%

Dr Daniel Branstetter performed immunostaining for RANK and RANKL on human breast tissue sections.
Dr Bhupinder Pal assisted with RNA-seq library preparation, and bioinformatic analysis was performed by Dr Gordon Smyth and Dr Goknur Giner.

Chapter 4 99%

Dr Francois Vaillant performed mammary fat pad transplantation experiments.
Ms Andrea Briffa performed mouse oophorectomy and sham operations.

Chapter 5 85%

Dr Daniel Branstetter assisted with immunostaining for RANK and RANKL on tissue microarrays.
Dr Francois Vaillant performed mammary fat pad transplantation experiments
Dr Daniel Gray and Ms Antonia Policheni analysed immune cell populations by flow cytometry.

Thus, the author's overall contribution to the results presented in this thesis was 93%.

Acknowledgements

I would like to thank my supervisors, Prof. Jane Visvader and Prof. Geoff Lindeman, for their incredible support, advice and mentorship over the last four years. Their talent and passion for research is inspirational, and I am incredibly grateful for the opportunity to work both as a research assistant and PhD candidate under their supervision. I have thoroughly enjoyed our discussions, and cannot thank you enough for your unwavering enthusiasm for these projects and your dedication to my research and career development.

I would like to thank all the members of the Stem Cells and Cancer Division for their friendship and support. I would particularly like to acknowledge Dr. Francois Vaillant for his technical assistance and for providing me with valuable training for aspects of this work. I also wish to thank Dr. Anne Rios, Dr. Ewa Michalak, Mr. Paul Jamieson and Dr. Florijn Dekkers for being fantastic mentors and friends during my time in the Breast Cancer Laboratory. In addition, I would like to thank Dr. Nai Yang Fu, Ms. Clare Weeden, Ms. Bianca Capaldo, Dr. Bhupinder Pal, Dr. James Whittle, Dr. Lily Lee, Dr. Sarah Best, Dr. Felicity Jackling, and Mr. Caleb Dawson for their advice, technical assistance and friendship.

I would like to thank my PhD committee for their time and support, Dr. Ruth Kluck, Dr. Marie-Liesse Asselin-Labat, Dr. Kate Sutherland and Dr. James Vince. I would like to acknowledge the services and departments at WEHI that have supported my research, particularly flow cytometry, bioservices, histology, imaging, instrumentation and communications. I would like to make special mention of Kim Birchall, who provided excellent animal husbandry. I would also like to thank kConFab, Heather Thorne, the Victorian Cancer Biobank, Leanne Taylor and Kathryn Goss for the provision of human material, as well as every woman who donated their breast tissue for research. I am very grateful to have had the opportunity to use human material for these projects, and these samples were the backbone for many of the discoveries described in this thesis. I would also like to acknowledge the contribution to these projects made by our collaborators Dr. William Dougall, Dr. Daniel

Branstetter, Ms. Antonia Policheni and Dr. Daniel Gray, and I wish to thank them for their technical assistance and scientific discussions.

Finally, I would like to thank my friends and family for their encouragement and unwavering support. To my family, Mr. Derek Nolan, Mrs. Christine Nolan, Mrs. Jess Nolan, Mr. Simon Pilkinton, Mrs. Sarah Mitchell and Mr. Alistair Mitchell, and to Mr. Tristan Benfield, I am incredibly grateful for your love and understanding over these past years. You have been my rock and I cannot thank you enough. I would like to dedicate this thesis to my parents, Mr. Derek Nolan and Mrs. Christine Nolan, whose incredible work ethic has been such an inspiration to me throughout my life, and who have always supported me unconditionally and encouraged me to strive for excellence.

Publications arising from this work

Nolan E, Vaillant F, Branstetter D, Pal B, Giner G, Whitehead L, Lok SW, Mann GB, kConFab, Rohrbach K, Huang L, Soriano R, Smyth GK, Dougall WC, Visvader JE*, Lindeman GJ* (2016) RANK ligand as a potential target for breast cancer prevention in *BRCA1* mutation carriers. *Nature Medicine*, 22(8):933–939
* These authors contributed equally
PMID: 27322743

Sau A, Lau R, Cabrita M, **Nolan E,** Crooks P, Visvader JE, Pratt MAC (2016) Persistent activation of NF-kappaB in *BRCA1*-deficient mammary progenitors drives aberrant proliferation and accumulation of DNA damage. *Cell Stem Cell*, 19(1):52-65.
PMID: 27292187

Nolan E, Lindeman GJ, Visvader JE (2017) Out-RANKing BRCA1 in Mutation Carriers. *Cancer Research*, 1;77(3):595-600
PMID: 28104682

Non-standard abbreviations

3D	3 dimensional
α	Anti-/alpha
ALDH	Aldehyde dehydrogenase
ATB	Amgen tissue bank
BAAA	BODIPY^{TM}-aminoacetaldehyde
BALB/c	Bagg albino
bFGF	Basic fetal growth factor
bp	Base pair
BrdU	Bromodeoxyuridine
CC3	Cleaved caspase 3
cDNA	Complementary DNA
CFC	Colony-forming capacity
Cre	Cre recombinase
CtIP	CtBP-interacting protein
DEAB	Diethylaminobenzaldehyde
DMBA	7,12-dimethylbenzen(a)anthracene
DMEM	Dulbecos modified eagle medium
DNA	Deoxyribonucleic acid
DNase	Deoxyribonuclease
dNTP	Deoxyribonucleotide triphosphate
dP	Days pregnant
DSB	Double-strand break
E	Embryonic day
ECL	Enhanced chemiluminescence
EDTA	Ethylenediaminetetracetic acid
EGF	Epidermal growth factor
EGTA	ethylene glycol-bis(β-aminoethyl ether)-N,N,N',N'-tetraacetic acid
eLLRCs	Embryonically-derived long label-retaining cells
ER	Oestrogen receptor
EtOH	Ethanol

FACS	Flow activated cell sorting
FCS	Fetal calf serum
FDA	Food and drug administration
FVB/N	Friend virus B NIH
GFP	Green fluorescent protein
GO	Gene ontology
Gy	Gray
HER2	Human epidermal growth factor receptor 2
HR	Homologous recombination/Hormone receptor
HRP	Horse raddish peroxidase
HRT	Hormone replacement therapy
IDC	Invasive ductal carcinoma
IgG	Immunoglobulin G
IKK	IκB kinase
K	Cytokeratin
kConFab	Kathleen Cuningham Foundation Consortium for Research into Familial Breast Cancer
kDa	Kilo dalton
KEGG	Kyoto encyclopedia of genes and genomes
Lin	Lineage
LOH	Loss of heterozygosity
LP	Luminal progenitor
MaSC/MS	Mammary stem cell
MEC	Mammary epithelial cell
MFI	Mean fluorescence intensity
ML	Mature luminal
MLPA	Multiplex ligation-dependent probe amplification
MMTV	Mouse mammary tumour virus
MPA	Medroxyprogesterone
MRI	Magnetic resonance imaging
mRNA	Messenger ribonucleic acid
NEMO	NF-κB essential modulator
NF-κB	Nuclear factor kappa-B
NHEJ	Non-homologous end joining

OPG	Osteoprotegerin
PARP	Poly ADP ribose polymerase
PARPi	Poly ADP ribose polymerase inhibitor
PBS	Phosphate buffered saline
PCR	Polymerase chain reaction
PDX	Patient-derived xenograft
PI-MEC	Parity-identified mammary epithelial cell
PR	Progesterone receptor
PRLR	Prolactin receptor
PTEN	Phosphatase and tensin homologue
PyMT	Polyoma middle T
RANK	Receptor activator of nuclear factor kappa-B
RANKL	Receptor activator of nuclear factor kappa-B ligand
RNA-seq	RNA sequencing
RPM	Revolutions per minute
RRSO	Risk-reducing salphingo-oophorectomy
RT	Room temperature
RT-PCR	Reverse transcriptase polymerase chain reaction
s.e.m.	Standard error of the mean
SLCs	Small light cells
SSB	Single-strand break
STIC	Serous tubal intraepithelial carcinomas
TCGA	The cancer genome atlas
TDLU	Terminal ductal alveolar unit
TEB	Terminal end bud
Th	T helper
TIL	Tumour-infiltrating lymphocyte
TMA	Tissue microarray
TNBC	Triple-negative breast cancer
Treg	Regulatory T cell
Tx	Transplantation
Veh	Vehicle
WAP	Whey acidic protein
WT	Wild-type

Table of Contents

List of Figures

List of Tables

Chapter 1: Introduction

1.1 The Mammary Gland

1.1.1 Structure and function

The mammary gland is a highly specialised organ that functions to produce and secrete milk for the nourishment of offspring. It is exquisitely dynamic, and undergoes growth, remodelling, cell death and regeneration with each reproductive cycle (Daniel and Smith, 1999). The mammary gland comprises both an epithelial compartment and the surrounding stroma containing a matrix of connective tissues, adipocytes, endothelial cells, fibroblasts and immune cells. In addition to providing structural support, signalling between the epithelium and stroma is essential for proper mammary gland development and function (reviewed in Hovey et al., 1999; Sakakura et al., 2013). Two main cellular lineages constitute the mammary epithelium: luminal epithelial cells that surround a central lumen and elongated myoepithelial cells that lie adjacent to the basement membrane (Visvader, 2009) (Figure 1.1). The contractile function of myoepithelial cells enables the circulation of milk through the ductal tree during lactation. Together these cells form a branching network of ducts that undergo extensive morphogenesis throughout the lifespan of a mammal.

While functionally analogous, there are key morphological differences between human and mouse mammary tissues (Figure 1.2). The human breast exhibits greater lobule complexity compared to the mouse mammary gland, and the functional portion of the breast is the terminal ductal lobular unit (TDLU). The TDLU comprises a small cluster of lobules emerging from a terminal duct that is surrounded by loose intralobular connective tissue and then denser interlobular connective tissue (Russo et al., 1990). In contrast, the mouse mammary gland lacks TDLUs but develops lobuloalveolar units during mid-pregnancy that are responsible for milk production. The human and mouse mammary stroma also exhibit significant differences. In humans, the stroma is enriched for fibrous

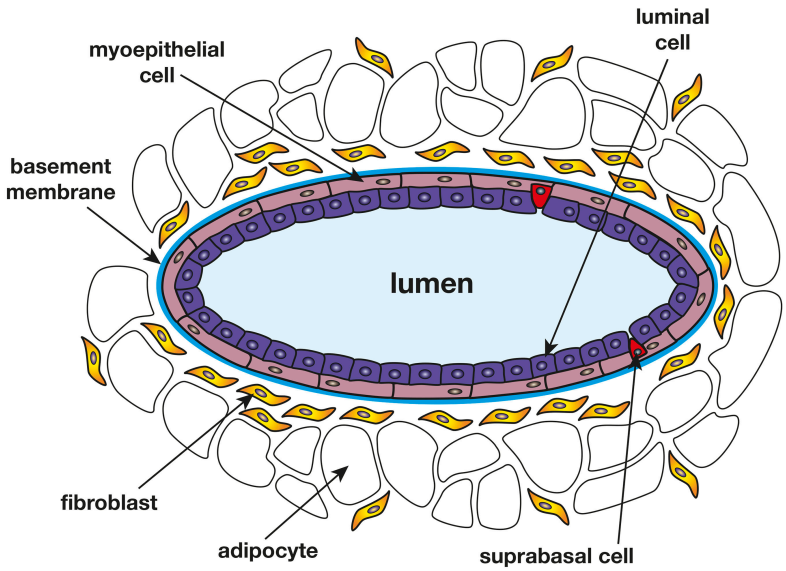

Figure 1.1: Schematic representation of a cross-section through a mammary duct

Within the mammary gland, ducts are organised as a bi-layer of epithelial cells: luminal cells surround the central lumen and elongated myoepithelial cells lie adjacent to the basement membrane. During lactation, milk is produced and secreted into the lumen by specialised luminal cells, termed alveolar cells, while myoepithelial cells contract to enable the expulsion of milk. The ductal tree lies in a mammary stroma/fat pad that predominantly comprises adipocytes and fibroblasts. Figure taken from Visvader, 2009.

connective tissue compared to the adipocyte-rich microenvironment in the mouse mammary gland (Parmar and Cunha, 2004). This difference may relate to the decreased requirement for physical support particularly during lactation in the mouse mammary gland, given its flattened position under the skin (Hovey et al., 1999). Despite these differences, the cellular composition of the epithelial compartment within human and mouse mammary tissues is remarkably similar and will be detailed later in this section.

1.1.2 Embryonic mammary gland development

There are three major stages during mammary gland development – embryonic, pubertal and reproductive, with the majority of changes occurring postnatally (reviewed in Macias and Hinck, 2012) (Figure 1.3). Mammary morphogenesis is initiated at embryonic day (E) 10.5 in mice with the formation of ectoderm-derived bilateral mammary lines that extend from the anterior to posterior limb bud (Hens and Wysolmerski, 2005). By E11.5, migration and aggregation of ectodermal cells at specific locations along the mammary line give rise to five pairs of multilayered structures called placodes (Propper, 1978). The subsequent invagination of placodes into the underlying mesenchyme leads to the formation of mammary epithelial buds, which continue to descend and generate a stalk that connects the mammary bud with the epidermis. Mesenchymal cells surrounding the epithelial bud condense and differentiate to form the mammary mesenchyme, a compact layer of fibroblastic cells. Importantly, factors secreted by the mesenchyme exert significant influence on the mammary line, stimulating differentiation towards the mammary epithelial lineage. This was demonstrated by elegant recombination experiments in which alternative combinations of mesenchyme and epithelial tissues were grafted into host mice, demonstrating that the morphology of the resulting epithelium was largely determined by the tissue origin of the mesenchyme (Kratochwil, 1969; Sakakura et al., 1976). At E15.5, the epithelial bud begins to proliferate, and a single sprout extends into the less compact fat pad precursor mesenchyme, a cluster of preadipocytes located within the dermis. At this point, ductal branching morphogenesis is initiated, yielding a rudimentary ductal tree comprising a primary duct and 10-15 secondary branches, which is present at birth and remains largely quiescent until puberty (Hens and Wysolmerski, 2005). This

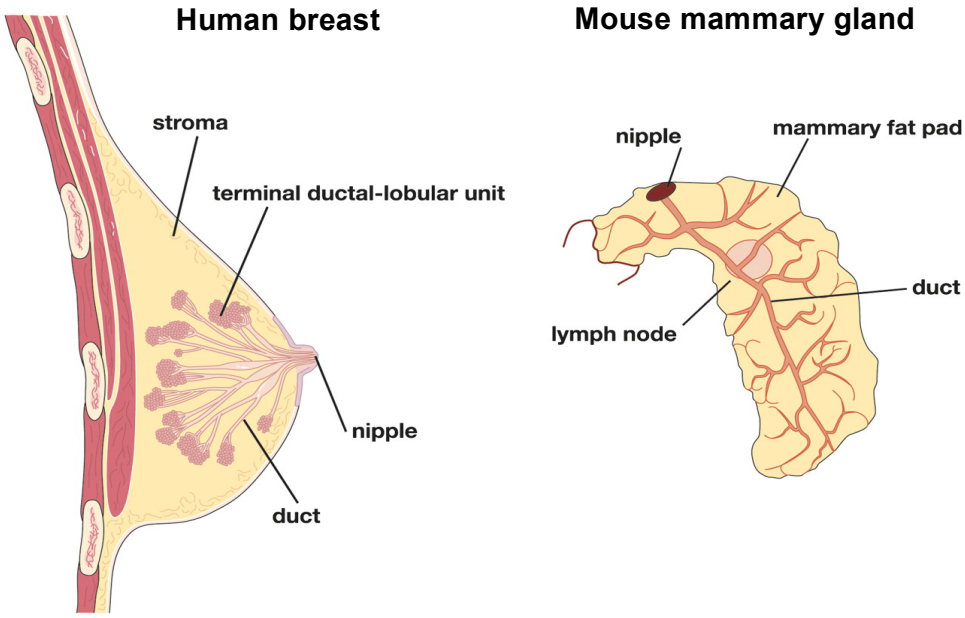

Figure 1.2: Schematic diagram of the human breast and mouse mammary gland

There are key differences in the structure and organisation of the human and mouse mammary glands. The human breast has a more complex ductal system, with 12 – 15 major ducts in the nipple region that terminate in clusters of ductules called terminal ductal-lobular unit (TDLUs). In the mouse mammary gland, the ductal branches terminate in terminal end buds during puberty or alveolar buds during pregnancy. Figure adapted from Visvader, 2009.

process is generally conserved in humans, in which mammary lines arise during the first trimester but then resolve into a single pair of placodes (Howard and Gusterson, 2000). Multiple sprouts extend from the epithelial bud, creating numerous ductal trees that unite at the nipple.

1.1.3 Pubertal mammary gland development

At the onset of puberty, in response to hormonal cues and growth factors, expansive ductal morphogenesis occurs and the epithelial tree extends and fills the entire mammary fat pad (Figure 1.3). Within the mouse mammary gland, cell proliferation occurs predominantly within terminal end buds (TEBs), specialised club-shaped structures present at the tips of growing ducts. TEBs are composed primarily of two distinct cell types, an inner layer of body cells that are the precursors to ductal epithelial cells, and the surrounding cap cells that give rise to myoepithelial cells (Williams and Daniel, 1983). Ductal morphogenesis and lumen formation require a precise balance between cell proliferation and cell death within the TEB (Humphreys et al., 1996). Progression into the mammary fat pad is largely driven by the highly proliferative cap cells present at the tip of the TEB, suggesting the presence of mammary stem cells (MaSCs) at this site (Williams and Daniel, 1983). Bifurcation of the TEB leads to the formation of primary ducts while secondary branches emerge laterally, generating a comprehensive ductal tree. Once ductal elongation extends to the boundaries of the mammary fat pad, TEBs are no longer present (Faulkin and Deome, 1960). Additional changes to ductal morphology occur with each oestrus cycle, whereby cyclical proliferation and differentiation gives rise to short tertiary branches terminating in alveolar buds (Sternlicht et al., 2006).

In the human breast, puberty-induced arborization leads to the formation of a more complex, highly elaborate ductal tree with primary ducts branching into segmental and smaller subsegmental ducts (Howard and Gusterson, 2000). Further subdivision of subsegmental ducts leads to terminal ducts, which culminate in a collection of several blind-ended ductules termed acini. A cluster of acini extending from one terminal duct and encased in stroma is referred to as a TDLU. The degree of lobular complexity within a TDLU has been classified into types I – IV

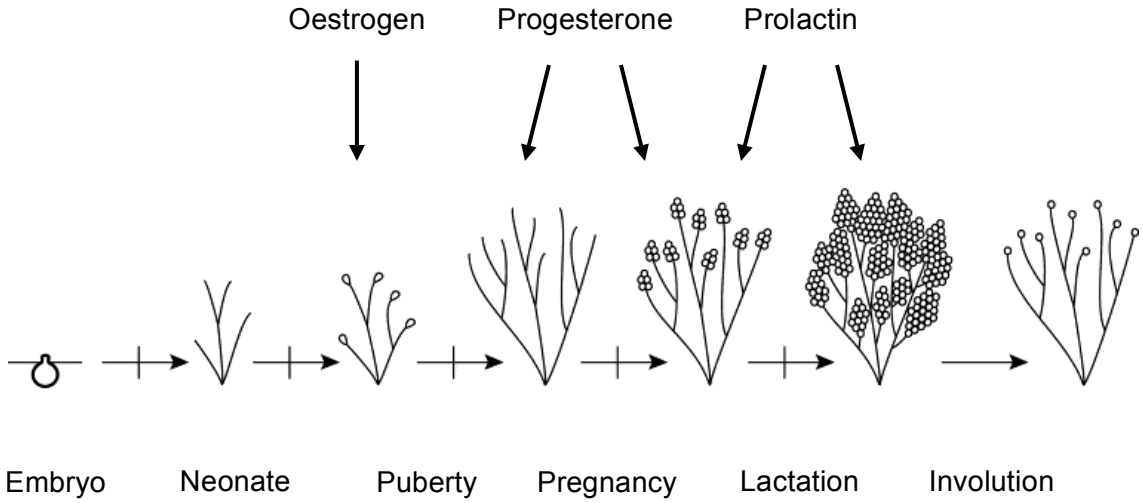

Figure 1.3: Schematic diagram of ductal development in the mouse mammary gland

In the neonate, only a rudimental ductal tree is present. In the pubertal mammary gland, oestrogen drives ductal elongation from terminal end buds at the tips of the ducts. The ducts extend and bifurcate until the edge of the fat pad is reached, coinciding with sexual maturity. Exposure to progesterone during oestrous cycling results in the formation of side branches. During pregnancy, progesterone stimulates further ductal expansion, followed by the generation of specialised alveolar units that produce milk during lactation. Prolactin is also essential for alveologenesis and lactogenic differentiation. During involution, the gland returns to a pre-pregnancy state. Figure adapted from Visvader and Lindeman, 2003.

(Russo and Russo, 1987). Type I lobules consist of short terminal ducts ending in a collection of acini, while the more complex Type II and III lobules encompass numerous ductules branching from the terminal duct, resulting in large numbers of acini. Type IV lobules are only present in lactating women (Russo et al., 1992). Significant variation in both the epithelial and stromal content of the nulliparous human breast has been documented (Howard and Gusterson, 2000; Page et al., 1987), between individuals and within the breast tissue of the same individual.

1.1.4 Reproductive mammary gland development

In both mice and humans, full mammary epithelial maturation takes place during pregnancy. The architecture of the mammary gland becomes markedly transformed, forming complex alveoli that contain specialised epithelial cells capable of synthesising and secreting milk for lactation (Macias and Hinck, 2012) (Figure 1.3). These changes are largely orchestrated by hormonal cues, in particular progesterone and prolactin (reviewed in Brisken, 2002; Brisken and O'Malley, 2010). In the initial phase of pregnancy, progesterone induces a profound surge in cellular proliferation, leading to extensive secondary and tertiary branching of the ductal tree. As with nulliparous mammary tissue, heterogeneity is observed during pregnancy in the human breast whereby some acini are essentially quiescent while nearby acini undergo dramatic proliferation and expansion (Howard and Gusterson, 2000). Progesterone and prolactin coordinate alveolar development during the next phase of pregnancy, whereby proliferation declines in favour of epithelial differentiation and secretory lineage commitment, leading to the formation of specialised alveolar units. Angiogenesis is concurrent with this process, thus alveolar buds become encased in a network of capillaries (Djonov et al., 2001). Interestingly, cytokinesis failure results in the majority of secretory alveolar cells becoming binucleated in late pregnancy (Rios et al., 2016). This is an evolutionary conserved mechanism likely to enhance milk production and thus promote offspring survival. Substantial stromal remodelling also occurs during this period; by late pregnancy adipose tissue is highly compressed due to the expanding alveoli. During the secretory phase in late pregnancy, the expression of milk proteins (whey acidic protein and α-lactalbumin) is markedly upregulated and lipid droplets begin to form (Watson and Khaled, 2008). The production of vast

quantities of protein and other nutrients by secretory alveolar cells can induce considerable stress upon the cellular machinery. To ensure luminal cell survival and milk production, epidermal growth factor (EGF)-mediated induction of the pro-survival gene *Mcl-1* occurs at the lactogenic switch in late pregnancy (Fu et al., 2015).

Following weaning, the mammary gland undergoes another period of remarkable remodelling, whereby alveolar cells are removed by cell death and the epithelial tree returns to a state comparable to the virgin gland. In a tightly regulated series of events, 80% of the mouse mammary epithelium is removed within a few days (Watson and Khaled, 2008). In mice, there are two key phases of involution, a reversible and irreversible phase (reviewed in Macias and Hinck, 2012). In the first, suckling can reinstate the milk supply. Studies have demonstrated that the first phase is largely regulated by local cues, in contrast to the second irreversible phase where systemic hormones exert significant influence (Li et al., 1997). The first phase is largely regulated by Signal Transducer and Activator of Transcription 3 (STAT3), which induces apoptosis, cell detachment and the accumulation of alveolar cells in the lumen of the duct. At 48 hours, the irreversible phase of involution is initiated and is characterised by marked apoptosis, alveoli collapse and adipocyte differentiation. Matrix metalloproteinases and plasmin cooperate to remodel the extracellular matrix, and eventually the majority of the secretory cells are removed and the mammary stroma is re-established (Macias and Hinck, 2012). Collectively, changes occurring within the human breast and mouse mammary gland during reproduction are a remarkable example of tissue remodelling and elasticity, allowing mammary tissue to continually adapt throughout life to meet its physiological requirements.

1.2 Dissecting the Mammary Epithelial Hierarchy

The epithelial compartment of the mammary gland is organised into a hierarchical structure (Figure 1.4). The hierarchical model of mammary epithelium is based on decades of elegant transplantation and *in vitro* studies that have demonstrated the existence of both stem and progenitor cells within mouse and human mammary

tissue. Isolation and characterisation of cellular subsets within the differentiation hierarchy has been achieved using multiple techniques including flow cytometry, gene expression analysis and *in vitro* and *in vivo* functional assays. Despite differences in the architecture of human and mouse mammary tissue, remarkable similarities are observed between their epithelial hierarchies. Located at the tip of the hierarchy, bipotent MaSCs are presumed to undergo asymmetric cell division to give rise to fully differentiated myoepithelial and luminal cells via lineage-restricted progenitor cells (Visvader and Stingl, 2014) (Figure 1.4). MaSCs must also be capable of self-renewal by symmetric cell division, enabling rapid expansion of the ductal tree and preventing exhaustion of progenitor cells. Within the luminal lineage, progenitor cells differentiate to either generate alveolar progenitor or ductal progenitor subsets. These in turn give rise to fully differentiated alveolar cells capable of milk production or mature ductal cells that constitute the inner layer of ducts. While not yet characterised, it is presumed that mature myoepithelial cells, the specialised contractile cells located at the basal surface of the mammary epithelium, arise from myoepithelial progenitor cells.

1.2.1 Identification of mouse mammary stem cells

Stem cells, regardless of their origin, are defined as unspecialised cells with the capacity to both self-renewal and generate progeny that can differentiate down multiple lineages to produce all the mature cell types present in that tissue (Visvader and Stingl, 2014). The dynamic nature of epithelial cell proliferation, differentiation and turnover within the mammary gland coupled with the remarkable plasticity through successive cycles of pregnancy suggests the existence of a renewable stem cell population.

The existence of mouse MaSCs was first suggested by DeOme et al. when transplantation of normal mammary epithelial fragments into cleared (de-epithelised) fat pads of three-week old recipient mice generated morphologically comparable outgrowths containing both luminal and myoepithelial cells (DeOme et al., 1959). These outgrowths could be serially transplanted, demonstrating the self-renewal capacity of cells within the mammary epithelium. This finding was

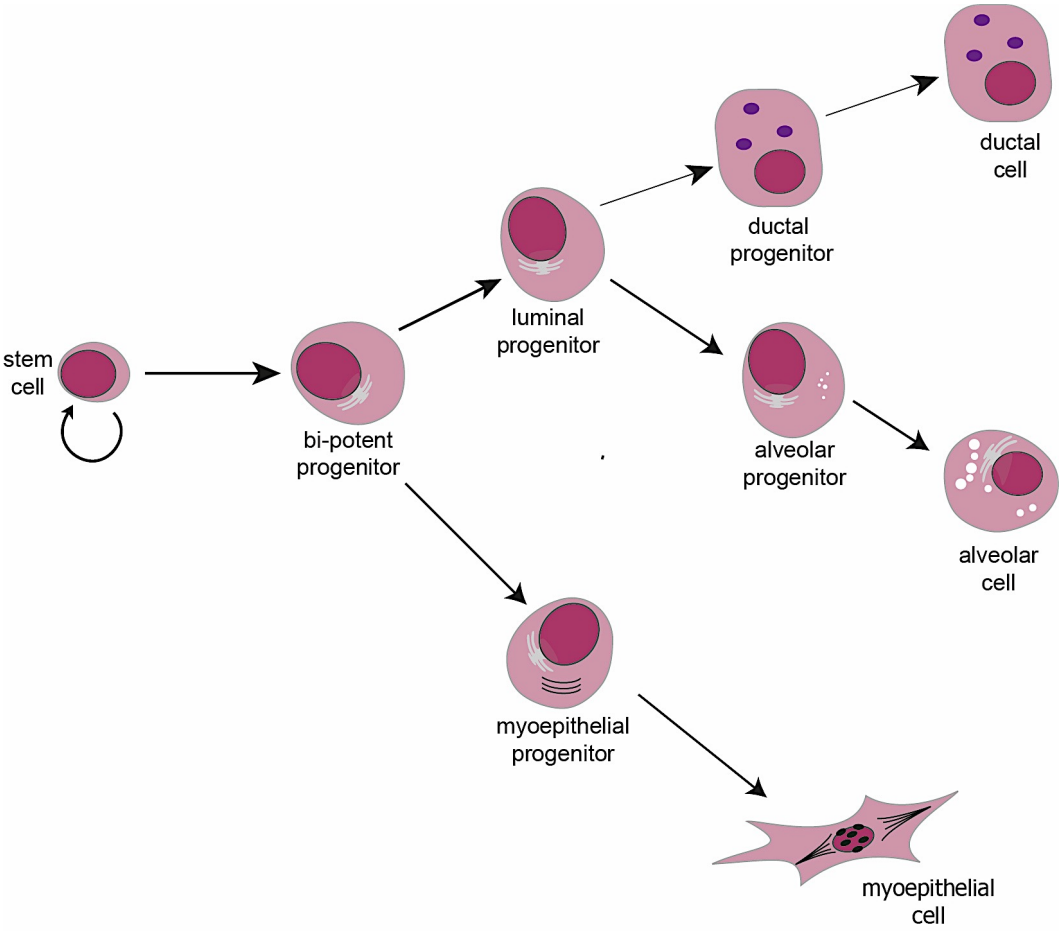

Figure 1.4: Schematic model of the mammary epithelial hierarchy

At the apex of the epithelial hierarchy are bipotent stem cells, which can undergo self-renewal and give rise to cells of two distinct lineages: myoepithelial and luminal. Luminal epithelial cells can be further subdivided into the ductal or alveolar lineages. Figure adapted from Visvader, 2009.

confirmed by additional studies (Daniel et al., 1968; Hoshino, 1962; Hoshino, 1964; Smith and Medina, 1988), and it was further shown that epithelium harvested from donor mice at any age, developmental stage or location in the mammary gland could give rise to fully functional mammary outgrowths (Smith and Medina, 1988). Both the highly proliferative cap cells within the TEB (Williams and Daniel, 1983) and the small light cells (SLCs) visualised by electron microscopy (Chepko and Smith, 1997; Smith and Medina, 1988), have been proposed to represent the mammary stem cell population, but this remains an open question. During adulthood, stem cells are thought to be dispersed throughout the epithelial tree and contribute to ductal maintenance.

Early lineage tracing experiments using retrovirally-marked mammary cells proposed that progeny from a single multipotent stem cell could generate a functional mammary gland upon transplantation (Kordon and Smith, 1998). This was demonstrated by two landmark publications in 2006, where it was revealed that a single MaSC could be isolated by flow cytometry and regenerate an entire mammary epithelial tree upon transplantation (Shackleton et al., 2006; Stingl et al., 2006). As well as demonstrating multi-lineage differentiation, clonal outgrowths were capable of generating functional lobuloalveolar units during pregnancy. The repopulating MaSCs were found to reside within the heterogeneous basal/myoepithelial compartment of the mammary gland, defined as $CD24^{+}/CD29^{hi}$ or $CD49^{hi}$, at a frequency of approximately 1 in 64 cells (Shackleton et al., 2006; Stingl et al., 2006). Expression profiling and immunohistochemistry confirmed $CD24^{+}CD29^{hi}/CD49^{hi}$ cells were enriched for genes associated with the myoepithelial lineage including *Krt5*, *Krt14* and *Vimentin*. Furthermore, *in vitro* clonogenic assays confirmed the multi-lineage potential of MaSCs, since colonies from $CD24^{+}CD49^{hi}$ cells were primarily enriched for basal markers but could also give rise to luminal cells. Concomitantly, another group demonstrated the utility of CD24 in flow cytometry as a marker of cells enriched for mammary repopulating activity (Sleeman et al., 2006).

Accumulating evidence suggests heterogeneity exists within the MaSC population. During pregnancy, alveologenesis may be driven by a transient MaSC subset that undergoes profound expansion (Asselin-Labat et al., 2010; Pal et al., 2013). It is

presumed that this pool provides an expanded compartment of alveolar progenitors which then undergoes alveolar differentiation. Slow-cycling stem cells, likely to be important for maintenance of the adult ductal tree, have also been identified in the adult mammary gland based on long-term label retention, using either synthetic DNA nucleotides (Shackleton et al., 2006; Smith, 2005) or an inducible histone 2B (H2B) promoter linked to a GFP reporter (dos Santos et al., 2013). It is not known whether these cells are distinct from a population of embryonically-derived label-retaining cells (eLLRCs) recently identified in the nipple region of the adult mammary gland (Boras-Granic et al., 2014). eLLRCs become quiescent at birth, however, a subset of these cells can re-enter the cell cycle in response to ovarian hormones and may contribute to the pool of slow-cycling stem cells during periods of mammary growth. Finally, a unique population of fetal MaSCs has been isolated from E18.5 mammary rudiments (Makarem et al., 2013; Spike et al., 2012). These cells have markedly higher repopulating activity compared to adult MaSCs, and are capable of self-renewal and multi-lineage differentiation.

1.2.2 Luminal compartment of the mouse mammary gland

The luminal cell compartment of the mammary epithelium is a heterogeneous collection of mature and progenitor cells restricted to either a ductal or alveolar cell fate. Luminal progenitor cells are not capable of mammary gland repopulation following transplantation yet exhibit robust clonogenic activity *in vitro*. Flow cytometry-based fractionation followed by the demonstration of *in vitro* clonogenic activity is a highly effective tool to distinguish progenitor subsets from terminally differentiated luminal cells. This can be achieved by culturing cells in two-dimensions on a feeder layer of fibroblasts (Asselin-Labat et al., 2007), or in three-dimensions using Matrigel as the extracellular matrix to support colony growth (Shackleton et al., 2006; Stingl et al., 2006). Matrigel assays are considered more physiologically relevant than feeder layers, allowing progenitors to form 3D acinar colonies. The luminal compartment can be fractionated from the mouse mammary epithelium by flow cytometry based on a $CD24^{+}CD29^{lo}$ or $CD24^{+}CD49f^{lo}$ expression profile (Shackleton et al., 2006; Stingl et al., 2006). These cells express transcripts typical of luminal cells and are capable of forming milk–producing colonies when cultured in the presence of a lactogenic stimulus (prolactin). Subsequently, it was

demonstrated that CD61 (β_3-integrin) expression, in combination with CD24 and CD29, is capable of discerning committed luminal progenitor cells ($CD24^+CD29^{lo}CD61^+$) from mature luminal cells ($CD24^+CD29^{lo}CD61^-$) (Asselin-Labat et al., 2007). Importantly, $CD61^+$ cells demonstrated markedly enhanced clonogenic activity in 3D cultures compared to $CD61^-$ cells. Furthermore, a dramatic decline in the proportion of $CD61^+$ cells was observed during pregnancy, consistent with enhanced alveolar differentiation.

Further fractionation of the luminal compartment can be achieved based on the expression of Sca1 and CD49b (α_2-integrin). Following discrimination between luminal and basal populations using CD24 and CD29, the expression of Sca1 and CD49b can resolve the luminal compartment into three distinct subpopulations (Pal et al., 2013; Shehata et al., 2012). The $Sca1^+CD49b^-$ subset distinguishes non-clonogenic mature luminal cells that express oestrogen receptors (ER) and progesterone receptors (PR). High CD49b expression plus differential Sca1 expression separates two distinct types of luminal progenitors with clonogenic capacity, ER-positive ($Sca1^+CD49b^+$) and ER-negative ($Sca1^-CD49b^+$). ER-positive progenitors likely represent ductal progenitors since they express high levels of *FoxA1* and transcription factors essential for ductal morphogenesis during mammary gland development (Bernardo et al., 2010). In contrast, ER-negative progenitors are likely alveolar progenitors since they express high levels of milk protein transcripts, *Elf5* and *LM04*, which are transcription factors that specialise alveolar cell fate (Oakes et al., 2008; Sum et al., 2005). Additional studies have reported the distinction between ductal and alveolar-restricted progenitors based on the differential expression of c-Kit and Sca1 (Regan et al., 2012) or c-Kit and CD14 (Asselin-Labat et al., 2011). In the latter study, the $CD29^{lo}CD24^+CD14^+cKit^-$ subset expressed milk protein transcripts in the virgin mouse and was expanded during late pregnancy, suggesting commitment to the alveolar lineage (Asselin-Labat et al., 2011). However variation in the expression of c-Kit (as well as CD61) has been observed between different mouse strains, in particular in C57BL6/J mice where c-Kit/CD61 expression is minimal (Shehata et al., 2012; Asselin-Labat unpublished). Alveolar progenitors with a $CD24^{high}$Prominin-1^- phenotype have also been reported (Sleeman et al., 2007).

1.2.3 Lineage tracing to map cell fate in the mouse mammary gland

While transplantation studies utilising mammary fat pads devoid of endogenous epithelium is considered the gold standard method for detecting MaSCs, this method only reads out the potential of a given cell as a stem cell. To understand the role of stem and progenitor cells *in vivo*, it is necessary to perform lineage tracing. Lineage tracing involves tracking genetically tagged stem and progenitor cells *in situ* over time to determine the progeny they produce. This method preserves tissue architecture and provides a physiological setting in which to track the activity of a particular cell subset. An early example of lineage tracing was using the mouse mammary tumour virus (MMTV) (Kordon and Smith, 1998), which randomly inserts its proviral DNA into the genome during the replication cycle (Ringold et al., 1979). Following serial transplantation of mammary tissue from infected donor mice into uninfected hosts, identical viral insertion sites were detected in primary and secondary outgrowths (Kordon and Smith, 1998), suggesting the existence of self-renewing cells capable of reconstituting mammary epithelium.

More recently, lineage-tracing studies have utilised inducible gene promoters to achieve both spatial and temporal control of cell tracking (Rios et al., 2014; Van Keymeulen et al., 2011; Wagner et al., 2002). Using *K14*-driven and doxycycline-inducible labeling of cells, van Keymeulen and colleagues reported that independent unipotent stem cells restricted to the luminal and myoepithelial lineages drive postnatal mammary gland morphogenesis. They concluded that bipotent stem cells do not exist. However this was later disputed, when *K5*-driven lineage tracing coupled with a novel 3D imaging strategy provided direct evidence for the existence of bipotent MaSC within the postnatal mammary gland (Rios et al., 2014). This study utilised a multi-colour cre reporter (Confetti, Schepers et al., 2012) together with a doxycycline-inducible system, and could trace stem cells and their progeny over expansive areas of the mammary tree at single-cell resolution. Importantly, clonal analysis revealed K5-labelled MaSC could generate offspring in both luminal and myoepithelial cell lineages, a finding that was validated in *K14* and *Lrg5*-driven systems (Rios et al., 2014). Furthermore these bipotent cells were long-lived and are likely to be essential for maintenance of ductal architecture. In

support of the bipotent stem cell hypothesis, a small subset of basal cells marked by Procr expression was shown to be highly enriched for bipotent stem cells: clonal lineage tracing analysis demonstrated that 93% of labelled $Procr^{+}$ clones contained both luminal and basal cells after a 6-week chase and the data indicated that these cells are cycling (Wang et al., 2015). The disparity between these studies (Rios et al., 2014; Van Keymeulen et al., 2011) highlights the need for great accuracy with the initial targeting of cells by using highly specific gene promoters, combined with advanced imaging techniques to track cells in 3D such as multi-colour reporters for clonal analysis.

Lineage tracing has also proved useful for tracking luminal progenitors within the mouse mammary gland. Rare populations of luminal progenitors expressing Notch signalling genes have been identified using this technique (Lafkas et al., 2013; Rodilla et al., 2015). Recently, tracing experiments demonstrated that Notch1 marks alveolar progenitor cells that expand during pregnancy and are responsible for the formation of lobuloalveolar units (Rodilla et al., 2015). In addition, these cells survived multiple rounds of involution. It is not known whether they overlap with parity-identified mammary epithelial cells (PI-MEC) isolated by an earlier cell mapping experiment (Wagner et al., 2002), shown to survive through involution and function as self-renewing progenitors in subsequent pregnancies. Furthermore, lineage tracing performed with an inducible *Elf5* promoter, a marker of luminal progenitor cells (Lim et al., 2010), showed that luminal progenitor cells are key drivers of ductal morphogenesis during puberty and alveolar formation during pregnancy, but are not as long-lived as MaSCs (Rios et al., 2014).

1.2.4 Human mammary epithelial hierarchy

Remarkably, the hierarchical model of mammary epithelium appears largely conserved between human and mouse mammary tissue. The existence of MaSCs in adult human breast tissue was first proposed following analysis of X-chromosome inactivation patterns, whereby entire lobules and ducts of normal breast tissue were found to have the same X chromosome inactivated, suggesting they were clonally derived (Tsai et al., 1996). The subsequent identification of bipotent, luminal-restricted and myoepithelial-restricted progenitors based on flow

cytometry and *in vitro* clonogenic assays lent support to the proposed differentiation hierarchy (Arendt et al., 2014; Stingl et al., 2001). Substantial evidence suggests that the human MaSC resides within the basal compartment of the mammary epithelium that is distinguished by an $EpCAM^{-}CD49f^{hi}$ phenotype (Eirew et al., 2008; Lim et al., 2009; Stingl et al., 2001). Repopulating activity *in vivo* was demonstrated using transplantation assays optimised for human MaSCs, either in renal capsule or mammary fat pad transplantation assays. In the former, dissociated human epithelial cells and mouse fibroblasts were suspended in collagen gels and then implanted under the renal capsule of immunocompromised mice (Eirew et al., 2008). This technique elegantly demonstrated only $EpCAM^{-}CD49f^{hi}$ cells were capable of regenerating polarised, bilayered structures containing both luminal and myoepithelial cells bound by a basement membrane. In addition, this subset exhibited self-renewal activity demonstrated by secondary transplantation. In a parallel approach (Lim et al., 2009), epithelial cells were co-injected into cleared mouse mammary fat pads along with human fibroblasts (Kuperwasser et al., 2004), to provide a more favourable environment for human cell growth and differentiation. Similarly, only the $EpCAM^{-}CD49f^{hi}$ population showed mammary regenerative capacity, at a frequency of 1 in 20,000 cells (Lim et al., 2009). This subpopulation expresses myoepithelial proteins including p63, cytokeratin 14 and vimentin, and is equivalent to the basal $CD24^{+}CD29^{lo}$ subset shown to harbour mouse MaSCs (Lim et al., 2009). In addition, marked similarities in the transcriptomes of human and mouse MaSC-enriched populations have been observed (Lim et al., 2010). In earlier reports, it was instead proposed that multipotent stem cells reside within the luminal ($EpCAM^{high}CD49f^{+}$) compartment of ducts (Ginestier et al., 2007; Villadsen et al., 2007), or that separate multipotent populations exist within the luminal and myoepithelial compartments (Keller et al., 2012). However, it is now well accepted that the $EpCAM^{-}CD49f^{hi}$ population contains MaSCs and that the discrepancies likely arose because of the inconsistent methods used to dissociate human mammary epithelial cells as well as the different downstream assays applied to assess stem cell activity (Visvader and Stingl, 2014).

Characterisation of sorted cell populations by expression analysis and *in vitro* clonogenic assays has delineated the luminal progenitor ($EpCAM^{+}CD49^{+}$) and

mature luminal ($EpCAM^+CD49f^-$) compartments of the human breast. Both subsets express markers of the luminal lineage including cytokeratin 8, 18 and 19, yet only $EpCAM^+CD49^+$ cells display clonogenic activity when cultured in Matrigel (Eirew et al., 2008; Lim et al., 2009). Further fractionation of the luminal progenitor population has been achieved based on the expression of ALDH and ERBB3, revealing three subpopulations of cells: $ALDH^+ERBB3^+$ ($ALDH^+$), $ALDH^-ERBB3^+$ ($ALDH^-$) and $ALDH^-ERBB3^-$ ($ERBB3^-$) (Eirew et al., 2012; Shehata et al., 2012). The $ALDH^+$ subset is highly clonogenic and likely analogous to the ER-negative alveolar progenitors identified in mouse mammary tissue ($Sca1^-CD49b^+$) since they share a gene signature closely associated with the alveolar lineage (Shehata et al., 2012). In contrast, $ALDH^-$ cells displayed the highest mRNA levels for genes involved in luminal differentiation and exhibited significantly lower clonogenic activity compared to the $ALDH^+$ population, consistent with a more differentiated phenotype. The high expression of *FOXA1* in this subset is also comparable to the ER-positive ductal progenitors identified in mouse tissue (Shehata et al., 2012). The $ERBB3^-$ subpopulation displayed low levels of luminal differentiation genes but the highest levels of basal-specific transcripts, implying an intermediate phenotype (Shehata et al., 2012). Intriguingly, in some patient samples this subset was the most dominant (up to 65% of the total luminal progenitor population), however its biological relevance is unknown given it was only present in the minority of patient samples analysed. Finally, a recent report has suggested that the luminal lineage may show increasing complexity with lobule maturity (Arendt et al., 2014). Specifically, a computational approach to model the cellular hierarchy from flow cytometry data (termed SPADE, Qiu et al., 2011) indicated that the highly arborized Type III breast lobules have clusters of rare but distinct luminal populations while Type I and II lobules appeared more homogeneous (Arendt et al., 2014).

1.3 Hormonal Regulation of Mammary Gland Development

Hormone signalling in the mammary epithelium is essential for the morphogenesis that takes place during puberty, oestrus cycling and pregnancy (Figure 1.3). In both human and mouse, the rapid ductal elongation and arborization that occurs at the onset of puberty is primarily regulated by oestrogen, while side branching during

oestrus cycling and functional lobuloalveolar development during pregnancy is largely driven by progesterone signalling. Prolactin also plays an essential role in alveologenesis and lactogenesis. Across species, proliferating cells in the adult mammary gland rarely express steroid receptors, and are regulated by hormones via paracrine mechanisms (Clarke et al., 1997; Grimm et al., 2002; Russo et al., 1999; Seagroves et al., 2000). This has been elegantly demonstrated in the mouse mammary epithelium, where MaSCs were shown to be highly responsive to steroid hormone signalling despite being hormone receptor-negative (HR^-), via paracrine signals secreted from HR^+ mature luminal cells (Asselin-Labat et al., 2010; Joshi et al., 2010). Oophorectomy markedly diminished MaSC number and repopulating capacity *in vivo*, while both pregnancy and exogenous hormone treatment significantly increased the number of repopulating cells (Asselin-Labat et al., 2010). HR^+ mature luminal cells can also signal to HR^- luminal progenitor cells in a paracrine fashion (Pal et al., 2013). Thus, HR^+ mature luminal cells appear to act as "sensor" cells that receive mitogenic signals encoded by systemic hormones, and secrete paracrine factors to instruct neighbouring HR^- stem and progenitor cells ("responder" cells) to proliferate (reviewed in Brisken, 2013). The use of paracrine signalling mechanisms ensures the precise coordination of multiple cell types and facilitates signal amplification.

1.3.1 Oestrogen

The steroid hormone oestrogen is primarily produced by the ovary, catalysed by the enzyme aromatase within the granulosa cells of maturing follicles and the luteal cells of the corpus luteum (Simpson et al., 1994). There are three major naturally occurring oestrogens: oestrone (E1), 17β-oestradiol (E2) and oestriol (E3). E2 is the most potent circulating oestrogen and mediates the majority of oestrogen action in the mammary gland. Oestrogen is the major mitogenic stimulus during puberty, necessary for the rapid growth and expansion of the ductal tree into the mammary fat pad (Brisken and O'Malley, 2010). Early experiments using oophorectomised mice revealed that the administration of 17β-oestradiol was sufficient to induce cell proliferation in the pubertal gland and rescue ductal outgrowth (Daniel et al., 1987). Oestrogen signals via two distinct nuclear oestrogen receptors, ERα and ERβ, which upon ligand binding function as transcription factors that modulate gene

transcription by binding to specific DNA sequences (hormone response elements) in target gene promoters (Beato et al., 1995; Tsai and O'Malley, 1994). ERα appears to be the critical mediator of oestrogen signals within the mammary epithelium since *ERα*$^{-/-}$ mice showed no development at puberty beyond a primitive ductal rudiment that was devoid of TEBs (Korach et al., 1996; Mallepell et al., 2006). In contrast, loss of *ERβ* had no adverse effects on ductal development (Forster et al., 2002). The phenotype observed in *ERα*$^{-/-}$ mice is presumably due to the paucity of functional MaSCs, since aromatase knockout animals harbour markedly fewer MaSCs and significantly reduced regenerative capacity (Asselin-Labat et al., 2010).

Elegant tissue recombination experiments indicated oestradiol elicits proliferation and morphogenesis by a paracrine mechanism, since *ERα*$^{-/-}$ epithelial cells could proliferate and contribute to all cellular compartments only when co-transplanted with wild-type (WT) cells (Mallepell et al., 2006). The growth factors amphiregulin, FGF7 and FGF10 are candidate paracrine mediators of oestrogen-induced proliferation and ductal outgrowth, since their transcription is strongly induced by 17-β-oestradiol and genetic ablation causes a phenotype similar to that of *ERα*-deficient epithelium (Ciarloni et al., 2007; Kenney et al., 1996; Lu et al., 2008; Luetteke et al., 1999).

1.3.2 Progesterone

Progesterone biosynthesis occurs primarily within the ovary, and is synthesised from cholesterol via the intermediate pregnenolone (Fritz and Speroff, 2012). Progesterone signalling is initiated upon binding to intracellular progesterone receptors that are members of the nuclear receptor superfamily of transcription factors and are expressed as two isoforms, PR-A and PR-B. Within the adult mouse mammary gland, progesterone orchestrates ductal side-branching during each oestrus cycle and the expansion of the alveolar compartment during pregnancy (reviewed in Brisken, 2013). Mammary epithelium from *PR*$^{-/-}$ mice lacked secondary and tertiary side branches, and failed to form milk-producing lobuloalveolar units during pregnancy that are essential for lactation (Brisken et al.,

1998; Lydon et al., 1995). Progesterone signals within the mammary gland are largely mediated by the PR-B receptor, since severely impaired ductal proliferation and alveolar morphogenesis were only observed following genetic deletion of *PR-B* and not *PR-A* (Mulac-Jericevic et al., 2003; Mulac-Jericevic et al., 2000). During adulthood, progesterone is a more potent mitogenic signal than oestrogen, since progesterone levels peak in the luteal phase of the menstrual cycle in humans or diestrus in mice, when mammary epithelial cell proliferation is highest (Arendt and Kuperwasser, 2015). *Ex vivo* culture of human reduction mammoplasties revealed that progesterone treatment stimulated cell proliferation whereas 17β-oestradiol did so only in a fraction of breast tissue samples (Tanos et al., 2013). In addition, treatment of oophorectomised adult mice with progesterone and 17β-oestradiol elicited profound cell proliferation, whereas the mitogenic effect of 17β-oestradiol alone was negligible (Beleut et al., 2010; Wang et al., 1990).

Progesterone exerts mitogenic effects predominantly via paracrine signalling in the mammary gland. Analogous to $ER\alpha^{-/-}$ cells, transplantation of $PR^{-/-}$ epithelial cells resulted in normal ductal branching and functional alveoli development only when co-mixed with WT cells (Brisken et al., 1998). Progesterone-induced proliferation occurs in two distinct waves, demonstrated by experiments in which oophorectomised mice were treated with exogenous progesterone and proliferating cells were distinguished using BrdU incorporation (Beleut et al., 2010). In the initial shorter wave, PR^+ cells themselves proliferate, consistent with a cell-intrinsic mechanism. This is followed by a larger second wave of proliferation in neighbouring PR^- cells mediated by paracrine signals. Both Wnt4 and RANKL have emerged as crucial paracrine mediators of progesterone action and their expression in PR^+ luminal cells is dramatically increased in mice following progesterone treatment (Brisken et al., 2000; Joshi et al., 2010; Mulac-Jericevic et al., 2003; Pal et al., 2013).

Interestingly, accumulating evidence suggests that progesterone-induced mammary epithelial expansion during pregnancy may be partly attributable to changes in the mammary epigenome. The expression and phosphorylation of EZH2, a histone methyltransferase that forms the catalytic component of the

polycomb repressive complex PRC2, is profoundly upregulated during early to mid pregnancy (Michalak et al., 2013; Pal et al., 2013). This expression pattern correlates with histone methylation changes and gene expression modulation, for example luminal genes required for differentiation and milk production showed strongly decreased H3K27 trimethylation marks and upregulated gene expression at mid-pregnancy (Pal et al., 2013). Loss of *Ezh2* led to reduced alveolar expansion and a failure of lactation (Michalak et al., 2013; Pal et al., 2013). Progesterone (but not prolactin) treatment *in vivo* led to a striking elevation in *Ezh2* expression and phosphorylation/activation, confirming the role of progesterone in this pathway (Pal et al., 2013). Moreover, *Ezh2* expression was enriched in the PR^- luminal progenitor population whereas *Rankl* was highly induced in differentiated PR^+ mature luminal cells, indicating a paracrine mode of stimulation. Collectively these findings indicate that progesterone-induced upregulation of *Ezh2* in pregnancy is a key event that facilitates changes in the mammary epigenome and modulation of gene expression.

1.3.3 Prolactin

Prolactin is primarily produced by lactotrophs in the anterior pituitary gland, however, local production in the mammary epithelium has also been reported (Vonderhaar, 1999). Within the mammary epithelium, prolactin plays a critical role in alveologenesis and lactogenic differentiation during pregnancy. This occurs indirectly through positive regulation of progesterone biosynthesis, and through direct mechanisms via its effect on mammary epithelial cells (Trott et al., 2008). Binding of prolactin to its cognate receptor PRLR induces receptor dimerisation and the activation of Janus Kinase 2 (JAK2), which results in phosphorylation and activation of STAT5 (Schindler and Darnell, 1995). Activated STAT5 translocates to the nucleus and induces expression of its target genes including milk proteins casein β (*Csn2*) and whey acidic protein (*Wap*) (Gouilleux et al., 1994; Li and Rosen, 1995). Genetic inactivation of *Prlr*, *Jak2* or *Stat5* leads to normal ductal expansion during puberty, however, the mutant epithelium is devoid of luminal cell proliferation or functional lobuloalveolar units during pregnancy (Brisken et al., 1999; Cui et al., 2004; Liu et al., 1997; Ormandy et al., 1997; Wagner et al., 2004). Transplantation experiments indicated that the alveologenesis defect in $Prlr^{-/-}$

glands was autonomous to the mammary epithelium and not a consequence of reduced levels of circulating progesterone (Brisken et al., 1999; Gallego et al., 2001). Furthermore progesterone supplementation in *Prlr*$^{-/-}$ mice was able to rescue ductal side branching but not alveologenesis (Ormandy et al., 2003). Paracrine-mediated signals have also been associated with prolactin signalling, for instance IGF-2 has been implicated as an essential paracrine mediator (Brisken et al., 2002). Reports have suggested RANKL may also be a paracrine meditator of prolactin (Fata et al., 2000; Srivastava et al., 2003), however, this has been disputed by other studies (Brisken, 2002; Obr et al., 2013).

1.3.4 RANKL: essential paracrine mediator of progesterone action

Receptor Activator of Nuclear Factor-κB Ligand (RANKL) is a cytokine member of the tumour necrosis factor (TNF) superfamily that was originally identified in bone tissue as the critical driver of osteoclast formation, differentiation and activation (Lacey et al., 1998; Yasuda et al., 1998). RANKL signals via its cognate receptor Receptor Activator of NF-κB (RANK) and can be inhibited by the soluble decoy receptor osteoprotegerin (OPG), thus the RANKL/OPG ratio is critical for bone remodelling and skeletal integrity. RANKL also plays a pivotal role in mammary gland morphogenesis, functioning as a key paracrine mediator of progesterone-induced mitogenic signals. In mice, RANKL expression is markedly induced by progesterone in mature PR^{+} luminal cells and mediates mitogenic signalling to neighbouring MaSC and luminal progenitor cells that express RANK but lack hormone receptors (Asselin-Labat et al., 2010; Fata et al., 2000; Fernandez-Valdivia et al., 2009; Gonzalez-Suarez et al., 2007; Joshi et al., 2010; Mulac-Jericevic et al., 2003; Pal et al., 2013) (Figure 1.5). RANK and RANKL are essential for the expansion of the stem/progenitor compartment that occurs during pregnancy and oestrus cycling (Asselin-Labat et al., 2010; Joshi et al., 2010), and for orchestrating the formation of functional lobuloalveolar structures required for lactation (Fata et al., 2000). Analogous to *PR*$^{-/-}$ epithelium, mice deficient in either *Rankl* or *Rank* developed normally during puberty but then failed to lactate due to a

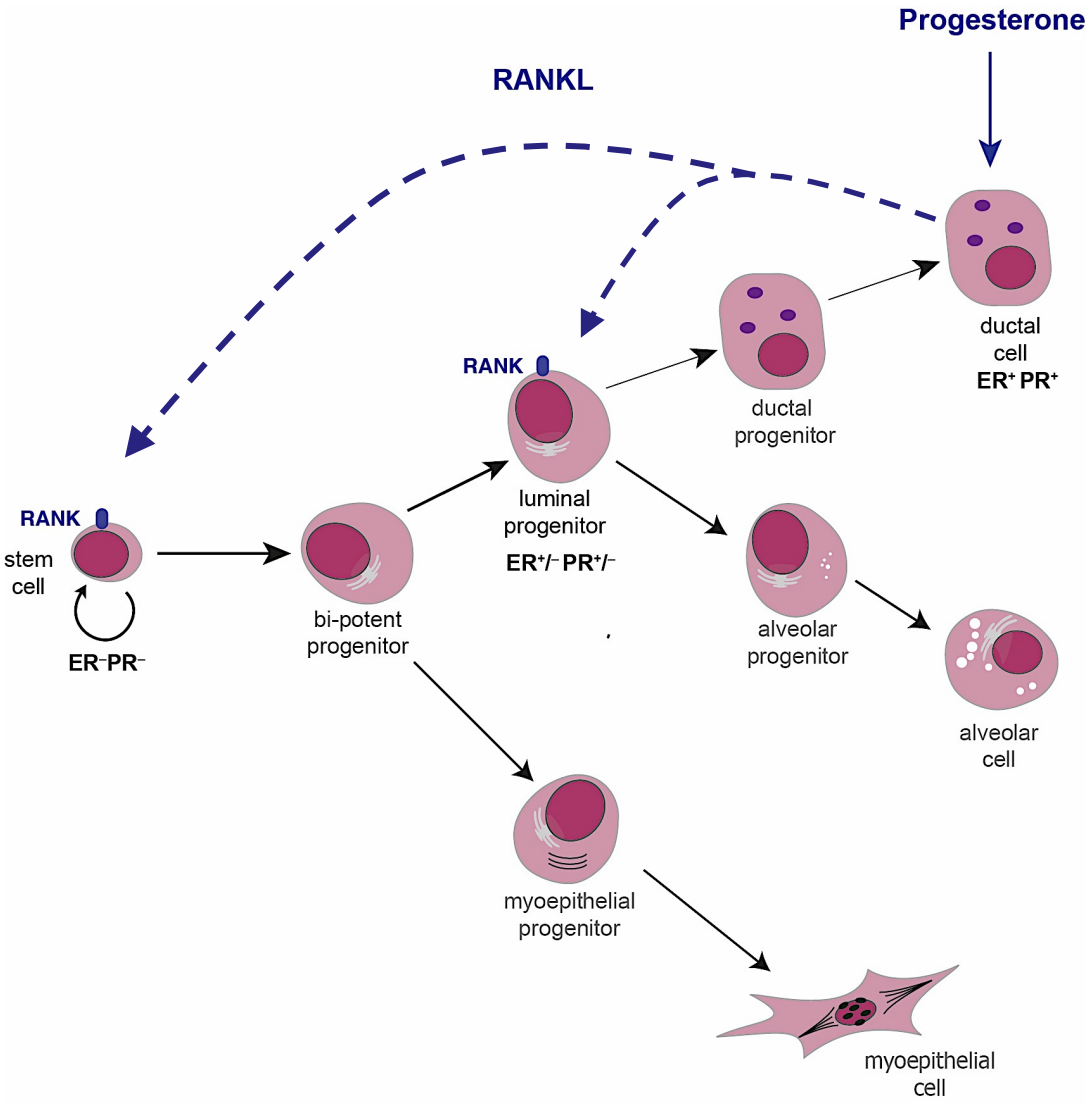

Figure 1.5: Schematic model of RANKL-mediated progesterone signalling in the mouse mammary gland

Mammary stem cells and luminal progenitor cells express RANK but lack expression of the hormone receptors ER and PR. These cells can receive mitogenic signals from progesterone via the secretion of RANKL from mature ductal cells. Figure adapted from Visvader, 2009.

lack of functional lobuloalveolar structures (Fata et al., 2000). This lactation defect was underpinned by an absence of RANKL-induced proliferation, differentiation and survival of the mammary epithelium (Fata et al., 2000). Ectopic expression of *Rankl* in $PR^{-/-}$ epithelial cells rescued branching morphogenesis and alveolar development, indicating that the RANKL signalling pathway is the major mediator of progesterone signalling to mouse mammary epithelium during lactational morphogenesis (Beleut et al., 2010; Mukherjee et al., 2010). The role of RANKL as an effector of mitogenic progesterone signalling has been confirmed in human breast tissue (Azim et al., 2015; Hu et al., 2014; Tanos et al., 2013). *Ex vivo* analysis of human breast tissue microstructures isolated from reduction mammoplasties demonstrated expression of RANKL in PR^{+} luminal cells and showed that progesterone induces cell proliferation with RANKL as an essential mediator (Tanos et al., 2013).

The spatially and temporally restricted expression of RANK and RANKL governs their control of mammary morphogenesis. RANKL mRNA and protein expression is exclusively induced in differentiated PR^{+} luminal cells in response to progesterone, peaking at mid-pregnancy and decreasing after 18.5 dP (Fernandez-Valdivia et al., 2009; Gonzalez-Suarez et al., 2007; Mulac-Jericevic et al., 2003). While *Rank* mRNA is unchanged, marked protein upregulation occurs specifically within HR^{-} MaSC and luminal progenitor cells during mid-pregnancy and is attenuated during maturation of the alveolar compartment (Fernandez-Valdivia et al., 2009; Gonzalez-Suarez et al., 2007). Interfering with this finely tuned regulation of RANK-RANKL signalling can have profound effects. As discussed above, *Rank*- and *Rankl*-deficient mammary glands lack functional lobuloalveolar structures required for successful lactation. Overexpression of *Rank* in the mouse mammary gland during pregnancy enhanced epithelial cell proliferation and markedly impaired alveolar differentiation (Gonzalez-Suarez et al., 2007). The observation that both *Rank* overexpression and loss result in the same striking lactation defect is paradoxical, but suggests that RANK upregulation during at mid-pregnancy is essential for epithelial expansion, and that dampening of RANK pathway activity is required later in pregnancy to initiate secretory differentiation. In addition, overexpression of *Rankl* in virgin mice leads to precocious ductal side-branching due to accelerated mammary epithelial proliferation, similar to the effects of

progesterone stimulation or *Rank* overexpression (Fernandez-Valdivia et al., 2009). In contrast to *Rank* transgenic mice, *Rankl*-overexpressing mice could undergo alveologenesis as a result of a compensatory reduction in *Rank* expression to attenuate the RANKL response. Taken together, these results suggest tight control of RANK and RANKL expression is required for proper hormone-induced mammary morphogenesis.

A critical downstream event in RANKL signalling is the activation of the NF-κB pathway (Anderson et al., 1997) (Figure 1.6). The NF-κB family of transcription factors, which are expressed in virtually all cell types, consists of five members: p50, p52, p65 (RelA), c-Rel and RelB, encoded by *NFKB1*, *NFKB2*, *RELA*, *REL* and *RELB*, respectively (reviewed in Hayden and Ghosh, 2008). These family members share an N-terminal Rel homology domain (RHD), responsible for DNA binding and dimerisation. NF-κB dimers bind to κB sites within the promoters/enhancers of target genes involved in a range of biological processes including inflammation, cell survival and proliferation, and regulate their transcription through the recruitment of coactivators and corepressors (Hayden and Ghosh, 2008). There are two distinct activating mechanisms referred to as the canonical (classical) and non-canonical (alternative) NF-κB pathway. In the canonical pathway, activation of the IκB kinase complex (IKKα, IKKβ and IKKγ/NEMO) induces proteasomal-mediated degradation of the inhibitory IκB protein, releasing the p50/p65 heterodimer and enabling nuclear translocation. In contrast, non-canonical signalling involves the activation of NF-κB inducing kinase (NIK) and IKKα, leading to the phosphorylation and partial processing of p100 into the mature p52 subunit. p52/RelB heterodimers are then free to translocate into the nucleus. Within the mammary gland, RANKL-RANK interactions promote the activation of IKKα (Cao et al., 2001), inducing transcriptional upregulation of the cell-cycle regulator *cyclin D1* and licensing cell proliferation (Cao et al., 2001; Fernandez-Valdivia et al., 2009; Mulac-Jericevic et al., 2003). Genetic inactivation of either *cyclin D1* or *IKKα* prevented the development of functional lobuloalveolar structures in pregnant mice (Cao et al., 2001; Fantl et al., 1995; Sicinski et al., 1995). The lactation defect observed in *IKKα*–deficient mice could be rescued by expression of a *cyclin D1* transgene (Cao et al., 2001). Alternative downstream

targets of RANKL signalling have also been revealed, including RANKL-triggered nuclear retention of the helix-loop-helix transcription factor Id2 (Kim et al., 2006; Kim et al., 2011) (Figure 1.6). *Id2*-deficient mice display impaired lobuloalveolar development during pregnancy and intrinsic defects in cellular proliferation and lactogenic differentiation (Miyoshi et al., 2001; Mori et al., 2000). RANK activation by RANKL triggers the activation of cyclin-dependent kinase 2 (Cdk2), which subsequently phosphorylates Id2 at serine 5 and prevents nuclear export. Nuclear localisation of Id2 is critical for the downregulation of *p21* promoter activity and cell cycle progression, eliciting proliferation and survival of mammary epithelial cells (Kim et al., 2006; Kim et al., 2011).

Following progesterone/RANKL-induced amplification of the mammary stem/progenitor cell compartment, commitment to the secretory lineage during pregnancy is achieved in part by RANKL-mediated induction of *Elf5*. Elf5 is an ETS transcription factor expressed by luminal progenitor cells that specifies their commitment towards the secretory alveolar lineage (Oakes et al., 2008). *Elf5* deletion prevents the formation of functional lobuloalveolar structures during pregnancy, while overexpression stimulates alveolar differentiation and milk secretion in virgin mice (Oakes et al., 2008). Elegant work has demonstrated significant induction of *Elf5* expression in luminal progenitors in response to progesterone treatment *in vivo*, or upon forced *Rankl* expression using the *MMTV* promoter (Lee et al., 2013). Blockade of RANKL signalling using a neutralising antibody prevented progesterone-induced side branching and the expansion of the $Elf5^+$ epithelial population (Lee et al., 2013). Thus RANKL-induced *Elf5* appears to drive the differentiation of luminal progenitor cells towards the secretory cell fate.

In addition to RANKL, Wnt-4 likely acts as a paracrine mediator of progesterone signalling, since the expression of *Wnt-4* is upregulated in response to progesterone in both human and mouse mammary glands (Brisken et al., 2000; Joshi et al., 2010; Tanos et al., 2013). In addition, its expression in the mouse epithelium colocalises with PR (Brisken et al., 2000). However, while mammary glands deficient in *Wnt-4* had reduced side-branching and alveologenesis during

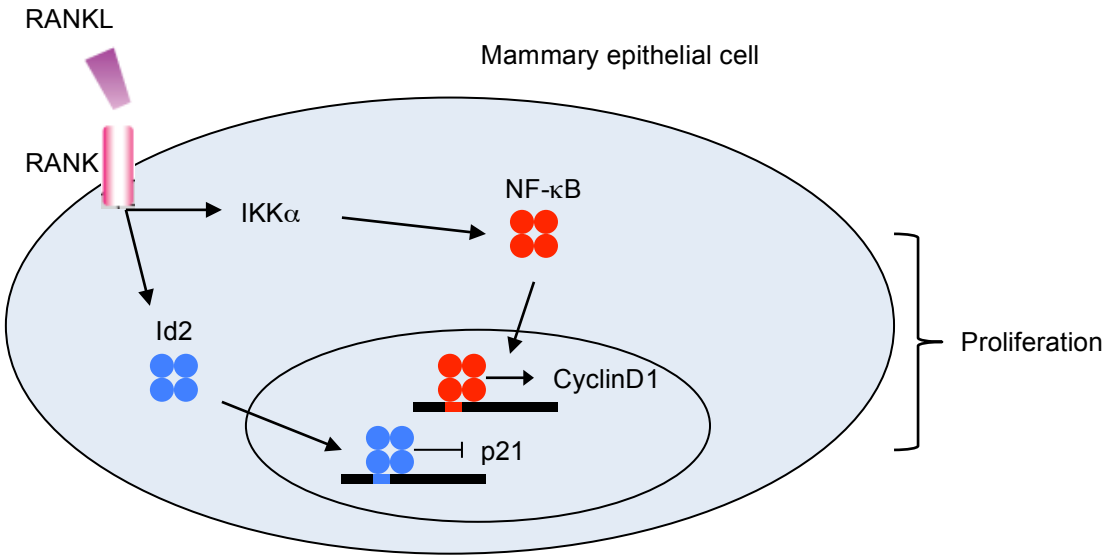

Figure 1.6: Schematic diagram depicting the signalling pathways downstream of the RANK receptor

RANKL-RANK interactions promote the activation of IKKα and subsequently NF-κB, which induces the transcriptional upregulation of *cyclin D1*. RANK activation also triggers nuclear retention of Id2, which leads to downregulation of *p21*. Both signalling pathways stimulate cell cycle progression and the proliferation of mammary epithelial cells. Adapted from Schramek et al., 2011.

early pregnancy, this phenotype was rescued as pregnancy progressed suggesting compensation by other Wnt ligands (Brisken et al., 2000). In addition, *Wnt-4* overexpression in the mammary gland failed to elicit a morphogenic response (Kim et al., 2009). These studies suggest that progesterone-induced Wnt-4, unlike RANKL, is not sufficient for ductal expansion and alveolar development in the mouse mammary gland. Intriguingly, an interaction between the RANKL and Wnt pathways was recently proposed (Joshi et al., 2015), in which progesterone-induced RANKL enables Wnt responsiveness by triggering the upregulation of *R-spondin1*, a secreted protein known to enhance Wnt signalling via stabilisation of the Wnt receptor complex (de Lau et al., 2014). This facilitates the proliferation of Wnt-responsive mammary stem/progenitor cells in response to progesterone-induced Wnt4 secretion.

1.4 Breast Cancer

1.4.1 Breast cancer heterogeneity

Breast cancer is the most common cancer affecting women worldwide, accounting for approximately 30% of all new cancer cases diagnosed each year and 15% of all deaths (Siegel et al., 2015). It is not a single disease but a heterogeneous collection of tumour subtypes with diverse pathological features, molecular signatures, therapeutic responses and clinical outcomes. Traditionally, breast cancers were classified based on the expression of ER, PR and human epidermal growth factor receptor 2 (HER2) by immunohistochemistry. As a consequence of elegant gene profiling studies, breast cancers can now be robustly stratified into five distinct subtypes on the basis of their transcriptome: luminal A, luminal B, HER2-positive, claudin-low and basal-like (Herschkowitz et al., 2007; Perou et al., 2000; Sorlie et al., 2001). Classification of newly diagnosed tumours into a breast cancer subtype has had important implications for tailoring treatments and predicting patient outcomes, however patient response to targeted therapy or chemotherapy remains highly variable. Intertumoral heterogeneity is hypothesised to reflect both the distinct breast epithelial cells that serve as the cell of origin for malignant transformation (reviewed in Visvader, 2011) and the nature of the

initiating genetic lesions (reviewed in Ellis and Perou, 2013). Comparisons between the molecular signatures of normal mammary epithelial populations with those representing the breast cancer subtypes has been a valuable tool for interrogating distinct cell of origin populations. Breast cancer subtypes appear to segregate along the normal mammary differentiation hierarchy starting with undifferentiated claudin-low tumours, followed by basal-like, then $HER2^+$ tumours and finally both luminal tumour subtypes (Lim et al., 2009; Prat et al., 2010) (Figure 1.7). Determining the cells of origin as well as the biomarkers they express could enable earlier detection of breast cancer and the development of effective preventive therapies (Visvader, 2011). In addition to cells of origin and genetic events, the microenvironment including stromal and immune cells likely plays a pivotal role in influencing tumour histopathology and behaviour (reviewed in Polyak and Kalluri, 2010).

1.4.2 Luminal A and B breast tumours

Luminal A and B tumours represent the majority of breast cancers and are typically associated with more favourable clinical outcomes compared to other tumour subtypes. Luminal tumours share a gene expression signature that aligns with that of differentiated ER^+ luminal cells including high expression of *ER* and the transcription factors *GATA3*, *XBP1* and *FOXA1* (Lim et al., 2009). Luminal A cancers are typically low-grade ER^+ tumours with low expression of proliferation genes, while luminal B tumours have lower *ER* expression and a higher proliferative index and tumour grade. Accordingly, patients with luminal A tumours show more favourable relapse-free and survival outcomes after treatment compared to luminal B tumours (Fan et al., 2006). The expression of ER by the majority of luminal A and B tumours permits the use of endocrine therapy for targeted treatment (in combination with chemotherapy or as a single agent), the use of which has dramatically increased the survival of patients with ER^+ breast cancer (Early Breast Cancer Trialists' Collaborative Group, 2005). Endocrine therapies typically involve the use of tamoxifen, a selective oestrogen-receptor modulator (Borras et al., 1994), or aromatase inhibitors such as letrozole that block oestrogen biosynthesis (Bulun et al., 2005). The 10-year relapse-free survival for luminal A patients treated with tamoxifen alone is approximately 70% compared to

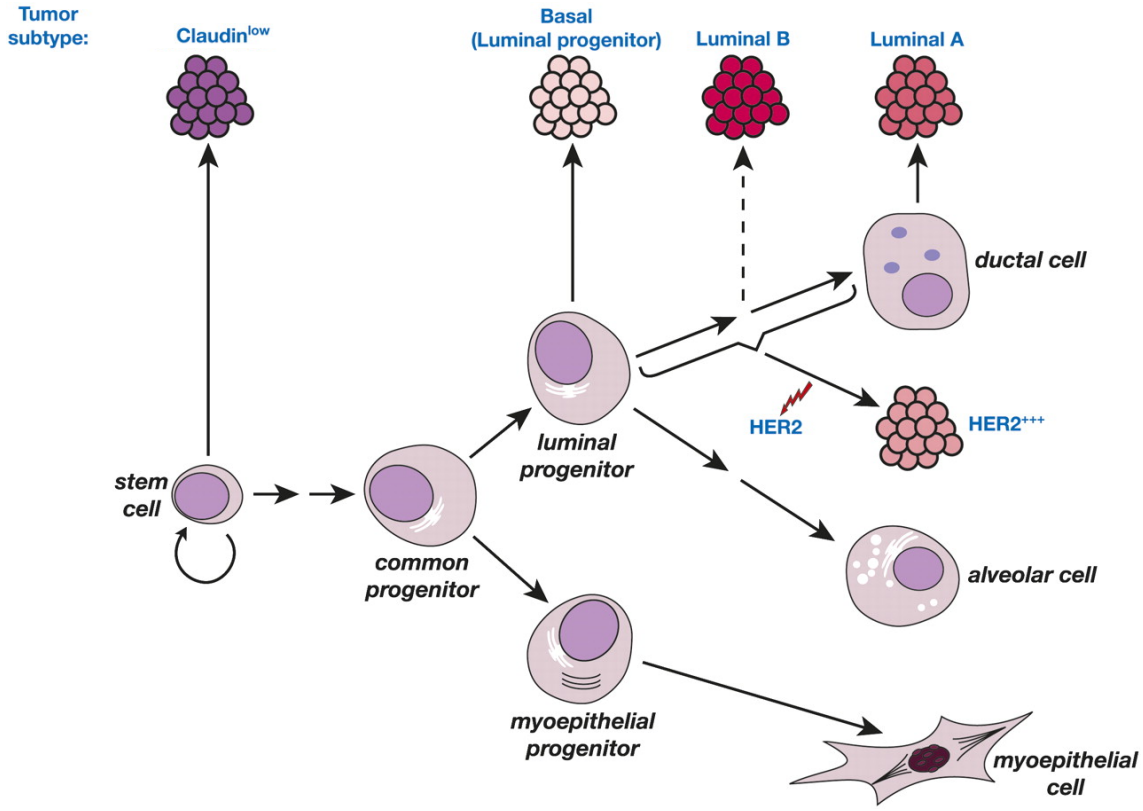

Figure 1.7: Schematic model of the human breast epithelial hierarchy and the potential association with breast cancer subtypes.

Depicted are the five major breast tumour subtypes along with their closest normal epithelial counterpart, based on the comparison of gene expression signatures. $HER2^{+}$ tumours may arise through amplification of the *HER2* locus in a target cell within the luminal lineage. Figure adapted from Visvader, 2009.

50% for patients with luminal B tumours (Cheang et al., 2009; Nielsen et al., 2010). Luminal A and B tumours also exhibit a distinct genetic mutational profile compared with other tumour subtypes, including mutations in key regulators of luminal cell differentiation and hormone signalling such as *PI3K*, *MAP3K1*, *GATA3*, *FOXA1* and *TBX3* (The Cancer Genome Atlas Network, 2012). Activating mutations in the PI3K pathway, a key intracellular signalling system that drives cellular growth and survival, are the most prevalent genetic events in ER^+ luminal breast tumours and have been implicated in both tumorigenesis and resistance to endocrine therapy (Ciruelos Gil, 2014). This, in combination with the observation that many patients with ER^+ breast cancer encounter *de novo* or acquired resistance to endocrine therapies, provides a powerful rationale for highly specific therapies targeting the PI3K pathway (Ellis and Perou, 2013; Li et al., 2013). Preclinical studies have revealed that pharmacological or genetic inactivation of PI3K induces marked apoptosis of ER^+ breast cancer cells particularly when combined with loss of oestrogen signalling (Crowder et al., 2009; Sanchez et al., 2011). Several agents that target the PI3K pathway are currently being evaluated for the treatment of ER^+ luminal breast cancer in clinical trials (reviewed in Ciruelos Gil, 2014).

1.4.3 HER2-positive tumours

Breast tumours that have overexpression/amplification of the *HER2/ErbB2* locus represent approximately 20% of breast cancers (Slamon et al., 1987). HER2 is a member of the human epidermal growth factor receptor family that promotes cell proliferation and survival. $HER2^+$ breast cancers are typically highly proliferative tumours that lack expression of basal-associated genes, have variable expression of hormone receptors (approximately 50% are ER^+) and lower expression of luminal-specific genes compared to luminal A and B tumours (Prat and Perou, 2011). These tumours have no clear association with a normal epithelial cell subset as yet, but their molecular signature implies they may derive from amplification of the *HER2* locus in an epithelial cell with an intermediate differentiation state between luminal progenitor and mature luminal cells (Visvader, 2009). Although $HER2^+$ breast cancers have been traditionally associated with a poor prognosis, treatment of these patients has been revolutionised by the development of Herceptin/Trastuzumab that specifically targets the HER2 receptor (Hudziak et al.,

1989; Vogel et al., 2002). The administration of trastuzumab in combination with chemotherapy results in improved recurrence-free survival as well as overall-survival in a significant proportion of patients with $HER2^+$ breast cancer (Piccart-Gebhart et al., 2005; Romond et al., 2005).

1.4.4 Basal-like breast cancer

Basal-like tumours are the most heterogeneous of the breast cancer subtypes and comprise 15 – 20% of all tumours. The majority of basal-like tumours exhibit a triple-negative phenotype ($ER^-PR^-HER2^-$) (>90%, Cheang et al., 2015), express high levels of EGFR and the basal markers cytokeratin 5, 6 and 14, and are associated with a poor prognosis. Basal-like cancers comprise 80 – 90% of all triple negative breast cancers (Reis-Filho and Lakhani, 2008). Interrogation of the gene expression signature of basal-like breast tumours with human mammary epithelial cells unexpectedly revealed striking similarities with the normal luminal progenitor gene signature, and not that of the MaSC-enriched population as had been widely presumed (Lim et al., 2009). Thus, the luminal progenitor could represent the cell of origin for basal-like breast tumours. These cells were further defined as $ALDH^+$ and ER^- luminal progenitor cells (Shehata et al., 2012). The mutational profile of basal-like tumours is distinct from other tumour subtypes as they carry an extremely high rate of *TP53* mutations (85% mutation frequency in TCGA database), a higher number of somatic mutations per tumour and a higher degree of genomic instability (The Cancer Genome Atlas Network, 2012). PI3K/Akt pathway activating mutations are also common in basal-like tumours, frequently via the loss of negative regulators such as *PTEN* (35% mutation frequency). Although triple negative basal-like tumours often display chemosensitivity, disease-free and overall survival are still significantly worse than ER^+ tumours due to higher rates of relapse in patients with residual disease (known as the “triple-negative paradox”, Carey et al., 2007). The absence of ER and HER2 expression precludes the use of endocrine or anti-HER2 therapy, thus cytotoxic chemotherapy remains the mainstay of treatment for basal-like breast tumours. Therefore a challenge for the field is the identification of effective targeted therapies for these highly aggressive tumours. Current molecular targets that are being evaluated include poly(adenosine diphosphate (ADP)-ribose) polymerase 1 (PARP1), vascular endothelial growth factor (VEGF), EGFR, MAPK

and PI3K/mTOR. Of particular interest is the inhibition of PARP1, a key player in the repair of DNA breaks that is typically found to be highly expressed in basal-like tumours, along with other DNA-repair pathway genes (Prat and Perou, 2011). Clinical trials have demonstrated the efficacy of PARP1 inhibitors particularly in patients with basal-like tumours that carry germline mutations in the DNA-repair genes *BRCA1* or *BRCA2*, or sporadic basal-like breast tumours that share common phenotypic features with familial *BRCA* tumours (termed "BRCAness", Lord and Ashworth, 2016; Turner et al., 2004).

1.4.5 Claudin-low tumours

Claudin-low tumours are the least frequent breast cancer subtype and are mostly triple-negative invasive ductal carcinomas that are associated with a poor prognosis (Herschkowitz et al., 2007). Tumours typically have mesenchymal features, express immune response genes implying lymphocytic infiltration and are characterised by low levels of genes involved in tight junctions, cell-cell adhesion and luminal differentiation (Prat et al., 2010). In contrast to the other poor outcome subtypes such as $HER2^+$ and basal-like, claudin-low tumours express low levels of proliferation-associated genes and thus appear to be slow-cycling tumours (Prat et al., 2010). Their response rate to standard neoadjuvant chemotherapy is intermediate between luminal and basal-like tumours (Prat et al., 2010). Interestingly, metaplastic carcinomas have been also linked with the claudin-low profile; these are rare, poorly differentiated breast tumours that are associated with poor prognosis and treatment resistance (Al Sayed et al., 2006; Hennessy et al., 2005). Molecular profiling studies have revealed the gene signature of the MaSC subset is most closely aligned with the claudin-low subtype (Herschkowitz et al., 2007; Lim et al., 2009; Prat et al., 2010), suggesting that this is the likely target population for malignant transformation. Functional evidence for MaSCs as the cells of origin for claudin-low tumours has come from the genetic transformation of human basal/myoepithelial cells, which resulted in the development of rare metaplastic tumours reminiscent of the claudin-low subtype following transplantation into mice (Keller et al., 2012).

1.5 Ovarian Hormones and Breast Cancer

The connection between ovarian hormones and breast cancer was established more than a century ago, when Sir George Beatson demonstrated that breast cancer progression could be drastically attenuated by bilateral oophorectomy in premenopausal women (Beatson, 1896). Subsequent evidence has implicated both exogenous and endogenous oestrogen and progesterone levels in breast cancer pathogenesis. Breast cancer risk robustly increases with early menarche, late menopause and shorter menstrual cycles (Colditz et al., 2004), clearly correlating cancer risk with the number of menstrual cycles a woman experiences during her lifetime, and hence the exposure time of the mammary epithelium to ovarian hormones. Conversely, early menopause or ovarian ablation is protective against breast cancer development (Parker et al., 2009b; Pike et al., 1993). Furthermore, exogenous hormone-replacement therapy (HRT) has been highly implicated as a risk factor for breast cancer in postmenopausal women (Collaborative Group on Hormone Factors in Breast Cancer, 1997; Hulka, 1997).

Breast cancer risk following exposure to ovarian hormones appears to be largely mediated by progesterone signalling (reviewed in Brisken, 2013). As discussed earlier in this chapter, progesterone is the major stimulus of cell proliferation in the adult female, and the majority of proliferation in the human breast occurs during the luteal phase when progesterone levels are highest. Importantly, a substantial increase in breast cancer risk was observed in women taking a combination of oestrogen and progestin (a synthetic progesterone agonist) for HRT compared to no or a small increase in risk conferred by oestrogen alone (Beral, 2003; Chlebowski et al., 2010; Rossouw et al., 2002). This is likely attributed to the substantial increase in cell proliferation observed in the breast epithelium of women taking combination therapy (Hofseth et al., 1999). The use of combination HRT significantly declined following publication of these findings, and has been followed by a reduction in breast cancer incidence (Farhat et al., 2010).

It is conceivable that the breast cancer risk associated with sustained progesterone exposure (via repeated menstrual cycles or combination HRT) is attributable to recurrent activation of paracrine effectors downstream of PR. As described earlier,

progesterone-induced RANKL stimulates proliferation and expansion of mammary stem/progenitor cells via the activation of downstream signalling pathways, specifically NF-κB and Id2. The expanded pool of stem/progenitor cells likely translates to increased targets for carcinogen or genetic mutation-induced malignant transformation (Asselin-Labat et al., 2010; Joshi et al., 2010). Indeed *in vivo* administration of medroxyprogesterone (MPA), a progestin commonly used in HRT, triggered an enormous induction (2000 fold) of *Rankl* mRNA in the mouse mammary epithelium, and stimulated mammary epithelial proliferation (Gonzalez-Suarez et al., 2010; Schramek et al., 2010). Together with the observation that elimination of RANKL signalling markedly delayed the onset and frequency of hormone-driven mouse mammary tumours (Gonzalez-Suarez et al., 2010; Schramek et al., 2010), this suggests that RANKL may be a principle mediator of the pro-tumorigenic effects of progesterone.

1.6 Familial Breast Cancer

The clustering of breast cancer in families was first documented in 1866 by the French surgeon Broca (Broca, 1866). It is estimated that 5 – 10% of all breast cancer cases are directly attributable to the inheritance of mutations in breast cancer susceptibility genes (Rahman and Stratton, 1998). A number of high-penetrance genes have been implicated in breast cancer susceptibility, including the tumour suppressor genes *BRCA1*, *BRCA2*, *TP53*, *PTEN, CHK2 and ATM* that are predominantly associated with the maintenance of genome integrity and DNA repair. Germline mutations in *BRCA1* and *BRCA2* have an autosomal dominant inheritance pattern, confer a high lifetime risk of developing breast and ovarian cancer and together account for approximately 30 – 40% of all hereditary breast cancer cases (Antoniou et al., 2008; Ford et al., 1998; Mavaddat et al., 2010; Peto et al., 1999). The risk of developing cancer is not identical for all carriers of *BRCA1* and *BRCA2* mutations, and can be influenced by allelic heterogeneity, modifier genes and environmental and hormonal cofactors (reviewed in Couch et al., 2014; Narod and Foulkes, 2004). While less common, germline mutations in *TP53* can lead to Li-Fraumeni syndrome, a multicancer syndrome that includes sarcoma, early-onset breast cancer, leukaemia and brain tumours (Li and Fraumeni, 1969).

There are likely to be additional moderate- and low- penetrance genes that contribute to a significant proportion of breast tumours and hence play an important role in genetic predisposition to breast cancer within the general population (Pharoah et al., 2008; Shuen and Foulkes, 2011). The difficulty in identifying these genes suggests they may influence breast cancer risk in a more subtle or complex manner, such as through gene-gene interactions or gene-environment interactions (Peto, 2002).

1.6.1 *BRCA1/2* breast cancer susceptibility genes

The first genetic linkage analysis of breast and ovarian cancer pedigrees led to the localisation of the susceptibility gene *BRCA1* on chromosome 17q21 (Hall et al., 1990), which was subsequently cloned in 1994 and shown to harbour truncating mutations in families with multiple cases of breast cancer (Miki et al., 1994). Germline mutations in *BRCA1* confer a 50 – 80% lifetime risk of developing breast cancer, as well as a 30 – 50% risk of ovarian cancer (Chen and Parmigiani, 2007; Rahman and Stratton, 1998). The frequency of *BRCA1* mutations in the general population is estimated at 1/500 to 1/1000 individuals (Easton et al., 1993). While inactivating mutations in *BRCA1* are found throughout the coding region of the gene, specific mutations are more common within certain populations as a consequence of genetic founder effects. This is particularly prominent in the Ashkenazi Jewish population, in which 1% carry the mutation 185delAG and 0.1 to 0.2% harbour the mutation 5382insC (FitzGerald et al., 1996; Roa et al., 1996; Struewing et al., 1995). Although somatic mutations in *BRCA1* are rarely observed in sporadic breast cancers, hypermethylation of the *BRCA1* promoter resulting in gene silencing has been demonstrated in 13% of sporadic breast tumours (Catteau et al., 1999; Esteller et al., 2000; Rice et al., 2000). Notably, breast tumours with *BRCA1* hypermethylation are histologically similar to tumours associated with a germline mutation.

Analysis of breast and ovarian cancer pedigrees that were not linked to *BRCA1* led to the mapping of a second susceptibility locus termed *BRCA2* at chromosome 13q12-13, which was cloned the following year (Wooster et al., 1995; Wooster et al., 1994). Like *BRCA1,* the inheritance of a germline mutation in *BRCA2* conveys a

significant breast cancer predisposition, while the risk of ovarian cancer is lower (approximately 20%, Risch et al., 2001). *BRCA2*-mutation carriers often present with cancer at an older age compared to *BRCA1*-mutation carriers, and have an overall lower penetrance of cancer risk (Moynahan, 2002). Notably, *BRCA2* is also important for the suppression of male breast, pancreatic, gastrointestinal and prostate cancer (Bancroft et al., 2014; Hahn et al., 2003; Moynahan and Jasin, 2010; Murphy et al., 2002). Specific pathogenic mutations in *BRCA2* are common within certain populations, particularly the 6174delT mutation that has a frequency of 1.3% in the Ashkenazi Jewish population (Oddoux et al., 1996; Roa et al., 1996), and 999del5 with a prevalence of 0.4% in the Icelandic population (Johannesdottir et al., 1996). Although an inherited *BRCA1* biallelic mutation has not been observed presumably due to embryonic lethality, rare *BRCA2* biallelic mutations lead to a severe form of Fanconi anaemia (Fanconi anaemia D1) characterised by the frequent occurrence of medulloblastoma, Wilms' tumour (a pediatric malignancy of the kidney) and haematological malignancies (Howlett et al., 2002; reviewed in Meyer et al., 2014).

Breast cancers that arise in *BRCA1*-mutation carriers often manifest as early onset, proliferative, high-grade infiltrating ductal carcinomas. Tumours typically exhibit a triple-negative phenotype, express basal/myoepithelial markers (e.g. K14) and have a molecular and pathological signature that is closely aligned with sporadic basal-like tumours (Foulkes et al., 2003; Larsen et al., 2013; Mavaddat et al., 2012; Sorlie et al., 2001; Waddell et al., 2010). Tumours are typically associated with a poor prognosis and are more aggressive than sporadic breast cancers (Evans and Howell, 2004; Robson et al., 2001) and hence often present as interval tumours (i.e. they arise between mammography screens, Brekelmans et al., 2001). *TP53* mutations are more frequent in *BRCA1*-mutated breast tumours than in sporadic cases (Greenblatt et al., 2001), indicating that the loss of cell cycle control might be a critical step in carcinogenesis. In contrast to *BRCA1*, 60 – 90% of *BRCA2*-mutated breast tumours are ER^+, and 40 – 80% are PR^+ (Honrado et al., 2006). Tumours are typically the luminal A or luminal B molecular subtype (Larsen et al., 2013; Mavaddat et al., 2012; Waddell et al., 2010). Approximately 15% of *BRCA2* tumours demonstrate overexpression/amplification of HER2, and triple-negative breast cancers are rarely observed.

Most ovarian cancers associated with germline *BRCA1/2* mutations are high-grade and advanced-stage serous carcinomas (Lakhani et al., 2004). Endometrioid and clear cell carcinomas have also been reported although at a significantly lower frequency. Similar to breast tumours, *TP53* mutations are found at a higher frequency than in sporadic ovarian tumours, with frequencies of 60%, 50% and 30% reported in *BRCA1*-mutant, *BRCA2*-mutant and sporadic ovarian cancers, respectively (Lakhani et al., 2004). High-grade serous ovarian carcinomas are thought to arise from secretory cells within the fallopian tube, and cancer precursor lesions known as serous tubal intraepithelial carcinomas (STIC) are often observed in specimens from asymptomatic *BRCA1/2*-mutation carriers (reviewed in Zeppernick et al., 2015).

1.6.2 Functions of BRCA1 and BRCA2

BRCA1 plays an essential role in a number of cellular processes including DNA repair, cell cycle-checkpoint control, protein ubiquitylation and chromatin remodelling (Deng, 2006; Huen et al., 2010; Narod and Foulkes, 2004; Rosen, 2013; Yoshida and Miki, 2004). *BRCA1* is a large gene comprising 24 exons and encodes a protein of 1863 amino acids. The N-terminus contains a RING domain that has E3 ubiquitin ligase activity and a nuclear export signal, while the C-terminus harbours two BRCT domains, which are sequence repeats of approximately 90 amino acids that facilitate interactions with a number of phosphorylated proteins involved in the DNA damage response (Moynahan and Jasin, 2010). Centrally located, there are two nuclear localisation signals, and a SQ cluster domain (SQCD) that contains several serine and threonine residues that act as phosphorylation sites for BRCA1 activation. The BRCA2 protein is larger than BRCA1 (3418 amino acids). The central region of the protein contains a DNA-binding domain and a series of eight short repeat motifs, termed BRC repeats that are protein-binding domains essential for its function in DNA repair. Two nuclear localisation signals are located in the C-terminus region.

Both BRCA1 and BRCA2 are critical for the maintenance of genomic integrity, largely facilitated by their role in homologous recombination (HR)-mediated repair of DNA double-strand breaks (DSBs) (reviewed in Huen et al., 2010; Moynahan

and Jasin, 2010; Roy et al., 2012; Sung and Klein, 2006; Tutt and Ashworth, 2002) (Figure 1.8). DSBs can occur as by-products of DNA replication or upon exposure to ionizing radiation or other genotoxic compounds. HR repair is the most accurate DNA repair mechanism, the absence of which can result in gross chromosomal rearrangements and genomic instability. HR repair occurs during late S phase to G2 phase of the mammalian cell cycle, whereby the homologous sequence of the sister chromatid acts as a template to guide precise DNA repair (Moynahan and Jasin, 2010). Repair is initiated by resection of the 5' and 3' ends of the DSB by exonucleases, producing a 3' single-stranded end that can invade the homologous "donor" sister chromatid and pair with the complementary DNA strand, allowing the initiation of repair. At the molecular level, a protein complex consisting of Mre11-RAD50-Nbs1 (termed MRN complex) binds to the ends of the DSB upon DNA damage, and recruits the DNA damage sensors ataxia telangiectasia mutated (ATM) and ataxia telangiectasia mutated rad3-related (ATR) (Lee and Paull, 2005). ATM and ATR are serine/threonine protein kinases that phosphorylate H2AX, facilitating the recruitment of repair proteins including BRCA1 (Celeste et al., 2002). ATM/ATR then phosphorylate and activate BRCA1 (Cortez et al., 1999; Tibbetts et al., 2000). Active BRCA1 can then form a protein complex with BRCA2 and PALB2, which binds RAD51 to form damage-induced nuclear foci at the site of the DSB (Scully et al., 1997; Wong et al., 1997; Xia et al., 2006; Zhang et al., 2009). Together this complex, along with other BRCA1-interacting proteins such as Abraxas, CtBP-interacting protein (CtIP) and the DNA helicase BRIP1, facilitate HR-mediated repair. Therefore, BRCA1 plays a central role in DNA repair by acting as a protein scaffold and signal integrator, linking DNA damage sensors with repair effectors (reviewed in Caestecker and Van de Walle, 2013; Roy et al., 2012). In contrast, BRCA2 appears to be more directly involved in the repair process, particularly in RAD51-mediated strand invasion (Wong et al., 1997). In cells deficient in functional BRCA1 or BRCA2, HR-mediated repair is impaired and more error-prone mechanisms such as non-homologous end-joining (NHEJ) and single-strand break (SSB) repair are employed to facilitate DNA repair, leading to increased chromosomal instability and rearrangements. *BRCA1/2*-mutated tumours show a significantly higher degree of genomic alterations compared to sporadic breast cancers (Nik-Zainal et al., 2016; Rahman and Stratton, 1998; Tirkkonen et al., 1997). The destabilised genome of *BRCA1*/2-deficient cells likely increases the

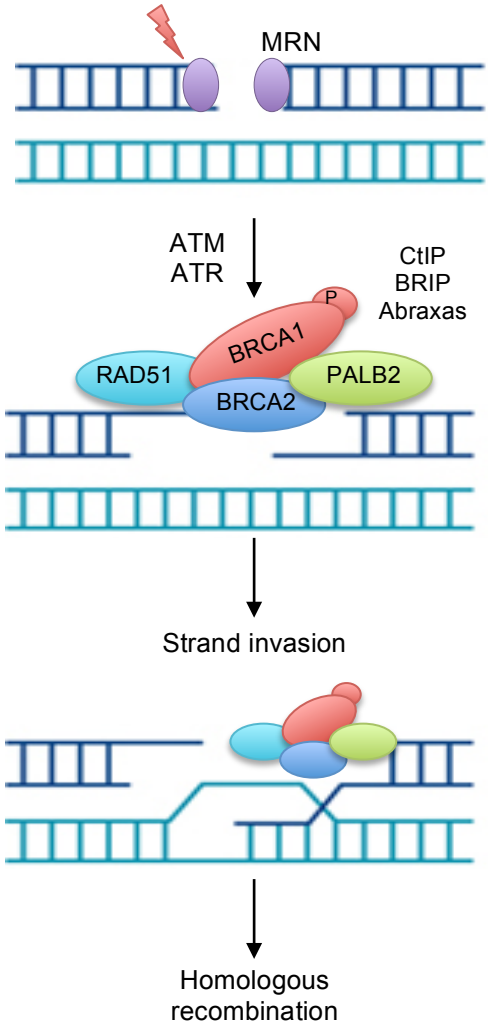

Figure 1.8: Schematic diagram depicting the role of BRCA1 and BRCA2 in homologous recombination-mediated DNA repair

DNA double-strand breaks (DSBs) are detected by the MRN complex, leading to the recruitment of ATM and ATR. The subsequent phosphorylation and activation of BRCA1 enables the formation of a multi-protein repair complex, containing the DNA repair effectors BRCA2 and RAD51. During homologous-recombination, the sister chromatid is used as a template for high-fidelity DNA repair. Adapted from Roy et al., 2012.

mutation rates of genes including tumour suppressors and oncogenes, ultimately leading to tumour formation.

Unlike BRCA2, BRCA1 has a number of broader roles within the cell. BRCA1 E3 ubiquitin ligase activity is enhanced when associated with the RING domain of its partner protein, BRCA1-associated RING domain protein 1 (BARD1). BRCA1-BARD1 heterodimers act as ubiquitin ligases to target proteins for proteasomal degradation (Wu et al., 1996). The ubiquitylation function of BRCA1 also contributes to its role in DNA repair, since the BRCA1/BARD1 complex exhibits post-damage ubiquitin ligase E3 activity at DSB sites, resulting in the modification of other DNA repair proteins such as CtIP and H2AX (Yu et al., 2003; Yu et al., 2006). RNA polymerase II and the coupled 3'-RNA processing machinery stalled at the sites of DNA damage are also targets of BRCA1/BARD1 ubiquitin ligase activity, leading to their degradation and permitting access for the repair machinery (Hashizume et al., 2001; Kleiman et al., 2005). BRCA1 can also act as either a coactivator or corepressor of gene transcription via its ability to recruit the basal transcription machinery (through an interaction with RNA polymerase II, Anderson et al., 1998), the histone deacetylases HDAC1 and HDAC2 (Yarden and Brody, 1999) and components of the SWI/SNF-related chromatin-remodelling complex (Bochar et al., 2000). Through its transcriptional regulation of genes involved in cell cycle checkpoint control, BRCA1 can elicit cell cycle arrest at several phases of the cell cycle. For example, BRCA1 promotes transcription of the cyclin dependent kinase (CDK) inhibitor *p21* and hence activation of the G1/S phase checkpoint (Somasundaram et al., 1997), and can transcriptionally repress *CyclinB*, the cyclin responsible for activating Cdc2 kinase to enable mitotic entry (MacLachlan et al., 2000). Checkpoint regulation also complements the role of BRCA1 in DNA damage repair processes, allowing adequate time for repair to occur so that genetic errors are not transmitted to subsequent generations.

1.6.3 Cells of origin for *BRCA1*-mutated breast cancers

Dissecting the early cellular changes that arise in premalignant *BRCA1/2*-mutant breast tissue is a critical step in identifying effective prevention strategies, and could also inform the development of targeted therapies. It was initially proposed

that putative breast stem cells residing within the basal layer of the mammary epithelium were the 'cell of origin' for *BRCA1*-mutated basal-like tumours (Foulkes, 2004). This was based primarily on histological studies noting similarities between basal-like tumours and basal mammary epithelial cells, for instance high expression of basal cytokeratins and a lack of hormone receptor expression. However, compelling evidence suggests that an aberrant luminal progenitor subpopulation residing within preneoplastic tissue from *BRCA1*-mutation carriers is the probable target population for neoplastic transformation (Lim et al., 2009; Molyneux et al., 2010; Proia et al., 2011). The luminal progenitor compartment within *BRCA1*-mutant tissue is expanded and exhibits factor-independent growth properties *in vitro* (Lim et al., 2009). Notably, the luminal progenitor subset harbours a molecular profile more closely aligned with that of basal-like tumours compared to any other breast cancer subtype, while the MaSC-enriched/basal subset is more closely aligned to the claudin-low subtype (Lim et al., 2009). Conditional deletion of *Brca1* in the luminal compartment of the mammary epithelium predisposes mice to the development of basal-like tumours that resemble the histological, pathological and molecular features of human basal-like tumours, whereas deletion in the basal compartment does not (Molyneux et al., 2010). Furthermore, transduction of human breast epithelial cells with a cocktail of potent oncogenic lentiviruses followed by implantation into the humanised mammary fat pads of immunocompromised mice (Kuperwasser et al., 2004) led to preferential transformation of *BRCA1*-mutated luminal cells compared to basal cells (Proia et al., 2011). Moreover, transformed cells from wild-type breast tissue gave rise to both luminal and basal-like tumours, whereas transformation of *BRCA1*-mutant cells predominantly yielded basal-like tumours. Thus *BRCA1*-deficient breast tissue exhibits an inherent defect that dictates tumour phenotype. The predilection for forming basal-like tumours may be mediated by the *BRCA1*-regulated transcription factor *SLUG*, which is profoundly upregulated in *BRCA1*-deficient tissues and blocks luminal cell differentiation, biasing cells towards a basal fate (Proia et al., 2011). Together, these studies provide valuable insights into the target cells prone to tumorigenesis and the potential molecular mechanisms underlying neoplastic transformation.

1.6.4 Tissue specificity of *BRCA1*-mutated tumours

Given the requirement for high-fidelity DSB repair in all cells to ensure survival, the loss of genomic stability associated with a germline *BRCA1* mutation would be anticipated to promote tumour formation in all tissues. However, *BRCA1*-mutation carriers are almost exclusively predisposed to developing breast and ovarian cancers. Several hypotheses have been put forward to explain this remarkable tumour-specificity. High-fidelity DNA repair in breast and ovarian tissues has been postulated to rely critically on functional BRCA1 protein, whereas other tissues may utilise compensatory mechanisms. This functional redundancy has been disputed based on the embryonic lethality associated with *Brca1*-null mice (Gowen et al., 1996), although it is possible that compensatory pathways are triggered post-natally (Monteiro, 2003). Secondly, it has been proposed that breast and ovarian tissues experience an accelerated rate of loss-of-heterozygosity (LOH) at the *BRCA1* locus compared to other tissues (Monteiro, 2003), perhaps via enhanced mitotic recombination. This has been speculated based on studies of somatic LOH in mice heterozygous for the adenine phosphoribosyltransferase (*Aprt)* locus, where rates of mitotic recombination were shown to have tissue-specific variation (Shao et al., 2001). However, evidence suggests that loss of the wild-type *BRCA1* allele may not be the rate-limiting initiating step of tumorigenesis, and may not be present in all cancer cells within *BRCA1*-mutated tumours (King et al., 2007; Martins et al., 2012). Indeed loss of *PTEN* has been shown to be the most probable first event in *BRCA1*-mutated human breast tumours, followed by mutations in *TP53* or *BRCA1* LOH with equal probability (Martins et al., 2012).

These hypotheses are primarily based on data using cells where both *BRCA1* alleles have been lost, or on events directly preceding this (in the case of an accelerated LOH). However it seems likely that the tissue-specificity associated with *BRCA1*-mutated tumours is facilitated by much earlier events that are initiated in heterozygous *BRCA1* breast tissue. Thus, the tumorigenesis process may begin long before cancer becomes clinically apparent. In line with this, Sedic et al. recently observed a significant increase in genomic instability and telomere erosion exclusively in human *BRCA1*-mutant breast epithelial cells relative to breast fibroblasts (Sedic et al., 2015). *BRCA1*-deficient epithelial cells also underwent

premature senescence in the absence of LOH (termed haploinsufficiency-induced senescence), likely imposing a strong selective pressure on cells to mutate or lose p53 and pRb pathways in order to bypass this barrier. Collectively, their findings demonstrate that substantial haploinsufficiency exists in *BRCA1*-mutant breast epithelial cells but is not present in mammary fibroblasts, cumulating in an increased propensity for neoplastic transformation.

Importantly, extrinsic influences such as hormone signalling likely act in concert with these cell intrinsic properties to promote neoplastic transformation specifically within breast and ovarian tissues. Indeed, amplified progesterone signalling has been identified in both human and mouse *BRCA1*-deficient mammary tissue (King et al., 2004; Ma et al., 2006; Poole et al., 2006; Widschwendter et al., 2013). Furthermore oestrogen signalling may confer a survival advantage to *BRCA1*-deficient cells in the breast and ovary. *Brca1*-deficient mouse mammary epithelial cells accumulate reactive oxygen species, however, oestrogen could overcome oxidative-stress induced cell death in these cells by the induction of NRF2-regulated antioxidant enzymes (Gorrini et al., 2013; Gorrini et al., 2014). The potential role of perturbed hormone signalling in the etiology of *BRCA1*-mutated tumours is substantiated by reports that prophylactic bilateral oophorectomy confers a marked reduction in cancer risk in *BRCA1*-mutation carriers (Domchek et al., 2006; Domchek et al., 2010; Eisen et al., 2005; Kauff et al., 2008; Kramer et al., 2005; Rebbeck et al., 1999; Rebbeck et al., 2002).

1.7 Modelling Breast Cancer

The development of models that recapitulate aspects of human breast cancer is essential for understanding the mechanisms that govern transformation and the role of specific genes and pathways in this process. Furthermore they are useful tools for the development of prevention strategies and novel therapeutics. Cancer cell lines propagated *in vitro* provide a renewable source of material and are typically associated with low costs and rapid results. However, cancer cell lines represent overly simplified tumour biology with a loss of context from systemic factors and tumour microenvironment. Another significant limitation is that the

continual passage of cells is accompanied by extensive clonal selection and loss of heterogeneity (Ellis and Fidler, 2010; Gillet et al., 2011); heterogeneity is a critical feature of human breast cancer. The genomes of cancer cell lines are not stable over time, with different isolates displaying variation at both the genomic and transcriptional levels (Nugoli et al., 2003). Moreover, there is an absence of correlation between clinical results and *in vitro* and *in vivo* data obtained from cell lines (Johnson et al., 2001), suggesting a lack of predictive value (Whittle et al., 2015).

Importantly, many of the molecular mechanisms governing neoplastic transformation are highly conserved throughout evolution (Sharpless and Depinho, 2006). In addition, accumulating evidence suggests that normal mouse mammary gland development relies on similar pathways in humans (Lim et al., 2010). This conservation across species supports the validity of using mouse mammary tumour models to mimic human breast cancer. Mouse tumour models are genetically engineered mouse strains that undergo spontaneous tumour development in response to loss or overexpression of a particular gene (Hutchinson and Muller, 2000). Models have been designed to emulate genetic alterations found in human breast cancers, including the overexpression of oncogenes including *ErbB2/Neu*, *Wnt1* and *c-Myc*, and inactivation of tumour suppressors such as *Trp53* and *Brca1*. These tumour models can address the significance of these genetic lesions in the pathogenesis of breast cancer.

1.7.1 *BRCA1/2*-deficient mouse models

The generation of engineered mouse models with mammary gland-specific deletion of *Brca1* has been critically important for addressing the diverse biological functions of BRCA1, both in normal development and tumorigenesis, as well as testing novel therapeutics (reviewed in Evers and Jonkers, 2006). Homozygous mice carrying germline mutations in both *Brca1* alleles die at mid-gestation between embryonic day 7.5 and 13.5, due to severe developmental delay and proliferation defects (Drost and Jonkers, 2009). In contrast to human *BRCA1*-mutation carriers, mice carrying heterozygous mutations do not develop tumours. These two features led to the generation of conditional mouse models in which inactivation of *Brca1* is

achieved by Cre recombinase (cre)-mediated deletion of one or more *Brca1* exons flanked by *loxP* recombination sites. Spatially controlled deletion is achieved using tissue-specific gene promoters for *cre* expression. The first conditional mouse model to directly demonstrate the tumour suppressive function of *Brca1* was reported by Xu and colleagues (Xu et al., 1999). Transgenic mice expressing *cre* from either the whey acidic protein (*Wap*) or mouse mammary tumour virus (*MMTV*) promoter induced mammary-specific deletion of *Brca1* exon 11. Mice developed diverse mammary tumours after a long latency, nonetheless tumours recapitulated several aspects of human *BRCA1*-associated carcinogenesis such as gross genomic instability, a triple-negative phenotype and altered *Trp53* expression. The introduction of one loss-of-function *Trp53* allele significantly reduced tumour latency and resulted in a striking increase in tumour incidence from 25% to 100%, suggesting cooperation of *Brca1* and *Trp53* in oncogenesis (Brodie et al., 2001; Xu et al., 1999).

Additional *Brca1* conditional mouse models have subsequently been generated, utilising alternative tissue-specific promoters and different floxed *Brca1* alleles (Table 1.1) (Liu et al., 2007; McCarthy et al., 2007; Molyneux et al., 2010; Poole et al., 2006; Shakya et al., 2008). Variations in the efficiency and specificity of *cre*-excision, mouse genetic backgrounds and floxed alleles likely account for the different features observed between models. Two models in particular generated a high incidence of tumours displaying hallmarks of human *BRCA1*-mutated basal-like breast tumours (Liu et al., 2007; Molyneux et al., 2010). These tumours were typically high grade, poorly differentiated, genomically unstable and proliferative, and lacked expression of ER and PR. Furthermore, the tumours showed increased expression of basal epithelial markers and unsupervised clustering of gene expression profiles demonstrated marked alignment with human *BRCA1*-deficient tumours and sporadic basal-like tumours. As discussed, deletion of *Brca1* in luminal progenitor cells was demonstrated to closely mimic the pathology of the human disease (Molyneux et al., 2010). Interestingly, breast tumours arising in mice following conditional inactivation of *Brca1* or its interacting protein *Bard1* were indistinguishable. Although these tumours arose after a long latency (17 months), it suggests that the ubiquitin E3 ligase function of BRCA1-BARD1 heterodimers could play a role in tumorigenesis (Shakya et al., 2008).

Table 1.1 Conditional *Brca1*-deficient mouse models

Reference	Mouse model	Back-ground	Latency (mo)	ER/ PR	Basal-like?	Features
Xu et al., 1999	*MMTV-cre/Brca*$^{F11/-}$ *Wap-cre/Brca1* $^{F11/-}$	NIH-BL(S)	>13	?	Some	Histologically diverse, low frequency, genomic instability, *Trp53* mutations
	MMTV-cre/Brca1 $^{F11/-}$ */p53*$^{+/-}$		6 – 8	?	Some	*Trp53* loss accelerated tumour frequency and onset, similar tumour features
Brodie et al., 2001	*MMTV-cre/Brca1*$^{F11/F11}$	NIH-BL(2), C57BL/6, 129/Sv	>12	ER$^-$ PR$^-$	Some	Diverse but mainly high-grade adenocarcinomas. Severe chromosomal abnormalities. Overexpression of ErbB2, c-Myc, cyclin d1.
	MMTV-cre/Brca1$^{F11/F11}$*/p53*$^{+/-}$		8	ER$^-$ PR$^-$	Some	Latency reduced with null *Trp53* loss, similar tumour features
Poole et al., 2006	*Wap-cre/Brca1*$^{F11/F11}$ */p53*$^{F5-6/F5-6}$	C57BL/6, 129/Sv or C57BL/6, BALB/c	7	PR$^+$ ER?	No	Diverse tumour spectrum. Tumours prevented by progesterone antagonist
Liu et al., 2007	*K14-cre/Brca1*$^{F5-13/F5-13}$*/p53*$^{F2-10/F2-10}$	FVB, 129/Ola	7	ER$^-$ PR$^-$	Yes	Poorly differentiated IDCs, genomic instability, basal epithelial markers. Gene profile aligned with human *BRCA1*-mutated tumours.
McCarthy et al., 2007	*Blg-cre/Brca1*$^{F22-24/F22-24}$*/p53*$^{+/-}$	C57bl/6, 129/Sv	7	ER$^-$ PR$^-$	Yes	High grade, metaplastic elements, basal markers and EGFR expression.
Shakya et al., 2008	*Wapcre/Brca1*$^{F2/F2}$	C57bl/6, 129/Sv	17	ER$^-$ PR$^-$	Yes	Invasive adenocarcinomas, basal markers, *Trp53* mutations, indistinguishable from *Bard1*-mutant mice
Molyneaux et al., 2010	*Blg-cre/Brca1*$^{F22-24/F22-24}$*/p53*$^{+/-}$	C57bl/6, 129/Sv	10	ER$^-$ PR$^-$	Yes	IDCs, high grade, genomic instability, basal markers, expression aligns with human sporadic basal-like tumours
	K14-cre/Brca $^{F22-24/F22-24}$*/p53*$^{+/-}$		8	ER$^-$ PR$^-$	No	Basal markers but predominantly adenomyoepitheliomas. Expression aligns with human sporadic basal-like tumours

IDC = invasive ductal carcinoma; F = floxed allele

Similar to *Brca1*, homozygous germline mutations in *Brca2* are embryonic lethal and spontaneous tumour development is not observed in heterozygous mice (reviewed in Evers and Jonkers, 2006). *Cre*-mediated deletion of *Brca2* under control of the *Wap* or *MMTV* promoter resulted in mammary tumour formation after a long latency (approximately 1.5 years) (Cheung et al., 2004; Ludwig et al., 2001). Comparable to human *BRCA2*-mutated cancer, tumours were typically adenocarcinomas, displayed chromosomal aberrations, frequently exhibited mutations in *Trp53* and 50% of tumours were ER^+ positive. The long tumour latency could be circumvented by co-deletion of *Trp53*. In contrast to these models, *K14*-specific deletion of *Brca2* does not promote mammary carcinogenesis unless in the presence of a *Trp53* mutation (Jonkers et al., 2001).

1.7.2 Alternative mouse models of basal-like breast cancer

Activation of the Wnt signalling pathway has been implicated in breast cancer, particularly in basal-like tumours. Both nuclear and cytosolic accumulation of β-catenin, a read-out of Wnt pathway activation, is enriched in basal-like tumours and predictive of a poor outcome (Khramtsov et al., 2010). The proto-oncogene *Wnt-1* was first identified as a frequent site of integration by the MMTV (Nusse and Varmus, 1982). *MMTV-Wnt1* mice develop extensive ductal hyperplasia early in life and mammary adenocarcinomas at approximately 6 - 12 months of age (Li et al., 2000; Tsukamoto et al., 1988). Tumours are typically triple-negative and mimic aspects of basal-like tumours such as keratin 14 and 17 expression (Herschkowitz et al., 2007; Lim et al., 2010; Pfefferle et al., 2013). Notably, activation of Wnt1 appears to target at least two cell types in mammary tissue. *MMTV-Wnt1* preneoplastic mammary glands harbour an expanded mammary stem cell pool as well as an aberrant population of $CD61^+$ progenitor cells that have *in vivo* repopulation capacity and high tumour-forming capacity (Shackleton et al., 2006; Vaillant et al., 2008). These aberrant bipotent progenitors also express high levels of the basal marker K14, suggesting Wnt1 activation may provoke de-differentiation to a more stem-like state (Visvader, 2009), consistent with its role in cell fate determination and self-renewal during normal development (Clevers and Nusse, 2012).

Mice on a BALB/c genetic background that carry a single copy of the *Trp53* gene (*p53*$^{+/-}$) also display a predilection for the development of mammary tumours that mimic aspects of human basal-like tumours (Herschkowitz et al., 2007; Kuperwasser et al., 2000). Mammary tumours have a latency of 8 – 14 months, typically display chromosomal abnormalities and express markers of basal/myoepithelial cells. Although tumours are predominantly triple-negative, a low frequency of ER^{+} tumours has also been reported (Dabydeen and Furth, 2014). Similar to *MMTV-Wnt1* mice, preneoplastic mammary tissue from p53$^{+/-}$ mice showed an enrichment of CD61^{+} progenitor cells that have high tumorigenic capacity (Vaillant et al., 2008).

1.7.3 Modelling luminal breast tumours

In human breast cancers, high expression of both ER and ER-regulated genes including PR are a defining feature of luminal tumours (Perou et al., 2000; Sorlie et al., 2001). In contrast, ER expression is low to absent in most mouse tumour models (Herschkowitz et al., 2007; Pfefferle et al., 2013) as is the expression of most ER-responsive genes, signifying an important caveat to the use of mouse models to recapitulate luminal breast cancers. Despite this, molecular signature analysis demonstrated that the *MMTV-Neu*, *MMTV-PyMT*, and *WAP-Myc* mouse tumour models clustered together and all showed a potential luminal tumour phenotype (Herschkowitz et al., 2007; Lim et al., 2010). This suggests human luminal tumours have many ER-independent features. A distinguishing feature of these mouse mammary tumours was high expression of *Xbp1* and *Gata3*, both human luminal tumour-defining genes (Sotiriou et al., 2003), as well as high expression of the luminal markers K8 and K18. More recently, gene expression analysis demonstrated that *MMTV-PyMT* tumours were somewhat similar to the luminal B subtype, while *MMTV-Neu* mouse tumours were specifically correlated with luminal A tumours (Pfefferle et al., 2013). Given that the *MMTV-Neu* mouse model overexpresses the *neu/erbB2* oncogene that is analogous to the *HER2* oncogene in human breast tumours, the correlation with luminal A tumours and not HER2^{+} tumours suggests that the *MMTV-Neu* model does not accurately mimic human HER2-overexpressing cancers. Furthermore, *MMTV-Neu* tumours display sensitivity to CDK4/6 inhibition (Roberts et al., 2012), consistent with findings from

human clinical trials utilising CDK4/6 inhibitors to treat luminal/ER$^+$ breast cancer (Finn et al., 2016).

1.7.4 Patient derived xenograft models

Patient-derived xenograft (PDX) models are valuable preclinical tools for testing new therapeutics and exploring the biological basis of drug sensitivity and resistance. They are based on the direct engraftment of fresh patient tumour fragments into immunocompromised mice. Oestrogen supplementation as well as the addition of mesenchymal stem cells and/or Matrigel to alter the tumour microenvironment has improved the success rate of engraftment (Whittle et al., 2015). PDX models maintain many features of the original patient tumour such as the cell differentiation and morphology, copy number variations, architecture, and molecular signature (reviewed in Hidalgo et al., 2014; Whittle et al., 2015). This conservation of tumour characteristics likely underlies the predictive value of PDX models, with reports indicating concordant drug responses of xenografts with that of patient tumours in some cases (Marangoni et al., 2007; Zhang et al., 2013). Thus, PDX models show promise of enabling a more personalised approach to cancer treatment.

PDX models have been essential for the preclinical testing of new classes of treatment for breast cancer. Basal-like breast cancer xenografts have established the biological rational for clinical trials investigating inhibitors of the PI3K/mTOR pathway (Lehmann et al., 2014; Xu et al., 2013), checkpoint kinase 1 (Ma et al., 2013), Aurora Kinase (Romanelli et al., 2012), and blockade of Wnt signalling (Gurney et al., 2012). Luminal breast cancer xenografts, unlike most mouse tumour models, express ER and are dependent on oestrogen for growth. A recent study utilising ER$^+$ PDX models demonstrated that targeting the pro-survival molecule BCL-2 using the BH3-mimetic ABT-199 profoundly improved the responsiveness of tumours to tamoxifen therapy, with one model showing complete remission following ABT-199/tamoxifen treatment (Vaillant et al., 2013). This study provided the rationale for an ongoing phase II clinical trial (ACTRN12615000702516). Studies utilising HER2$^+$ PDX tumour models have demonstrated encouraging

findings from combining anti-HER2 therapies with additional targeted therapies such as PI3K/Akt/mTOR pathway inhibitors (García-García et al., 2012).

As with any model of human disease, there are caveats to the use of PDX models for breast cancer (reviewed in Aparicio et al., 2015; Whittle et al., 2015). The requirement for immunocompromised mice results in the loss of interactions between the tumour and immune cells within the tumour microenvironment, and prevents the testing of immunotherapeutics. Currently the generation of PDX cohorts is biased towards more aggressive tumours and thus luminal A breast tumours are largely under-represented (DeRose et al., 2011; Eirew et al., 2015; Kabos et al., 2012; Zhang et al., 2013). While PDX models frequently undergo spontaneous metastasis, it remains unclear whether these sites faithfully recapitulate the metastasis observed in patients. Indeed, PDX tumour cells in mice appear to have predilection for lung metastasis (Zhang et al., 2013). Furthermore, the direct transplantation of tumour cells precludes analysis of the mechanisms underlying neoplastic transformation as well as the testing of cancer prevention strategies. Despite this, PDX models currently provide one of the best model systems to advance cancer drug discovery efforts.

1.8 Aims and Objectives of Thesis

The overall goal of this work was to gain insights into the molecular and cellular mechanisms governing oncogenesis and tumour progression in *BRCA1*-mutation carriers. The work presented in this thesis is divided into two specific research aims: firstly, to identify a targetable pathway in preneoplastic *BRCA1*-mutant breast epithelium that could be exploited as a cancer prevention strategy (Chapters 3 and 4), and secondly, to identify novel molecular targets for the treatment of established *BRCA1*-mutant tumours (Chapter 5).

To address the first aim, we have focussed on the role of the RANKL signalling pathway in *BRCA1*-associated oncogenesis. This was based upon the prior link between deregulated progesterone signalling and breast cancer risk in *BRCA1*-mutation carriers (King et al., 2004; Ma et al., 2006; Poole et al., 2006; Widschwendter et al., 2013), and the role of RANKL as a key paracrine effector of progesterone action (Asselin-Labat et al., 2010; Beleut et al., 2010; Joshi et al., 2010; Tanos et al., 2013). Chapter 3 of this thesis reports the identification and characterisation of a novel RANKL-responsive $RANK^+$ cell population within the $BRCA1^{mut/+}$ breast epithelium, utilising preneoplastic breast tissue from *BRCA1*-mutation carriers who underwent a prophylactic mastectomy. The value of targeting this population for breast cancer prevention via RANKL blockade was described in Chapter 4, utilising human $BRCA1^{mut/+}$ breast tissue and a *Brca1*-deficient mouse model.

For the second research aim, presented in Chapter 5, both RANKL and immune checkpoints were examined as potential molecular targets for the treatment of *BRCA1*-mutated breast tumours, either alone or as an adjunct to chemotherapy. Drug studies were performed *in vivo* using *BRCA1*-mutated PDX models and *Brca1*-deficient mice, and the mechanisms underlying the tumour response were investigated. Together, the work described in this thesis has significant implications for the prevention and treatment of breast cancer in *BRCA1*-mutation carriers and possibly other women at high risk.

Chapter 2: Materials and Methods

2.1 Human Tissue Samples

2.1.1 Human breast specimens

Human breast tissue was obtained through the Royal Melbourne Hospital Tissue Bank, Kathleen Cuningham Foundation Consortium for Research into Familial Breast Cancer (kConFab) and the Victorian Cancer Biobank. Fresh samples were either normal breast tissue (confirmed by pathology) from reduction mammoplasties and prophylactic mastectomies of known *BRCA1* or *BRCA2* mutation carriers, or breast tumour samples from *BRCA1*-mutation carriers or non-carriers undergoing surgical resection. Informed consent was obtained from all subjects and approval was granted by the Human Research Ethics Committees of The Walter and Eliza Hall Institute of Medical Research (WEHI). All normal breast specimens (reduction mammoplasties or prophylactic mastectomies) were from premenopausal women who were unaffected by cancer and who were not taking tamoxifen.

2.1.2 Human tissue dissociation

Normal human breast tissue dissociation was performed as previously described (Lim et al., 2009). Samples were minced with razor blades and digested at 37 °C for 8 - 9 h with 150 U/mL collagenase (Sigma), 50 U/mL hyaluronidase (Sigma) and 100 U/mL DNase (Worthington) in DMEM with nutrient mixture F-12 Ham (DME-HAM, Gibco) supplemented with 5 % fetal calf serum (FCS), 2 mM glutamine, 500 ng/mL hydrocortisone, 5 µg/mL insulin, 20 ng/mL cholera toxin and 10 ng/mL epidermal growth factor (EGF). Digestion was performed at 140 RPM in a shaking orbital incubator (Ratek Laboratory Equipment). The resulting organoid suspension was digested with 0.25 % trypsin and 1 mM EGTA for 2 min at 37 °C and red blood cells were removed by lysis (IOTest 3 Lysing Solution, Beckman Coulter). A single-cell suspension was generated by filtration through a 100 µM cell strainer (BD-Falcon). Antibody labelling and flow cytometry was performed on cell suspensions to fractionate epithelial populations.

2.1.3 Breast tumour preparation

Human breast tumours (either primary or tumour xenografts passaged in mice) were minced and digested at 37 °C for 1 h with 300 U/mL collagenase, 100 U/mL hyaluronidase and 100 U/mL DNase in supplemented DME-HAM medium as detailed above. The resulting single-cell suspensions were used for antibody labelling and flow cytometry and/or transplanted into immunocompromised mice. Frozen stocks were prepared (50 % FCS, 6 % Dimethyl sulfoxide, 44 % supplemented DME-HAM) for subsequent *in vivo* experiments.

2.1.4 Breast organoid preparation

Breast organoids were isolated from human breast tissue (reduction mammoplasties or prophylactic mastectomies) using a protocol based on Tanos et al., 2013. Tissue was minced and digested at 37 °C for 9 h at 140 RPM in a shaking orbital incubator (Ratek Laboratory Equipment) with 150 U/mL collagenase, 50 U/mL hyaluronidase and 100 U/mL DNase in phenol-free serum-free DME-HAM supplemented with 2 mM glutamine. The following day, the resulting organoids were harvested by centrifugation (250 x g, 4 min, 4 °C) and plated in ultra-low attachment 24 well plates (Corning) in phenol-free DME-HAM + 2 mM glutamine in a 5 % CO_2, 5 % O_2, 37 °C incubator. Six hours after plating, organoids were treated with ethanol (vehicle control), progesterone (20 nM, Sigma) or both progesterone and denosumab (10 μg/mL, Amgen) for 24 h. At experimental endpoint, organoids were washed with phosphate-buffered saline (PBS) and fixed in 4 % paraformaldehyde for 1 h before being sequentially embedded in agarose (2 % low melting point agarose (w/v), PBS) and paraffin.

2.1.5 BRCA-D pilot clinical study

The BRCA-D pilot, registered on the Australian New Zealand Clinical Trials Registry (ACTRN12614000694617), is an ongoing investigator-initiated study approved by the Human Research Ethics Committees of WEHI and Melbourne Health (Royal Melbourne Hospital) and sponsored by Melbourne Health. It is a pre-operative window study designed to evaluate the biological effects of the RANKL inhibitor denosumab on normal breast tissue from *BRCA1* and *BRCA2*-mutation carriers and non-carriers with a strong family history. The primary endpoint of the study is a change in cell proliferation, determined by immunostaining for Ki67.

Results from the first three *BRCA1*-mutation carriers participating in the study are reported in this thesis. Subjects underwent pre-treatment breast tissue biopsies followed by three months of denosumab therapy (120 mg, subcutaneous injection on Day 1, 15, 28, 56). A post-treatment biopsy was carried out approximately one month after the last dose. Both pre- and post-treatment biopsies were performed during the luteal phase of the menstrual cycle, confirmed by analysis of serum LH, FSH, oestradiol and progesterone. All patients participating in the study provided informed consent.

2.2 Experimental Animals

2.2.1 Mouse strains

All mouse strains were maintained in the WEHI animal facility according to institutional guidelines. All experiments were performed with Animal Ethics Approval and conformed to regulatory standards set by the WEHI Animal Ethics Committee. *MMTV-cre* mice (*Cre-A* strain) were provided by K. U. Wagner (Wagner et al., 1997); *Brca1*$^{fl/fl}$ mice were from the US National Cancer Institute (Xu et al., 1999); *BALB/c-p53*$^{+/-}$ mice were from the Jackson Laboratory (Jacks et al., 1994); *MMTV-Wnt1* mice were provided by the Jackson Laboratory (Tsukamoto et al., 1988); *MMTV-PyMT* mice were from the US National Cancer Institute (Guy et al., 1992a) and *MMTV-Neu* mice were from the Jackson Laboratory (Guy et al., 1992b). FVB/N and BALB/c wild-type mice and immunocompromised *RAG1*$^{-/-}$ (Mombaerts et al., 1992) and *NOD-SCID-IL2*γ*R*$^{-/-}$ (Shultz et al., 2005) mice were obtained from the Kew breeding facility of WEHI.

2.2.2 Mouse genotyping

Mouse tail biopsies were digested at 55 °C overnight in DirectPCR Tail lysis buffer (Viagen) containing 1 mg/mL Proteinase K to extract genomic DNA, followed by 1 h at 85 °C. Polymerase chain reactions (PCR) were performed with 1 μL DNA and 19 μL GoTaq Green (Promega) containing the appropriate primers (Table 2.1). PCR products were separated by gel electrophoresis performed in TAE buffer (40 mM Tris.Acetate pH 8.2, 1 mM EDTA) using agarose gels (1.5 % agarose (w/v), TAE buffer, 60 ng/mL SYBR Safe (Invitrogen)) and visualised by ultraviolet light.

2.2.3 Bromodeoxyuridine labelling

Mice were given an intraperitoneal injection of Bromodeoxyuridine (BrdU) Cell Labelling Reagent (0.5 mg/10 g body weight, Amersham Biosciences) 1.5 h prior to tissue collection. Mammary tumours were fixed in 4 % paraformaldehyde and BrdU incorporation was determined by immunohistochemistry.

2.2.4 Mammary gland preparation

Single cell suspensions from mouse mammary glands were prepared as previously described (Shackleton et al., 2006). Freshly harvested mammary tissue was mechanically dissociated with a McIlwain tissue chopper (Mickle Laboratory Engineering), and then digested at 37 °C in a shaking orbital incubator (Ratek Laboratory Equipment) at 160 RPM for 1 h in 300 U/mL collagenase, 100 U/mL hyaluronidase and 100 U/mL DNase in DME-HAM medium supplemented with 5 % FCS, 2 mM glutamine, 250 ng/mL hydrocortisone, 5 µg/mL insulin, 20 ng/mL cholera toxin and 10 ng/mL EGF. The resulting suspension was then sequentially digested with 0.25 % trypsin/EGTA for 3 min and 5 mg/mL dispase (Roche Diagnostics) for 5 min. Red blood cells were removed by lysis with 0.64% NH_4Cl and a single-cell suspension was generated following filtration through a 40 µM cell strainer (BD-Falcon). Cells were then labelled with antibodies and flow cytometry was performed.

2.2.5 Mammary tumour dissociation

Mice bearing mammary tumours up to 600 mm^3 were euthanised and the tumour was excised. Tumours were minced with a razor blade and digested at 37 °C for 1 h as described above for mammary gland preparation. The resulting tumour suspension was digested with 0.25 % trypsin/EGTA for 3 min and filtered through a 100 µM cell strainer (BD-Falcon) to generate a single-cell suspension. Cells were used for antibody labelling and flow cytometry and/or mammary gland transplantation.

2.2.6 Mammary fat pad transplantation

Freshly prepared single-cell suspensions or freshly sorted cells were counted and resuspended in 25 % growth-factor-reduced Matrigel (BD Pharmingen) and 75 % transplantation buffer (50 % FCS, 40 % PBS and 10 % Trypan blue). Mammary

gland transplantation was performed on virgin female mice aged three to four weeks, as previously described (DeOme et al., 1959; Shackleton et al., 2006). Depending on the subsequent *in vivo* experiment, the following mouse strains were used: *RAG1*$^{-/-}$, *NOD-SCID-IL2*γ*R*$^{-/-}$ or syngeneic (F1 FVB x BALB/c) mice. Mice were anaesthetised with 20 μL/g ketamine intraperitoneal anesthesia and the fourth (inguinal) mammary gland was exposed via an abdominal incision. The mammary fat pad from nipple to inguinal lymph node was removed, and in doing so the endogenous epithelium was removed. Cells (10 μL) were then injected into the remaining fat pad. Epithelial reconstitution was confirmed 6 weeks post-surgery by wholemount analysis.

2.3.7 *Ex-vivo* colony formation assay

8-week old female FVB/N mice were given a single subcutaneous injection of an anti-mouse RANKL neutralising monoclonal antibody (Clone OYC1, 5 mg/kg, Oriental Yeast Company) or an isotype-matched control antibody (Rat IgG2a, 5 mg/kg, WEHI Monoclonal Antibody Facility). Mammary glands were harvested after 7 days and a single-cell suspension was generated, as detailed above. Colony assays were performed on fractionated cell populations following flow cytometry.

2.2.8 *In vivo* tumour prevention studies

Freshly sorted epithelial cells from the mammary glands of three *MMTV-cre/Brca1*$^{fl/fl}$*/p53*$^{+/-}$ mice (10 – 12 weeks old) were transplanted into the fat pads of 36 recipient mice (50,000 cells per recipient mouse). Six weeks following surgery, two mice were sacrificed and the presence of ductal outgrowths confirmed by wholemount analysis. The remaining mice were randomised to receive subcutaneous injections of either the RANKL inhibitor OPG-Fc (3 mg/kg, Amgen) or an isotype-matched control antibody (mouse IgG1, 3 mg/kg, Amgen). Thereafter, mice were injected three times per week and monitored for the development of mammary tumours three times per week. Where required, a third treatment arm was included whereby mice received an oophorectomy six-weeks following transplantation, and the vehicle control group received a sham operation in addition to mouse IgG1.

For prevention studies that did not require transplantation, female *MMTV-cre/Brca1*$^{fl/fl}$*/p53*$^{+/-}$ were randomly allocated to receive subcutaneous injections at 9 weeks of age with either an anti-mouse RANKL neutralising antibody (5 mg/kg) or an isotype-matched control antibody (Rat IgG2a, 5 mg/kg). Treatment was repeated every three weeks, and mice were palpated three times weekly to monitor tumour formation. Alternatively, 9-week old *MMTV-Wnt1* mice were randomly allocated to receive subcutaneous injections of OPG-Fc (3 mg/kg) or mouse IgG1 (3 mg/kg) three times per week. All prevention experiments were blinded and the group allocation was unknown when assessing for tumour development. In all experiments, mice were euthanised once tumours reached the ethical size limit of 600 mm^3.

2.2.9 *In vivo* treatment studies

Single-cell suspensions from freshly harvested *MMTV-cre/Brca1*$^{fl/fl}$*/p53*$^{+/-}$ tumours were transplanted into the mammary fat pads of 4-week old syngeneic (F1 FVB/N x BALB/c) recipient mice (40,000 cells per recipient). At 3 weeks post-transplantation, when tumours had reached a size of approximately 100 mm^3, mice were randomly assigned treatment groups and injected with combinations of the following drugs: Cisplatin (4 mg/kg, intravenous), Anti-PD1 (200 μg/mouse, intraperitoneal), Anti-CTLA4 (150 μg/mouse, intraperitoneal) or a vehicle control (PBS, intravenous or intraperitoneal). Cisplatin was injected on day 1, followed by anti-PD1/anti-CTLA4 injections on days 2, 5 and 8. This treatment regime was repeated every 21 days, for a total of four treatments. Tumours were measured 3 times per week, and mice were euthanised once the ethical end point (tumour volume of 600 mm^3) was reached. For short-term *in vivo* studies, tumours were harvested either the day before treatment initiation (day 0) or at day 14.

For patient-derived xenograft tumours, frozen stocks of early passage tumour cell suspensions were thawed, washed and resuspended in DME-HAM media supplemented with 10% FCS for 1 h at 4 °C. Cells were then transplanted into the mammary fat pad of *NOD-SCID-IL2γR*$^{-/-}$ mice (200,000 cells per mouse). Once tumours had reached a size of approximately 100 mm^3, mice were randomised to receive either OPG-Fc (3 mg/kg, subcutaneous), mouse IgG1 (3 mg/kg, subcutaneous), docetaxel (10 mg/kg, intraperitoneal) or a combination of docetaxel

and OPG-Fc. OPG-Fc and mouse IgG1 were injected three times per week, and docetaxel was injected every 21 days. Tumours were measured three times per week and mice were euthanised once the tumour volume reached 600 mm^3. For all treatment studies, tumour volume was determined by the following formula: $(\text{smallest diameter})^2(\text{largest diameter})/2$ (Marangoni et al., 2007). All studies were blinded and the group allocation was unknown when determining tumour volume.

2.3 Flow Cytometry

2.3.1 Cell antibody labelling

The primary and secondary antibodies used for cell labelling are detailed in Table 2.2. To label human breast epithelial cells, cells were blocked in PBS containing 5 % normal goat serum (Merck) and 10 % DNase for 10 min at 4 °C, then incubated with mouse anti-human RANK for 30 min at 4 °C. Cells were then washed with PBS containing 2 % FCS and incubated with APC-conjugated anti-mouse IgG for 30 min at 4 °C. Cells were washed twice and blocked with mouse and rat immunoglobulin (Jackson Immunolabs), and anti-CD16/CD32 Fcγ III/II receptors (anti-Fcγ, WEHI Monoclonal Antibody Facility) for 10 min, followed by incubation with the following human-specific primary antibodies for 25 min at 4 °C: anti-CD31, anti-CD45, anti-CD235α, anti-EpCAM and anti-CD49f. Cells were washed, incubated with secondary antibody and resuspended in 0.5 μg/mL propidium iodide for live cell discrimination. The same protocol was applied for antibody labelling of patient-derived xenograft tumour cells, however, mouse-specific antibodies were utilised for CD31 and CD45, so that mouse endothelial cells and immune cells could be excluded.

To label mouse mammary epithelial cells or mouse mammary tumours, cell suspensions were blocked in rat immunoglobulin, 10 % DNase and anti-Fcγ for 10 min at 4 °C. Cells were then incubated with the following mouse-specific primary antibodies for 25 min at 4 °C: anti-CD31, anti-CD45, anti-Ter119, anti-CD24 and anti-CD29. Where required, anti-PD-L1 (CD274), anti-Sca-1 and anti-CD49b were also included in the primary antibody mix. Cells were then washed and incubated

with secondary antibody for 15 min at 4 °C, and resuspended in 0.5 μg/mL propidium iodide.

2.3.2 Analysis of ALDH activity (Aldefluor assay)

Single-cell suspensions from fresh human breast tissue specimens (reduction mammoplasties or prophylactic mastectomies) were incubated for 50 min at 37 °C with BODIPY^{TM}-aminoacetaldehyde (BAAA) using the ALDEFLUOR kit (STEMCELL Technologies). To control for background fluorescence, an aliquot of cells was incubated with 15 μM diethylaminobenzaldehyde (DEAB) under the same conditions. Cells were then washed with PBS/2 % FCS, and incubated with primary antibodies, as described above.

2.3.3 Cell sorting and analysis

Cell sorting was performed on a FACSAria flow cytometer (Becton Dickinson) and cell analysis was performed on a LSRFortessa^{TM} X-20 (Becton Dickinson). Data was later analysed using FlowJo software (Tree Star). The lineage-negative population was defined as $CD31^{-}CD45^{-}CD235\alpha^{-}$ for human cells and $CD31^{-}CD45^{-}Ter119^{-}$ for mouse cells.

2.4 In vitro assays

2.4.1 2D colony assay

Freshly sorted cells were counted and seeded in 24-well plates at a density of 100 cells/well along with irradiated NIH3T3 feeder cells (25,000 cells per well) in DME-HAM supplemented with 5 % FCS, 250 ng/mL hydrocortisone, 5 μg/mL insulin, 2 mM glutamine, 10 ng/mL EGF and 20 ng/mL cholera toxin. Cultures were maintained in a 5 % CO_2, 5 % O_2, 37 °C incubator. The following day, the media was replaced with supplemented DME-HAM containing 1 % FCS. Media was changed after 3 days, and then after 7 days the cells were fixed in an ice-cold 1:1 Acetone:Methanol solution for 1 min. Colonies were then stained with Giemsa (Merck) for 1 min, before being rinsed with water and imaged using a Zeiss upright microscope with Zen software (Zeiss).

2.4.2 3D colony assay

Freshly sorted cell subsets were counted and pelleted by centrifugation at 1200 RPM for 5 min at 4 °C. Cells were then resuspended in ice-cold Matrigel (BD Biosciences) at a density of 50,000 cells/mL, and 20 μL droplets dispensed into Permanox 4-well chamber slides (LabTex) and allowed to set at 37 °C. Wells were filled with 0.8 mL DME-HAM, supplemented with B27, 500 ng/mL hydrocortisone, 2 mM glutamine, 5 μg/mL insulin, 10 ng/mL EGF and 20 ng/mL cholera toxin. Cells were cultured in 5 % CO_2, 5 % O_2 in a 37 °C incubator, with the media changed every 3 days. After 14 days, Matrigel drops were imaged on a Nikon TiE microscope using Metamorph Inc. software, and colonies were quantified using ImageJ (NIH).

2.4.3 Lentiviral production

Second-generation lentivirus production was performed using HEK293T cells. Cells were cultured in DMEM media (Gibco) supplemented with 10 % FCS and penicillin/streptomycin at 37 °C in a 5 % CO_2 incubator. For virus production, cells were seeded in 10 cm tissue culture treated dishes at a density of 3 x 10^6 cells per dish. The following day, a calcium-phosphate transfection was performed, whereby 2 x HEPES-Buffered Saline (1.64 % NaCl, 0.075 % KCl, 0.054 % $Na_2HPO_4.12H_2O$, 0.22 % Glucose, 1.2 % HEPES) was bubbled through a solution containing 10 μg plasmid of interest, 0.25 M $CaCl_2$, 7.5 μg packaging plasmid (pSPAX2) and 3 μg envelope plasmid (pMD2.6-VSVG). Once a precipitate was visible (25 – 30 min), the solution was added dropwise to HEK293T cells. The media was changed after 12 h, and lentivirus was collected at 48 h and 60 h. Virus was filtered through a 0.45 μm membrane (Sartorius Stedim Biotech) and concentrated by ultracentrifugation (Optima L-90K Ultracentrifuge, Beckman Coulter) at 25,000 RPM using a SW28 rotor (Beckman Coulter). Virus was stored in aliquots at -80 °C.

2.4.4 Reporter assays

Freshly sorted cells were seeded in 24-well ultralow adherence plates (Corning) at a density of 10,000 cells/mL in DME-HAM medium supplemented with B27, 5 μg/mL insulin, 10 ng/mL EGF, 5 ng/mL bFGF, 4 μg/mL heparin, 500 ng/mL hydrocortisone and 2 mM glutamine. Plates were incubated for 6 h in a 5 % CO_2,

5% O_2, 37 °C incubator. Cells were then transduced with a lentiviral NF-κB reporter plasmid (multiplicity of infection value of 5) using Polybrene® transfection reagent (Sigma), followed by centrifugation at 2500 RPM at 32 °C for 2 h. Plates were returned to a 5 % CO_2, 5 % O_2, 37 °C incubator for 48 h, with fresh media added after 12 h. At experimental endpoint, cells were harvested, washed and the percentage of GFP^+ cells was determined by flow cytometry.

2.4.5 Comet assays

Freshly sorted cells were seeded in 24-well ultralow adherence plates at a density of 20,000 cells/mL in DME-HAM medium supplemented with B27, 5 μg/mL insulin, 10 ng/mL EGF, 5 ng/mL bFGF, 4 μg/mL heparin, 500 ng/mL hydrocortisone and 2 mM glutamine. Plates were incubated overnight in a 5 % CO_2, 5 % O_2, 37 °C incubator. The following morning, cells were treated with hydroxyurea (10 mM, Sigma), irradiated at 3 Gray (Gy) or left untreated. After 4 h, cells were harvested, washed with PBS and alkaline comet assays were performed in duplicate using the CometAssay® kit (Trevigen), according to the manufacturer's instructions. As a positive control for DNA damage, cells were treated with 100 μM hydrogen peroxide for 20 min at 4 °C. Slides were imaged using a Nikon Upright 90i microscope and olive tail moment was quantified using Metamorph software.

2.5 Histological Analysis

2.5.1 Wholemount analysis

Mammary glands were placed onto superfrost plus coated slides (Menzel Glaser) and fixed overnight in Carnoy's solution (60 % ethanol, 30 % chloroform, 10 % acetic acid). Slides were then washed in 70 % ethanol and stained overnight in Carmine alum (0.2 % carmine, 0.5 % potassium aluminum sulphate). Glands were sequentially dehydrated in ethanol and cleared in xylene prior to coverslipping and imaging on a Zeiss upright microscope using Zen software (Zeiss).

2.5.2 Immunohistochemistry

Tissues were fixed in 4 % paraformaldehyde at 4 °C for 24 h and embedded in paraffin. 5 μm sections were cut onto superfrost plus coated slides, which were then de-waxed in xylene and re-hydrated. Antigen-retrieval was performed using Diva Decloaker antigen retrieval buffer (Biocare Medical), citrate buffer (1.8 mM citric acid, 8.2 mM sodium citrate, pH 6.0) or DAKO pH 9.0 antigen retrieval buffer (DAKO), with a pressure cooker (DAKO, 125 °C for 30 sec). Slides were then washed and endogenous peroxidase activity was quenched with 3 % hydrogen peroxide in distilled water for 5 min. Sections were washed in PBS containing 0.05 % Tween20 (Sigma) and blocked for 1 h at room temperature (RT) with 5 % goat or horse serum (Merck) in a humidifier box. Sections were incubated with primary antibodies (Table 2.3) diluted in blocking solution for 1 h at RT or overnight at 4 °C. Cells were then washed and incubated with secondary antibody (Table 2.3) for 30 min at RT, followed by a 30 min incubation at RT with ABC reagent (Vector Laboratories). 3,3'-diaminobenzidine was used as the substrate for streptavidin-biotin peroxidase detection (DAKO). Counterstaining (30 sec haematoxylin, 30 sec schotts tap water) was then performed, followed by coverslipping and imaging on a Nikon Eclipse 50i microscope using Zen software (Zeiss). Alternatively, slides were de-waxed and stained for haematoxylin and eosin (H & E) for visualisation of mammary gland morphology. When staining quantification was required, slides were imaged with an Aperio Digital Pathology Slide Scanner (Leica) and quantification was performed using ImageJ software (NIH).

2.5.3 Cytospins

Freshly sorted cell subsets were counted and pelleted by centrifugation at 1200 RPM for 5 min at 4 °C. Cells were then resuspended in PBS at a density of 100,000 cells/mL and spun onto superfrost plus slides (Menzel Glaser) using a Thermo Cytospin machine (Thermo Fisher Scientific) at 700 RPM for 3 min. Slides were air-dried for 5 min, then fixed in 4 % paraformaldehyde for 5 min, washed twice in PBS and stored in 70 % ethanol prior to immunohistochemistry.

2.5.4 kConFab tissue microarrays and Amgen tissue bank samples

Breast tumour tissue microarrays (TMAs) were generated from tumours arising in high-risk women with a strong family history (kConFab cohort, Mann et al., 2006),

with relevant IRB approval. kConFab cases had undergone germline sequencing and MLPA of the *BRCA1* and *BRCA2* genes. TMAs comprised 628 breast tumours and 466 normal breast tissue samples (tumour-adjacent), from 676 breast cancer patients. The Amgen Tissue Bank (ATB) contained tissue sections from anonymised breast tumour samples obtained from the MT Group, Van Nuys, CA. Samples were genotyped for *BRCA1* and *BRCA2* mutations. Information on menstrual cycle status or oral contraceptive use was unknown.

2.6 General Molecular Biology

2.6.1 Bacterial transformation

Plasmid DNA was introduced into Stb13™ chemically-competent bacteria by adding 1 μg DNA to 100 μL bacteria and incubating on ice for 30 min. Tubes were then heat-shocked at 42 °C for 1 min and then incubated on ice for 5 min. 700 μL Super Optimal with Catabolite repression (SOC) broth (2 % tryptone (w/v), 0.5 % yeast extract (w/v), 10 mM NaCl, 2.5 mM KCl, 10 mM $MgCl_2$, 10 mM MgSO4 and 20 mM glucose) was added to each tube and cells were allowed to recover at 37 °C for 1 h in an orbital shaker at 225 RPM (Ratek Laboratory Equipment). Cells were then plated onto pre-warmed agarose plates (1 % tryptone (w/v), 2 % yeast extract (w/v), 0.5 % NaCl (w/v), 0.2 % glucose (w/v), 1.5 % (w/v) difco agar 10 mM Tris pH 7.4, 1 mM $MgCl_2$) containing Ampicillin (0.2 mg/mL, Ampicillin Sodium Salt, Sigma) and incubated overnight at 37 °C.

2.6.2 Plasmid preparations

Single colonies of transformed bacteria were picked and starter cultures were grown in 2 mL Lennox Luria broth (LLB) (2 % tryptone (w/v), 1 % yeast extract (w/v), 0.5 % NaCl pH 7.1 (w/v)) at 37 °C for 6 h at 225 RPM before being transferred to 200 mL of LLB broth and cultured overnight at 37 °C at 225 RPM. The following morning, a large-scale DNA extraction (maxi-prep) was performed using the PureLink® HiPure Plasmid Maxiprep Kit (Invitrogen), according to manufacturer's instructions.

2.6.3 Western blot analysis

Freshly sorted cells that had been snap-frozen and stored at –80 °C were lysed in ice-cold RIPA buffer (10 mM Tris HCL, 150 mM NaCl, 1 % Triton X-100 (w/v), 0.1 % SDS (w/v), 1 % Sodium Deoxycholate (w/v) and 0.01 % Sodium Azide (w/v)) containing protease inhibitors (Protease Inhibitor Cocktail, Roche) and phosphatase inhibitors (PhosSTOP™, Roche). After the addition of RIPA buffer, cells were incubated on ice for 15 min and vortexed every 5 min, then briefly homogenised by sonication. Samples were then centrifuged (15,000 x g, 10 min at 4 °C) and protein was quantified using BCA analysis (Thermo Fisher) on a Chameleon Plate Reader (HIDEX). Mammary tumours that had been snap-frozen were crushed in liquid nitrogen using a mortar and pestle and lysed with ice-cold RIPA buffer, as above. Aliquots of each sample (15 μg protein) were then mixed with Sample Reducing Agent (Invitrogen) and LDS Sample Buffer (Invitrogen), and heated at 70 °C for 10 min. Proteins were then separated by SDS-PAGE using a 4 – 12 % gradient gel (Life Technologies) in MES Buffer (Life Technologies), and transferred to polyvinylidene difluoride membranes (Millipore) by wet-transfer (Bio-Rad Criterion Blotter) in transfer buffer (20 % (w/v) Methanol, 2.42 g/L Tris Base, 11.26 g/L Glycine). Membranes were blocked with milk (5 % skim milk powder (w/v) in PBS with 0.1 % Tween20 (PBS-T)) before being probed overnight with primary antibodies at 4 °C (provided in Table 2.4). The following day, membranes were washed with PBS-T and probed with HRP-conjugated secondary antibodies (Table 2.4) for 1 h at RT. For detection, membranes were incubated with ECL or ECL Prime (GE Healthcare Life Sciences) for 1 min, then exposed to X-ray film (GE Healthcare) and developed (Kodak X-OMAT 3000 RA Processor).

2.6.4 RNA extraction and quantitative reverse-transcription PCR

RNA was isolated from sorted cells using the RNeasy Mini kit (Qiagen) together with an on-column DNase treatment (Qiagen), according to the manufacturer's instructions. cDNA was synthesised with the First Strand Synthesis Kit (Invitrogen), using an oligo(dT) primer. Quantitative reverse-transcription (RT)-PCR was performed in duplicate with the Rotorgene RG-6000 (Corbett Research) using SYBR Green PCR Master Mix (Life Technologies) together with sequence specific primers (Table 2.5). Standard curves were generated using known quantities of

PCR products, and used to determine the expression in experimental samples. Expression analysis was performed using Rotorgene software.

2.6.5 RNA-seq

Total RNA was extracted from sorted cells as described above. Libraries for whole transcriptome analysis were generated using 100 ng total RNA, following the Illumina's TruSeq RNA v2 sample preparation protocol. Libraries were sequenced on an Illumina HiSeq 2000 at the Australian Genome Research Facility (AGRF), Melbourne. Between 15.8 and 23.1 million 100 bp read pairs were obtained for each sample. Reads were aligned to the hg19 genome using Rsubread 1.16.1 (Liao et al., 2013). The number of fragments overlapping each Entrez gene was counted using featureCounts (Liao et al., 2014) and NCBI RefSeq annotation (build 37.2). Genes were filtered as unexpressed if they failed to achieve a count per million of 0.5 in at least three samples. Genes with no official gene symbol in the NCBI gene information file were also removed. Compositional differences between libraries were normalised using the trimmed mean of M-values (TMM) method (Robinson et al., 2010). Subsequent analysis used the limma software package (Ritchie et al., 2015). Counts were transformed to log2 counts per million with associated precision weights using voom (Law et al., 2014). Differential expression between samples was assessed using empirical Bayes moderated t-statistics with robust estimation of prior parameters (Smyth, 2004). A paired design was used to adjust for baseline differences between patients. Genes were considered differentially expressed if they achieved a false discovery rate of 0.05. Gene and KEGG ontology analysis was performed using limma's 'goana' and 'kegga' functions, respectively.

2.6.6 Comparison of RNA-seq profiles

The RNA-seq profiles of 882 breast cancer tumours in the form of genewise read counts were downloaded from The Cancer Genome Atlas (TCGA) Data Portal (https://tcga-data.nci.nih.gov). PAM50 tumour subtype calls were obtained for each sample from the TCGA analysis working party (K.A. Hoadley and C.M. Perou). This included 132 basal-like, 65 $HER2^{+}$, 391 luminal A, 183 luminal B and 111 normal-like breast tumours. Genes were considered unexpressed if there was not at least 0.1 read per million in at least 100 samples. Entrez Gene IDs without official gene

symbols were also excluded, leaving 16479 genes. Using the edgeR package (Robinson et al., 2010), counts were normalised by the trimmed mean of M-values method (Robinson and Oshlack, 2010). The voom method (Law et al., 2014) was then used to transform counts to $\log_2$ counts per million with associated precision weights. The concordance of the $RANK^+$ expression signature with tumour subtypes was tested used the roast function of the limma package (Wu et al., 2010) with 9999 rotations. The $\log_2$ fold changes between $RANK^+$ and $RANK^-$ cells were used as gene weights in the ROAST tests. Enrichment plots were drawn using the barcode plot function. $RANK^+$ signature scores were calculated for each tumour using a method described previously (Lim et al., 2009).

2.6.7 Telomere length measurement

Genomic DNA from sorted cell populations was extracted using the Illustra tissues & cells genomicPrep mini spin kit (GE Healthcare), according to manufacturers instructions. Analysis of telomere length was performed as previously described (Cawthon, 2009). Briefly, 20 ng DNA was mixed with 0.75x SYBR Green 1 (Thermo Fisher), 0.625 U AmpliTaq Gold DNA Polymerase (Thermo Fisher), 25 mM $MgCl_2$, 0.1 M DTT, 5 M Betaine and 10 mM dNTPs in a final reaction volume of 25 μL. Sequence-specific primers for the telomere signal (T) and a single-copy gene signal (S) were also added to each sample (900 nM final concentration, Table 2.5). Samples were run in triplicate and thermal cycling was performed with a Rotorgene RG-6000 (Corbett Research). The cycling profile was as follows: Stage 1: 15 min at 95 °C; Stage 2: 2 cycles of 15 s at 94 °C, 15 s at 49 °C; and Stage 3: 32 cycles of 15 s at 94 °C, 10 s at 62 °C, 15 s at 74 °C with signal acquisition, 10 s at 84 °C, 15 s at 88 °C with signal acquisition. After raw data collection, Rotorgene software was used to generate two standard curves (one for the telomere signal and one for single-copy gene signal), using DNA extracted from HEK293T cells as the standard DNA control. This results in an average T/S ratio for each experimental sample, which is proportional to the average telomere length per cell.

2.7 Statistical Analysis

Unless otherwise stated, a two-tailed *t*-test was used to determine statistical significance using Prism software (GraphPad). For RNA-seq data, statistical

analysis was performed using the limma software package (Ritchie et al., 2015). For analysis of RANK immunohistochemistry in normal human breast tissue and human breast tumours, a Wilcoxon Rank Sum test or a Fisher's exact test was used, respectively. Significance is indicated on the figures using the following convention: *$P < 0.05$, **$P < 0.01$, ***$P < 0.001$, ****$P < 0.0001$.

Table 2.1 Oligonucleotide primers for genotyping

Gene	Primer Sequence (5' – 3')	Annealing temp
Brca1 floxed allele	CTGGGTAGTTTGTAAGCATGC CAATAAACTGCTGGTCTCAGG CTGCGAGCAGTCTTCAGAAAG	60 °C
MMTV-cre transgene	CTGATCTGAGCTCTGAGTG CATCACTCGTTGCATCGACC	60 °C
Trp53 knockout	TTATGAGCCACCCGAGGT TATACTCAGAGCCGGCCT TCCTCGTGCTTTACGGTATC	52 °C
MMTV-Wnt transgene	CTCTAGAGGATCTTTGTGAAGG GGACAAACCACAACTAGAATGC	55 °C
MMTV-PyMT transgene	CTCTAGAGGATCTTTGTGAAGG GGACAAACCACAACTAGAATGC	55 °C
MMTV-Neu transgene	CTCTAGAGGATCTTTGTGAAGG GGACAAACCACAACTAGAATGC	55 °C

Table 2.2 Antibodies for flow cytometry

Antibody	Clone	Conjugate	Specificity	Dilution	Species	Supplier
RANK	N1H8	None	Human	1:4000	Mouse	Amgen Inc.
CD31	WM59	PE	Human	1:40	Mouse	BD Pharmingen
CD45	H130	PE	Human	1:120	Mouse	BD Pharmingen
CD235α	GA-R2	PE	Human	1:120	Mouse	BD Pharmingen
EpCAM	VU-1D9	FITC	Human	1:40	Mouse	STEMCELL Technologies
EpCAM	VU-1D9	Pacific Blue	Human	1:40	Mouse	Cell Signalling
CD49f	GoH3	Biotin	Human	1:80	Rat	Abcam
CD31	MEC 13.3	PE	Mouse	1:80	Rat	BD Pharmingen
CD45	30-F11	PE	Mouse	1:80	Rat	BD Pharmingen
CD31	MEC 13.3	APC	Mouse	1:40	Rat	Biolegend
CD45	30-F11	APC	Mouse	1:80	Rat	Biolegend
Ter119	Ter-119	APC	Mouse	1:80	Rat	Biolegend
CD24	M1/69	Pacific Blue	Mouse	1:200	Rat	Biolegend
CD29	HMβ1-1	FITC	Mouse	1:300	Hamster	Biolegend
Sca-1	E13-161.7	PE	Mouse	1:200	Rat	BD Pharmingen
CD49b	HMa2	Biotin	Mouse	1:200	Hamster	eBioscience
PD-L1	MIH5	Biotin	Mouse	1:100	Rat	eBioscience
Streptavidin-APC-Cy7	-	-	-	1:300	-	BD Pharmingen

Table 2.3 Antibodies for immunohistochemistry

Antibody	Clone	Conjugate	Specificity	Dilution	Species	Supplier
RANK	N1H8	None	Human	1:1000	Mouse	Amgen Inc.
RANKL	M366	None	Human	1:500	Mouse	Amgen Inc.
Ki67	B56	None	Human	1:200	Mouse	BD Pharmingen
PR-A	16	None	Human	1:400	Mouse	Novacastra
CK14	LL002	None	Human	1:80	Mouse	Novacastra
CK18	5D3	None	Human	1:300	Mouse	Novacastra
p63	4A4	None	Human	1:100	Mouse	DAKO
RANK	-	None	Mouse	1:80	Goat	R & D
RANKL	-	None	Mouse	1:300	Goat	R & D
Ki67	D3B5	None	Mouse	1:200	Rabbit	Cell Signalling
K8/18 (TROMA-1)	-	None	Mouse/ Human	1:1800	Rat	DSHB
K14	-	None	Mouse	1:1000	Rabbit	Covance
ERα	MC-20	None	Mouse/ Human	1:300	Rabbit	Santa Cruz
PR	C-19	None	Mouse/ Human	1:400	Rabbit	Santa Cruz
Cleaved caspase 3	-	None	Mouse/ Human	1/100	Rabbit	Cell Signalling
BrdU	-	None	Mouse/ Human	1/750	Rat	Becton Dickinson
CD8	-	None	Mouse	1/1000	Rabbit	Synaptic Systems
Rabbit IgG	-	Biotin	-	1:300	Rabbit	Vector Labs
Mouse IgG	-	Biotin	-	1:300	Mouse	Vector Labs
Rat IgG	-	Biotin	-	1:300	Rat	Vector Labs
Goat IgG	-	Biotin	-	1:300	Goat	Vector Labs

Table 2.4 Antibodies for western blotting

Antibody	Clone	Conjugate	Dilution	Species	Supplier
p100/p52	-	None	1/500	Rabbit	Cell Signalling
Phospho-AKT	M89-61	None	1/500	Mouse	BD Biosciences
Phospho-ERK1/2	-	None	1/750	Rabbit	Cell Signalling
GAPDH	71.1	None	1/5000	Mouse	Sigma
Cyclin D1	-	None	1/1000	Rabbit	Cell Signalling
Cleaved Caspase 3	-	None	1/1000	Rabbit	Cell Signalling
Mouse IgG	-	HRP	1:10000	Mouse	Southern Biotech
Rabbit IgG	-	HRP	1:10000	Rabbit	Southern Biotech

Table 2.5 Oligonucleotide primers for quantitative PCR

Gene	Primer Sequence (5' – 3')	Product size (bp)
MKI67	F: GAATTGAACCTGCGGAAGAGC R: AGCGCAGGGATATTCCCTTATTTT	105
CDK1	F: CTAGAAAGTGAAGAGGAAGGGGT R: CATAAGCACATCCTGAAGACTGAC	105
PBK/TOPK	F: GCCAAGATCCTTTTCCAGCAG R: TCTTGGTGCAGATACTTTAACCCT	79
TOP2A	F: TCCTGCCTGTTTAGTCGCTT R: ATTTACAGGCTGCAATGGTGAC	83
GAPDH	F: CGCTCTCTGCTCCTCCTGTT R: CCATGGTGTCTGAGCGATGT	115
BRCA1	F: AAGCAGCGGATACAACCTCAA R: TGATCTCCCACACTGCAATAAGT	104
RSPO1	F: AAAGGCAGAGGCGGATCAGT R: CGGATGTCGTTCCTCTCCAG	130
TCF1	F: CCTTCGACCGCAACCTGAAGA R: TCTGCAATGACCTTGGCTCTC	130
TCF4	F: GCCTCTTATCACGTACAGCAAT R: GCCAGGCGATAGTGGGTAAT	147
Telomere repeat sequence (T)	Telg: ACACTAAGGTTTGGGTTTGGGTTTGGGTTT GGGTTAGTGT Telc: TGTTAGGTATCCCTATCCCTATCCCTATCCC TATCCCTAACA	79
Single-copy gene (S) (albumin)	Albu: CGGCGGCGGGCGGCGCGGGCTGGGCGGA AATGCTGCACAGAATCCTTG Albd: GCCCGGCCCGCCGCGCCCGTCCCGCCGG AAAAGCATGGTCGCCTGTT	98

Chapter 3: Identification of a novel population of RANK^{+} luminal progenitor cells in preneoplastic *BRCA1*$^{mut/+}$ human breast tissue

3.1 Introduction

Despite tremendous progress in understanding the cellular functions of BRCA1, the precise molecular mechanisms governing the transition from normal breast epithelium to malignancy in *BRCA1*-mutation carriers remain largely obscure. There is accumulating evidence for deregulated hormone signalling in *BRCA1*-mutant breast tissue. The risk of breast cancer in mutation carriers is substantially higher during pregnancy, when there are high circulating levels of steroid hormones (Jernstrom et al., 1999; Narod, 2001) while a sharp decline in cancer risk occurs after menopause (Antoniou et al., 2003). Moreover, a recent analysis of serum oestradiol and progesterone indicated that premenopausal *BRCA1*/*2*-mutation carriers have higher titres of serum progesterone during the luteal phase of the menstrual cycle compared to non-carriers (Widschwendter et al., 2013). Defects in hormone receptor activity have also been implicated in *BRCA1*-deficient breast epithelial cells. BRCA1 can interact with both the PR and ER to repress their transcriptional activities (reviewed in Katiyar et al., 2006). *BRCA1*-deficiency would therefore be predicted to promote the activity of these receptors in hormonally-regulated tissues such as the breast and ovary. Indeed, disrupted receptor turnover and enhanced PR expression have been observed in the mammary epithelium of *Brca1*/*p53*-deficient mice (Poole et al., 2006) and in normal human breast tissue adjacent to *BRCA1*-mutated tumours (King et al., 2004). Furthermore, treatment of *Brca1*-deficient mice with exogenous progesterone led to increased tertiary branching (Ma et al., 2006), while the progesterone antagonist mifepristone prevented mammary tumorigenesis in mice lacking functional BRCA1 and p53 (Poole et al., 2006). Collectively, these studies suggest amplified hormonal signalling exists in *BRCA1*-mutant breast tissue as a consequence of perturbed steroid hormone and receptor regulation.

Despite these findings, the mechanism by which aberrant hormone signalling in *BRCA1*-deficient preneoplastic breast tissue leads to neoplastic transformation is undefined. A candidate pathway underlying this process is the RANKL signalling axis. As discussed in Chapter 1, *RANKL* is a major target gene of progesterone and is a key paracrine effector of mitogenic progesterone signalling in normal breast tissue. Notably, the RANKL signalling pathway has also been implicated in hormone-driven mammary tumorigenesis. RANK overexpression in mice treated with the carcinogen 7,12-dimethylbenzen(a)anthracene (DMBA) and medroxyprogesterone acetate (MPA) led to an increase in preneoplastic lesions and accelerated mammary tumour formation (Gonzalez-Suarez et al., 2010). *MMTV-RANK* mice also spontaneously developed preneoplastic lesions and adenocarcinomas after multiple rounds of pregnancy (Gonzalez-Suarez et al., 2010). Conversely, ablation of RANKL signalling by pharmacological inhibition or genetic deletion markedly decreased the incidence, onset and progression of MPA/DMBA-driven mammary cancer (Gonzalez-Suarez et al., 2010; Schramek et al., 2010). Notably, systemic RANK blockade reduced tumour incidence by 90% in the DMBA/MPA-treated mice (Gonzalez-Suarez et al., 2010). Tumour attenuation was preceded by a reduction in preneoplastic lesions and a rapid reduction in cell proliferation and *cyclin D1* expression, suggesting that decreased proliferation 'protects' against early events in tumorigenesis (Gonzalez-Suarez et al., 2010). Together these observations suggest that amplified signalling through the RANKL pathway has pro-tumorigenic effects. This may be mediated in part by RANKL-mediated activation of NF-κB, since the inhibition of canonical NF-κB activation in *MMTV-IκBα* mice reduced the burden of both premalignant and malignant mammary lesions following DMBA/MPA treatment (Pratt et al., 2009). In a separate study, Cao et al showed that mice expressing a mutant *IKKα* to inhibit the non-canonical NF-κB pathway displayed a significant delay in MPA/DMBA-induced mammary tumour onset and tumour burden compared to control mice (Cao et al., 2007).

These findings raise the possibility that the RANKL signalling axis may be the crucial link between deregulated progesterone signalling and breast cancer susceptibility in *BRCA1*-mutation carriers. This chapter will explore and characterise the role of the RANK-RANKL pathway in both normal human breast

epithelium and in premalignant *BRCA1*-mutant tissue obtained from mutation carriers that underwent a prophylactic mastectomy. The results highlight a novel role for this signalling axis in *BRCA1*-associated breast oncogenesis and, importantly, further delineate the 'cell of origin' population in *BRCA1*-mutation carriers.

3.2 Results

3.2.1 Prominent RANK expression on *BRCA1*$^{mut/+}$ luminal progenitor cells

To interrogate the expression of RANK and RANKL in human breast epithelium, we first delineated breast epithelial subsets within histologically normal human breast tissue using flow cytometry. Breast tissue was obtained from premenopausal women either undergoing reduction mammoplasties (WT, n = 33) or prophylactic mastectomies in the case of *BRCA1* (*BRCA1*$^{mut/+}$, n = 24) and *BRCA2* (*BRCA2*$^{mut/+}$, n = 10) mutation carriers (Table 3.1 and 3.2). Freshly isolated breast tissue was depleted of hematopoietic and endothelial cells (Lin$^-$) and further fractionated into mature luminal (CD49f$^-$EpCAM$^+$), luminal progenitor (CD49f$^+$EpCAM$^+$), basal/mammary stem cell (MaSC)-enriched (CD49f$^+$EpCAM$^-$) and stromal (CD49f$^-$ EpCAM$^-$) cells (Figure 3.1a,b). Co-staining for RANK revealed that its expression was confined to the luminal progenitor subset in both *BRCA1*$^{mut/+}$ and WT breast tissue, with no expression detected in the basal/MaSC-enriched, mature luminal or stromal subsets (Figure 3.1a - c). Quantitative RT-PCR analysis demonstrated *RANK* mRNA expression was also largely restricted to luminal progenitor cells (Figure 3.1d). Notably, a markedly larger fraction of RANK-positive (RANK$^+$) luminal progenitor cells was observed in *BRCA1*$^{mut/+}$ breast tissue (28.6 ± 2.5%) compared to age-matched WT (14.7 ± 1.2%) and *BRCA2*$^{mut/+}$ tissue (13.6 ± 3.5%) (Figure 3.1e). Consistent with these findings, immunostaining of normal breast tissue adjacent to *BRCA1*-mutated breast tumours also showed augmented RANK expression compared to *BRCA2* or WT tumour-adjacent tissue (Table 3.3). Thus *BRCA1*$^{mut/+}$ luminal progenitors exhibit prominent expression of RANK. As anticipated given its role as a paracrine effector, expression of *RANKL* was restricted to the mature luminal (HR$^+$) population (Figure 3.1f).

3.2.2 RANK$^+$ progenitors exhibit enhanced clonogenic and Aldefluor activity

To characterise the RANK-expressing luminal progenitor subset, the *in vitro* growth properties of freshly sorted RANK$^+$ and RANK$^-$ luminal progenitor cells were evaluated using 3D colony-forming assays with Matrigel. RANK$^+$ cells isolated from *BRCA1*-mutation carriers had significantly higher clonogenic capacity compared to

RANK$^-$ cells from the same tissue, and also exhibited higher proliferative capacity than WT RANK$^+$ cells (Figure 3.2). We next assessed the enzymatic activity of aldehyde dehydrogenase (ALDH) in the subsets defined by RANK expression using the Aldefluor flow cytometry assay. High ALDH activity is a biomarker of luminal progenitor cells (Eirew et al., 2012). Notably, RANK$^+$ luminal progenitor cells from both *BRCA1*$^{mut/+}$ and WT breast tissue exhibited higher ALDH activity compared to their RANK$^-$ counterpart cells, and this feature that was more pronounced in *BRCA1*$^{mut/+}$ tissue (Figure 3.3a,b). Furthermore, RANK and ALDH1 immunostaining was colocalised in sequential sections of TDLUs and ducts from *BRCA1*$^{mut/+}$ and WT tissue, with more intense RANK and ALDH expression evident in *BRCA1*$^{mut/+}$ epithelium (Figure 3.3c). RANK expression thus appears to mark an aberrant luminal progenitor subset in breast tissue from *BRCA1*-mutation carriers.

3.2.3 *BRCA1*$^{mut/+}$ RANK$^+$ luminal progenitors have enhanced mitotic activity

To interrogate the molecular pathways associated with RANK$^+$ luminal progenitor cells, RNA-seq was performed on freshly sorted RANK$^+$ and RANK$^-$ progenitors isolated from WT breast epithelium. We identified 632 genes that were differentially expressed between the two populations, with 367 upregulated and 265 downregulated genes in RANK$^+$ cells relative to the RANK$^-$ subset (Table 3.4 and 3.5). Importantly, gene ontology-analysis demonstrated a significant upregulation of cell cycle, proliferation and DNA repair genes in the RANK$^+$ subset, suggesting these cells are highly mitotically active (Figure 3.4a, Table 3.6). The most highly upregulated gene in the RANK$^+$ subset was *TOP2A,* which encodes a DNA topoisomerase that relieves torsional stress during DNA replication by introducing transient double-stranded breaks (Nitiss, 2009). *TOP2A* is highly expressed in proliferating cells and its overexpression is frequently observed in high-grade triple-negative breast cancers (Komatsu et al., 2013; Nakagawa et al., 2011; Rudolph et al., 1999; Tan et al., 2008). Other notable enriched genes include *PBK/TOPK,* which encodes a serine/threonine kinase that is activated by CDK1 and is required for mitotic cell division (Park et al., 2006; Rizkallah et al., 2015) and *FOXM1*, a member of the mammalian forkhead box family of transcription factors that is highly expressed in proliferating cells where it regulates transcription of cell cycle genes that promote DNA replication and mitosis progression (Wang et al., 2005).

Intriguingly, KEGG analysis revealed a marked enrichment of metabolic pathways in RANK$^+$ cells, particularly fatty acid metabolism (Figure 3.4b).

We next validated these findings by performing quantitative RT-PCR on RANK$^+$ and RANK$^-$ luminal progenitor cells from additional WT and *BRCA1*$^{mut/+}$ patient samples. Four highly differentially expressed genes were selected for validation (*TOP2A*, *MKi67*, *CDK1* and *PBK/TOPK*) based on their association with proliferative tissues and triple-negative breast cancer. Significant upregulation of all four genes was confirmed in the RANK$^+$ compared to the RANK$^-$ luminal progenitor subset (Figure 3.5a). Furthermore, these genes were significantly upregulated in RANK$^+$ luminal progenitors from *BRCA1*$^{mut/+}$ tissue relative to WT breast tissue (Figure 3.5a), consistent with their enhanced colony-forming activity in Matrigel (Figure 3.2). RANK$^+$ cells also harboured high levels of *BRCA1* transcripts (Figure 3.5a), suggesting BRCA1 normally performs an important role within these cells. The augmented expression of Ki67 in *BRCA1*$^{mut/+}$ RANK$^+$ progenitors was confirmed at the protein level by performing immunostaining on cytospins of freshly sorted cells (Figure 3.5b,c). Thus RANK$^+$ luminal progenitor cells within *BRCA1*$^{mut/+}$ tissue have higher mitotic activity compared to WT breast tissue. Notably, RNA-seq revealed that expression of PR and ER was downregulated in RANK$^+$ luminal progenitors relative to the RANK$^-$ subset. This is consistent with the paracrine mode of stimulation of these cells, and has also been observed in the mouse mammary gland (Pal et al., 2013). We confirmed this finding through immunostaining of PR on cytospins of freshly sorted RANK$^+$ and RANK$^-$ luminal progenitor cells from WT breast tissue, demonstrating a marked enrichment of PR expression in RANK$^-$ cells (Figure 3.5d,e).

Although Wnt pathway activation was not a feature of the RANK$^+$ gene signature, the recently proposed interaction between RANKL and Wnt, whereby RANK activation was shown to enhance Wnt signalling via the upregulation of *R-spondin1* (Joshi et al., 2015), prompted us to interrogate this pathway further. Consistent with the RNA-seq analysis, we did not observe enhanced expression of *R-spondin1* or the Wnt pathway transcription factors *TCF1* and *TCF4* in RANK$^+$ cells relative to their RANK$^-$ counterpart cells (Figure 3.6a). Thus, an interaction between RANK and Wnt signalling does not appear to be a prominent feature of human breast

epithelium. To explore alternative downstream signalling pathways responsible for the enhanced proliferation of *BRCA1*$^{mut/+}$ RANK^{+} cells, the activation of NF-κB within the human breast epithelium was next investigated. Western blot analysis of sorted total epithelial cells from WT and *BRCA1*$^{mut/+}$ breast tissue revealed elevated expression of p52 (NF-κB2) in 66% of *BRCA1*$^{mut/+}$ patient samples compared to 37.5% of WT samples (Figure 3.6b). We next transduced freshly sorted WT and *BRCA1*$^{mut/+}$ epithelial subsets with a lentiviral NF-κB-GFP reporter construct to provide a read-out of NF-κB-mediated transcriptional activation. Notably, a dramatic increase in reporter activity was observed in RANK^{+} luminal progenitor cells compared to the RANK^{-}, basal/MaSC and mature luminal subsets (Figure 3.6c). Moreover, GFP expression was profoundly elevated in *BRCA1*$^{mut/+}$ RANK^{+} cells compared to those isolated from WT breast tissue (Figure 3.6c). These findings are consistent with previous reports demonstrating RANKL-induced NF-κB activation in the mouse mammary epithelium (Cao et al., 2001). Thus NF-κB activation, a well-established pro-proliferative pathway (Karin et al., 2002), is a prominent feature of *BRCA1*$^{mut/+}$ RANK^{+} cells.

3.2.4 The RANK^{+} progenitor signature correlates with basal-like breast cancers

To interrogate the relationship between RANK^{+} and RANK^{-} progenitor cells and the different breast cancer subtypes, the gene signature of the RANK^{+} subset was compared to the molecular profiles of luminal A and B, basal-like, HER2^{+} and normal-like tumours from the TCGA dataset (n = 882 tumours). The RANK^{+} gene signature was more closely associated with basal-like cancers than all other breast cancer subtypes (Figure 3.7). Specifically, genes upregulated in RANK^{+} cells were also highly enriched in basal-like tumours, while downregulated genes were least expressed in basal-like tumours, relative to the other subtypes. Conversely, the RANK^{-} molecular signature was closer to all other subtypes of breast cancer than basal-like tumours. Thus, RANK^{+} but not RANK^{-} luminal progenitor cells share striking molecular properties with basal-like breast cancers, implicating this subset as a candidate cell of origin population for *BRCA1*-mutated breast tumours.

3.2.5 *BRCA1*$^{mut/+}$ RANK^{+} luminal progenitors have grossly aberrant DNA repair mechanisms

To explore whether the highly proliferative RANK^{+} population from *BRCA1*-heterozygous tissue was prone to acquiring DNA damage, we performed comet assays to quantify DNA lesions in breast epithelial cells from age-matched WT and *BRCA1*$^{mut/+}$ breast tissue. Freshly sorted cell subsets were allowed to recover overnight and then treated with hydroxyurea (to induce stalled DNA replication forks) or subjected to γ-irradiation (3 Gy) to induce double-strand breaks and harvested 4 hours later (Figure 3.8a). As expected, no DNA damage was evident in any epithelial subset from WT patients including RANK^{+} and RANK^{-} progenitors, owing to intact DNA repair mechanisms (Figure 3.8b). In contrast, a basal level of DNA damage was clearly discernable in *BRCA1*$^{mut/+}$ luminal progenitor cells, and these cells were highly sensitive to damage induced by either hydroxyurea or γ-irradiation (Figure 3.8b - f). The basal/MaSC population exhibited minimal damage either before or after treatment (Figure 3.8e). Importantly, the RANK^{+} luminal progenitor population was profoundly more sensitive to DNA damage following γ-irradiation compared to RANK^{-} cells, suggesting that the DNA-repair machinery is markedly perturbed in these cells as a consequence of *BRCA1* heterozygosity (Figure 3.8b - f). In addition, a moderate increase in DNA damage was observed in hydroxyurea-treated RANK^{+} cells compared to RANK^{-} cells, indicating that stalled fork repair is also defective in this cellular subset. Collectively, these data suggests *BRCA1*$^{mut/+}$ luminal progenitor cells, particularly RANK^{+} cells, exhibit striking haploinsufficiency for DNA repair.

The aberrant DNA repair mechanisms evident in *BRCA1*$^{mut/+}$ luminal progenitor cells prompted us to next analyse the telomere lengths in both WT and *BRCA1*$^{mut/+}$ tissue using quantitative PCR specific for the telomere repeat sequence (Cawthon, 2009). While shorter telomeres were observed in luminal progenitor cells relative to the basal/MaSC population consistent with previous reports (Kannan et al., 2013), we did not observe any significant differences in telomere length between RANK^{+} and RANK^{-} progenitors (Figure 3.8g). While this was surprising given the increased mitotic activity of RANK^{+} cells, a prolonged lifespan is required for a cell to

accumulate oncogenic lesions. Thus drastic telomere shortening in the probable target population of $RANK^+$ cells would not be conducive to cell survival.

3.3 Discussion

The development of novel chemoprevention and breast cancer treatment strategies for *BRCA1*-mutation carriers is reliant on understanding the mechanisms by which disruption of this tumour suppressor gene leads to cancer. Given the accumulating evidence implicating amplified progesterone signalling in *BRCA1*-associated breast oncogenesis, we have explored the possibility that the progesterone-responsive RANKL signalling axis is a key modulator of this process.

The use of prophylactic mastectomy tissue samples obtained from *BRCA1*-mutation carriers provides unique insights into the biological properties of heterozygous but ostensibly normal *BRCA1*-mutant mammary epithelium. Utilising flow cytometric fractionation of subsets within the mammary epithelium, we have identified a novel population of RANK-expressing luminal progenitor cells that are expanded in preneoplastic *BRCA1*-mutant human breast tissue compared to WT tissue. $RANK^+$ cells were highly proliferative, as demonstrated by gene expression analysis and colony-forming assays as a functional read-out of mitotic activity. This is consistent with a previous report demonstrating co-localisation of RANK and Ki67 immunostaining in a subset of breast epithelial cells from cynomolgus macaque monkeys (Wood et al., 2013), as well as the reported induction of DNA replication and cellular proliferation by progesterone (Graham et al., 2009). Notably, $RANK^+$ cells also exhibited markedly higher ALDH activity and protein expression compared to $RANK^-$ cells, a feature that was especially prominent in $BRCA1^{mut/+}$ tissue. ALDH1-positive cells comprising entire acini have been previously noted as a feature of $BRCA1^{mut/+}$ breast tissue (Liu et al., 2008). Interestingly, the presence of ALDH-positive acini was also associated with breast cancer risk, since four of five *BRCA1*-mutation carriers with ALDH1-positive lobules developed breast cancer, compared to only two of the eight carriers with no detectable ALDH1-positive acini (Liu et al., 2008). Although this dataset represents a small number of patients, these findings implicate ALDH1/RANK double-positive lobules in breast oncogenesis.

In addition to cell cycle genes, molecular profiling revealed a substantial enrichment of metabolic pathways in $RANK^+$ luminal progenitor cells compared to

RANK^{-} cells, particularly fatty acid metabolism. This suggests RANK^{+} luminal progenitor cells may represent a distinct population of alveolar-type progenitor cells within the breast epithelium, but this is yet to be determined. This is compatible with previous reports that ALDH^{+} luminal progenitor cells share a gene signature consistent with an alveolar progenitor population (Shehata et al., 2012). The similar *BRCA1* transcript levels observed between WT and *BRCA1*$^{mut/+}$ subsets are consistent with previous data from studies using cultured epithelial cells (Bellacosa et al., 2010; Sedic et al., 2015), implying that biological changes in *BRCA1*$^{mut/+}$ cells reflect perturbations at the protein level.

By quantifying DNA lesions using comet assays, our findings suggest that the DNA repair machinery is uncoupled in RANK^{+} luminal progenitor cells that have lost a single allele of *BRCA1*. Given the critical role of BRCA1 in high fidelity homologous recombination (HR)-mediated DNA repair, loss of function would render cells highly susceptible to DNA damage. The existence of defective DNA repair mechanisms in breast tissue heterozygous for *BRCA1* (i.e. haploinsufficiency) has been a contentious topic for the field. Long-standing results show that HR function is intact in *BRCA1*$^{+/-}$ embryonic stem cells until both copies of *BRCA1* are inactivated (Moynahan et al., 2001), while mice heterozygous for *Brca1* do not exhibit any detectable phenotype nor do they spontaneously develop mammary tumours (Drost and Jonkers, 2009). By contrast, others have recently demonstrated defective DNA repair upon loss of a single allele of *BRCA1* using immortalised cell lines or *BRCA1*$^{mut/+}$ breast epithelial cells that were cultured long-term *in vitro* (Konishi et al., 2011; Pathania et al., 2014; Savage et al., 2014; Sedic et al., 2015). Our data represents the first demonstration of *BRCA1* haploinsufficiency for DNA repair in highly fractionated breast populations, and in freshly sorted cells that were not passaged *in vitro*. Most importantly, we identified the RANK^{+} luminal progenitor population as an epithelial subset that is particularly susceptible to acquiring DNA damage, either in the basal-state or following γ-irradiation or replication fork stalling. This indicates that markedly perturbed DNA repair mechanisms exist in ostensibly normal *BRCA1*$^{mut/+}$ tissue. These results are consistent with the proliferative nature of RANK^{+} progenitors, since the genome is particularly susceptible to damage during DNA replication when lesions on a single strand can be converted to double strand damage (Roy et al., 2012). Given the alternative cellular roles of BRCA1, it

is also conceivable that the rapidly dividing RANK$^+$ population deprived of a full complement of intact BRCA1 has a high requirement for this tumour suppressor in checkpoint control or transcriptional regulation. This would dramatically reduce the available pool of functional BRCA1 that is able to coordinate DNA repair, and could explain the increased susceptibility of RANK$^+$ progenitors to accumulating DNA lesions. Collectively, our results imply that loss of a single *BRCA1* allele in the proliferating RANK$^+$ population could generate a pool of genetically unstable cells that are prime targets for the acquisition of additional mutations such as *BRCA1* LOH or loss of *TP53*. Thus, RANK$^+$ but not RANK$^-$ luminal progenitor cells are a likely target population for malignant transformation in *BRCA1*-mutant breast tissue. Fittingly, RANK$^+$ but not RANK$^-$ progenitors shared a molecular profile closely aligned with basal-like breast tumours. This is in line with the previous observation that the gene signature of the ALDH$^+$ luminal progenitor population in the human breast more strongly correlates with basal-like breast tumours compared to the ALDH$^-$ luminal progenitor population (Shehata et al., 2012).

Using NF-κB GFP reporter assays, we demonstrated prominent NF-κB activity in *BRCA1*$^{mut/+}$ RANK$^+$ cells. Given the established link between the RANK-NF-κB signalling axis and proliferation via cyclin D1 upregulation (Cao et al., 2001), NF-κB activity in *BRCA1*$^{mut/+}$ tissue could contribute to expansion of the RANK$^+$ subset as well as the mitotically active state. In a recent report (Sau et al., 2016), the perturbed growth properties of *BRCA1*-deficient luminal progenitors were linked to DNA damage-induced activation of NF-κB. Activation of the ATM checkpoint kinase and the NF-κB essential modulator (NEMO) in *BRCA1*-deficient luminal progenitors in response to DNA damage resulted in activation of canonical NF-κB signalling as shown by an increase in p65 phosphorylation, as well as prolonged non-canonical p52 activation. Notably, p52, ATM and IKKα were all shown to be essential for growth factor-independent proliferation of *BRCA1*-deficient luminal progenitor cells. Sau et al also showed that NF-κB inhibition *in vivo* markedly reduced γH2AX foci in *Brca1*-null mouse mammary glands, consistent with an additional role for NF-κB upstream of DNA damage in RANK$^+$ progenitors. Thus it appears that NF-κB is activated in a two-pronged manner in *BRCA1*-deficient cells, i.e. by progesterone-induced activation of the RANK pathway as well as by the DNA damage response.

The augmented NF-κB activity observed in *BRCA1*$^{mut/+}$ RANK^{+} cells is likely a consequence of both activation mechanisms. It is probable that DNA damage-induced NF-κB generates a positive feedback loop by stimulating proliferation of RANK^{+} cells, which further exacerbates genomic instability.

Deregulated systemic factors are additional features associated with a germline *BRCA1* mutation that likely contribute to the hyperactivation of the RANK^{+} luminal progenitor population in *BRCA1*$^{mut/+}$ preneoplastic tissue. As discussed, *BRCA1*-mutation carriers exhibit an amplified hormonal milieu, as a consequence of deregulated ER/PR expression and higher circulating levels of progesterone, which would promote RANKL-mediated stimulation of RANK^{+} cells during the luteal phase of the menstrual cycle. Furthermore, *BRCA1*-mutation carriers were recently reported to have lower serum OPG levels (Widschwendter et al., 2015). Since OPG is the decoy receptor for RANKL and plays an essential role in curbing RANK activation, reduced OPG levels would be anticipated to trigger amplification of the RANKL signalling pathway in *BRCA1*-mutant breast epithelium.

In summary, we have identified a novel subset of RANK^{+} luminal progenitor cells residing within the breast epithelium of *BRCA1*-mutation carriers that are actively proliferating yet are exquisitely sensitive to DNA damage compared to other breast epithelial cell types, likely setting the stage for neoplastic transformation. Notably, RANK^{+} luminal progenitors bear a unique molecular signature that is closely aligned to that of basal-like breast cancer. These findings implicate RANK^{+} and not RANK^{-} luminal progenitor cells as the primary target population for basal-like breast tumours in *BRCA1*-mutation carriers. Although alternative progesterone-responsive genes such as *Wnt4* could contribute to oncogenesis, we did not observe any alterations in the expression of Wnt pathway genes in *BRCA1*$^{mut/+}$ epithelial subsets. Based on our findings, we propose a model to explain the potential molecular mechanisms underlying oncogenesis in premenopausal *BRCA1*-mutation carriers (Figure 3.9). In this model, cell extrinsic influences such as amplified hormonal signalling act in concert with properties intrinsic to RANK^{+} cells including DNA repair haploinsufficiency and the ensuing DNA damage-induced NF-κB. The end result is a hyperactive pathway, initiated by progesterone

and amplified by NF-κB signalling. Together this culminates in a genetically unstable population of $RANK^+$ cells in *BRCA1*$^{mut/+}$ epithelium that is prone to malignant transformation, providing a molecular basis for the differential sensitivity of *BRCA1*$^{mut/+}$ versus WT luminal progenitor cells as well as the tissue-specific pattern of tumour formation. Overall, the potentially integral role for the RANKL signalling axis in tumour initiation in *BRCA1*-mutation carriers indicates RANKL as a potential novel chemoprevention target for these high risk women.

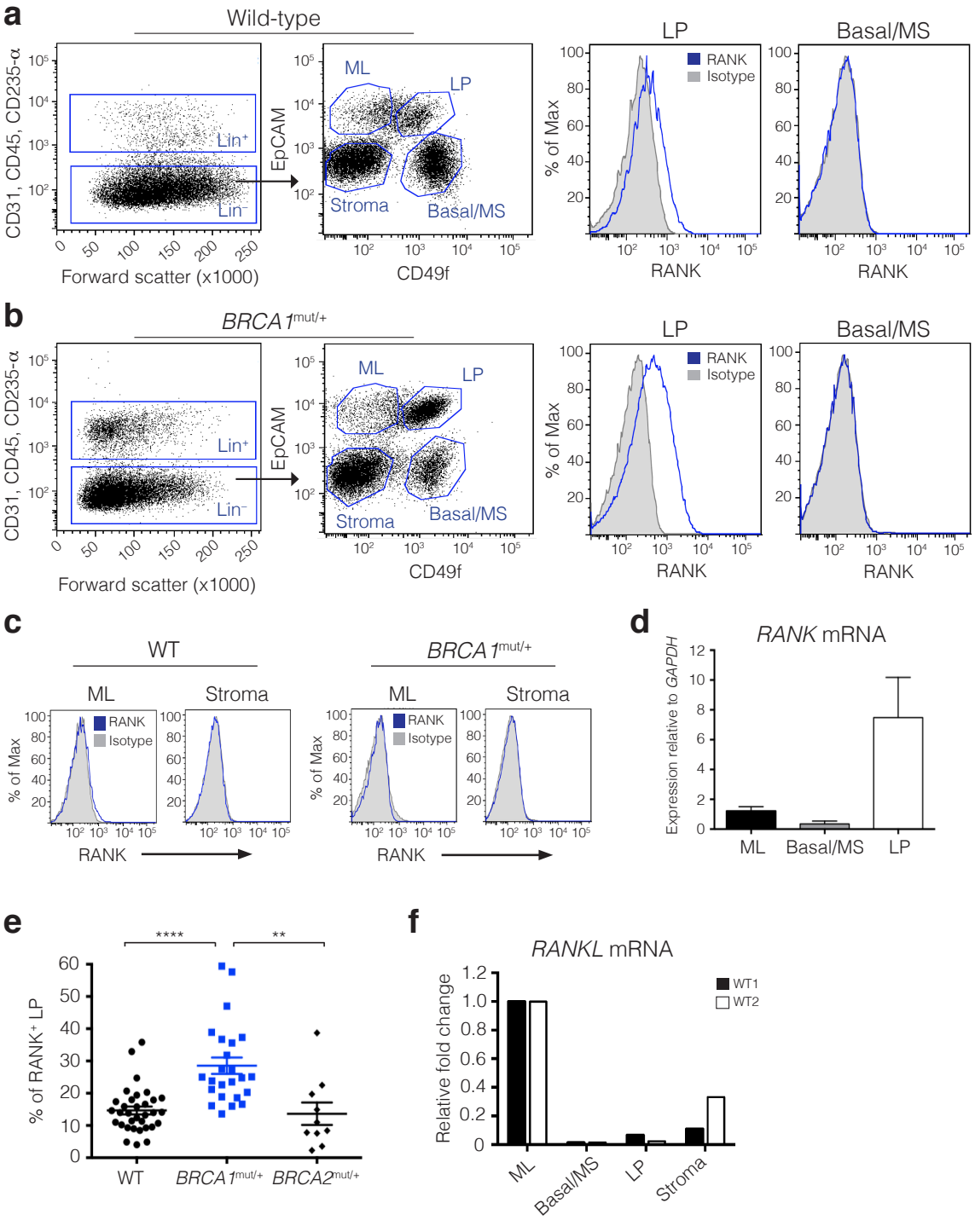
a
Wild-type
CD31, CD45, CD235-α
Lin+
Lin−
Forward scatter (x1000)
EpCAM
ML
LP
Stroma
Basal/MS
CD49f
LP
Basal/MS
RANK
Isotype
% of Max
RANK
b
BRCA1mut/+
c
WT
BRCA1mut/+
ML
Stroma
d
RANK mRNA
Expression relative to GAPDH
e
% of RANK+ LP
****
**
WT
BRCA1mut/+
BRCA2mut/+
f
RANKL mRNA
Relative fold change
WT1
WT2
Stroma

Figure 3.1: Prominent RANK expression on *BRCA1*$^{mut/+}$ luminal progenitors

(**a, b**) Representative FACS plots showing delineation of distinct subpopulations isolated from (**a**) wild-type (WT, n = 33 patients, reduction mammoplasty) or (**b**) pathologically normal *BRCA1* breast tissue (*BRCA1*$^{mut/+}$, prophylactic mastectomy, n = 24 patients) based on expression of CD31, CD45, CD235-α, EpCAM, CD49f and RANK. RANK expression (blue) was compared to an isotype-matched control antibody (grey). Cells negative for CD31, CD45 and CD235-α define the lineage negative (Lin$^-$) population. ML, mature luminal; LP, luminal progenitor; MaSC, mammary stem cell. (**c**) Representative histograms portraying the lack of RANK expression in the ML and stroma subsets within WT (n = 33 patients) or *BRCA1*$^{mut/+}$ breast tissue (n = 24 patients). (**d**) Expression analysis of *RANK* in the ML, basal/MaSC and LP subpopulations from WT breast tissue (n = 3 patients) by quantitative RT-PCR. Data is depicted as mean ± s.e.m. Expression was normalised to *GAPDH*. (**e**) Graph showing percentage of RANK$^+$ LP cells within *BRCA1*$^{mut/+}$ breast tissue (28.6 ± 2.5 %, n = 24 patients) compared to WT (14.7 ± 1.2 %, n = 33) and *BRCA2*$^{mut/+}$ (13.6 ± 3.5 %, n = 10) tissue. Bars represent mean ± s.e.m. $^{**}P < 0.01$, $^{****}P < 0.0001$. (**f**) Expression analysis of *RANKL* in ML, Basal/MaSC, LP and stroma subpopulations from WT breast tissue (n = 2 patients, WT1 and WT2) by quantitative RT-PCR. Expression was normalised to *GAPDH* and is depicted as fold-change relative to the mature luminal subset.

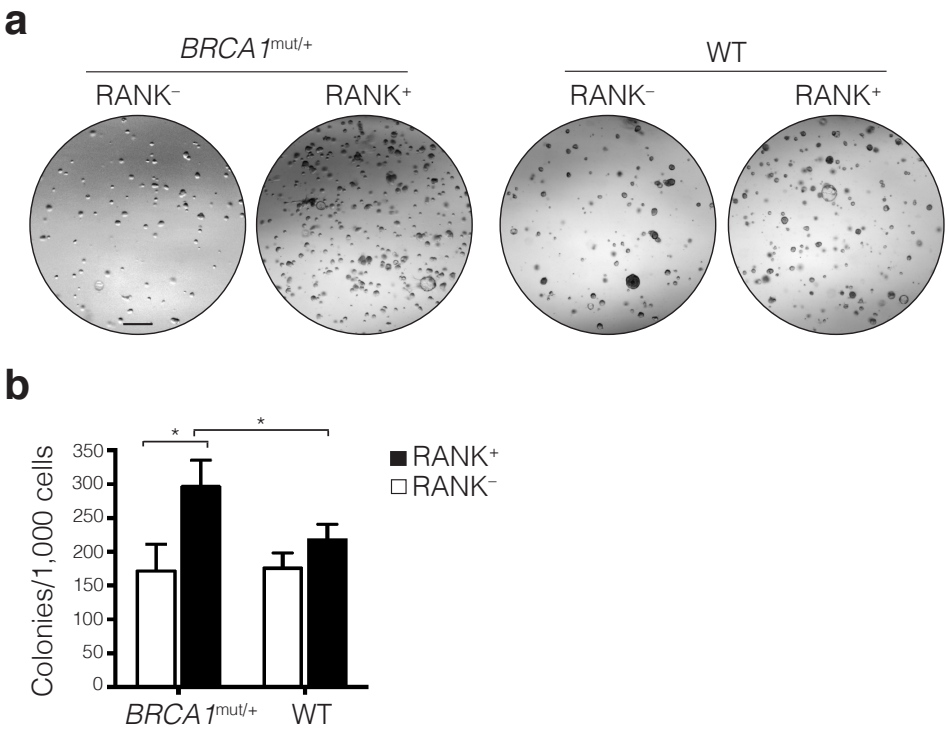

Figure 3.2: RANK^{+} progenitors from *BRCA1*$^{mut/+}$ tissue are highly clonogenic

(**a**) Representative images of 3D Matrigel droplets of freshly sorted RANK^{+} and RANK^{-} luminal progenitor cells from *BRCA1*$^{mut/+}$ (n = 6 patients) and WT (n = 5 patients) breast tissue (3 – 5 replicates per population per patient). Scale bar = 0.5 mm (**b**) Bar chart depicting colony-forming capacity of RANK^{+} and RANK^{-} luminal progenitor cells from *BRCA1*$^{mut/+}$ (n = 6 patients) and WT (n = 5 patients) breast tissue. Colonies were quantified using ImageJ software (NIH). Data represent mean ± s.e.m. *P < 0.05.

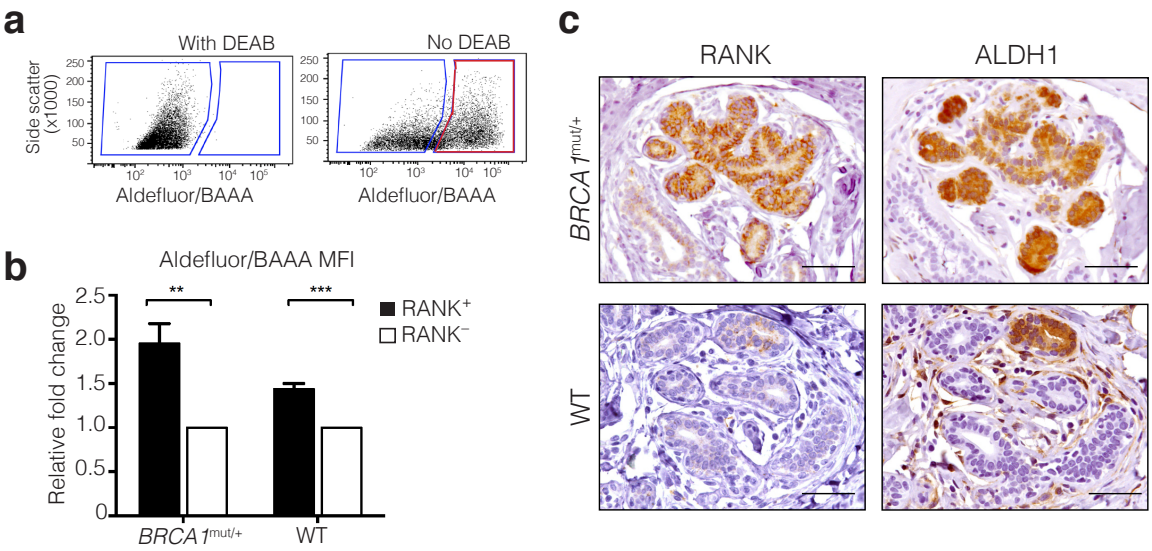

Figure 3.3: RANK^{+} progenitors exhibit enhanced ALDH activity

(**a**) Representative BODIPY-aminoacetaldehyde (BAAA) fluorescence profiles of luminal progenitor cells after incubation with Aldefluor in the presence (left) or absence (right) of the inhibitor diethylaminobenzaldehyde (DEAB). Aldefluor-positive cells are outlined in red. (**b**) Mean fluorescence intensity (MFI) values for the Aldefluor/BAAA fluorescence of RANK^{+} luminal progenitor cells isolated from *BRCA1*$^{mut/+}$ (n = 4 patients) and WT (n = 5 patients) breast tissue, relative to the MFI of the corresponding RANK^{-} luminal progenitor subset. Data are depicted as mean fold change ± s.e.m. $^{**}P < 0.01$, $^{***}P < 0.001$. (**c**) Images showing overlapping distribution of RANK and ALDH1 immunostaining in sequential sections from pathologically normal WT (n = 19 patients) and *BRCA1*$^{mut/+}$ (n = 23 patients) breast tissue. Scale bar = 50 μm.

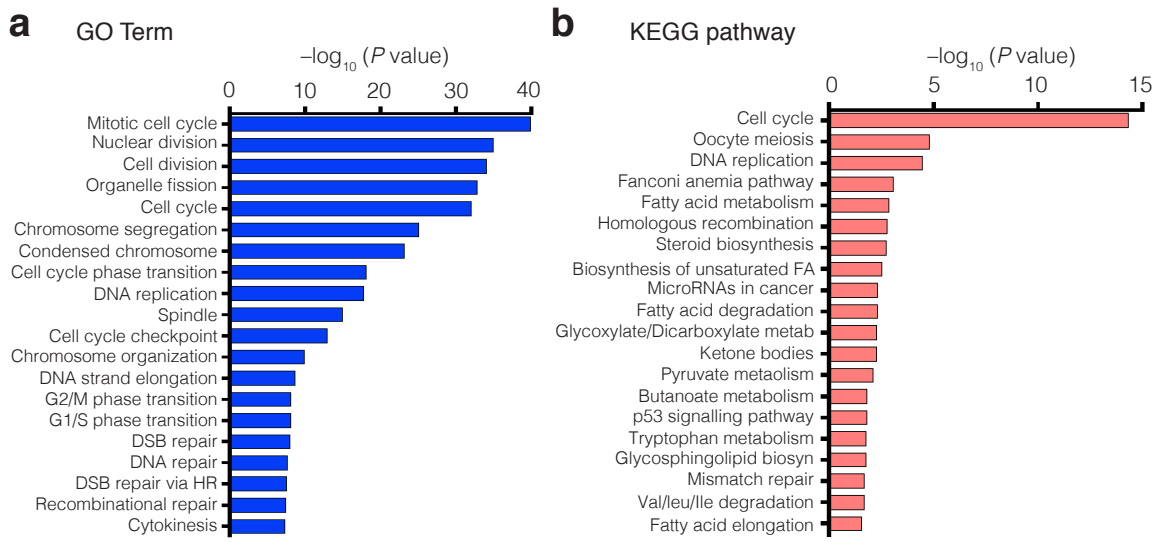

Figure 3.4: RNA-seq analysis of RANK$^+$ versus RANK$^-$ luminal progenitor cells

(**a, b**) Unbiased (**a**) gene ontology (GO) group and (**b**) Kyoto Encyclopedia of Genes and Genomes (KEGG) pathway enrichment in freshly sorted RANK$^+$ luminal progenitor cells from WT breast tissue (n = 4 patients), compared to RANK$^-$ luminal progenitors cells. Gene expression profiles of RANK$^+$ and RANK$^-$ cells were determined by RNA-seq. RANK$^+$ luminal progenitor cells exhibit a marked enrichment in cell cycle, DNA repair and metabolic pathway genes compared to RANK$^-$ cells.

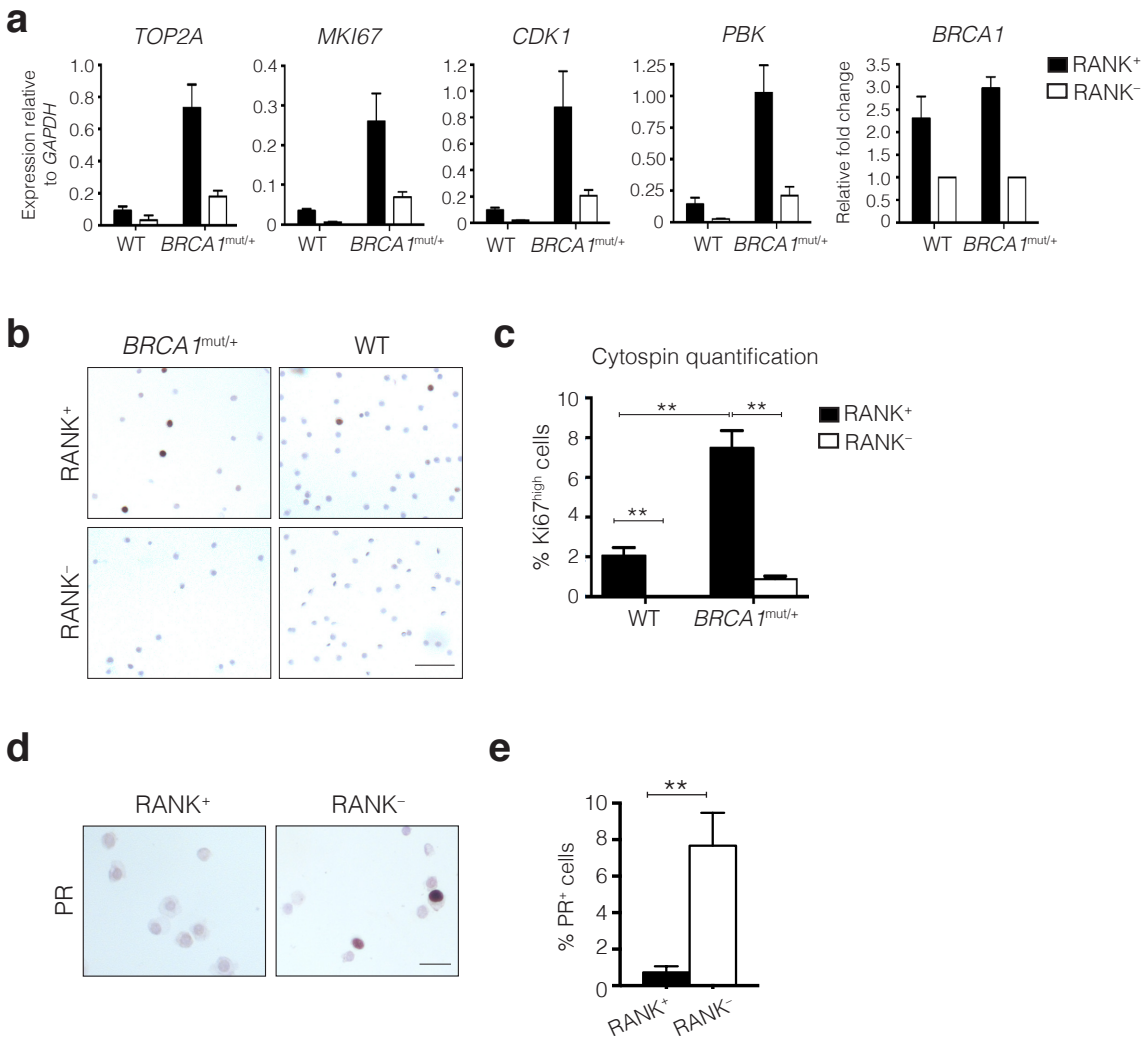

Figure 3.5: RANK$^+$ luminal progenitors are highly proliferative and PR$^-$

(**a**) Quantitative RT-PCR analysis of *TOP2A*, *MKI67*, *CDK1*, *PBK* and *BRCA1* expression in freshly sorted RANK$^+$ and RANK$^-$ luminal progenitor cells from WT (n = 3 patients) and *BRCA1*$^{mut/+}$ (n = 3 patients) breast tissue. Expression is shown relative to *GAPDH* for *TOP2A*, *MKI67*, *CDK1* and *PBK*, and as fold change in expression in RANK$^+$ cells relative to RANK$^-$ cells for *BRCA1*. Data represent mean ± s.e.m. (**b**) Representative images and (**c**) quantification of immunostaining for Ki67 on cytospins of freshly sorted RANK$^+$ and RANK$^-$ luminal progenitor cells from WT (n = 3 patients) and *BRCA1*$^{mut/+}$ (n = 3 patients) breast tissue. Scale bar, 100 μm. Data represent mean ± s.e.m. ***P* < 0.01. (**d**) Representative images and (**e**) quantification of immunostaining for progesterone receptor (PR) on cytospins of freshly sorted RANK$^+$ and RANK$^-$ luminal progenitor cells from WT breast tissue (n = 4 patients). Scale bar, 25 μm. Data represent mean ± s.e.m. ***P* < 0.01.

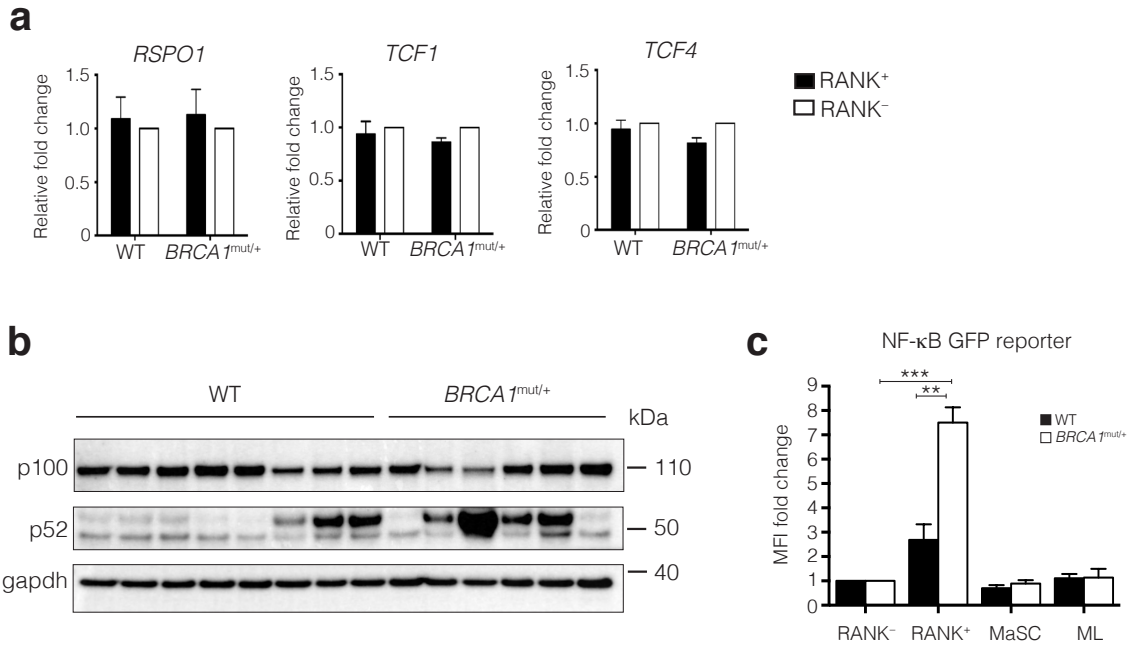

Figure 3.6: RANK$^+$ luminal progenitor cells have high NF-κB activity

(**a**) Quantitative RT-PCR analysis of *RSPO1, TCF1* and *TCF4* expression in freshly sorted RANK$^+$ and RANK$^-$ luminal progenitor cells from WT (n = 3 patients) and *BRCA1*$^{mut/+}$ (n = 3 patients) breast tissue. Expression is shown relative to *GAPDH.* Data represent mean ± s.e.m. (**b**) Western blot analysis of p100 (precursor) and p52 (active subunit) expression in sorted epithelial cells from WT (n = 8 patients) and *BRCA1*$^{mut/+}$ (n = 6 patients) breast tissue. GAPDH was used as a protein loading control. (**c**) NF-κB reporter activity in sorted RANK$^+$ luminal progenitor, RANK$^-$ luminal progenitor, MaSC and ML subpopulations from WT (n = 3 patients) and *BRCA1*$^{mut/+}$ (n = 3 patients) breast tissue. Freshly sorted cells were transduced with a lentiviral reporter and GFP was measured after 48 h by flow cytometry as a read out of reporter activity. Data are depicted as fold change in mean fluorescence intensity (MFI) of GFP in each subset relative to the RANK$^-$ luminal progenitor subset. Data represent mean ± s.e.m. $^{**}P < 0.01$, $^{***}P < 0.001$.

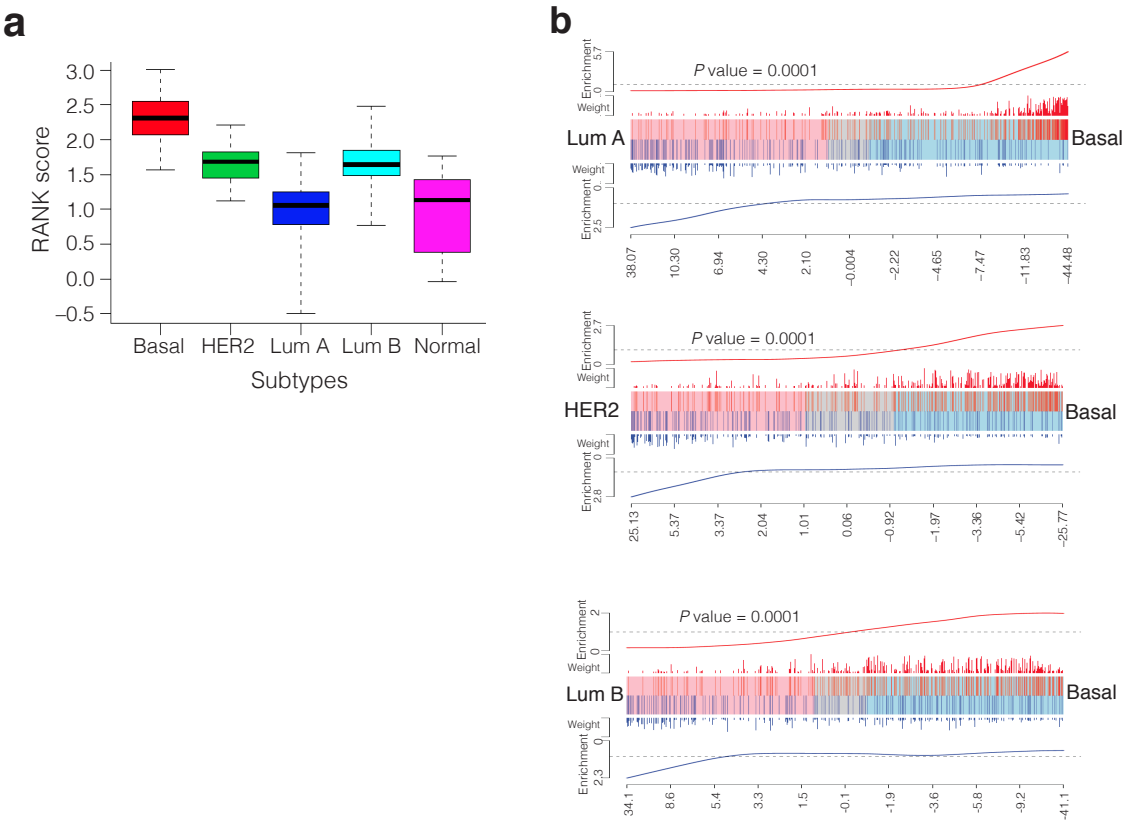

Figure 3.7: The RANK$^+$ gene signature correlates with basal-like breast cancers

(**a**) Box plots of RANK$^+$ signature expression scores by breast tumour subtype. The RANK signature (genes upregulated in RANK$^+$ compared to RANK$^-$ luminal progenitor cells, n = 4 patients) is strongly correlated with the basal subtype of breast cancer (n = 132 tumours). (**b**) Barcode plots showing association of the RANK$^+$ expression signature with the basal breast tumour subtype (n = 132 tumours), compared to luminal A (n = 391), luminal B (n = 183) or HER2$^+$ (n = 65) breast tumours. Genes are ordered from right to left as most upregulated to most downregulated in basal breast tumours. The *x*-axes show genewise *t*-statistics for the basal versus luminal A, luminal B or HER2$^+$ comparison. Vertical red bars designate genes upregulated in RANK$^+$ compared to RANK$^-$ cells, whereas blue bars designate downregulated genes. 'Weight' refers to the $\log_2$ fold-change in expression of each gene compared to RANK$^-$ cells, with a higher fold change represented as a greater bar length. ROAST *P* values measure the overall correlation.

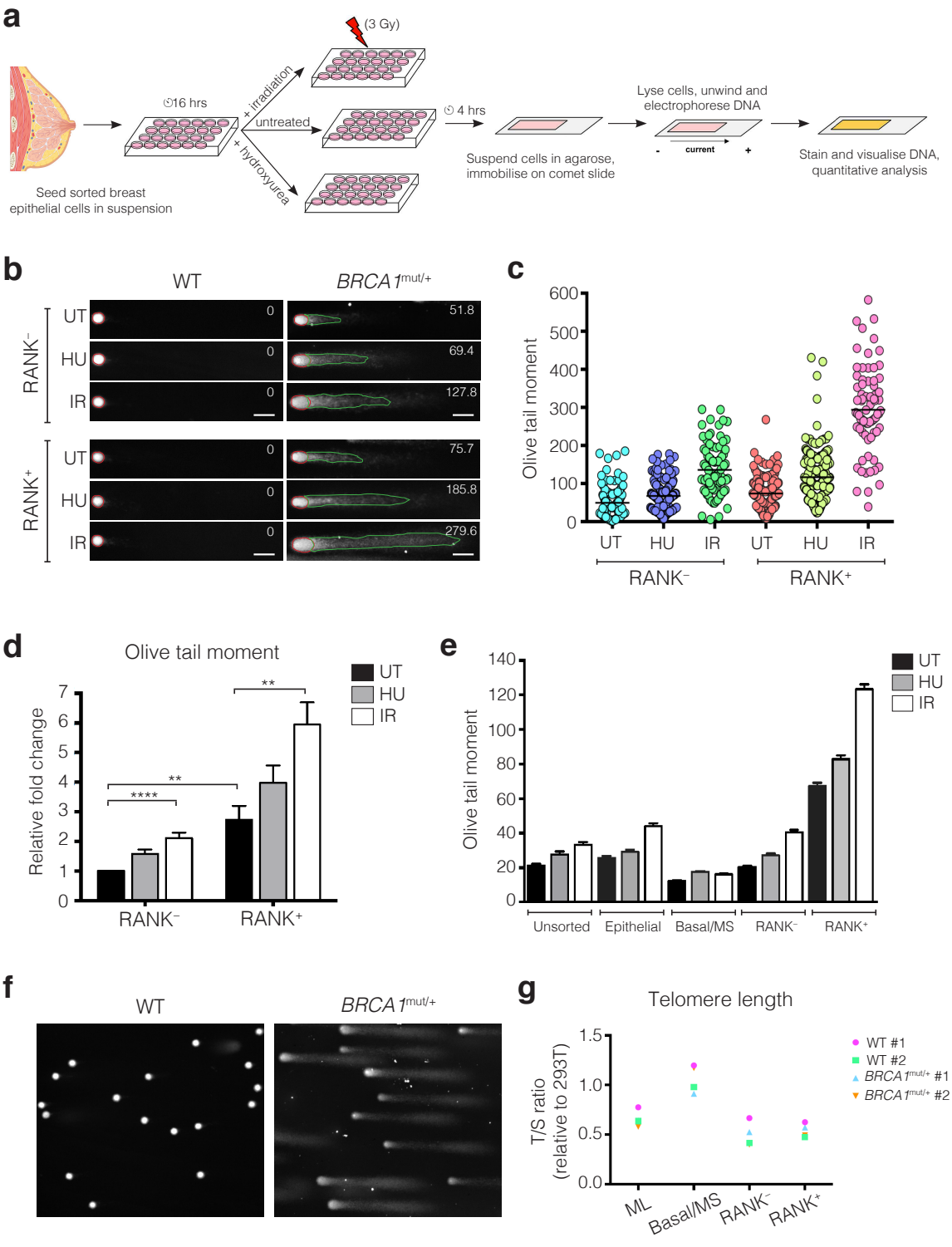
a
(3 Gy)
+ irradiation
untreated
+ hydroxyurea
16 hrs
4 hrs
Seed sorted breast epithelial cells in suspension
Suspend cells in agarose, immobilise on comet slide
Lyse cells, unwind and electrophorese DNA
current
Stain and visualise DNA, quantitative analysis
b
WT
BRCA1mut/+
RANK⁻
RANK⁺
UT
HU
IR
0
51.8
69.4
127.8
75.7
185.8
279.6
c
Olive tail moment
RANK⁻
RANK⁺
d
Olive tail moment
Relative fold change
UT
HU
IR
RANK⁻
RANK⁺
e
Olive tail moment
Unsorted
Epithelial
Basal/MS
RANK⁻
RANK⁺
f
WT
BRCA1mut/+
g
Telomere length
T/S ratio (relative to 293T)
ML
Basal/MS
RANK⁻
RANK⁺
WT #1
WT #2
BRCA1mut/+ #1
BRCA1mut/+ #2

Figure 3.8: *BRCA1*$^{mut/+}$ RANK^{+} progenitors have grossly deficient DNA repair mechanisms

(**a**) Overview of comet assay: freshly sorted human breast subsets were seeded into low-adherent plates and incubated for 16 h. Cells were then treated with hydroxyurea (10 mM), irradiated at 3 Gray (Gy) or left untreated. After 4 hours, cells were harvested and immobilised in agarose on a comet slide. Cells were then lysed, the DNA was unwound and gel electrophoresis was performed to induce migration of fragmented DNA. DNA was visualised with SyberGreen and imaged on a Nikon Upright 90i microscope. Quantification was performed using MetaMorph software. (**b**) Representative images of comets from RANK^{+} or RANK^{-} luminal progenitor cells isolated from WT (n = 5 patients) or *BRCA1*$^{mut/+}$ breast tissue (n = 6 patients). Values represent the olive tail moment (product of the tail length and the fraction of total DNA in the comet tail). Scale bar = 50 μm. UT, untreated; HU, hydroxyurea; IR, irradiated. (**c**) A representative *BRCA1*$^{mut/+}$ patient sample showing the olive tail moment for individual RANK^{+} or RANK^{-} cells. Bar, mean score. (**d**) Fold-change in olive tail moment in untreated versus treated RANK^{+} and RANK^{-} luminal progenitor cells isolated from *BRCA1*$^{mut/+}$ tissue (n = 6 patients). Data are depicted as fold-change relative to the untreated RANK^{-} subset. At least 200 cells per treatment condition were scored for each patient. Data represent mean ± s.e.m. $^{**}P < 0.01$, $^{****}P < 0.0001$. (**e**) Extended analysis of olive tail moment in *BRCA1*$^{mut/+}$ cell subsets. Shown are olive tail moments for unpurified cells (epithelium and stroma), epithelial cells, basal/MaSC, and RANK^{+} and RANK^{-} luminal progenitors cells. Comet tails are evident in all subsets, but are most pronounced in the RANK^{+} subset. Data represent mean ± s.e.m for n = 3 patients. (**f**) Representative image field showing irradiated RANK^{+} luminal progenitor cells from a WT or *BRCA1*$^{mut/+}$ patient sample. Dramatic differences in comet tail lengths between WT and *BRCA1*$^{mut/+}$ cells are clearly discernable. (**g**) Telomere length as determined by quantitative PCR using freshly sorted ML, Basal/MS, RANK^{-} and RANK^{+} luminal progenitor cells from WT (n = 2 patients) and *BRCA1*$^{mut/+}$ (n = 2 patients) breast tissue. Data are depicted as a T/S ratio, which is the ratio of the telomere gene signal to the signal-copy gene signal (albumin). Samples with a T/S > 1.0 have an average telomere length greater than that of the standard DNA (293T cells) while samples with a T/S < 1.0 have an average telomere length shorter than that of the standard DNA.

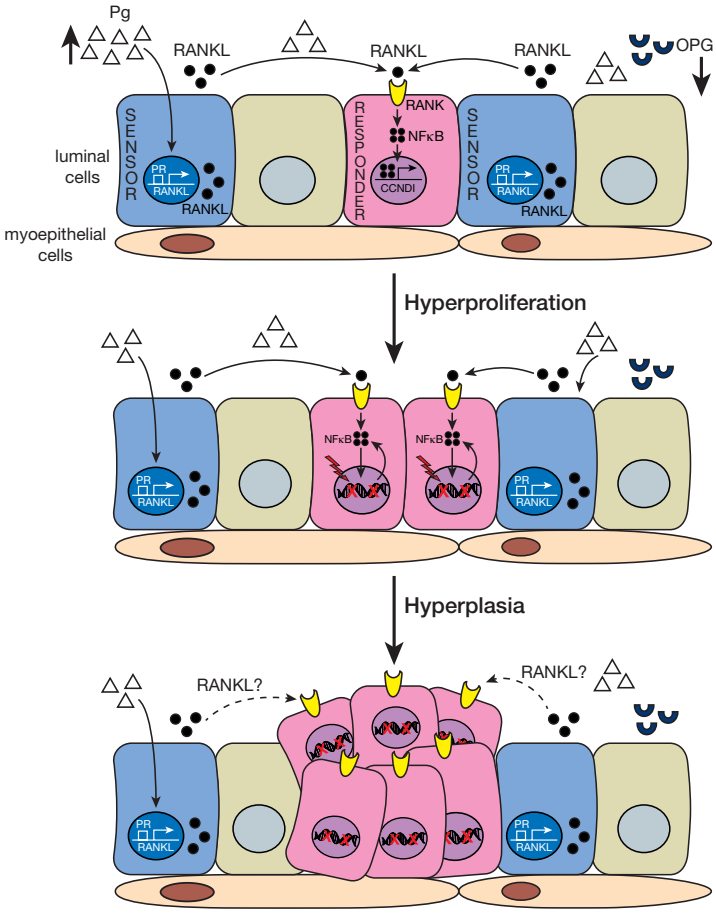

Figure 3.9: Schematic model of potential cellular and molecular mechanisms that drive hyperplasia in *BRCA1*-mutation carriers.

Progesterone-mediated activation of RANK in *BRCA1*$^{mut/+}$ luminal progenitor cells results in the activation of pro-proliferative signalling pathways such as NF-κB. Hyperactivation of this pathway in response to amplified hormonal signaling leads to augmented proliferation, and exerts undue pressure on the DNA repair machinery. Haploinsufficiency for DNA repair and the ensuing genomic instability in RANK^{+} cells leads to the acquisition of potentially deleterious mutations as well as the activation of NF-κB. Activation of the non-canonical p52 pathway results in a sustained response that further exacerbates genomic instability by triggering the proliferation of RANK^{+} cells, creating a positive feedback loop. NF-κB-mediated proliferation may be self-perpetuating (due to the DNA damage response), but RANK^{+} cells still remain highly responsive to progesterone-induced RANK signalling. Hyperplastic lesions are likely still progesterone-responsive, but transition to a hormone-independent state as tumorigenesis progresses.

Table 3.1 Classification of pathogenic *BRCA1* mutations in prophylactic mastectomy samples

Patient ID	Age (yrs)	BIC classification*	HGVS classification#
1	32	BRCA1 del exon 20	BRCA1g.71598-?_71681+?del (del exon20)
2	30	BRCA1 5632 T>A (V1838E)	BRCA1c.5513T>A (p.Val1838Glu)
3	40	BRCA1 5586 G>A (A1823T)	BRCA1c.5467G>A (p.Ala1823Thr)
4	27	BRCA1 IVS 6-2 del A	BRCA1c.302-2delA
5	44	BRCA1 185_186 del AG (STOP 39)	BRCA1c.68_69delAG (p.Glu23ValfsX17)
6	48	BRCA1 300 T>G (C61G)	BRCA1c.181T>G (p.Cys61Gly)
7	34	BRCA1 del exon 24	BRCA1g.82936-?_84436+?del (del exon24)
8	39	BRCA1 1996insTAGT	BRCA1c.1874_1877dupTAGT
9	33	BRCA1 5586 G>A (A1823T)	BRCA1c.5467G>A (p.Ala1823Thr)
10	29	BRCA1 3726 C>T (R1203X)	BRCA1c.3607C>T (p.Arg1203X)
11	30	BRCA1 4184_4187 del TCAA (STOP 1364)	BRCA1c.4065_4068delTCAA (p.Asn1355LysfsX10)
12	33	BRCA1 del exons 21_23	BRCA1g.77620-?_81094+?del (del exons21_23)
13	49	BRCA1 2919 C>T (Q934X)	BRCA1c.2800C>T (p.Gln934X)
14	39	BRCA1 3519 G>T (E1134X)	BRCA1c.3400G>T (p.Glu1134X)
15	26	BRCA1 2800_2801 del AA (STOP 901)	BRCA1c.2681_2682delAA (p.Lys894ThrfsX8)
16	41	BRCA1 Ex 13 Dup'n (STOP 1460) g44369_50449 dup 6kb	BRCA1g.44369_50449 dup6kb (dup exon13)
17	31	BRCA1 3374_3375 ins GA (STOP 1087)	BRCA1c.3254_3255dupGA (p. Leu1086AspfsX2)
18	32	BRCA1 2594 del C (STOP 845)	BRCA1c.2475delC (p.Asp825GlufsX21)
19	30	BRCA1 4744 del CT (STOP 1572)	BRCA1c.4625_4626delCT (p.Ser1542Trp)
20	31	BRCA1 5382_5383 ins C (STOP 1829)	BRCA1c.5266dupC (p. Gln1756ProfsX74)
21	42	BRCA1 633 del C (STOP 233)	BRCA1c.514delC (p.Gln172AsnfsX62)
22	35	BRCA1 2080 del A (STOP 700)	BRCA1c.1961delA (p.Lys654SerfsX47)
23	42	BRCA1 300 T>G (C61G)	BRCA1c.181T>G (p.Cys61Gly)
24	33	BRCA1 3600_3610 del GAAGATACTAG (STOP 1163)	BRCA1c.3481_3491delGAAGATACTAG (p.Glu1161PhefsX3)

*BIC: Breast cancer Information Core database (http://research.nhgri.nih.gov/bic/)

#HGVS: Human Genome Variation Society (http://www.hgvs.org)

Table 3.2 Classification of pathogenic *BRCA2* mutations in prophylactic mastectomy samples

Patient ID	Age (yrs)	BIC classification*	HGVS classification#
1	27	BRCA2 9106 C>T (Q2960X)	BRCA2c.8878C>T (p.Gln2960X)
2	25	BRCA2 2988 del C (STOP 959)	BRCA2c.2760delC (p.Ile921PhefsX39)
3	50	BRCA2 983_986 del ACAG (STOP 275)	BRCA2c.755_758delACAG (p.Asp252ValfsX24)
4	44	BRCA2 5910 C>G (Y1894X)	BRCA2c.5682C>G (p.Tyr1894X)
5	37	BRCA2 7895_7896 ins A (STOP 2565)	BRCA2c.7667dupA (p.Asn2556LysfsX10)
6	40	BRCA2 3036_3039 del ACAA (STOP 958)	BRCA2c.2808_2811delACAA (p.Ala938ProfsX21)
7	46	BRCA2 8803 del C (STOP 2862)	BRCA2c.8575delC (p.Gln2859LysfsX4)
8	40	BRCA2 5301_5302 ins A (STOP 1694)	BRCA2c.5073dupA (p.Trp1692MetfsX3)
9	33	BRCA2 1617_1618 del AG (STOP 466)	BRCA2c.1389_1390delAG (p.Val464GlyfsX3)
10	36	BRCA2 3199 A>G (N991D)	BRCA2c.2971A>G (p.Asn991Asp)

*BIC: Breast cancer Information Core database (http://research.nhgri.nih.gov/bic/)

#HGVS: Human Genome Variation Society (http://www.hgvs.org)

Table 3.3 RANK and RANKL expression in normal breast tissue

Gene	Mutation Status	No. samples	RANK H-score	*P* value	RANKL H-score	*P* value
BRCA1	*BRCA1*$^{mut/+}$	78	20.32	0.023	24.12	0.94
	Non-*BRCA1*	306	10.75		26.45	
BRCA2	*BRCA2*$^{mut/+}$	58	16.67	0.064	25.98	0.38
	Non-*BRCA2*	326	11.98		25.89	

Normal breast tissue (either tumour adjacent or contralateral breast) from the kConFab cohort was scored for BRCA1 and BRCA2 expression. The H-score incorporates intensity (scale of 0 - 3) multiplied by percent cells staining positive for RANK or RANKL. *P* values (Wilcoxon Rank Sum test) compare *BRCA1*-mutation carriers with non-*BRCA1* mutant tissue (i.e. women with a positive family history but no *BRCA1* germline mutation; includes *BRCA2*-mutation carriers) and *BRCA2*-mutation carriers with non-*BRCA2* mutant tissue (i.e. women with a positive family history but no *BRCA2* germline mutation; includes *BRCA1*-mutation carriers). Analysis was not adjusted for menopausal status or menstrual cycle stage.

Table 3.4 List of the 45 most upregulated genes in RANK$^+$ luminal progenitor cells compared to RANK$^-$ luminal progenitor cells.

No.	Gene ID	Symbol	Log fold change	Adjusted *P* value
1	7153	TOP2A	4.38	8.9E-07
2	10721	POLQ	4.11	2.6E-03
3	983	CDK1	4.06	8.9E-07
4	24137	KIF4A	4.01	2.1E-04
5	9212	AURKB	4.00	2.5E-04
6	10024	TROAP	3.90	4.8E-04
7	4605	MYBL2	3.88	5.7E-06
8	6241	RRM2	3.80	3.3E-03
9	4288	MKI67	3.78	8.9E-07
10	259266	ASPM	3.70	2.0E-05
11	9088	PKMYT1	3.70	6.2E-03
12	55872	PBK	3.54	8.0E-05
13	146909	KIF18B	3.54	1.1E-03
14	9787	DLGAP5	3.54	6.7E-03
15	55355	HJURP	3.53	2.9E-04
16	221150	SKA3	3.46	2.9E-02
17	150468	CKAP2L	3.38	1.9E-03
18	10403	NDC80	3.37	5.8E-03
19	55635	DEPDC1	3.37	5.3E-03
20	128239	IQGAP3	3.36	1.1E-05
21	23397	NCAPH	3.34	6.4E-04
22	83540	NUF2	3.32	1.6E-03
23	157570	ESCO2	3.27	2.0E-04
24	8318	CDC45	3.26	3.2E-04
25	1870	E2F2	3.26	1.2E-02
26	56992	KIF15	3.25	7.0E-04
27	699	BUB1	3.22	7.0E-04
28	57405	SPC25	3.21	4.8E-04
29	55771	PRR11	3.21	2.0E-04
30	220134	SKA1	3.21	2.1E-03
31	113130	CDCA5	3.20	1.8E-03
32	3161	HMMR	3.08	9.7E-03
33	2305	FOXM1	3.07	3.6E-04
34	9768	KIAA0101	3.04	1.2E-03
35	79801	SHCBP1	3.03	5.2E-04
36	64151	NCAPG	3.01	1.0E-04
37	1063	CENPF	2.99	1.5E-02
38	3833	KIFC1	2.87	1.0E-04
39	144455	E2F7	2.78	5.9E-03
40	7272	TTK	2.77	3.1E-03
41	54478	FAM64A	2.76	6.6E-03
42	374393	FAM111B	2.76	1.5E-03
43	332	BIRC5	2.75	8.1E-03
44	3832	KIF11	2.69	2.1E-04
45	9156	EXO1	2.67	3.4E-02

Table 3.5 List of the 45 most downregulated genes in RANK$^+$ luminal progenitor cells compared to RANK$^-$ luminal progenitor cells.

No.	Gene ID	Symbol	Log fold change	Adjusted *P* value
1	5999	RGS4	-3.16	0.029
2	118430	MUCL1	-2.94	0.015
3	3560	IL2RB	-2.84	0.038
4	6898	TAT	-2.82	0.019
5	399	RHOH	-2.77	0.025
6	63895	PIEZO2	-2.76	0.040
7	9077	DIRAS3	-2.66	0.026
8	10761	PLAC1	-2.64	0.026
9	7031	TFF1	-2.58	0.004
10	1734	DIO2	-2.51	0.000
11	6519	SLC3A1	-2.50	0.022
12	58	ACTA1	-2.46	0.004
13	10563	CXCL13	-2.43	0.010
14	652	BMP4	-2.42	0.023
15	4588	MUC6	-2.34	0.007
16	80832	APOL4	-2.14	0.014
17	51673	TPPP3	-2.09	0.043
18	139221	MUM1L1	-2.03	0.032
19	6236	RRAD	-2.03	0.004
20	5646	PRSS3	-2.03	0.020
21	9518	GDF15	-2.00	0.008
22	10551	AGR2	-1.97	0.019
23	8671	SLC4A4	-1.93	0.042
24	80736	SLC44A4	-1.85	0.005
25	91074	ANKRD30A	-1.77	0.003
26	57758	SCUBE2	-1.77	0.009
27	2354	FOSB	-1.76	0.015
28	8013	NR4A3	-1.74	0.003
29	7033	TFF3	-1.73	0.046
30	1264	CNN1	-1.71	0.024
31	11259	FILIP1L	-1.71	0.006
32	80008	TMEM156	-1.65	0.048
33	54855	FAM46C	-1.65	0.037
34	3899	AFF3	-1.64	0.008
35	29881	NPC1L1	-1.62	0.036
36	7021	TFAP2B	-1.62	0.009
37	83897	KRTAP3-2	-1.59	0.011
38	100126791	EGOT	-1.56	0.019
39	273	AMPH	-1.56	0.032
40	5744	PTHLH	-1.55	0.043
41	84665	MYPN	-1.47	0.046
42	26353	HSPB8	-1.47	0.001
43	10538	BATF	-1.42	0.018
44	143098	MPP7	-1.41	0.041
45	8821	INPP4B	-1.39	0.018

Table 3.6 GO groups upregulated in RANK$^+$ luminal progenitor cells compared to RANK$^-$ luminal progenitor cells

GOBPID	GO term	*P* value	No. genes
GO:0000278	mitotic cell cycle	1.32E-40	132
GO:0000280	nuclear division	1.16E-35	90
GO:0051301	cell division	8.28E-35	107
GO:0048285	organelle fission	1.59E-33	90
GO:1903047	mitotic cell cycle process	3.59E-33	112
GO:0007049	cell cycle	9.21E-33	161
GO:0022402	cell cycle process	4.41E-31	133
GO:0007067	mitotic nuclear division	1.66E-30	73
GO:0007059	chromosome segregation	8.36E-26	46
GO:0000793	condensed chromosome	7.49E-24	44
GO:0000777	condensed chromosome kinetochore	1.05E-20	30
GO:0044770	cell cycle phase transition	7.94E-19	66
GO:0044772	mitotic cell cycle phase transition	1.29E-18	65
GO:0006260	DNA replication	1.79E-18	51
GO:0000819	sister chromatid segregation	5.78E-17	24
GO:0005819	spindle	1.09E-15	44
GO:0006261	DNA-dependent DNA replication	3.15E-14	29
GO:0000075	cell cycle checkpoint	1.11E-13	40
GO:0010564	regulation of cell cycle process	1.90E-13	55
GO:0051276	chromosome organization	1.30E-10	69
GO:0022616	DNA strand elongation	2.24E-09	13
GO:0000086	G2/M transition of mitotic cell cycle	7.60E-09	26
GO:0000082	G1/S transition of mitotic cell cycle	9.39E-09	31
GO:0006302	double-strand break repair	1.00E-08	23
GO:0044843	cell cycle G1/S phase transition	1.16E-08	31
GO:0006281	DNA repair	2.47E-08	43
GO:0000724	double-strand break repair via HR	2.79E-08	16
GO:0007091	metaphase/anaphase transition of mitotic cell cycle	3.33E-08	13
GO:0044784	metaphase/anaphase transition of cell cycle	3.33E-08	13
GO:0000725	recombinational repair	3.48E-08	16
GO:0000910	cytokinesis	5.16E-08	20

Chapter 4: RANKL inhibition as a promising breast cancer prevention strategy for *BRCA1*-mutation carriers

4.1 Introduction

Despite their significant cancer predisposition, carriers of *BRCA1/2* mutations are currently faced with few effective clinical options to reduce their breast cancer risk. Heightened surveillance through regular breast examination can promote early detection of malignancy, and the introduction of breast magnetic resonance imaging (MRI) has improved screening effectiveness (Robson and Offit, 2007). However, interval cancers are common, and often present as advanced stage tumours (i.e. node positive) (Kriege et al., 2004). Coupled with this, *BRCA1*-mutated tumours are associated with a high incidence of disease recurrence and there are currently no therapies to supplement traditional chemotherapy. Therefore, breast cancer prevention remains the most viable approach for these high risk women.

Presently, the most effective means of primary prevention in *BRCA1*-mutation carriers is the surgical removal of breasts and ovaries. Prophylactic mastectomy ensures a very high protection from breast cancer (Domchek et al., 2010; Meijers-Heijboer et al., 2001; Rebbeck et al., 2004), while the benefit of risk-reducing salphingo-oophorectomy (RRSO) is less clear. Several retrospective studies have reported a breast cancer risk reduction of approximately 50% following RRSO (Domchek et al., 2006; Domchek et al., 2010; Eisen et al., 2005; Kauff et al., 2008; Kramer et al., 2005; Rebbeck et al., 1999; Rebbeck et al., 2002), although this was disputed in a recent study that utilised a revised study design (Heemskerk-Gerritsen et al., 2015). Bilateral oophorectomy, however, did delay tumour onset in *Brca1/p53*-deficient mice (Bachelier et al., 2005). Prophylactic mastectomy and RRSO, while significantly reducing breast cancer risk, are highly invasive and irreversible. Moreover, the long-term effects (such as loss of fertility following RRSO) can be highly distressing for young, asymptomatic women. Indeed clinical uptake is often low, with only 11% of *BRCA1/2*-mutation carriers currently opting for

prophylactic mastectomy in Australia (Kiely et al., 2010; Meiser et al., 2003; Phillips et al., 2006). This highlights the need for non-surgical alternatives. Importantly, despite the ambiguous effect on breast cancer risk, RRSO is still highly recommended to *BRCA1/2*-mutation carriers later in life (>35 years of age) due to their increased susceptibility to ovarian cancer.

In the previous chapter, we defined a novel role for the RANKL signalling axis in contributing to breast oncogenesis in *BRCA1*$^{mut/+}$ breast tissue. The augmented proliferation of RANK^{+} luminal progenitor cells combined with their predilection for DNA damage suggested they are prime cellular targets for basal-like breast tumours arising in *BRCA1*-mutation carriers. Based on these findings, we speculate that specific targeting of this progenitor subset via RANKL blockade could be a novel prevention strategy for these high-risk individuals (Figure 4.1). This approach would remove both the initialising mitogenic signal to RANK^{+} progenitors by disrupting their link to progesterone signalling as well as preventing further cyclical stimulation of the DNA-damage response/NF-κB pathway in RANK^{+} cells. Notably, the human-specific RANKL blocking antibody Denosumab (AMG-162) (Kostenuik et al., 2009) was fast-tracked by the FDA for the treatment of osteoporosis in postmenopausal women and for the prevention of skeletal-related events in patients with bone metastasis, and is now in routine clinical use (Lipton et al., 2007; McClung et al., 2006). This suggests that denosumab could be 'repurposed' as a breast cancer preventive therapy for *BRCA1*-mutation carriers.

In this chapter, we have investigated the efficacy of RANKL blockade in attenuating progesterone-induced cellular proliferation and *BRCA1*-associated mammary tumorigenesis. Several models of *BRCA1*-mutated breast cancer and the *BRCA1*$^{mut/+}$ preneoplastic phase were employed, including three-dimensional human breast organoids, breast biopsies from *BRCA1*-mutation carriers as well as the *MMTV-cre-Brca1*$^{fl/fl}$*p53*$^{+/-}$ mouse model. Importantly we have also directly compared pharmacological inhibition of RANKL with existing prevention strategies, and explored RANKL blockade in alternative mouse models of basal-like breast cancer. The findings have significant clinical implications and could directly impact the lives of *BRCA1*-mutation carriers.

4.2 Results

4.2.1 RANKL inhibition attenuates proliferation in breast organoids and breast tissue biopsies from *BRCA1*-mutation carriers

The first step in evaluating RANKL blockade as a prevention strategy was to investigate the significance of RANKL inhibition during the preneoplastic phase in *BRCA1*$^{mut/+}$ breast tissue. Given that primary human breast epithelial cells grown *in vitro* lose steroid hormone receptor expression, a requirement for studying paracrine factors, we optimised an *ex vivo* three-dimensional breast organoid system that is responsive to progesterone signalling based on the method of Tanos et al., 2013. The cellular architecture of breast epithelium was preserved in organoids isolated from fresh human breast specimens, with immunostaining confirming the presence of bilayered ducts and TDLUs comprising both luminal (K18 positive) and basal (K14 and p63 positive) cells, as well as retention of PR expression (Figure 4.2a). Organoids from both WT and *BRCA1*$^{mut/+}$ breast tissue responded to exogenous progesterone treatment and exhibited an increase in epithelial cell proliferation based on Ki67-positive cells (Figure 4.2b,c and Figure 4.3). However, the mitogenic response to progesterone was more profound in *BRCA1*$^{mut/+}$ tissue compared to WT (Figure 4.2c), consistent with findings in *Brca1*-deficient mice (Ma et al., 2006; Poole et al., 2006). Importantly, concomitant exposure to the RANKL-inhibitor denosumab blocked the progesterone-stimulated increase in Ki67^{+} cells in *BRCA1*$^{mut/+}$ organoids (Figure 4.2b,c and Figure 4.3). Thus, ostensibly normal human *BRCA1*$^{mut/+}$ breast tissue is hyper-responsive to progesterone and RANKL blockade attenuates this response.

The *in vivo* effect of RANKL inhibition on breast tissue from *BRCA1*-mutation carriers was next assessed via the first three subjects recruited to a pilot clinical study, 'BRCA-D' (ACTRN12614000694617). The BRCA-D study is a pre-operative window study evaluating the safety and biological effects of denosumab on normal breast tissue from premenopausal *BRCA1* and *BRCA2*-mutation carriers, as well as high risk WT patients with a strong family history of breast cancer. Three *BRCA1*-mutation carriers were treated with denosumab over a three-month period, and Ki67 expression was scored in pre- and post-treatment biopsies that were

collected during the luteal phase of the menstrual cycle (Figure 4.4a). Notably, a substantial reduction in Ki67 was observed in each subject, from a mean value of 2.5 ± 1.2% to 0.5 ± 0.2% (Figure 4.4b,c). Thus, RANKL blockade markedly attenuates breast epithelial proliferation in *BRCA1*-mutation carriers.

4.2.2 RANKL inhibition attenuates mouse mammary progenitor activity

To determine whether RANKL inhibition can block luminal progenitor activity *in vivo*, we injected adult virgin mice (8 weeks of age) with an anti-RANKL monoclonal antibody. Mammary glands were harvested after 7 days and *in vitro* colony-forming assays were performed with freshly sorted basal/MaSC cells ($Lin^{-}CD29^{hi}CD24^{+}$), hormone receptor-negative (HR^{-}) luminal progenitor cells ($Lin^{-}CD29^{lo}CD24^{+}CD49b^{+}Sca1^{-}$) and HR^{+} luminal progenitor cells ($Lin^{-}CD29^{lo}CD24^{+}CD49b^{+}Sca1^{+}$) (Figure 4.5a). Notably, clonogenic activity was markedly reduced in the HR^{-} luminal progenitor subset, previously shown to express RANK (Pal et al., 2013), while no difference in colony formation was observed in the HR^{+} luminal progenitor population that is $RANK^{-}$ (Figure 4.5b,c). As previously reported, a significant reduction in clonogenic activity was observed in the basal/MaSC subset (Asselin-Labat et al., 2010) (Figure 4.5b,c). Therefore RANKL inhibition can attenuate progenitor and stem cell activity *in vivo*. It was not possible to fractionate $RANK^{+}$ and $RANK^{-}$ subsets as in the case of human tissue, owing to a lack of suitable anti-RANK antibodies for flow cytometry.

4.2.3 RANKL inhibition curtails tumorigenesis in *Brca1*-deficient mice

To determine the efficacy of RANKL inhibition as a breast cancer prevention strategy, we utilised the *MMTV-cre/Brca1*$^{fl/fl}$*/p53*$^{+/-}$ mouse model, previously shown to develop basal-like tumours that recapitulate features of human *BRCA1*-mutated breast cancer (Brodie et al., 2001; Xu et al., 1999; Table 1.1). The relevance of this mouse tumour model was confirmed by immunostaining mammary tumours for ER, PR, K14, K18 and Ki67, demonstrating a basal-like phenotype (Figure 4.6). Importantly, immunostaining of *MMTV-cre/Brca1*$^{fl/fl}$*/p53*$^{+/-}$ tumours revealed abundant RANK expression (14/14 tumours), whereas the majority of tumours from *p53*$^{+/-}$ mice did not express RANK (3/10 tumours) (Figure 4.7a). $RANKL^{+}$ positive

cells were also present in *MMTV-cre/Brca1$^{fl/fl}$/p53$^{+/-}$* mammary tumours, albeit at a low frequency, while they were completely absent from *p53$^{+/-}$* tumours (Figure 4.7a). RANKL could therefore be important for sustaining proliferation within *MMTV-cre/Brca1$^{fl/fl}$/p53$^{+/-}$* tumours. Moreover, hyperplastic mammary tissue from *MMTV-cre/Brca1$^{fl/fl}$/p53$^{+/-}$* mice exhibited profoundly high levels of RANK (6/6 mice), in contrast to those from *p53$^{+/-}$* mice (0/4 mice) (Figure 4.7b). The specificity of the anti-RANK and anti-RANKL antibodies was validated by immunostaining mammary glands during different stages of development, revealing a marked increase in expression during pregnancy as expected (Figure 4.7c). These data demonstrate that the *MMTV-cre/Brca1$^{fl/fl}$/p53$^{+/-}$* strain represents a suitable mouse model to study prevention through RANKL inhibition.

We used two alternative strategies to test the effect of RANKL blockade on tumour development in the *MMTV-cre/Brca1$^{fl/fl}$/p53$^{+/-}$* mouse model. In the first approach, mammary gland transplantation studies were performed with preneoplastic (histologically normal) mammary glands isolated from *MMTV-cre/Brca1$^{fl/fl}$/p53$^{+/-}$* female mice at 12 weeks of age. Freshly sorted mammary epithelial cells (Lin$^-$ CD24$^+$) were transplanted into the cleared inguinal fat pads of four-week old immunocompromised *RAG1$^{-/-}$* recipients to generate ductal outgrowths (Figure 4.8a). Six weeks following reconstitution, recipients were randomised to receive either a mouse IgG1 control antibody or the RANKL inhibitor OPG-Fc, which acts as a decoy receptor through binding RANKL. Excitingly, a significant delay in tumour onset was observed in mice treated with OPG-Fc compared to control mice (P = 0.0002) (Figure 4.8b). Median tumour onset was 215 days in the control arm, whereas median onset was not reached in OPG-Fc-treated mice and only 6/17 (35%) of mice developed tumours by the experimental end-point (day 250) (Figure 4.8b). Notably, histological evaluation of mammary glands at this time-point revealed dramatically reduced hyperplasia in OPG-Fc-treated mice compared to control mice (Figure 4.8c).

In the second approach, *MMTV-cre/Brca1$^{fl/fl}$/p53$^{+/-}$* mice were randomised at 9 weeks of age to treatment with a neutralising anti-mouse RANKL monoclonal antibody or control antibody and monitored for tumour onset (Figure 4.9a). Similar to the OPG-Fc inhibitor, a significant delay in tumour onset was evident in mice

treated with anti-RANKL compared to control mice, with median tumour onset at 177 days compared to 123 days, respectively (P = 0.0044, Figure 4.9b). Thus, through two independent *in vivo* chemoprevention studies, we have demonstrated that pharmacologic inhibition of RANKL significantly impacts on mammary tumour development in *Brca1*-deficient mice.

4.2.4 The efficacy of RANKL blockade is comparable to oophorectomy

Given that risk-reducing salphingo-oophorectomy (RRSO) has shown efficacy as a breast cancer preventive therapy in *BRCA1*-mutation carriers and *Brca1*-deficient mice, we directly compared this highly invasive approach with pharmacological RANKL blockade. To generate a preclinical model, sorted epithelial cells (Lin^- $CD24^+$) cells were harvested from preneoplastic mammary tissue of young adult *MMTV-cre/Brca1*$^{fl/fl}$*/p53*$^{+/-}$ mice and transplanted into the cleared fat pads of syngeneic recipient mice (F1 FVB x BALB/c, Figure 4.10a). Six weeks after mammary gland reconstitution, mice were randomised to undergo an oophorectomy or a sham operation followed by treatment with a mouse IgG1 control antibody or to receive treatment with the RANKL inhibitor OPG-Fc (Figure 4.10a). Median tumour onset was 206 days in the vehicle group, whereas the tumour latency was significantly attenuated in mice that underwent an oophorectomy or received RANKL blockade (P < 0.05, Figure 4.10b). Thus, our data implicates RANKL inhibition as a prevention strategy that is comparable to the benefit of oophorectomy.

4.2.5 RANKL blockade delays tumour onset in *MMTV-Wnt1* mice

To explore whether RANKL blockade may be more broadly applicable for breast cancer prevention, the efficacy of RANKL inhibition in the *MMTV-Wnt1* mouse model was investigated. The *MMTV-Wnt1* strain was chosen following the observation of substantial RANK expression in tumours (5/8) and preneoplastic mammary tissue (10/10) harvested from these mice (Figure 4.11a,b). In contrast to *MMTV-cre/Brca1*$^{fl/fl}$*/p53*$^{+/-}$ mice, RANKL expression was not observed in *MMTV-Wnt1* tumours (Figure 4.11a). For the prevention study, 8-week old *MMTV-Wnt1* mice were assigned at random to receive either a mouse IgG1 control antibody or

OPG-Fc (Figure 4.11c). Importantly, a marked delay in tumour latency was observed in mice treated with OPG-Fc, with tumour latency increasing from 115 days in the control arm to 240 days in the OPG-Fc arm (P = 0.0058, Figure 4.11d). Thus, RANKL blockade may also be a useful prevention strategy for other individuals at a high risk of developing breast cancer.

4.3 Discussion

BRCA1-mutation carriers are currently faced with few options to reduce their risk of developing breast cancer. The identification of an effective, non-surgical prevention therapy remains a 'holy-grail' for the field. In this chapter we have explored RANKL blockade as a potential breast cancer prevention strategy for *BRCA1*-mutation carriers, and provide compelling evidence to suggest targeting this pathway may effectively minimise the breast cancer risk associated with a *BRCA1* mutation.

To study the effects of RANKL blockade during the preneoplastic phase in *BRCA1*$^{mut/+}$ breast tissue, a three-dimensional breast organoid culture system was utilised. The significance of the extracellular matrix and three-dimensional structure for mammary epithelial cell biology and cell signalling is well documented (Kass et al., 2007; Roskelley et al., 1994). Human breast epithelial cells grown in two-dimensions lose expression of hormone receptors, while three-dimensional cultures using Matrigel maintain hormone receptor expression although *Wnt4* and *RANKL* are not induced by progesterone in this system (Graham et al., 2009). By isolating three-dimensional breast organoids, we have generated a model of human *BRCA1*$^{mut/+}$ breast tissue that preserves key features of the *in situ* tissue. We demonstrated that *BRCA1*$^{mut/+}$ organoids were hyper-responsive to progesterone and that RANKL neutralisation profoundly inhibited progesterone-induced proliferation. Importantly, this was confirmed *in vivo*, where RANKL inhibition markedly diminished epithelial cell proliferation in breast biopsies from *BRCA1*-mutation carriers who were treated with denosumab over a three-month period. Thus, RANKL blockade showed remarkable efficacy in preneoplastic human *BRCA1*-mutant breast tissue.

Through multiple *in vivo* preclinical prevention studies, we provided evidence that RANKL inhibition significantly impacts on mammary tumour development and hyperplasia in *Brca1/p53*-deficient mice. A profound delay in tumour onset was observed in mice treated with either OPG-Fc or an anti-RANKL monoclonal antibody, comparable to the effects of oophorectomy. The use of two independent pharmacologic RANKL inhibitors in this study was informative, since OPG-Fc also exhibits some affinity for binding the TNF-related apoptosis-inducing ligand (TRAIL)

(Bossen et al., 2006; Truneh et al., 2000). The efficacy demonstrated by both OPG-Fc and the specific anti-RANKL neutralising antibody allowed us to exclude TRAIL-inhibition as the mechanism by which OPG-Fc delays tumour onset rather than through RANKL blockade. It is conceivable that the impact of RANKL inhibition may be more pronounced in human *BRCA1*-mutation carriers than in *Brca1/p53*-deficient mice because mice bearing heterozygous *Brca1* mutations do not develop spontaneous breast (or ovarian) tumours, and therefore prevention studies must be performed using mice in which both alleles have been lost. Therefore it is possible that the preneoplastic period is accelerated compared to the human setting. A delay in tumour onset following RANKL blockade was also observed in the *MMTV-Wnt1* mouse model, which develops $RANK^+$ tumours that have been previously shown to resemble basal-like cancers (Herschkowitz et al., 2007). This is consistent with a previous report demonstrating a delay in tumour onset in *MMTV-Wnt1* mice following oophorectomy (Bocchinfuso et al., 1999). This implies that RANKL inhibition may also be applicable to other women at high risk of developing breast cancer, although this would require identification of suitable biomarker(s) to identify those who would benefit since inclusion cannot be based on the presence of a germline mutation as in the case of *BRCA1*. It is not known whether post-menopausal *BRCA1*-mutation carriers would benefit from RANKL blockade, although it is unlikely given that the loss of progesterone would abrogate signalling through the RANKL axis. Indeed, the BRCA-D study included a fourth *BRCA1*-mutation carrier who was post-menopausal and for whom denosumab therapy did not influence cell proliferation (data not shown).

Notably, a concurrent study showed that genetic ablation of RANK in the mammary epithelium of *Brca1/p53*-deficient mice under the control of either the *WapCre*^{C} or *K5* promoter substantially delayed the onset of mammary tumours and hyperplasia, respectively (Sigl et al., 2016). While these findings support our data, it is important to note that genetic inactivation of *Rank* does not recapitulate a prevention study performed in humans, since the *K5* and *WapCre*^{C} promoters are active in embryogenesis (Van Keymeulen et al., 2011) and puberty (Lin et al., 2004), respectively. Interestingly, a previous chemoprevention study performed in *Brca1/p53*-deficient mice utilising the PR antagonist mifepristone demonstrated a complete abrogation of tumour development, with no tumours appearing over the

12-month study period. However, mifepristone is not a selective PR antagonist and it binds to glucocorticoid receptors with high affinity (Baulieu, 1989). Therefore, the observed prevention in this study may be partly attributable to the anti-glucocorticoid effects (Drost and Jonkers, 2009).

Alternative chemoprevention strategies for *BRCA1*-mutation carriers are currently under investigation, for example the selective oestrogen receptor modulator tamoxifen (reviewed in Phillips and Lindeman, 2014). There has only been one trial to specifically evaluate its efficacy in the primary prevention setting, whereby women at high risk of breast cancer were randomised to receive either daily tamoxifen or placebo for a period of 5 years (King et al., 2001). Although there was a 62% reduction in breast cancer risk among *BRCA2*-mutation carriers taking tamoxifen, the risk ratio for breast cancer in *BRCA1*-carriers was 1.67 (95% confidence interval 0.32 – 10.7) and the sample size was small (n = 19 *BRCA1*/2 carriers). Notably, tamoxifen treatment o*f Brca1/p53*-deficient mice has been reported to cause an acceleration of mammary tumour development, likely due to the alteration in tamoxifen agonist/antagonist activity following *BRCA1* loss (Jones et al., 2005). In the clinic, the uptake of tamoxifen for prevention has been poor. Given reports that endometrial cancer risk may be amplified in *BRCA1*-mutation carriers taking tamoxifen (Nelson et al., 2013; Phillips et al., 2013), it is unlikely that tamoxifen will be formally evaluated in a prevention study for these high-risk women. Tamoxifen does appear to significantly reduce the risk of contralateral breast cancer in patients carrying mutant *BRCA1* with primary unilateral breast cancer, with a relative risk of 0.47 (95% confidence interval 0.37 – 0.60) demonstrated in a recent meta-analysis (Xu et al., 2015).

Recently, it has been suggested that the PARP1 inhibitors, veliparib and olaparib, may delay tumour development in *Brca1*/*p53*-deficient mice (To et al., 2014). PARP inhibitors exploit the disrupted DNA repair machinery present in *BRCA1*-deficient cells, and induce apoptosis by increasing genomic instability. They have shown efficacy in the treatment of *BRCA1*-mutated breast tumours in phase II and III trials (reviewed in Drost and Jonkers, 2014), and could potentially be explored for breast cancer prevention. However, the implementation of PARP inhibitors for chemoprevention is potentially problematic, given that serious side effects such as

myelodysplastic syndrome/Acute Myeloid Leukemia have been reported (Audeh et al., 2010). There is also concern that the tumours that eventually develop (since treatment delayed but did not prevent tumorigenesis in mice, To et al., 2014) may be PARP-resistant and thus not amenable to PARP inhibitors or platinum-based therapies for treatment. Thus, RANKL blockade represents a more favourable prevention strategy. Finally, given that DNA damage-induced NF-κB activity is a key feature of *BRCA1*-deficient cells (Sau et al., 2016), NF-κB may be a potential target for chemoprevention in *BRCA1*-mutation carriers. However, the central role of NF-κB in many physiological processes such as innate and adaptive immunity, inflammation and cell death, suggests there will be significant toxicity and immunosuppression associated with long-term use (Baud and Karin, 2009). Thus, NF-κB inhibitors are unlikely to be evaluated in the clinic as a viable breast cancer prevention strategy.

In summary, the findings presented in this chapter point to RANKL inhibition as a compelling strategy for breast cancer prevention in *BRCA1*-mutation carriers who otherwise face few effective options to minimise their risk. These findings are likely to culminate in a large international prevention study in the future. We believe that denosumab could offer a favourable alternative to prophylactic mastectomy, or could at least 'buy time' for younger *BRCA1*-mutation carriers who are considering a mastectomy. In addition, given that RANKL blockade was shown to be as effective as oophorectomy for breast cancer prevention in *Brca1*-deficient mice, this could delay the need for *BRCA1*-mutation carriers to undergo RRSO, allowing them to remain pre-menopausal with intact ovarian function until later in life. As a corollary, continued denosumab therapy after RRSO could also help to abrogate the associated loss of bone mineral density. If RANKL inhibition proves to be an effective breast cancer prevention strategy, then it could potentially benefit thousands of *BRCA1*-mutation carriers and possibly other women at high risk of developing breast cancer.

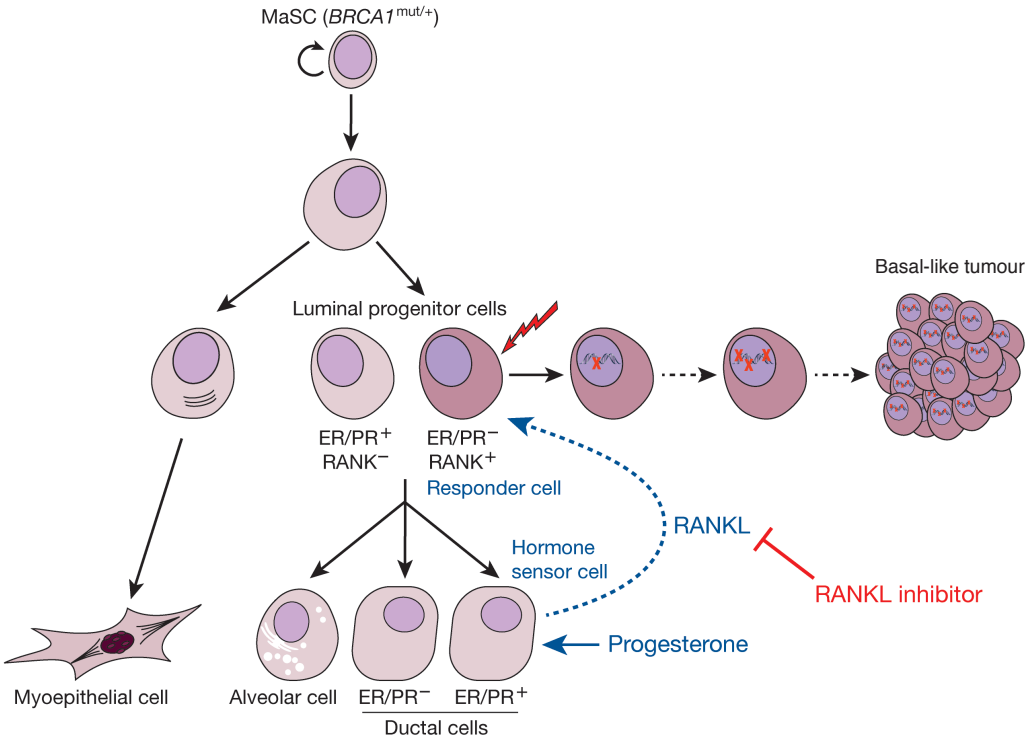

Figure 4.1: Schematic model of the human breast epithelial hierarchy and breast oncogenesis in *BRCA1*-mutation carriers

BRCA1$^{mut/+}$ breast epithelium contains both RANK^{+} and RANK^{-} luminal progenitor subsets. RANK^{+} progenitors (responder cells) do not express hormone receptors but can receive mitogenic signals from progesterone via the secretion of RANKL from mature ductal cells (hormone sensor cells). *BRCA1*-associated tumorigenesis may result from the acquisition of genetic alterations in the highly proliferative RANK^{+} luminal progenitor subset. RANKL inhibition blocks progesterone-induced signals from mature ductal cells to RANK^{+} cells, thereby reducing mitogenic stimulation and potentially delaying oncogenesis. ER, oestrogen receptor; PR, progesterone receptor. Figure taken from Nolan et al., 2016.

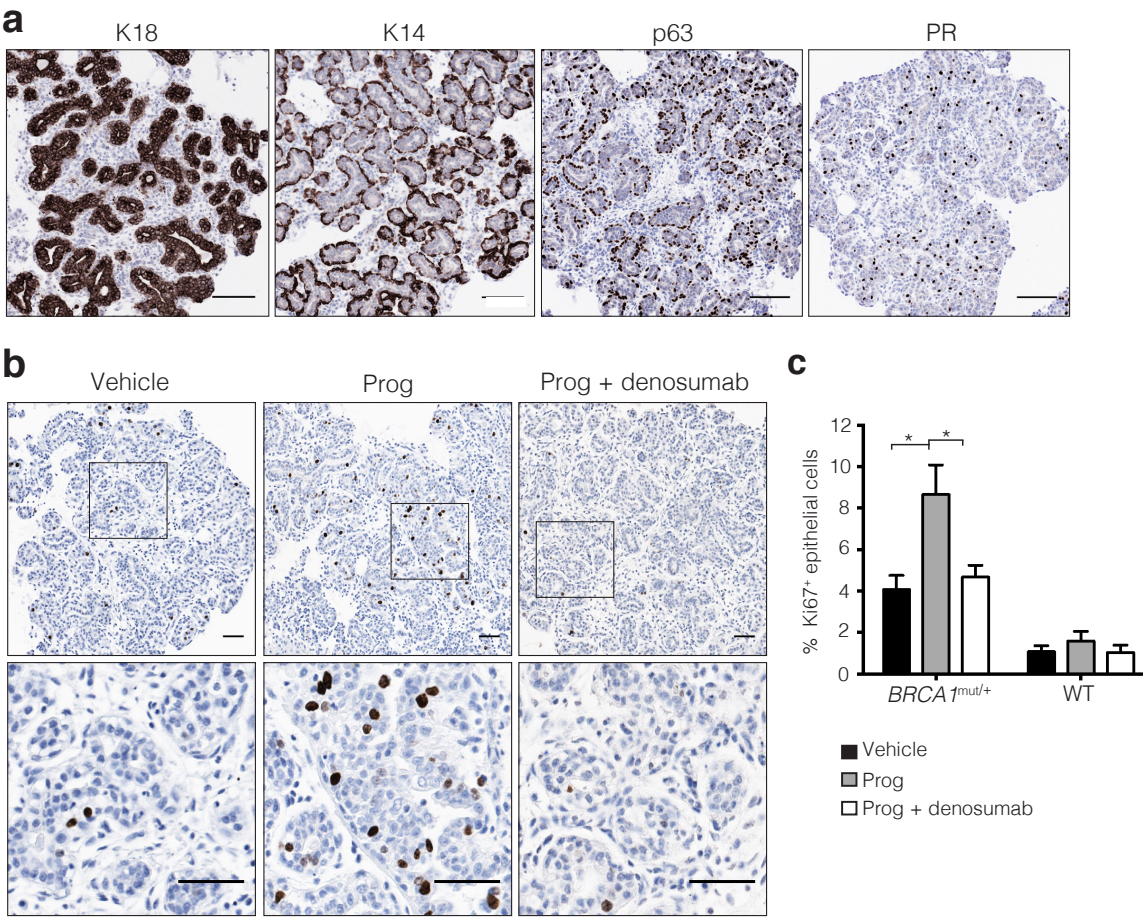

Figure 4.2: RANKL is required for progesterone-mediated cell proliferation in *BRCA1*$^{mut/+}$ breast organoids

(**a**) Representative images showing immunostaining of human breast organoids with antibodies to cytokeratin 8/18 (K18), cytokeratin 14 (K14), p63 and progesterone receptor (PR). Scale bars = 100 μm. (**b**) Representative images showing Ki67 immunostaining in organoids isolated from *BRCA1*$^{mut/+}$ breast tissue (n = 5 patients) and treated with vehicle (EtOH), progesterone (prog, 20 nM) or progesterone and the RANKL-inhibitor denosumab (10 μg/mL) for 24 h. The enlargement shows each image at 3x magnification. Scale bars = 50 μm. (**c**) Bar chart depicting the proliferative response of *BRCA1*$^{mut/+}$ (n = 5 patients) or WT (n = 4 patients) organoids to progesterone ± denosumab for 24 h. Organoids were quantified using ImageJ software (NIH) and data are depicted as mean percentage of Ki67^{+} cells within ducts ± s.e.m. *P < 0.05.

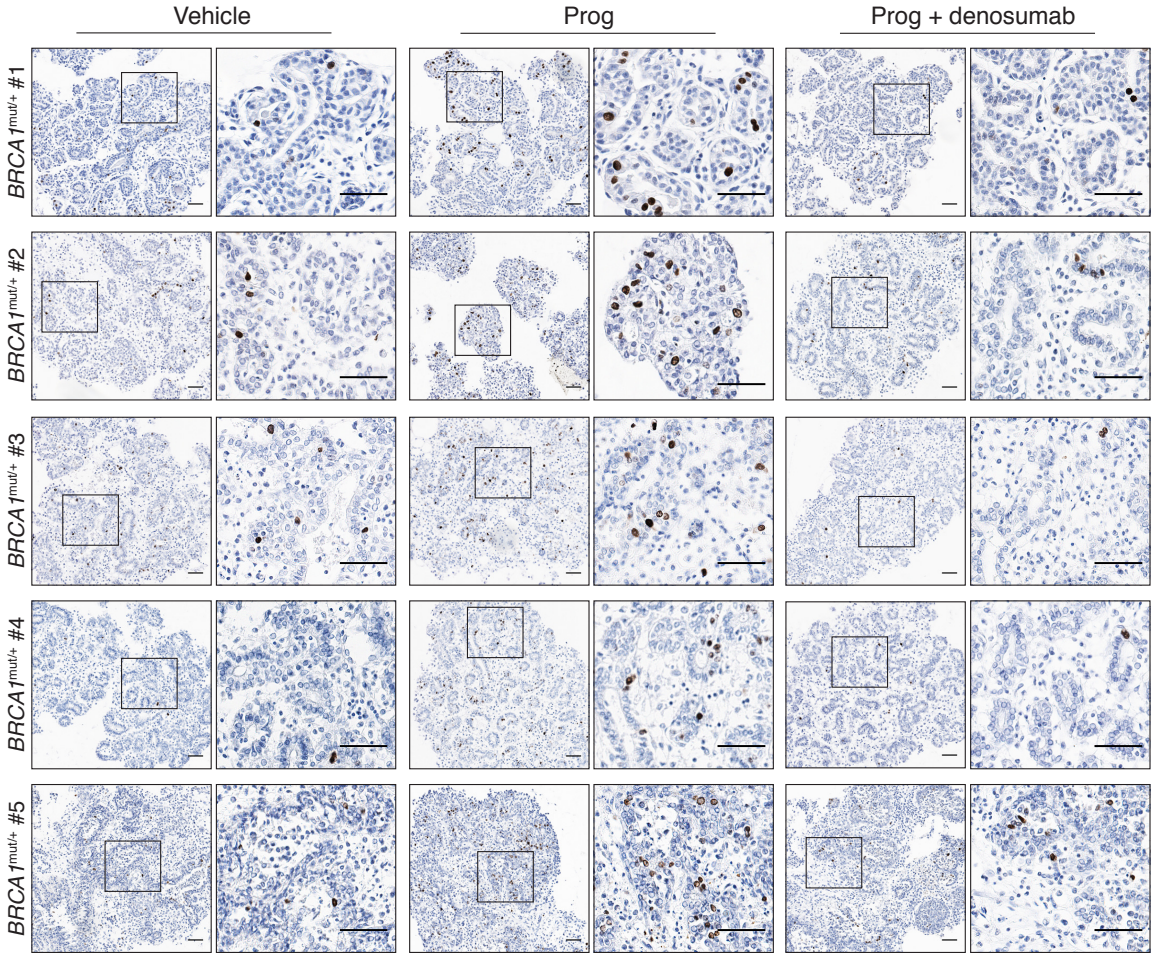

Figure 4.3: RANKL inhibition attenuates progesterone-induced proliferation in *BRCA1*$^{mut/+}$ organoids

Additional representative images from each of the five *BRCA1*$^{mut/+}$ patients showing Ki67 immunostaining in freshly isolated organoids that were treated with vehicle (EtOH), progesterone (20 nM) ± denosumab (10 µg/mL) for 24 h. The enlargement shows each image at 3x magnification. Scale bars = 50 µm.

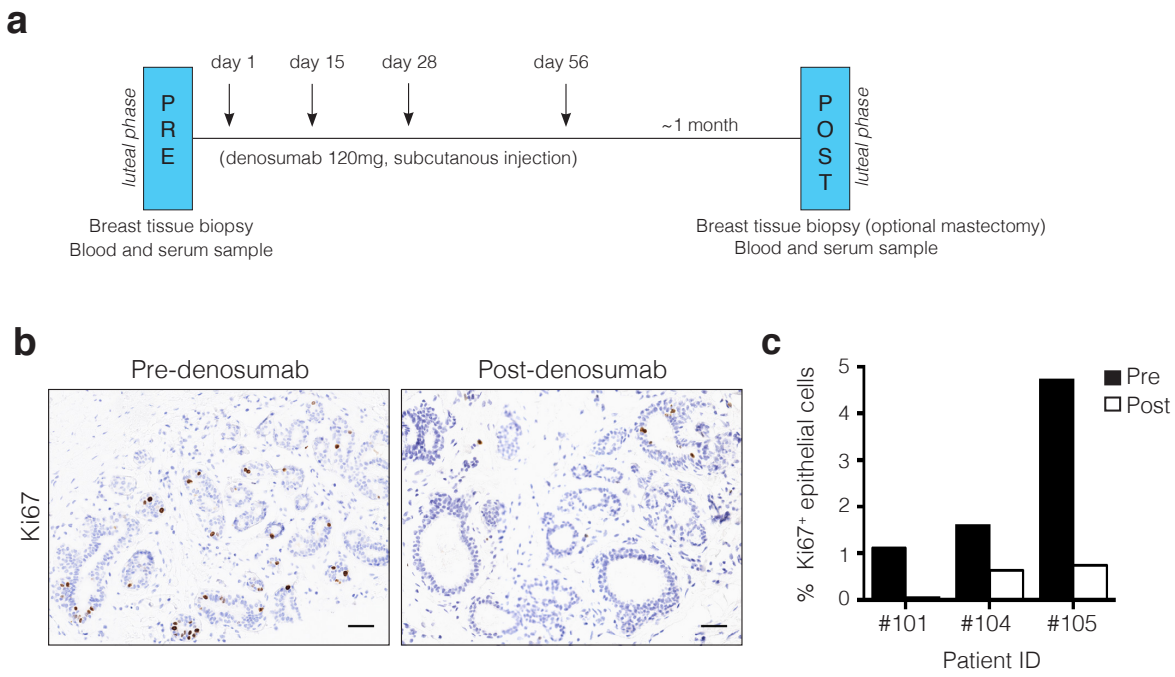

Figure 4.4: RANKL blockade attenuates cell proliferation in *BRCA1*-mutation carriers

(**a**) Overview of BRCA-D pilot study design: *BRCA1*-mutation carriers underwent pre-treatment breast tissue biopsies followed by three months of denosumab therapy (120 mg, subcutaneous injection on Day 1, 15, 28, 56). A post-treatment biopsy was carried out approximately one month after the final treatment. Both pre- and post- treatment biopsies were performed during the luteal phase of the menstrual cycle, confirmed by analysis of serum LH, FSH, oestradiol and progesterone. (**b**) Representative images showing Ki67 immunostaining of pre- (left) and post-denosumab treatment (right) breast tissue biopsies from subject #105 on the BRCA-D study. Scale bars = 50 μm (**c**) Histogram showing mean percentage of $Ki67^+$ epithelial cells following immunostaining of core breast biopsies from three *BRCA1*-mutation carriers before and after denosumab treatment. Two independent biopsies were quantified per patient.

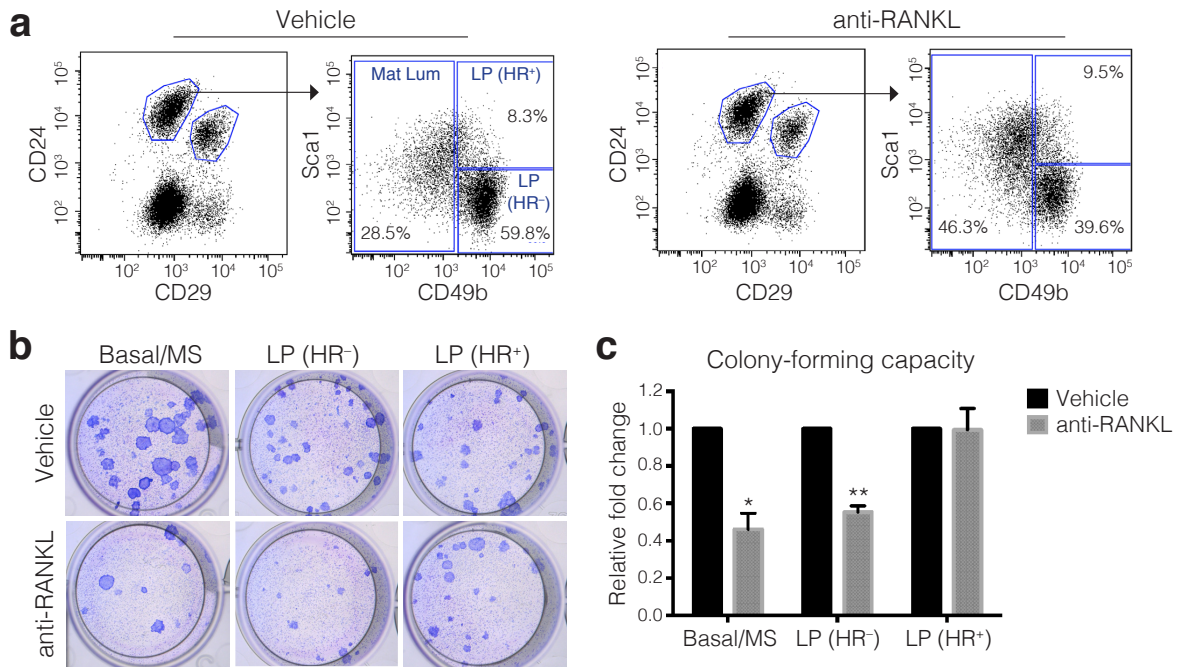

Figure 4.5: RANKL blockade attenuates stem and progenitor cell activity *in vivo*

(**a**) Representative FACS plots showing expression of CD24, CD29, Sca1 and CD49b in mouse mammary glands pooled from virgin FVB/N mice treated with either an anti-RANKL neutralising antibody (5 mg/kg) or an isotype-matched control antibody (vehicle, 5 mg/kg) for 7 days. Differential expression of Sca1 and CD49b was used to delineate mature luminal cells ($Sca1^{+}CD49b^{-}$), hormone receptor-positive luminal progenitor cells (HR^{+} LP, $Sca1^{+}CD49b^{+}$) and hormone receptor-negative luminal progenitor cells (HR^{-} LP, $Sca1^{-}$ $CD49b^{+}$). (**b**) Representative images showing Giemsa-stained colonies from basal/MaSC-enriched (basal/MS), HR^{+} LP and HR^{-} LP cells isolated from vehicle versus anti-RANKL treated mice, plated on fibroblast feeder layers for 7 days. (**c**) Bar graph depicting reduced clonogenic capacity in basal/MS and HR^{-} LP subsets isolated from anti-RANKL treated mice compared to vehicle mice. Data represent mean ± s.e.m of two independent experiments (n = 3 mice per group per experiment). **P* < 0.05, ***P* < 0.01.

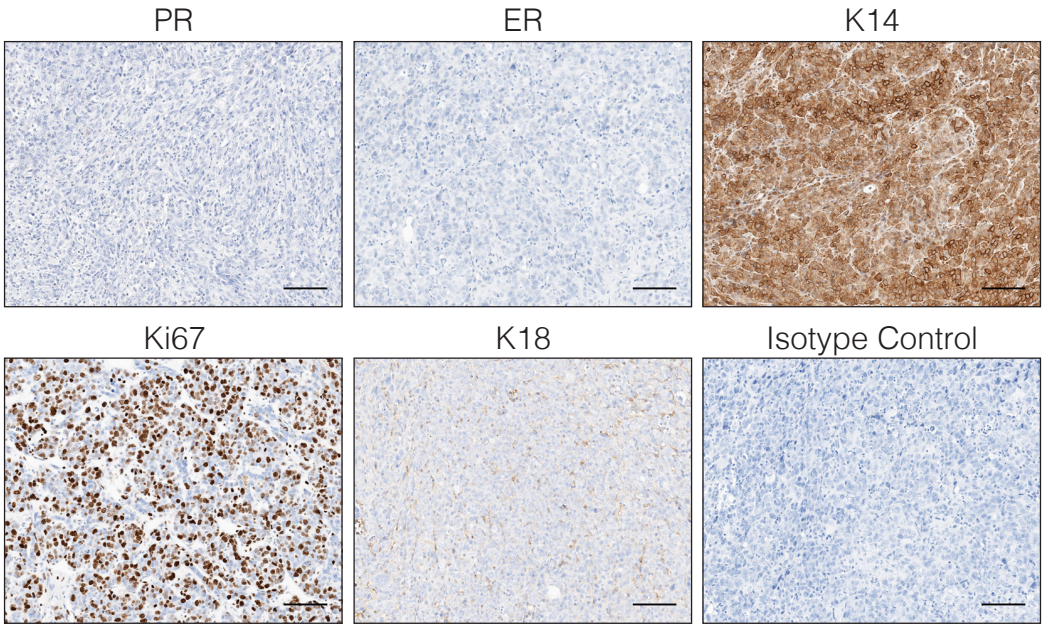

Figure 4.6: *MMTV-cre/Brca1$^{fl/fl}$/p53$^{+/-}$* mammary tumours resemble human *BRCA1*-mutated breast tumours

Representative images showing immunostaining of progesterone receptor (PR), oestrogen receptor (ER), cytokeratin 14 (K14), cytokeratin 8/18 (K18), Ki67 and an isotype-matched control antibody in *MMTV-cre/Brca1$^{fl/fl}$/p53$^{+/-}$* mouse mammary tumours (n = 5 tumours) harvested at ethical endpoint (tumour volume of 600 mm^3). Scale bars, 100 μm.

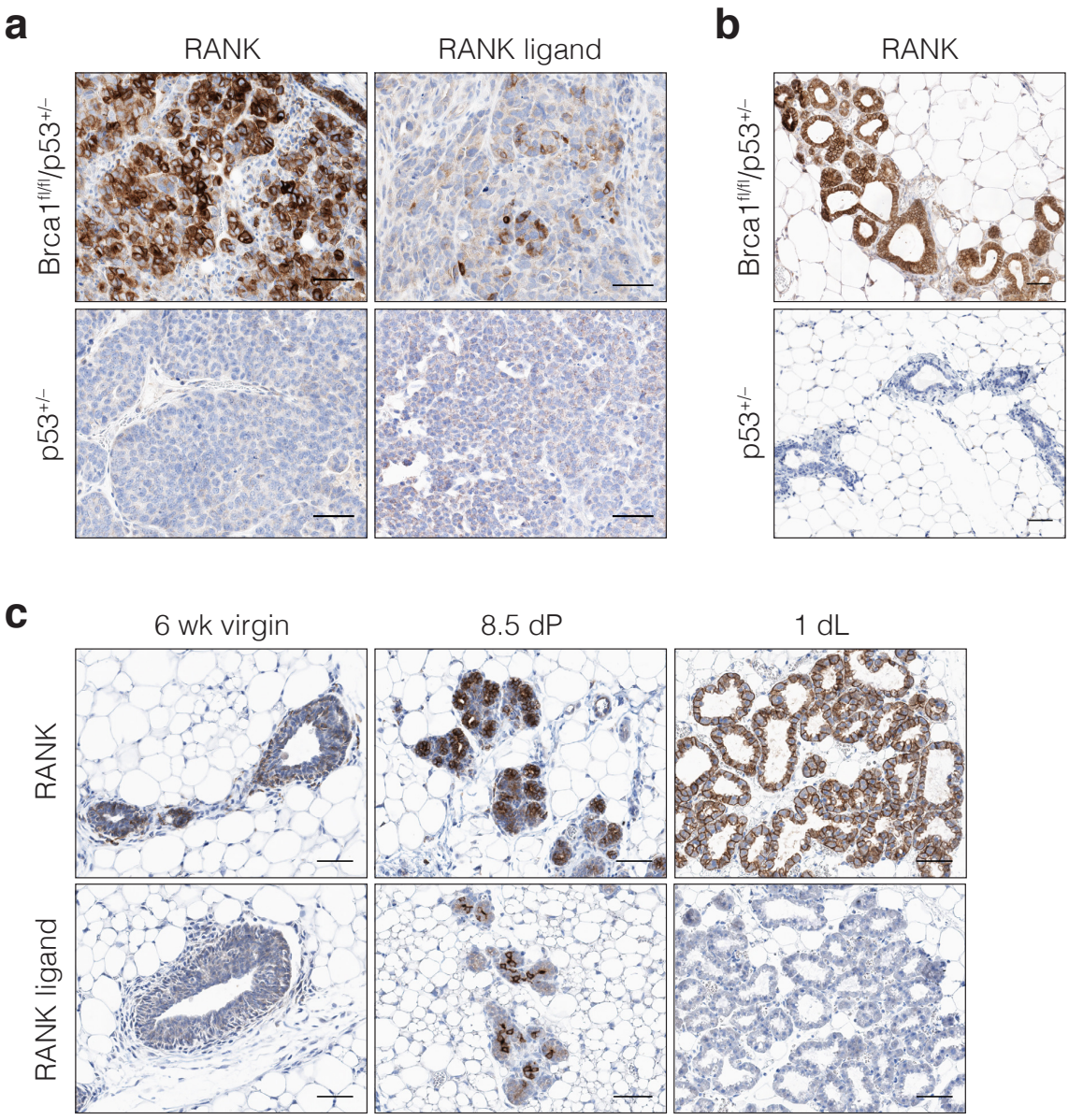

Figure 4.7: Prominent RANK expression in mammary tumours and preneoplastic mammary glands from *MMTV-cre/Brca1$^{fl/fl}$/p53$^{+/–}$* mice

(**a**) Representative image showing enrichment of RANK and RANKL immunostaining in *MMTV-cre/Brca1$^{fl/fl}$/p53$^{+/–}$* mouse mammary tumours (n = 14) compared to *p53$^{+/–}$* mammary tumours (n = 10). Scale bars = 100 μm. (**b**) Representative images showing RANK immunostaining in preneoplastic mammary glands harvested from *MMTV-cre/Brca1$^{fl/fl}$/p53$^{+/–}$* mice (n = 6) versus *p53$^{+/–}$* mice (n = 4). Scale bars = 50 μm. (**c**) Representative images showing RANK and RANKL expression in mammary glands harvested from 6-week virgin (n = 3), 8.5 day pregnant (dP, n = 3) or 1 day lactating (dL, n = 3) FVB/N mice. Scale bars = 50 μm.

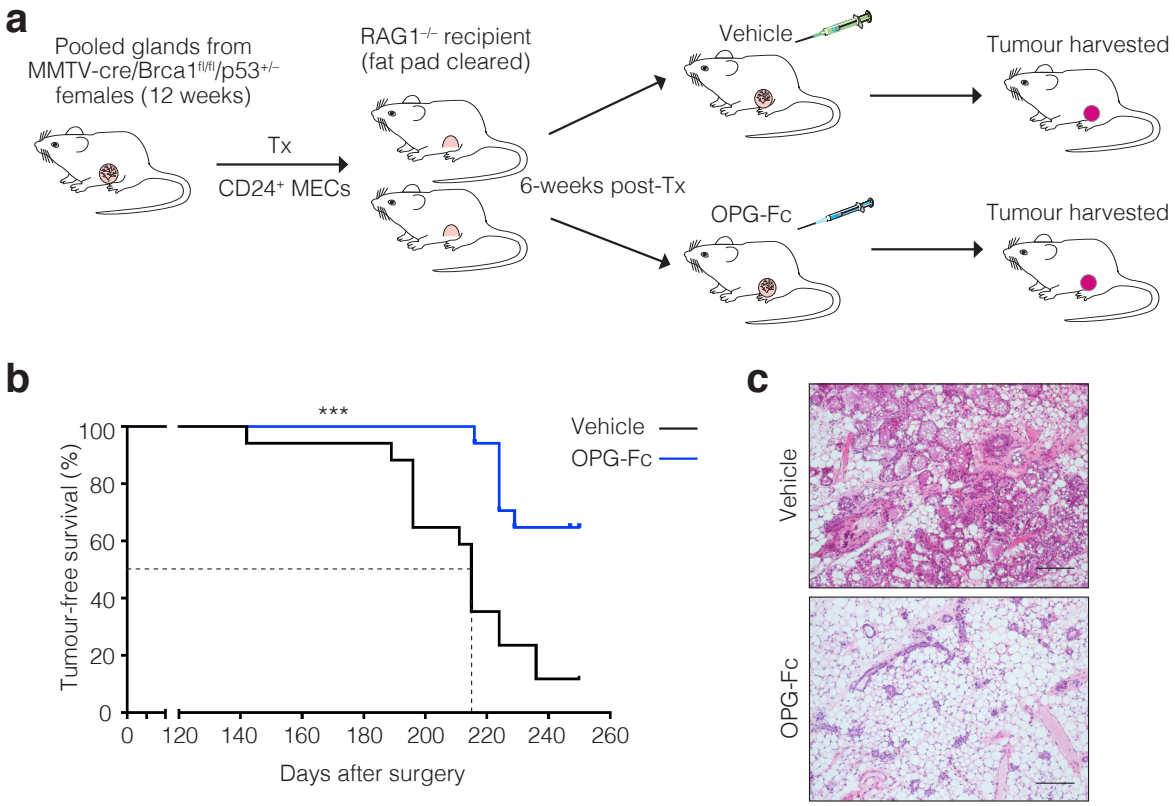

Figure 4.8: RANKL inhibition significantly attenuates tumorigenesis in *Brca1*-deficient mammary epithelial cells

(**a**) Overview of tumour prevention study: freshly sorted $Lin^{-}CD24^{+}$ mammary epithelial cells (MECs) harvested from three 12-week female *MMTV-cre/Brca1$^{fl/fl}$/p53$^{+/-}$* mice were injected into the cleared fat pads of *RAG1$^{-/-}$* recipient mice. Treatment with the RANKL-inhibitor OPG-Fc (3 mg/kg) or an isotype-matched control antibody (vehicle, 3 mg/kg) was commenced 6-weeks post-transplantation (Tx). Mice were monitored for tumour development, and tumours were harvested once ethical endpoint (tumour volume of 600 mm^3) was reached. (**b**) Kaplan-Meier survival curves of *RAG1$^{-/-}$* recipient mice treated with OPG-Fc (n = 17 mice) or vehicle (n = 17 mice). The dotted line depicts median tumour onset. ***P < 0.001. (**c**) Representative H & E sections for mammary glands harvested from *RAG1$^{-/-}$* recipients receiving either vehicle or OPG-Fc. Glands were harvested at day 250 and the presence of mammary outgrowths confirmed by wholemount analysis. Scale bar = 100 μm.

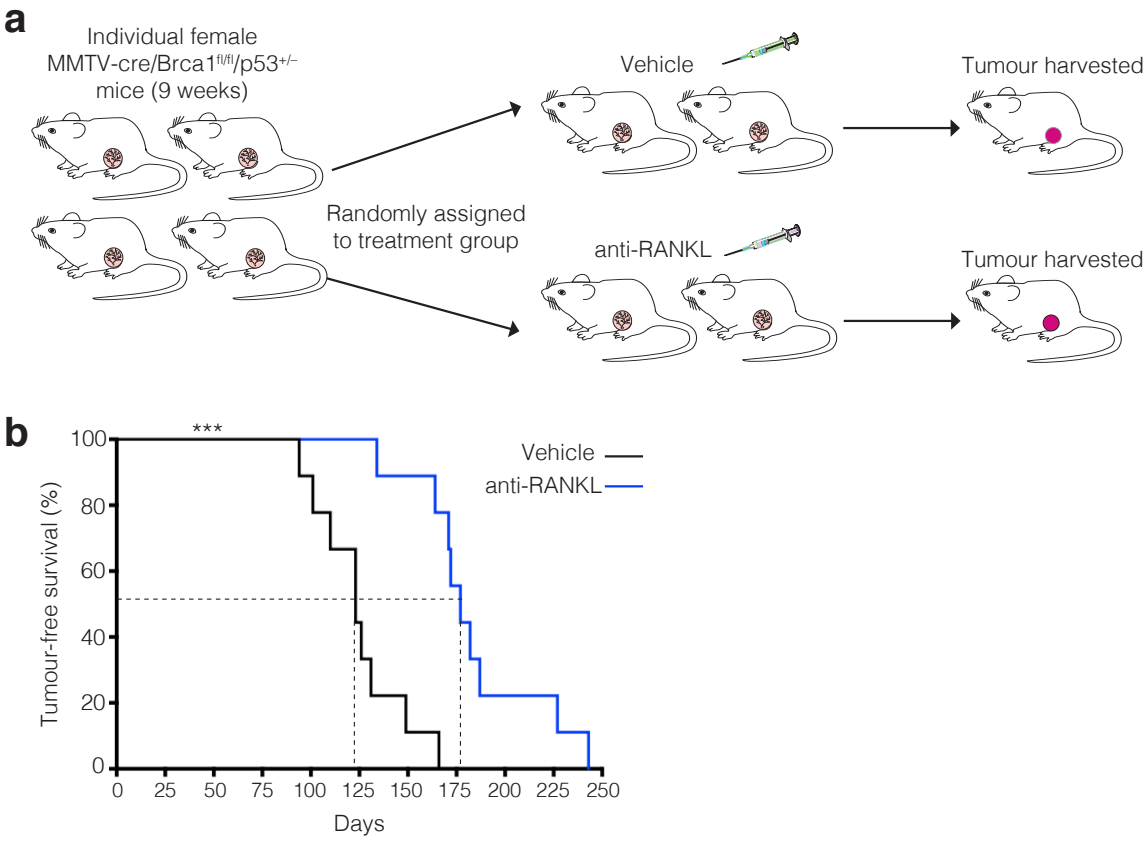

Figure 4.9: RANKL inhibition markedly curtails tumour development in *Brca1*-deficient mice

(**a**) Overview of alternative tumour prevention study: individual 9 week-old female *MMTV-cre/Brca1*$^{fl/fl}$*/p53*$^{+/-}$ mice were randomly assigned to receive either an anti-RANKL neutralising antibody (5 mg/kg) or an isotype-matched control antibody (vehicle, 5 mg/kg) every 21 days. Mice were monitored for tumour development, and tumours were harvested once ethical endpoint (600 mm^3) was reached. (**b**) Kaplan-Meier survival curves of *MMTV-cre/Brca1*$^{fl/fl}$*/p53*$^{+/-}$ mice following treatment with anti-RANKL (n = 9 mice) or vehicle (n = 9 mice). The dotted line depicts median tumour onset. ***P < 0.001.

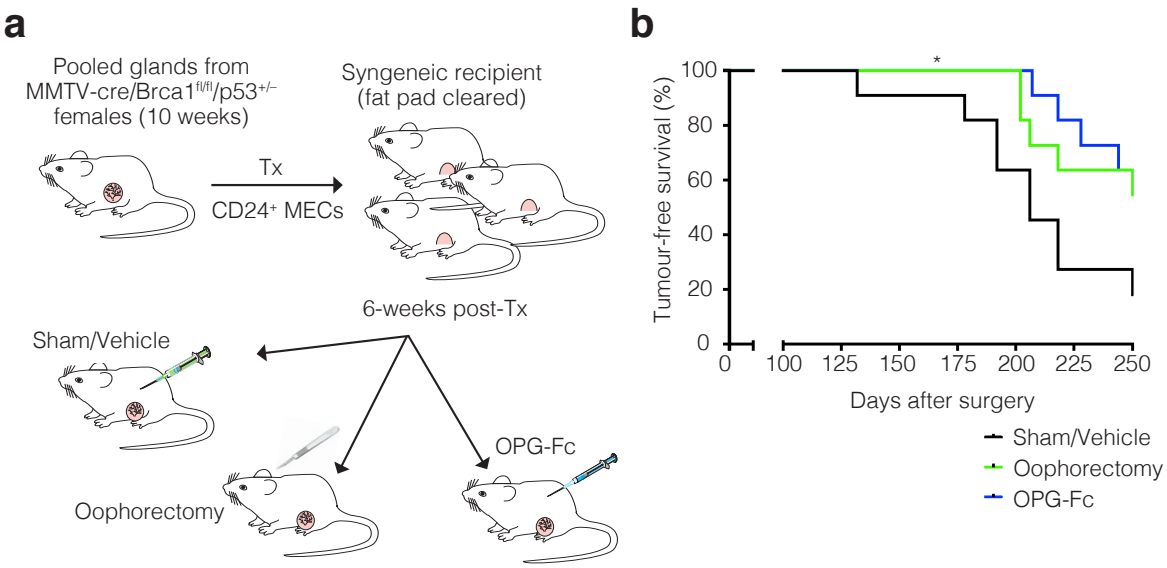

Figure 4.10: RANKL blockade in *Brca1*-deficient mice is comparable to an oophorectomy

(**a**) Overview of comparative prevention study: freshly sorted $Lin^{-}CD24^{+}$ mammary epithelial cells (MECs) harvested from three 10-week old female *MMTV-cre/Brca1$^{fl/fl}$/p53$^{+/-}$* mice were injected into the cleared fat pads of syngeneic (F1 FVB x BALB/c) mice. 6-weeks post-transplantation (Tx), mice were randomised to receive treatment with the RANKL-inhibitor OPG-Fc (3 mg/kg), or an oophorectomy or a sham operation followed by treatment with an isotype-matched control antibody (vehicle, 3 mg/kg). Mice were monitored for tumour development, and tumours were harvested once ethical endpoint (tumour volume of 600 mm^3) was reached. (**b**) Kaplan-Meier survival curves of *MMTV-cre/Brca1$^{fl/fl}$/p53$^{+/-}$* mice following an oophorectomy (n = 11), sham operation (n = 11) or OPG-Fc treatment (n = 11). **P* < 0.05.

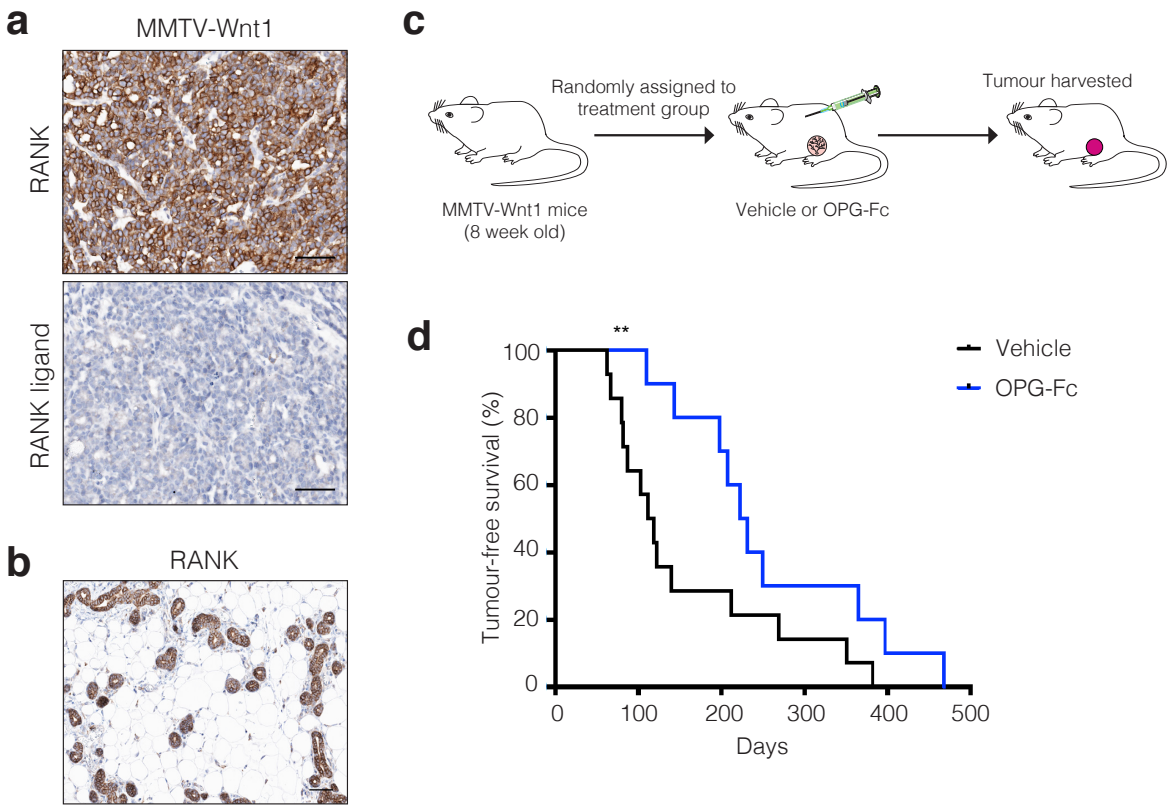

Figure 4.11: RANKL inhibition curtails tumorigenesis in *MMTV-Wnt1* mice

(**a**) Representative images showing RANK and RANKL immunostaining in *MMTV-Wnt1* mammary tumours (n = 8 mice). Scale bars = 100 μm. (**b**) Representative image of RANK immunostaining in preneoplastic mammary tissue from *MMTV-Wnt1* mice (n = 10). Scale bars = 100 μm. (**c**) Overview of prevention study: individual 8 week-old female *MMTV-Wnt1* mice were randomly assigned to receive the RANKL-inhibitor OPG-Fc (5 mg/kg) or an isotype-matched control antibody (vehicle, 5 mg/kg). Mice were monitored for tumour development, and tumours were harvested once ethical endpoint (600 mm^3) was reached. (**d**) Kaplan-Meier survival curves of *MMTV-Wnt1* mice following treatment with OPG-Fc (n = 12 mice) or vehicle (n = 14 mice). $^{**}P < 0.01$.

Chapter 5: Identification of novel therapeutic targets for the treatment of *BRCA1*-mutated breast cancer

5.1 Introduction

Breast cancers that arise in *BRCA1*-mutation carriers frequently exhibit a triple negative phenotype with respect to the expression of ER, PR and HER2, precluding the use of endocrine therapy or HER2-targeting therapeutics such as Trastuzumab. Cytotoxic chemotherapy therefore remains the mainstay of systemic treatment for breast cancer patients harbouring a *BRCA1* mutation. There are no specific chemotherapy guidelines for patients with *BRCA1*-mutated breast cancer and thus they are typically treated with a combination of anthracyclines and taxanes, the chemotherapeutic agents routinely used for triple-negative breast cancer (TNBC). Anthracyclines such as doxorubicin intercalate between DNA base pairs and prevent replication in rapidly dividing cancer cells (reviewed in Minotti et al., 2004). In addition, they inhibit topoisomerase II enzyme which is critical for relaxing supercoiled DNA during replication and transcription. Anthracycline treatment is usually followed by taxane therapy, such as docetaxel or paclitaxel. Taxanes bind and stabilise microtubules thus preventing their disassembly during mitosis. Both the accumulation of microtubules within the cell and the prevention of DNA replication promote apoptosis of tumour cells (Eisenhauer and Vermorken, 1998).

Accumulating evidence suggests that *BRCA1*-mutated breast tumours display differential chemotherapeutic sensitivity compared to TNBCs from non-carriers. Several *in vitro* studies have demonstrated a poor response of *BRCA1*-deficient tumour cells to taxane treatment, in comparison to *BRCA1*-proficient cells (Chabalier et al., 2006; Lafarge et al., 2001; Quinn et al., 2003; Tassone et al., 2003). This has also been observed in the clinic, where breast cancer patients harbouring a *BRCA1* mutation are less likely to achieve a response to neoadjuvant docetaxel treatment compared to non-carriers (Byrski et al., 2008). Using a *Brca1*-deficient mouse model, the stimulation of drug efflux transporters in *Brca1*-mutant

cells was reported to contribute to taxane resistance, although this finding has not yet been translated to human *BRCA1*-mutated breast tumours (Rottenberg et al., 2012).

Despite the poor response to taxanes, multiple reports suggest that *BRCA1*-deficient breast cancer cells respond more favorably to chemotherapeutics that induce DNA damage compared to *BRCA1*-proficient cells, consistent with the role of BRCA1 in high-fidelity DNA repair. Platinum compounds and PARP inhibitors are two promising drug classes that exploit the sensitivity of *BRCA1*-deficient cells to double-strand DNA breaks (DSBs), and are currently being evaluated in clinical trials. Platinums such as cisplatin or carboplatin induce DNA crosslinking, and thus prevent transcription and DNA replication, and also generate DSBs that require homologous-recombination (HR) for effective DNA repair (Bhattacharyya et al., 2000). In *BRCA1*-deficient cells that must rely on more error-prone repair mechanisms such as non-homologous end joining (NHEJ), the resulting genomic instability can induce apoptosis in cancer cells. Clinical trials of cisplatin (as an adjuvant or neoadjuvant therapy) resulted in high response rates in patients with *BRCA1*-mutated breast cancer, and these patients responded better than patients with intact BRCA1 function (Byrski et al., 2010; Byrski et al., 2009; Byrski et al., 2014; Moiseyenko et al., 2015; Silver et al., 2010). PARP inhibitors (PARPi), such as olaparib and veliparib represent a more targeted approach for exploiting the DNA repair defects inherent in *BRCA1*-mutated cancer cells. PARP enzymes are critical for single-strand break (SSB) repair, and their inhibition leads to the accumulation of SSBs, which can be converted into the more lethal DSBs during DNA replication. PARP inhibition is thus highly detrimental to HR-deficient *BRCA1/2*-mutated cancer cells (Farmer et al., 2005). Promising results from clinical trials of PARPi have been observed so far (reviewed in Drost and Jonkers, 2014): for example, olaparib resulted in tumour regression in >40% of patients with *BRCA1/2*-mutated breast cancer (Tutt et al., 2010), although the beneficial effects of olaparib were not observed in a separate cohort (Gelmon et al., 2011). However, while clinical trials for both platinum-based compounds and PARPi have demonstrated promising results, they have not yet translated into routine clinical use. Further trials are required to optimise the correct dosing schedule for these

therapies in combination with conventional chemotherapy to enhance efficacy and prevent toxicity.

Tumour recurrence and treatment resistance remain a foremost issue with breast cancer treatment in the clinic. Patients with TNBC, including those with a *BRCA1*-mutation, often respond well to initial chemotherapy (Parker et al., 2009a; Rouzier et al., 2005) yet they have a shorter recurrence-free survival compared to other breast cancer subtypes and a very poor prognosis once the disease becomes metastatic (Dent et al., 2007; Kassam et al., 2009). Treatment resistance is commonly observed in breast cancer patients with *BRCA1*-mutated tumours in the clinic (Lord and Ashworth, 2013; Rosen and Pishvaian, 2014). Tumour relapse and resistance in *BRCA1*-mutated breast cancers has been effectively modeled using *Brca1/p53*-deficient mice, with numerous reports demonstrating that mammary tumours cannot be completely eradicated by treatment with docetaxel, doxorubicin, olaparib, cisplatin or carboplatin, despite initial regression (Rottenberg et al., 2008; Rottenberg et al., 2007; Shafee et al., 2008; Zander et al., 2010). After multiple rounds of treatment and accompanying regression, eventually tumours become resistant to therapy. Thus, PARP inhibitors, platinum compounds and conventional chemotherapeutic agents are unlikely to be the ultimate treatment solution for *BRCA1*-mutated breast cancers. Hence, new drugs or combinations are required to achieve complete eradication of this highly aggressive disease.

There is increasing evidence to suggest that effective and sustained eradication of tumours requires efficient killing of tumour cells with an optimal chemotherapy regime as well as engagement of the immune system to keep residual tumour cells in check (Zitvogel et al., 2008). The crucial role of the immune system in cancer has been recognised for decades, with cells of both the innate (neutrophils, macrophages, monocytes and dendritic cells) and the adaptive (B and T lymphocytes) immune system working together to eradicate tumour cells. For an effective anti-cancer immune response, several stepwise events must be instigated and allowed to proceed iteratively. These steps are collectively termed the Cancer-Immunity Cycle (reviewed in Chen and Mellman, 2013). In the first step, tumour-specific antigens captured by antigen-presenting cells are processed and presented on major histocompatibility molecules (MHC) to naïve T cells within

lymphoid tissues. This prompts the priming and activation of effector T cell responses against tumour-specific antigens that, as a consequence of a myriad of genetic alterations found in most human cancers, are viewed as 'non-self'. The activated effector T cells then traffic to the tumour site and infiltrate the tumour bed, whereby they either directly induce cancer cell death (in the case of activated cytotoxic $CD8^+$ T cells), or indirectly through the release of cytokines to promote the immune response ($CD4^+$ T helper (Th) cells). In cancer patients, it is thought that the anti-tumour immune response does not perform optimally, and that many tumours likely arise as a failure of immune surveillance (Pardoll, 2012). Accordingly, the use of immunotherapy to stimulate the patient's own immune system to target and eradicate tumour cells has shown remarkable success across a broad range of tumour types, particularly in melanoma (reviewed in Mahoney et al., 2015; Mellman et al., 2011).

In addition to adoptive T-cell therapy and cancer vaccines, effective immunotherapy can be achieved via the inhibition of immune checkpoints (reviewed in Mellman et al., 2011; Pardoll, 2012; Topalian et al., 2015). Immune checkpoints include programmed cell death protein 1 (PD-1) and cytotoxic T-lymphocyte associated protein 4 (CTLA-4), which are inhibitory receptors that are constitutively expressed on regulatory T cells (Tregs) and are upregulated on activated cytotoxic $CD8^+$ T cells and activated $CD4^+$ Th cells (Chen and Flies, 2013). CTLA-4 is activated upon binding to its ligands B7.1 and B7.2, and its primary role is to dampen the activation of T cells during the priming stages within lymphoid tissues. In contrast, PD-1 is activated upon binding to its ligands PD-L1 and PD-L2, and primarily diminishes effector T cell activity (cytolytic function or cytokine production) within peripheral tissues. Both CTLA-4 and PD-1 also enhance the immunosuppressive activity of Tregs. Thus under normal physiological conditions, PD-1 and CTLA-4 are crucial for dampening the duration and amplitude of the immune response to promote tolerance to self-antigens and thus prevent autoimmunity (Pardoll, 2012). PD-1 (and CTLA4 to a lesser extent) is also critical during a chronic infection to minimise collateral tissue damage caused by a persistent immune response. Overall, targeting immune checkpoints for cancer therapy removes the 'brakes' on the immune system, reinvigorating and expanding the magnitude of the pre-existing anti-cancer immune response (Bianchini et al.,

2016). Checkpoint inhibitors are currently being examined in clinical trials for the treatment of a broad range of tumour types, including HER2-positive breast cancers and TNBC (reviewed in Savas et al., 2016).

The work presented in this chapter examines novel therapeutic strategies for the treatment of *BRCA1*-mutated breast cancer, with the goal of identifying approaches to enhance the effectiveness of current chemotherapeutic agents. Both RANKL inhibition and immune checkpoint blockade were identified as promising new strategies for the treatment of *BRCA1*-mutant tumours, providing proof-of-principal findings that could warrant further investigation in the clinic.

5.2 Results

5.2.1 RANK is highly expressed in *BRCA1*-mutated human breast tumours

We first explored the potential of RANKL blockade as a novel treatment strategy for *BRCA1*-mutated breast cancers, prompted by our discovery that $RANK^+$ luminal progenitor cells represent a key target for oncogenesis in preneoplastic $BRCA1^{mut/+}$ breast epithelium (described in Chapters 3 and 4). The expression of RANK and RANKL in primary human breast tumours was determined by immunohistochemistry using tissue microarrays (TMA) containing 628 tumours (the kConFab cohort, Mann et al., 2006). Both the frequency of RANK expression and the intensity of staining were significantly higher in *BRCA1*-mutated breast tumours compared to WT tumours, as reflected by a four-fold increase in the RANK incidence score ($P < 0.001$, Table 5.1) and an increase in the mean H-score from 2.3 in WT tumours to 13.6 in *BRCA1*-mutated tumours ($P < 0.0001$, Figure 5.1a). RANK expression was also markedly higher in *BRCA1*-mutated tumours compared to *BRCA2*-mutated tumours (Table 5.1, Figure 5.1a). To rule out the effect of selection bias given the small area of tumour sampled on the TMA, we confirmed our findings using large tissue sections from a separate cohort of breast tumour samples (the Amgen Tissue Bank cohort). Consistent with the TMA, a marked increase in H-score was observed in *BRCA1*-mutated breast tumours (mean 65.7) compared to WT tumours (mean 12.5) ($P = 0.0005$, Figure 5.1b,c). While there was no difference in the incidence of RANKL expression across patient genotypes (Table 5.1), RANKL staining was frequently observed in the stroma and normal breast tissue adjacent to $RANK^+$ *BRCA1*-mutated tumours (Figure 5.1d), implicating RANKL signalling in tumour cell proliferation.

To identify $RANK^+$ breast tumour models to use for preclinical studies, RANK immunostaining was performed on a TMA containing primary human breast tumour samples that had been subsequently engrafted into mice to generate patient-derived xenograft (PDX) models. Moderate to strong expression of RANK was observed in 6/51 cores (Figure 5.2a), with weak expression detected in an additional 7 cores (data not shown). We chose three tumour samples for further analysis: two *BRCA1*-mutated tumours with moderate RANK expression (PDX 110

and PDX 303) and a triple-negative, *BRCA1*-wild-type tumour that exhibited strong RANK expression (PDX 744). RANK protein expression was retained in all three tumour models following engraftment into mice, as determined by immunostaining (Figure 5.2b) and FACS analysis of tumour cell suspensions (Figure 5.2c).

5.2.2 RANK$^+$ tumour cells have enhanced tumour-initiating capacity

To explore the tumorigenic potential of RANK$^+$ versus RANK$^-$ tumour cells, we harvested PDX 303 tumours and transplanted equal numbers of freshly sorted RANK$^+$ and RANK$^-$ tumour cells into the mammary fat pads of recipient mice and monitored tumour growth (Figure 5.3a). RANK$^+$ tumour cells exhibited enhanced tumour-initiating capacity compared with RANK$^-$ cells, as demonstrated by the significantly accelerated growth of RANK$^+$-derived tumours across two independent experiments (Figure 5.3b,c). Thus, signalling pathways active in RANK$^+$ tumour cells may convey a growth and/or survival advantage compared to RANK$^-$ tumour cells.

5.2.3 RANKL blockade can significantly attenuate tumour growth and synergises with taxane chemotherapy

To assess the effect of RANKL blockade on tumour growth *in vivo*, we generated cohorts of mice bearing either PDX 110, PDX 303 or PDX 744 tumours and then randomised mice to receive either a mouse IgG1 control antibody or the RANKL inhibitor OPG-Fc. Treatment was initiated when tumours were first palpable (approximately 4 mm^3) and was continued until tumours reached approximately 600 mm^3, at which time the mice were euthanised. Notably, a marked attenuation of tumour growth was observed in all three PDX models treated with OPG-Fc compared to control mice (Figure 5.4), with the most dramatic effect observed with PDX 110 (Figure 5.4a).

Given that *BRCA1*-mutated breast tumours are highly aggressive tumours and often present as advanced-stage cancers (Kriege et al., 2004), the initiation of treatment upon first palpation of the tumour may not be an accurate representation of the clinical utility of this approach. We therefore generated additional cohorts of

tumour-bearing mice and once tumours had reached a size of approximately 100 mm^3, mice were randomised to one of four treatment groups: (1) vehicle (mouse IgG1); (2) OPG-Fc; (3) docetaxel or (4) OPG-Fc and docetaxel. Single-agent therapy with either OPG-Fc or docetaxel demonstrated little or no efficacy in these models (Figure 5.5). However, treatment of PDX 110 and PDX 744 tumours with the combination of OPG-Fc and docetaxel markedly attenuated tumour growth, and a significant improvement in survival was observed ($P < 0.0001$, Figure 5.5a,b). The addition of OPG-Fc to docetaxel therapy did not significantly impact on the growth of PDX 303 tumours (Figure 5.5c), however this model exhibits the lowest expression of RANK (Figure 5.2). Collectively, these data suggest that OPG-Fc can synergise with docetaxel to significantly inhibit tumour growth, and RANK expression may act as a biomarker of therapeutic response.

To determine which signalling pathways might mediate the synergy between docetaxel and RANKL blockade, a western blot was performed with PDX 110 tumours that were harvested either three or five days post-treatment. There were no discernable differences in the activation of NF-κB, Akt or ERK signalling pathways between treatment groups, and no change in caspase activation (Figure 5.6a). Furthermore, immunohistochemistry indicated no significant differences in BrdU incorporation or cleaved caspase-3 expression between treatment groups, suggesting cell proliferation and survival were unchanged (Figure 5.6b). Therefore the mechanisms underlying the synergistic effects of OPG-Fc and docetaxel remain elusive and warrant further investigation.

5.2.4 Combination therapy with immune checkpoint inhibitors significantly attenuates the growth of *Brca1*-deficient mammary tumours

The potential of immune checkpoint blockade was also explored as a novel treatment strategy for *BRCA1*-mutated breast tumours. Flow cytometry was first utilised to assess the expression of PD-L1 on tumour cells from a range of mouse mammary tumour models: *MMTV-cre/Brca1$^{fl/fl}$/p53$^{+/-}$*, *MMTV-Neu*, *MMTV-PyMT*, *MMTV-Wnt1* and *p53$^{+/-}$*. Notably, *MMTV-cre/Brca1$^{fl/fl}$/p53$^{+/-}$* tumours were significantly enriched for PD-L1 expression, with approximately 29% of tumour cells expressing PD-L1 compared to <5% of cells from *MMTV-Neu* and *MMTV-PyMT*

tumours (P < 0.01, Figure 5.7). PD-L1 expression was also observed on approximately 15% of cancer cells from *MMTV-Wnt1* and $p53^{+/-}$ tumours that recapitulate features of human basal-like breast cancers, similar to *Brca1*-deficient tumours (outlined in Chapter 1). The prominent expression of PD-L1 on *Brca1*-deficient tumour cells implies they are actively suppressing the anti-cancer immune response by triggering the PD-1 checkpoint, and provides a strong rationale for testing the efficacy of checkpoint inhibitors on tumour growth.

To produce a preclinical model, single-cell suspensions were generated from freshly harvested *MMTV-cre/Brca1*$^{fl/fl}$*/p53*$^{+/-}$ mammary tumours and cells were transplanted into the mammary fat pads of a large cohort of syngeneic recipient mice (Figure 5.8a). To recapitulate a treatment study relevant to patients with *BRCA1*-mutated breast tumours, we set up a six-arm study to evaluate the effects of the two checkpoint inhibitors (anti-PD1 and anti-CTLA4) on tumour growth, with or without the chemotherapeutic agent cisplatin (Figure 5.8a). Checkpoint inhibition alone was ineffective in this model, and tumours in this group and the vehicle arm were harvested shortly after treatment was initiated (Figure 5.8b,c). While cisplatin treatment initially induced tumour regression, tumours were not completely eradicated and eventually developed resistance by the third treatment cycle (Figure 5.8b). Although single-arm checkpoint blockade failed to improve the tumour response to cisplatin, a striking attenuation in tumour growth was observed in mice treated with the combination of cisplatin, anti-PD1 and anti-CTLA4 (Figure 5.8b). Tumour growth remained minimal throughout the treatment period, and a significant improvement in survival was observed compared to all other groups (P = 00025, Figure 5.8b,c). Importantly, no increase in toxicity was observed in mice treated with the combination group compared to chemotherapy alone, as determined by visual inspection and assessment of mouse weight. Therefore dual anti-PD1 and anti-CTLA4 therapy, when combined with cisplatin, confers a remarkable improvement in tumour response and could be a potential new treatment strategy for *BRCA1*-mutated breast tumours.

5.2.5 Checkpoint blockade induces an avid immune response in *Brca1*-deficient tumours

To explore the mechanism underlying the superior response of *Brca1*-deficient tumours to treatment with cisplatin and anti-PD1/anti-CTLA4 compared to cisplatin alone, we generated a preclinical model to assess the effects of treatment on the immune response within the tumour microenvironment. *MMTV-cre/Brca1*$^{fl/fl}$*/p53*$^{+/-}$ tumour cells were transplanted into the mammary fat pads of syngeneic recipients, and tumours were harvested either at baseline (untreated) or 14 days following treatment with either cisplatin alone or cisplatin and anti-PD1 and/or anti-CTLA4 (Figure 5.9a). Flow cytometry was used to characterise the composition and activation status of immune cell populations infiltrating the tumour microenvironment. Compared to chemotherapy alone, checkpoint inhibition and chemotherapy together provoked a marked increase in the proportion of tumour infiltrating cytotoxic CD8$^+$ T cells that coincided with a decrease in the proportion of immunosuppressive FOXP3$^+$ Tregs (Figure 5.9b,c). This effect was most pronounced in tumours from mice receiving combination therapy (i.e. cisplatin, anti-PD1 and anti-CTLA4), resulting in a substantial increase in the mean CD8$^+$:FOXP3$^+$ cell ratio compared to cisplatin treatment alone (Figure 5.9c). These data suggest that the combination of chemotherapy and checkpoint blockade induced changes in the tumour microenvironment that favour a cytotoxic rather than immunosuppressive immune response. Notably, a high CD8$^+$:FOXP3$^+$ cell ratio in breast cancer patients correlates with an improved response, progression-free survival and overall survival in patients receiving neoadjuvant chemotherapy (Ladoire et al., 2008; Ladoire et al., 2011). The enrichment of cytotoxic CD8$^+$ T cells within the tumour infiltrate in the combination group was also evident by immunohistochemistry (Figure 5.9d).

We next examined the T cell activation status following treatment by assaying the expression of the activation markers Inducible T-cell Co-Stimulator (ICOS), CD44, Neuropilin 1 (NRP1) and PD-1. ICOS, CD44 and NRP1 were substantially upregulated on CD4$^+$FOXP3$^-$ Th cells and CD8$^+$ T cells within tumours treated with the combination therapy compared to cisplatin alone (Figure 5.10a). Furthermore, the proportion of activated PD-1$^+$CD8$^+$ T cells infiltrating the tumour was markedly

increased by cisplatin and dual checkpoint blockade, when compared to cisplatin alone or together with individual checkpoint inhibitors (Figure 5.10b,c). Notably, cisplatin treatment alone was associated with a moderate increase in CD44, NRP1 and PD-1 expression relative to the untreated group, suggesting chemotherapy itself can induce immune cell activation (Figure 5.10). Taken together, these findings suggest that the combination of chemotherapy and dual checkpoint inhibitors triggers an avid immune response within the tumour microenvironment.

5.3 Discussion

The current treatment paradigm for *BRCA1*-mutated breast tumours is typically a combination of surgery, local radiotherapy and chemotherapy. Despite initial sensitivity to chemotherapy and tumour regression, residual tumour cells frequently lead to tumour relapse and therapeutic failure, highlighting the need to identify new treatment strategies for an effective and durable response.

In the previous chapters, we demonstrated that the RANKL signalling pathway may drive tumour initiation in *BRCA1*-mutant breast epithelium. In this chapter, we investigated a role for RANKL in the progression of *BRCA1*-mutated breast cancers. Both the frequency and intensity of RANK expression was found to be significantly higher in *BRCA1*-mutated breast tumours compared to WT and *BRCA2*-mutated tumours. The retention of RANK expression in *BRCA1*-mutated tumours as well as RANKL expression in the tumour stroma adjacent to $RANK^+$ domains suggests that the RANKL signalling pathway may be important for driving proliferation of these tumours. This is further supported by the increased tumour-initiating capacity of $RANK^+$ tumour cells compared to $RANK^-$ cells isolated from the same tumour. RANK expression has previously been detected in several human breast cancer cell lines such as MDA-MB-231, MCF-7 and T47Ds (Labovsky et al., 2012; Schramek et al., 2010; Thomas et al., 1999). Consistent with our findings, expression analysis of RANK mRNA and protein in primary human breast cancer samples revealed RANK is predominantly expressed in high grade, proliferative tumours that lack expression of PR and ER (Azim et al., 2015; Palafox et al., 2012; Pfitzner et al., 2014; Santini et al., 2011). Notably, high RANK expression correlates with a high incidence of metastasis, a shorter disease-free survival and a shorter overall survival in breast cancer patients (Palafox et al., 2012; Pfitzner et al., 2014; Santini et al., 2011). RANKL protein is rarely found in tumour cells, and is more commonly expressed in infiltrating lymphocytes and fibroblast-like cells in the surrounding stroma of breast tumours (Gonzalez-Suarez et al., 2010; Tan et al., 2011). Interestingly, the secretion of RANKL by tumour infiltrating Tregs has been proposed to stimulate metastatic progression of RANK-expressing breast tumour cells (Jones et al., 2006; Tan et al., 2011). These

findings strengthen the notion of RANKL inhibition as a potent therapeutic approach for *BRCA1*-mutated breast cancer patients.

Importantly, treatment of a $RANK^{+}$ PDX that was established from a *BRCA1*-mutation carrier (PDX 110) with docetaxel plus OPG-Fc significantly attenuated tumour growth and markedly prolonged survival of recipient mice. Single-agent therapy with docetaxel was ineffective in these tumours, consistent with the poor response of *BRCA1*-mutated tumours to taxane therapy in the clinic (Byrski et al., 2008). This synergistic relationship was also observed in a PDX model derived from a *BRCA1*-wild-type TNBC with prominent RANK expression (PDX 744), suggesting RANKL could be more broadly applicable as a therapeutic target for TNBCs that express high levels of RANK. Minimal treatment response to docetaxel plus OPG-Fc was observed in the $RANK^{low}$ PDX 303, implying that a threshold level of RANK expression may be required for an effective response. Notably, a clinical trial to test the efficacy of denosumab as an adjunct to neoadjuvant chemotherapy in patients with TNBC is currently under development by the German Breast Group (NCT02682693). In addition to assessing the ability of denosumab to increase response rates and improve outcomes for participants, this study aims to correlate therapeutic response with the degree of RANK expression. Although the number of *BRCA1*-mutation carriers included in this study is likely to be small, it will provide important insights into the broader use of RANKL inhibition as a treatment for TNBC.

The efficacy of immune checkpoint inhibitors, specifically anti-PD1 and anti-CTLA4, for the treatment of *BRCA1*-mutated breast tumours was also investigated in this chapter. There are several key features of *BRCA1*-mutated breast cancer that provided a strong rationale for this study. Firstly, tumours that typically respond best to checkpoint inhibitors are those associated with a high degree of somatic mutations (Hugo et al., 2016; Snyder et al., 2014; Van Allen et al., 2015). For example, a high mutational load in melanoma tumours correlates with a sustained clinical benefit from anti-CTLA4 therapy and improved overall survival (Snyder et al., 2014). The high mutational diversity found in these tumours likely exposes an array of neoantigens for potential immune recognition and activation (Topalian et al., 2015). Although breast cancers are not characteristically associated with a high

mutational burden (Alexandrov et al., 2013), elevated genomic instability is a hallmark feature of *BRCA1*-mutated breast tumours (Rahman and Stratton, 1998; Tirkkonen et al., 1997). A significant enrichment for non-silent mutations (missense mutations and indels) has also been observed in *BRCA1/2*-mutated human breast tumours compared to WT tumours (S. Loi, unpublished observation). Thus, *BRCA1*-mutated breast tumours would be anticipated to have a high proclivity for generating neoantigens that can be recognised by the immune system as 'non-self'. Secondly, *BRCA1*-mutated breast cancers are associated with a prominent immune infiltrate (Lakhani et al., 1998). This suggests that the immune system is already actively engaged with *BRCA1*-mutated tumour cells, a response that could be strengthened by the use of checkpoint inhibitors. Importantly, the presence of an immune response within *BRCA1*-mutated tumours correlates with our observation that *Brca1*-deficient mouse mammary tumours express high levels of PD-L1. PD-1 ligands, particularly PD-L1, are commonly upregulated in many cancers, particularly those associated with a prominent immune infiltrate (Dong et al., 2002). This is thought to occur primarily as an acquired resistance mechanism of tumour cells upon sensing immune engagement, since inflammatory cytokines produced by immune cells within the tumour microenvironment such as interferon gamma (IFNγ) can stimulate PD-L1 expression (Blank et al., 2004; Spranger et al., 2013). Alternatively, intrinsic resistance mechanisms have been reported, whereby genomic alterations or activation of signalling pathways such as PI3K/Akt within tumour cells can promote PD-L1 upregulation (Marzec et al., 2008; Parsa et al., 2007). These two mechanisms are not mutually exclusive and may co-exist within the same tumour microenvironment (Topalian et al., 2015). Our demonstration of prominent expression of PD-L1 on *Brca1*-deficient tumour cells is consistent with a recent finding that *BRCA1/2*-mutated high grade serous ovarian tumours express high levels of PD-L1 (Strickland et al., 2016) and the report of high *PD-L1* mRNA expression in breast tumours from *BRCA1*-mutation carriers (Basu et al., 2014). Importantly, PD-L1 expression by tumour cells has significant implications for the anti-tumour immune response, as it suggests that even though the tumour microenvironment may contain a significant repertoire of tumour-specific T cells capable of inducing cancer cell death, the activity of T cells is restricted due to activation of the PD-1 checkpoint. This is substantiated by reports that forced expression of PD-L1 in mouse tumour cells inhibits local anti-tumour T cell

responses (Dong et al., 2002; Iwai et al., 2002; Konishi et al., 2004). Therefore, the true potential of the immune response within the tumour microenvironment could be restored via PD-1 inhibition. Collectively, the high genomic instability, prominent immune infiltrate and PD-L1 upregulation provided strong justification for testing the efficacy of immune checkpoint inhibitors as a treatment strategy for *BRCA1*-mutated breast cancers.

Through an *in vivo* preclinical treatment study, we demonstrated that dual checkpoint blockade with cisplatin had a striking effect on the growth of *Brca1*-deficient tumour cells when compared to cisplatin alone. Tumours underwent a marked regression that was sustained throughout the treatment period, and a significant improvement in the survival of recipient mice was observed. A comprehensive analysis of immune cell populations within the tumour microenvironment revealed that combination treatment significantly enhanced the recruitment of $CD8^+$ effector T cells to the tumour site, and promoted the activation of both $CD8^+$ and $CD4^+$ T cells. Together this results in a superior anti-cancer immune response and accompanying tumour regression. The synergistic anti-cancer effect of anti-PD1 and anti-CTLA4 treatment is compatible with the biology of these checkpoints, since the two agents act at distinct points of the immune response: T cell activation (anti-CTLA4) and T cell effector function (anti-PD-1). Concomitant use of cisplatin was required for a treatment response to checkpoint blockade, since no attenuation in tumour growth was observed with the use of anti-CTLA4 and anti-PD1 alone. This is consistent with reports suggesting chemotherapy can act as an immunological adjuvant in the tumour microenvironment by promoting the release of tumour antigens via immunogenic cell death, thereby priming *de novo* T cell responses and improving the efficacy of checkpoint blockade (reviewed in Zitvogel et al., 2008). Neoadjuvant chemotherapy in some TNBC patients has also been shown to stimulate lymphocytic infiltrate in the residual tumour by altering the tumour microenvironment, turning it from “cold” containing few tumour-infiltrating lymphocytes (TILs) to “hot” with high TIL presence and permitting a more productive immune response (Dieci et al., 2015; Kang et al., 2013). Chemotherapy is also likely to reduce the tumour bulk, enabling the immune system to eradicate residual tumour cells. However, studies have shown that care must be exercised with the dual use of chemotherapy and immunotherapy, to

ensure that chemotherapeutic agents are used at appropriate doses and schedules that do not suppress the immune system by depleting proliferating lymphocytes (reviewed in Mahoney et al., 2015).

Our findings suggest that the use of inhibitors targeting PD-1 and CTLA-4 could have a profound effect on the response of *BRCA1*-mutated tumours to chemotherapy. There are currently eleven clinical trials ongoing to establish the role of checkpoint inhibitors either alone, in combination or as an adjunct to chemotherapy in patients with TNBC (detailed in Bianchini et al., 2016). Our findings support the implementation of clinical studies to specifically assess the efficacy of chemotherapy and checkpoint blockade for the treatment of *BRCA1*-mutated TNBCs. The inclusion of *BRCA1*-germline mutations as exploratory biomarkers in current immunotherapy clinical trials for TNBC could also provide insights into the potential of this therapeutic approach. Notably, clinical trials for metastatic melanoma have reported an increase in the incidence of grade 3 – 4 adverse events in patients receiving both anti-PD1 and anti-CTLA4 compared to monotherapy, although higher objective response rates and a significantly longer progression-free survival were observed (Larkin et al., 2015). Although many adverse events (e.g. diarrhea, nausea) were treatable with the use of immune-modulatory agents, this highlights the need to identify predictive biomarkers of benefit from therapy (in addition to *BRCA1*-mutation status). This will allow clinicians to make more informed decisions about the benefit-risk ratio of treatment, and is an important focus of current research (reviewed in Meng et al., 2015). Although we did not observe increased toxicity in mice receiving the combination therapy compared to cisplatin alone, clinical trials to thoroughly assess the potential side effects of this proposed treatment regime for *BRCA1*-mutation carriers would be essential.

Overall, the findings presented this chapter reveal an exciting potential for both RANKL inhibition and immune checkpoint blockade in the treatment of *BRCA1*-mutated breast cancer. Both of these approaches were shown to increase the efficacy of chemotherapy alone, and thus could be used to augment the response of *BRCA1*-mutation carriers to current treatment options and prevent treatment resistance. Through the combination of chemotherapy with more targetted

therapies, particularly via the activation of a patient's immune system using checkpoint inhibitors, there is the potential for a more effective and durable benefit from therapy.

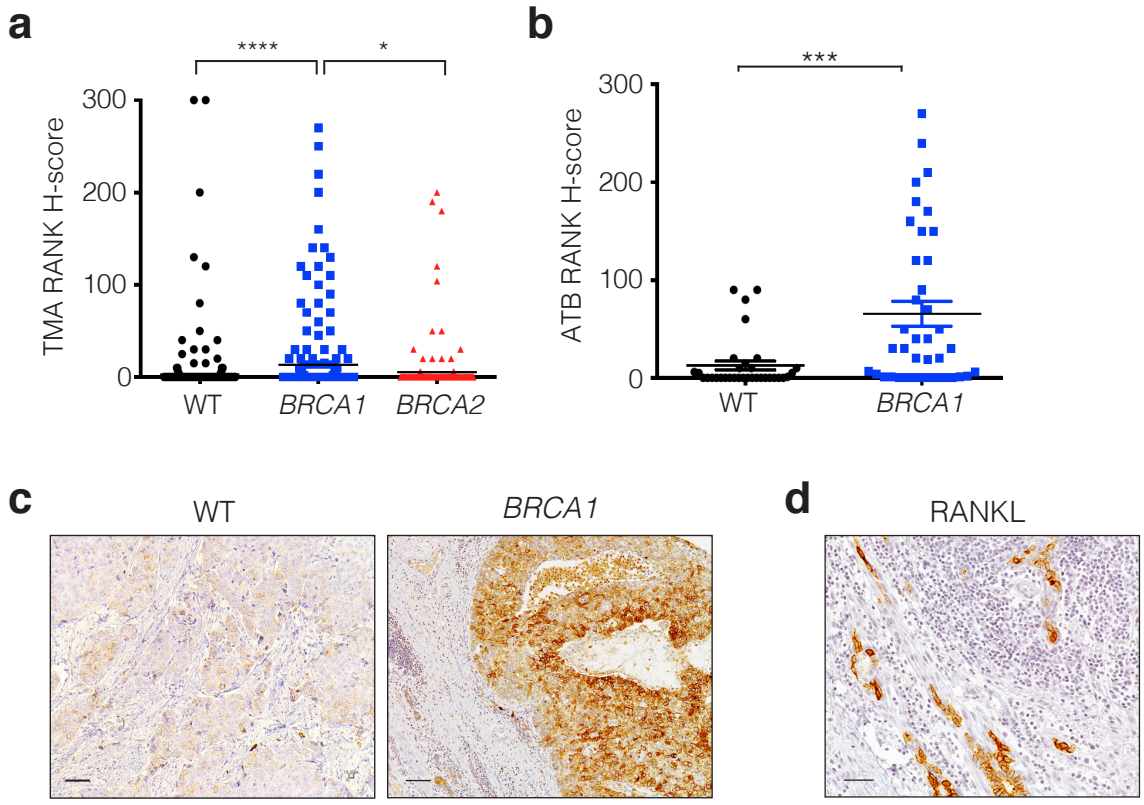

Figure 5.1: RANK is highly expressed in *BRCA1*-mutated human breast tumours

(**a**) RANK expression in wild-type (WT), *BRCA1*- and *BRCA2*-mutated human breast tumours from kConFab tissue microarrays (TMAs). Expression was determined by immunohistochemistry and is depicted as an H-score (staining intensity (scale of 0 – 3) multiplied by percent positive cells, resulting in a range of 0 – 300). Bar, mean score. **P* < 0.05, *****P* < 0.0001. (**b**) RANK H-scores of WT and *BRCA1*-mutated human breast tumours from the Amgen Tissue Bank cohort. Data represent mean ± s.e.m. ****P* < 0.001. (**c**) Representative images of RANK immunostaining on sections from WT and *BRCA1*$^{mut/+}$ breast tumours. Scale bars = 100 μm. (**d**) Representative image showing RANKL immunostaining on serial sections of a RANK^{+} *BRCA1*-mutated breast tumour showing distribution within normal breast tissue adjacent to the tumour. Scale bar = 100 μm.

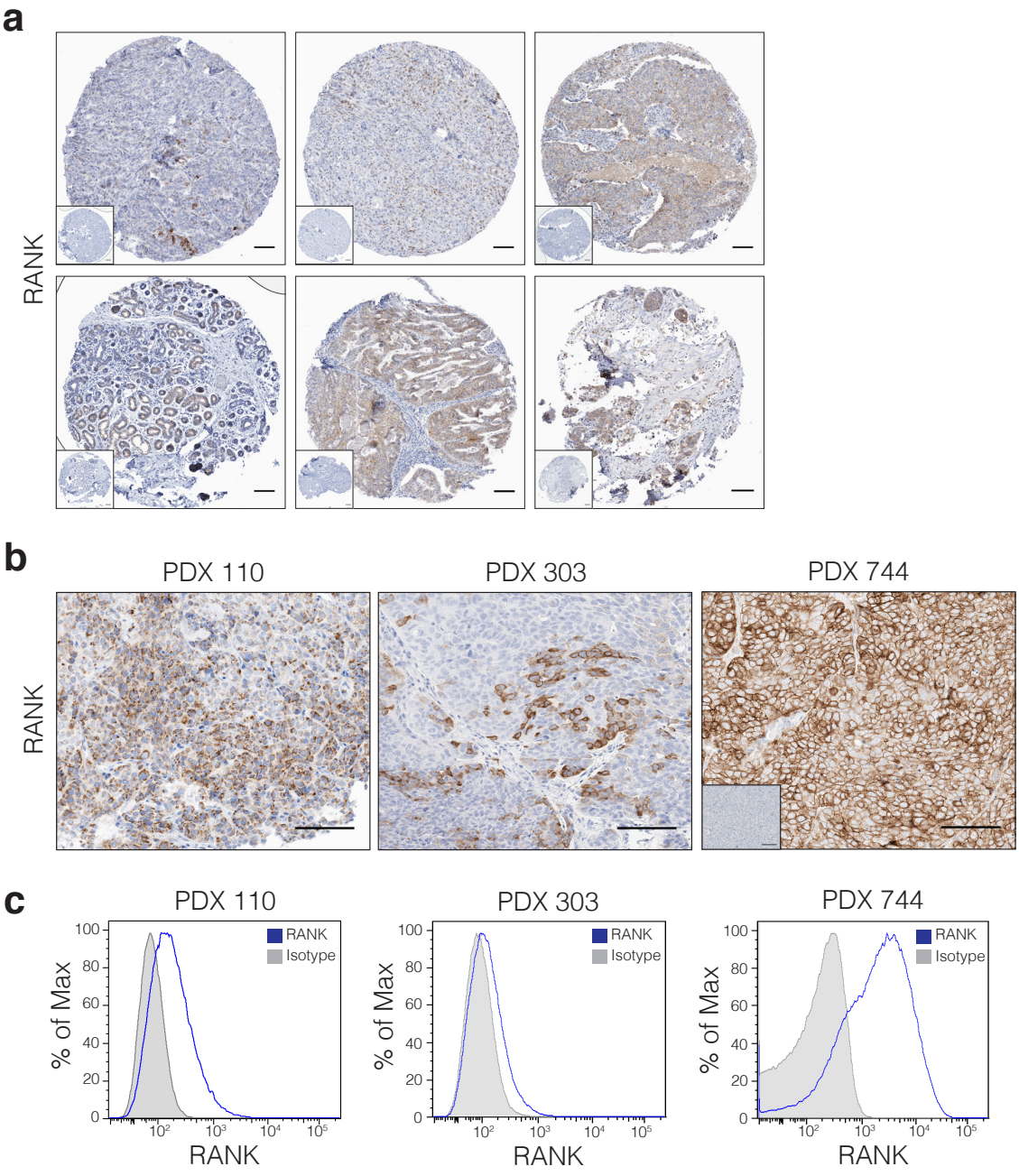

Figure 5.2: RANK expression in patient-derived xenograft tumours

(**a**) RANK immunostaining on a TMA containing primary human breast tumours that were subsequently engrafted into mice to generate patient-derived xenograft (PDX) models (inserts, isotype-matched control antibody). Scale bars = 100 μm. (**b**) Representative images showing retention of RANK expression in PDX tumour models #110, #303 and #744 that were passaged in mice (n = 4 mice per model). Scale bars = 100 μm. (**c**) Representative FACS plots showing expression of RANK in PDX tumour models (n = 4 mice per model). RANK expression (blue) was compared to an isotype-matched control antibody (grey).

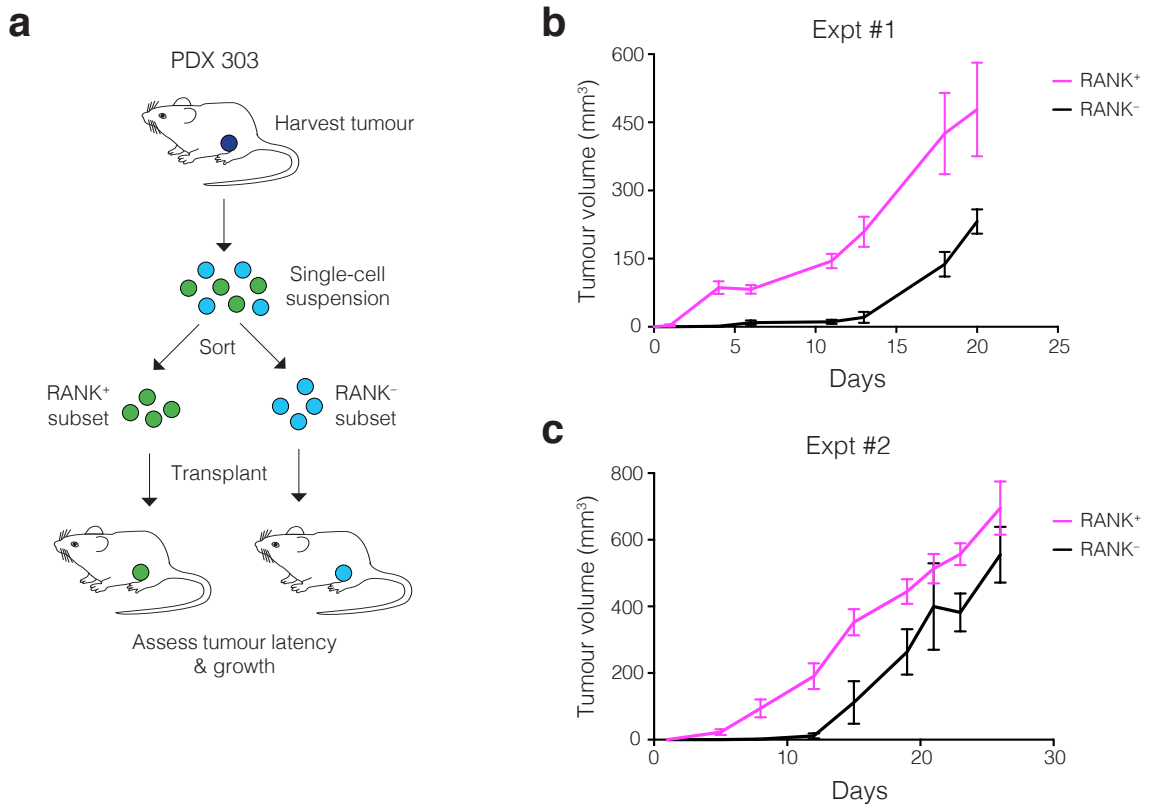

Figure 5.3: RANK$^+$ tumour cells have enhanced tumour-initiating capacity

(**a**) Experimental outline: tumours from PDX model #303 were harvested and RANK$^+$/RANK$^-$ tumour cells were isolated by flow cytometry. Equal numbers of freshly sorted cells were then injected into the cleared fat pad of *NOD-SCID-IL2γR*$^{-/-}$ mice (10,000 cells per recipient), and tumour growth was monitored. (**b**, **c**) Tumour growth curves from two independent experiments showing accelerated tumour onset and enhanced growth of RANK$^+$ tumour cells compared to RANK$^-$ cells. On each curve, data represent mean tumour volume ± s.e.m for n = 6 mice per treatment arm.

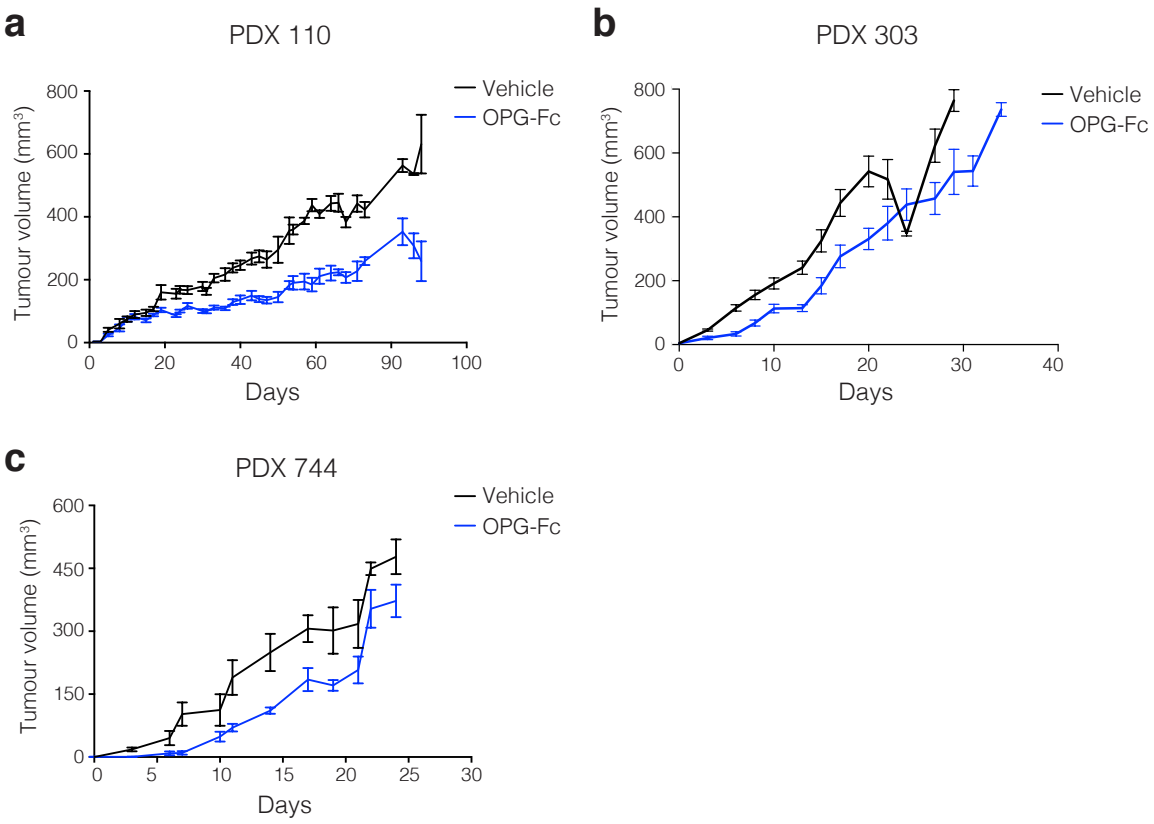

Figure 5.4: RANKL inhibition markedly attenuates tumour growth

Tumour growth curves showing (**a**) PDX 110 (**b**) PDX 303 and (**c**) PDX 744 tumours treated with either the RANKL inhibitor OPG-Fc (5 mg/kg) or an isotype matched control antibody (vehicle, 5 mg/kg). Treatment was initiated once tumours were first palpable (approximately 4 mm^3). For each graph, data represent mean tumour volume ± s.e.m for n = 10 mice per treatment arm. In (**b**), a drop in mean tumour volume in the vehicle arm was observed because the majority of mice were euthanised at this timepoint due to the ethical endpoint (600 mm^3) being reached. Only mice with smaller tumours remained after this time.

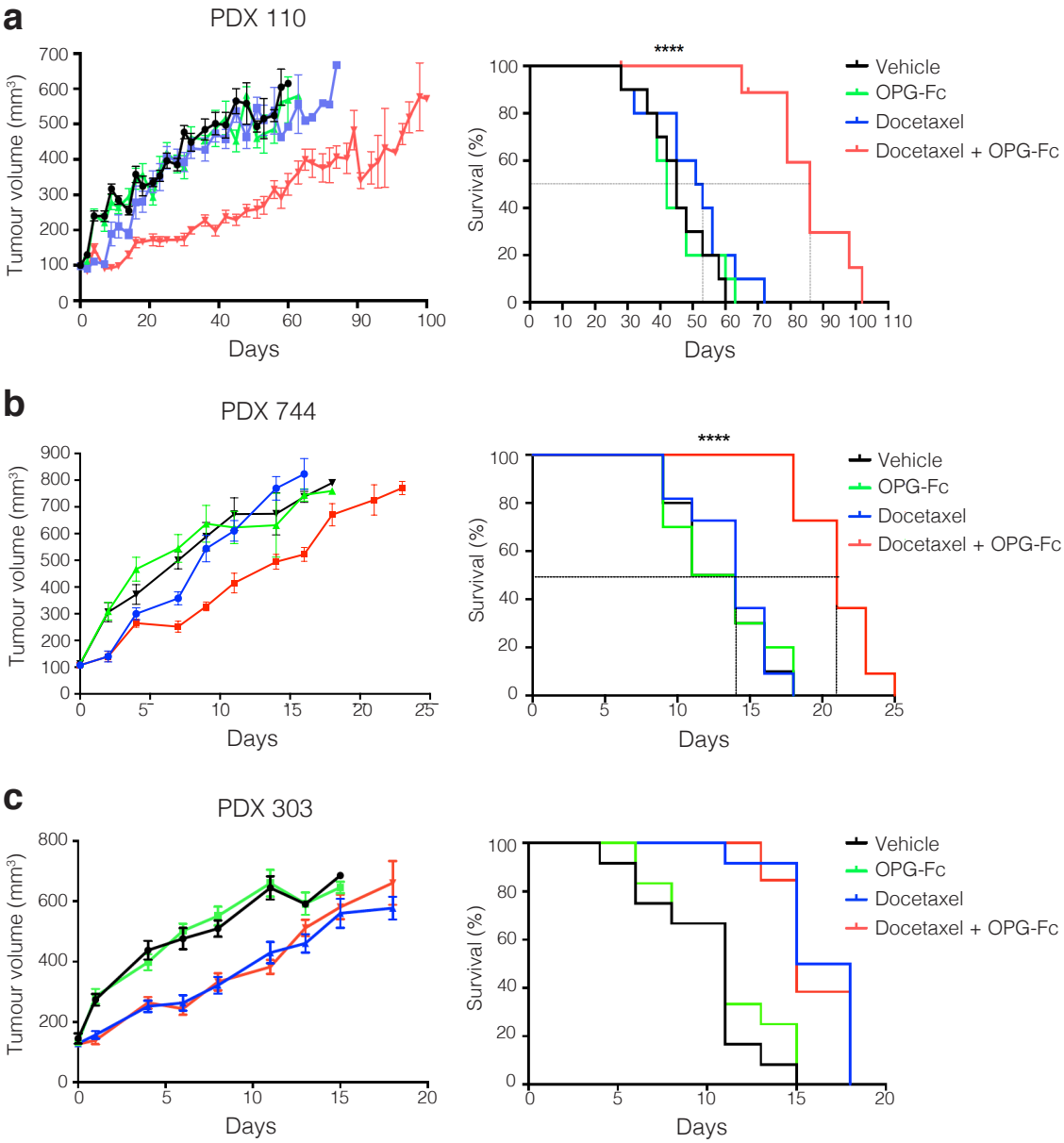

Figure 5.5: RANKL blockade synergises with docetaxel chemotherapy

Tumour growth and Kaplan-Meier survival curves depicting the response of (**a**) PDX 110 (**b**) PDX 744 and (**c**) PDX 303 tumours treated with vehicle (mouse IgG1, 5 mg/kg), docetaxel (10 mg/kg), OPG-Fc (5 mg/kg) or both docetaxel and OPG-Fc. Treatment was initiated once tumours reached a size of 100 mm^3 and mice were sacrificed once ethical endpoint (600 mm^3) was reached. For tumour growth curves, data represent mean tumour volume ± s.e.m for n = 10 mice per treatment arm. The dotted line on Kaplan-Meier curves depicts median tumour onset. ****P < 0.0001.

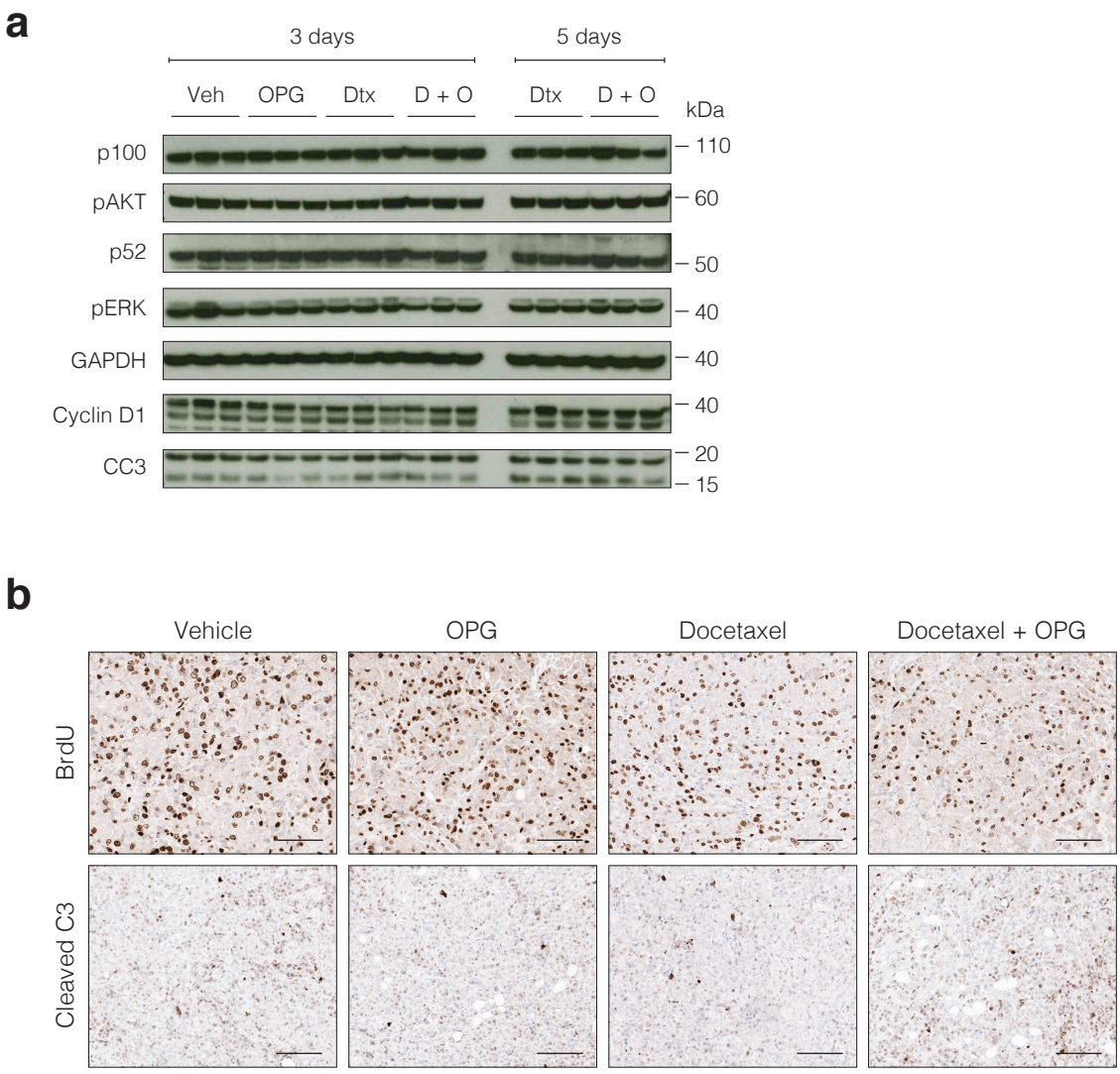

Figure 5.6: Synergy between anti-RANKL and docetaxel treatment does not appear to be due to alterations in cell proliferation or apoptosis.

(**a**) Western blot analysis of p100/p52, phospho-AKT, phospho-ERK1/2, cyclin D1 and cleaved caspase 3 (CC3) expression in PDX 110 tumours. Mice were treated with vehicle (Veh), OPG-Fc, docetaxel (Dtx) or both docetaxel and OPG-Fc (D + O) for three days before tumours were harvested (n = 3 mice per group). Additional mice in the docetaxel and docetaxel/OPG-Fc groups were harvested after five days of treatment (n = 3 mice per group). GAPDH was used as a protein loading control. (**b**) Representative images showing immunostaining for BrdU (top) and cleaved caspase 3 (bottom) in tumours harvested after three days of treatment (n = 3 mice per group). Scale bars = 100 μm.

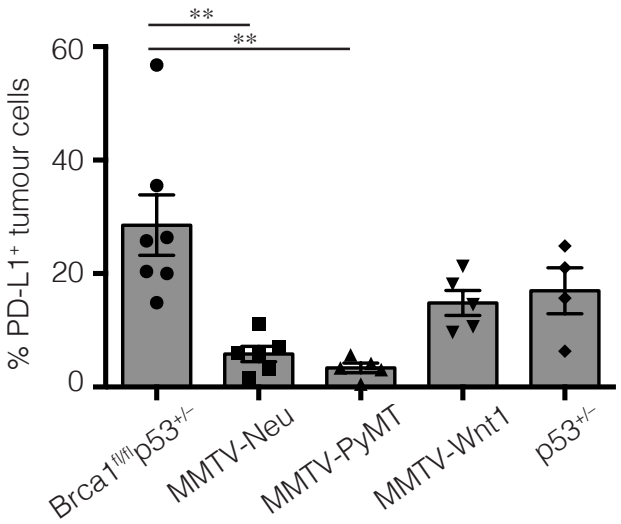

Figure 5.7: *Brca1*-deficient tumours are enriched for PD-L1 expression

Graph depicting the percentage of PD-L1^{+} tumour cells within mammary tumours harvested from *MMTV-cre/Brca1$^{fl/fl}$/p53$^{+/–}$*, *MMTV-Neu*, *MMTV-PyMT*, *MMTV-Wnt1* and *p53$^{+/–}$* mice. PD-L1 expression was determined by flow cytometry on freshly harvested tumours, and the percentage of positive cells was determined by comparing PD-L1 expression to an isotype-matched control antibody. Data represent mean ± s.e.m, each data point depicts an individual tumour. $^{**}P < 0.01$.

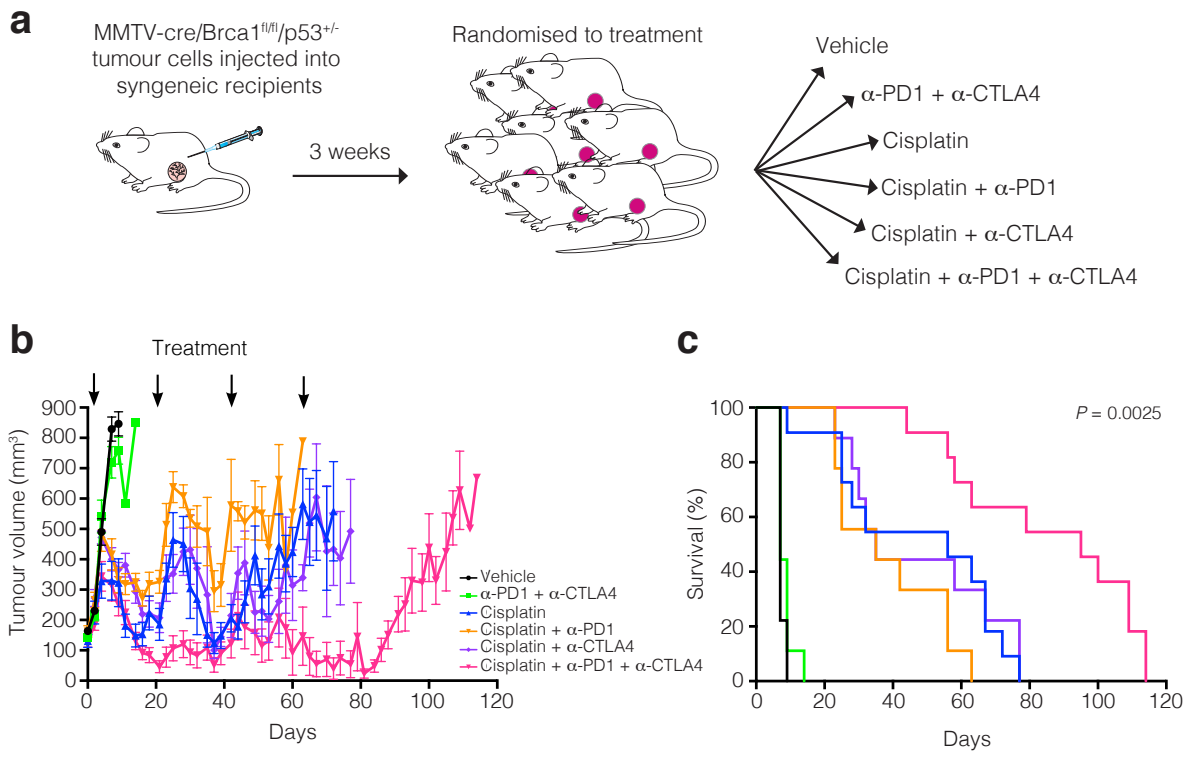

Figure 5.8: Combination therapy with checkpoint inhibitors significantly attenuates the growth of *Brca1*-deficient tumours

(**a**) Overview of treatment strategy: freshly harvested *MMTV-cre/Brca1*$^{fl/fl}$*/p53*$^{+/-}$ tumour cells were injected into the mammary fat pads of syngeneic (F1 FVB x BALB/c) mice. 3-weeks post-transplantation, mice were randomised to one of six treatment arms: (1) vehicle (PBS), (2) anti-PD1 and anti-CTLA4, (3) cisplatin, (4) cisplatin and anti-PD1, (5) cisplatin and anti-CTLA4 and (6) cisplatin, anti-CTLA4 and anti-PD1. Mice received treatment on days 1, 21, 42 and 63. (**b**) Tumour growth curve and (**c**) Kaplan-Meier survival curves depicting the augmented response of *MMTV-cre/Brca1*$^{fl/fl}$*/p53*$^{+/-}$ tumours to combination therapy. In (**b**), arrows depict treatment days and data represent mean ± s.e.m for n = 11 mice per treatment arm.

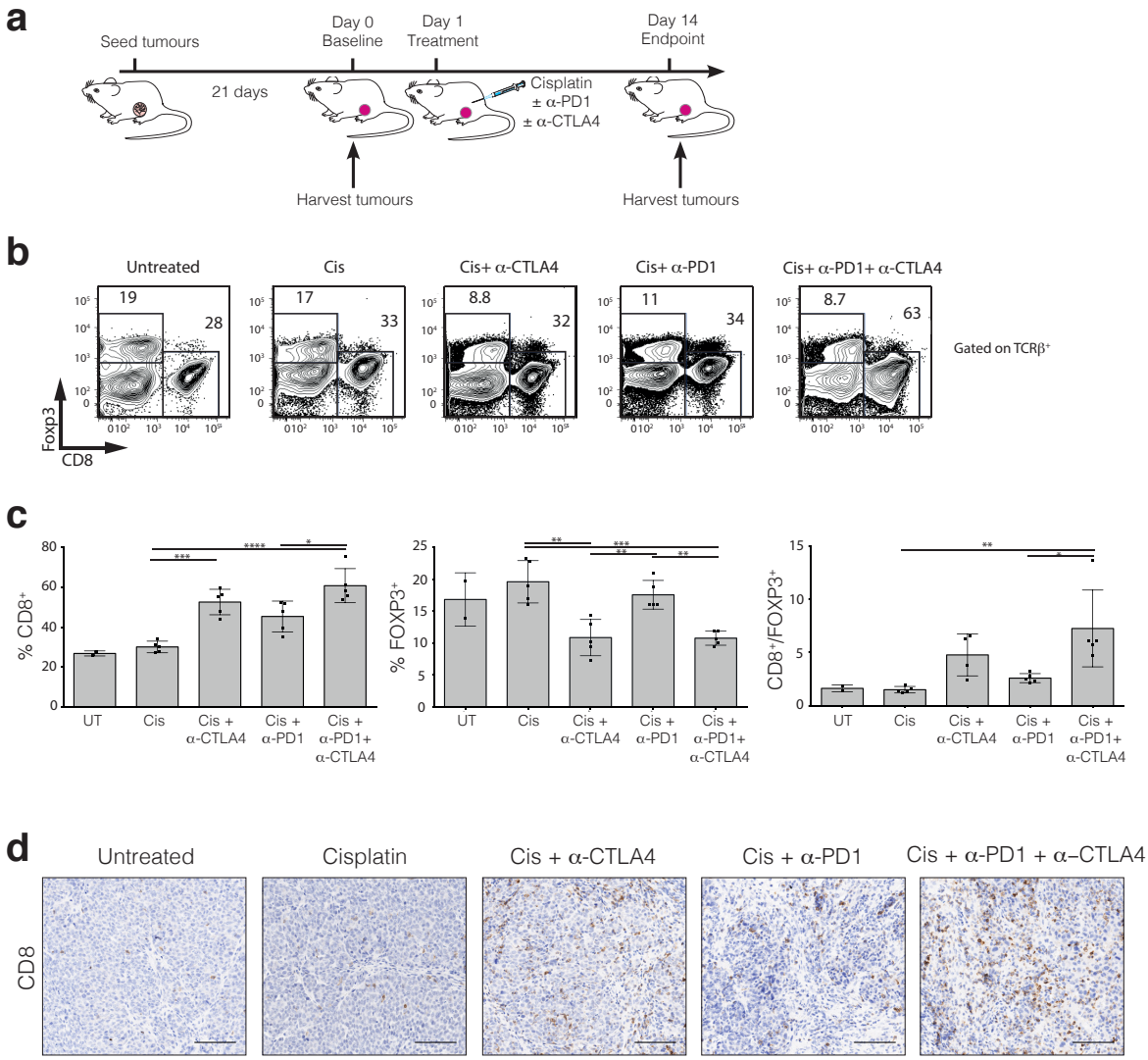
a
Seed tumours
Day 0
Baseline
Day 1
Treatment
Day 14
Endpoint
21 days
Cisplatin
± α-PD1
± α-CTLA4
Harvest tumours
Harvest tumours
b
Untreated
Cis
Cis+ α-CTLA4
Cis+ α-PD1
Cis+ α-PD1+ α-CTLA4
19
28
17
33
8.8
32
11
34
8.7
63
Foxp3
CD8
Gated on TCRβ+
c
% CD8+
% FOXP3+
CD8+/FOXP3+
UT
Cis
Cis + α-CTLA4
Cis + α-PD1
Cis + α-PD1+ α-CTLA4
d
Untreated
Cisplatin
Cis + α-CTLA4
Cis + α-PD1
Cis + α-PD1 + α–CTLA4
CD8

Figure 5.9: Checkpoint blockade induces a cytotoxic immune response within the tumour microenvironment

(**a**) To assess the effects of cisplatin and anti-CTLA4/anti-PD1 treatment on anti-tumour immunity, *MMTV-cre/Brca1*$^{fl/fl}$*/p53*$^{+/-}$ tumour cells were transplanted into the fat pads of syngeneic (F1 FVB x BALB/c) mice. Tumours were either harvested prior to treatment initiation (day 0), or 14 days after treatment with cisplatin ± anti-CTLA4/anti-PD1. The composition and activation status of immune cells infiltrating the tumour was assessed by flow cytometry on tumour cell suspensions. Two independent experiments were performed (n = 5 mice per group per experiment). (**b**) Representative FACS plots and (**c**) bar graphs showing the percentage of $CD8^+$ and $FOXP3^+$ T cells within the $TCR\beta^+$ population in tumours from mice receiving the indicated treatment. In (**c**) data represent mean ± s.e.m, and each data point represents an individual mouse. **P* < 0.05, ***P* < 0.01, ****P* < 0.001, *****P* < 0.0001. (**d**) Representative images showing immunostaining for CD8 within tumours from mice receiving the indicated treatment (n = 3 tumours per group). Scale bars = 100 μm.

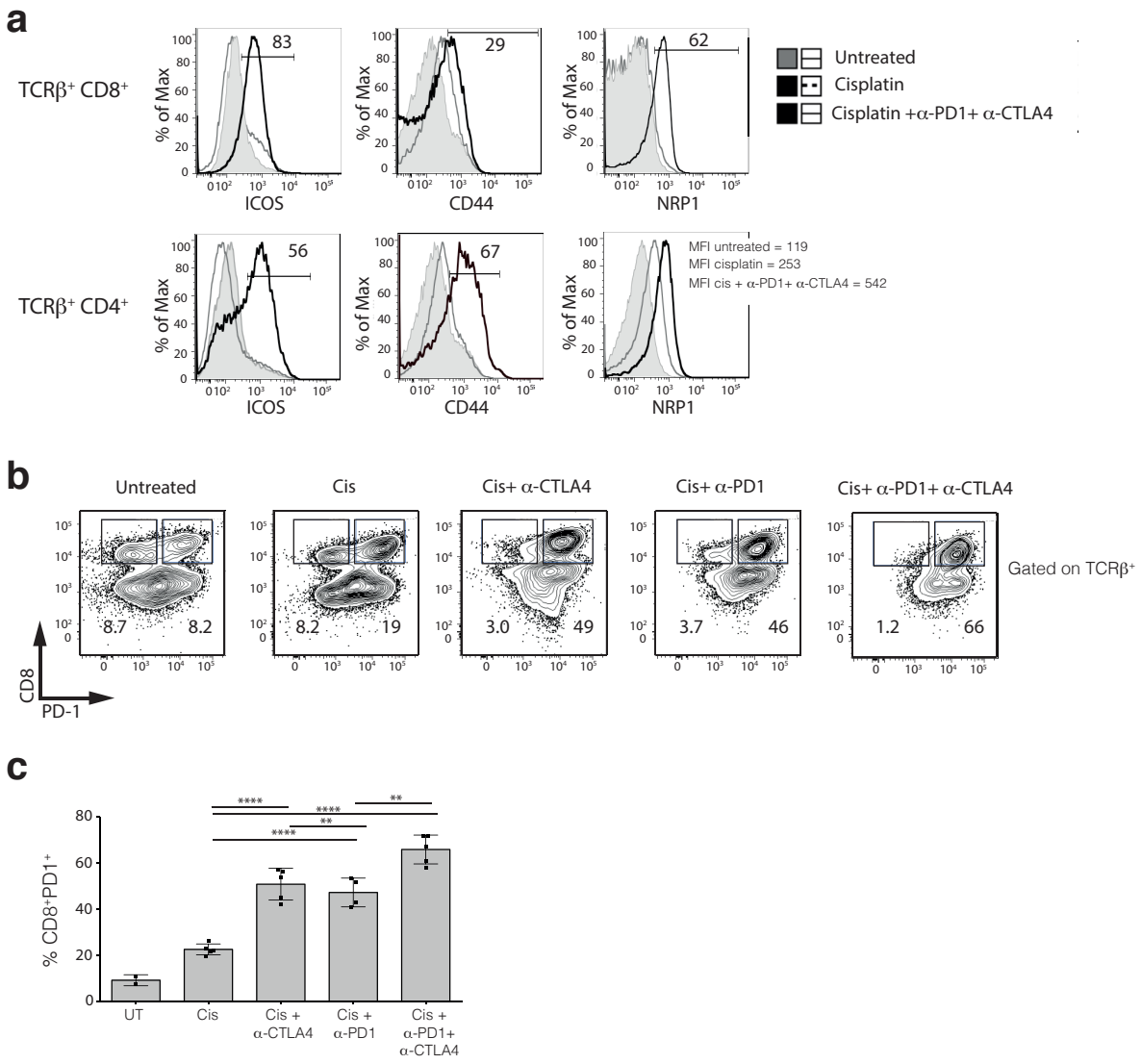

Figure 5.10: Combined checkpoint blockade induces effector T cell activation

(**a**) Representative histograms of ICOS, CD44 and NRP1 expression on TCRβ$^+$ CD4$^+$ and CD8$^+$ T cells in tumours from untreated mice versus mice treated with cisplatin or cisplatin and anti-CTLA4/anti-PD1 (n = 5 mice per group, two independent experiments). (**b**) Representative FACS plots and (**c**) bar graphs showing expression of PD-1 on CD8$^+$ T cells within tumours from mice receiving the indicated treatment (n = 5 mice per group). In (**c**) data represent mean ± s.e.m, and each data point represents an individual mouse. ***P* < 0.01, *****P* < 0.0001.

Table 5.1 Incidence scores of RANK and RANKL expression in primary breast tumours

Patient genotype	RANK-positive (%)	RANKL-positive (%)
WT	31/311 (10%)	37/312 (12%)
BRCA1$^{mut/+}$	61/144 (42%)	13/141 (9%)
BRCA2$^{mut/+}$	17/115 (15%)	5/116 (4%)

Tumours were scored from tissue microarrays from the kConFab cohort. *BRCA1*- and *BRCA2*-mutated tumours were from known mutation carriers, while WT were from 'BRCAX' cases with a positive family history, where no *BRCA1* or *BRCA2* germline mutation was identified by germline testing. *BRCA1*-mutated tumours are more frequently RANK-positive than WT (Fisher's exact test, P = 1.8e-14) or *BRCA2*-mutated tumours (P = 1.4e-6). No association was observed for RANKL staining between different groups.

Chapter 6: Concluding Remarks

6.1 Discussion and future directions

Understanding the cellular and molecular mechanisms that culminate in breast carcinogenesis in *BRCA1*-mutation carriers is pivotal for the identification of novel cancer prevention and treatment strategies. This thesis has primarily explored the possibility that the RANKL signalling axis plays a crucial role in *BRCA1*-associated breast tumorigenesis, and thus serves as the link between ovarian hormones and breast cancer risk in *BRCA1*-mutation carriers. The efficacy of RANKL inhibition for the treatment of established *BRCA1*-mutated tumours was also examined. Finally, given that lymphocytic infiltrate is a salient feature of *BRCA1*-mutated tumours, this thesis has explored the utility of immune checkpoint inhibitors as an adjunct to chemotherapy in the treatment of *BRCA1*-mutated tumours.

6.1.2 Identification of a perturbed RANK$^+$ progenitor population within *BRCA1*$^{mut/+}$ breast epithelium

Using primary human breast tissue obtained from *BRCA1*-mutation carriers who underwent a prophylactic mastectomy, we identified an expanded population of RANK$^+$ luminal progenitor cells that are highly proliferative yet exquisitely sensitive to DNA damage in the haploinsufficient state compared to other breast epithelial cell types. This likely results in a genetically unstable pool of RANK$^+$ progenitors with *BRCA1*-mutant breast epithelium. NF-κB pathway activation within RANK$^+$ cells may be the critical driver of proliferation given its previous link with RANKL-induced mammary cell proliferation (Cao et al., 2001; Schramek et al., 2010) and the augmented activity in *BRCA1*$^{mut/+}$ progenitors (Sau et al., 2016). Importantly, in addition to providing a growth advantage, NF-κB activation may also confer a survival advantage to genetically unstable RANK$^+$ cells through the induction of anti-apoptotic genes (Dutta et al., 2006). RANKL treatment has been shown to provide a marked protection from cell death in response to γ-irradiation in breast cancer cell lines, a response dependent on the NF-κB family member IKKα

(Schramek et al., 2010). Therefore by stimulating proliferation and blocking apoptosis, RANKL-mediated NF-κB activation may predispose *BRCA1*$^{mut/+}$ RANK^{+} luminal progenitor cells to acquiring a myriad of genetic alterations that promotes neoplastic transformation.

Importantly, the RANK^{+} but not RANK^{-} luminal progenitor subset shared a molecular profile more closely aligned with basal-like breast tumours than any other breast cancer subtype. Together, these findings suggest that RANK^{+} luminal progenitor cells are an important cancer-initiating population in *BRCA1*-mutation carriers. *In vivo* lineage-tracing studies will ultimately be required to conclusively prove that the RANK^{+} population is the key cellular target for transformation, analogous to elegant lineage tracing experiments performed with crypt stem cells (Barker et al., 2009). Importantly, our findings build on current knowledge of *BRCA1*-mutated breast epithelium. Although aberrant growth properties of *BRCA1*$^{mut/+}$ luminal progenitor cells have been previously reported, and the molecular profile of these cells has been correlated with basal-like breast tumours (Lim et al., 2009), our results identify for the first time a 'targetable' subpopulation of luminal progenitors that have a higher propensity for transformation. The identification of a molecular pathway that could be inhibited to switch off the proliferation of *BRCA1*$^{mut/+}$ luminal progenitor cells has important implications for the prevention of breast tumorigenesis. Intriguingly, single-nucleotide variants (SNPs) in the human *RANK* locus were recently reported to be associated with a modified breast cancer risk specifically in *BRCA1*-mutation carriers (Sigl et al., 2016), as well as the general population (Bonifaci et al., 2011). Although this requires validation in larger cohorts, it would be interesting in future studies to examine the biological effect of these variants on RANK signalling and oncogenesis.

The findings presented in Chapter 3 also provide insight into the tissue specificity of *BRCA1*-mutated breast tumours, as *BRCA1*-mutation carriers almost exclusively develop breast and ovarian tumours. The model for neoplastic transformation in *BRCA1*-mutated breast epithelium (Figure 3.9) suggests that haploinsufficiency for DNA repair in RANK^{+} luminal progenitor cells, together with the progesterone-responsiveness of these cells, culminates in an increased susceptibility to

oncogenesis compared with other cell types and tissues within *BRCA1*-mutation carriers. Future studies will be important to determine whether this mechanism extends to the ovary. We are currently assessing the expression of RANK within the fallopian tubes and cancer precursor lesions (STICs) of *Brca1*-deficient mice as well as human tissue sections obtained from *BRCA1*-mutation carriers who underwent an RRSO. If prominent expression is observed, this could lead to *in vivo* studies to assess the effect of RANKL blockade on the development of *BRCA1*-mutated ovarian carcinomas.

6.1.2 RANKL blockade as a potential breast cancer prevention strategy for *BRCA1*-mutation carriers

The findings described in Chapter 3 provided a strong rationale for the evaluation of RANKL as a therapeutic target for breast cancer prevention in *BRCA1*-mutation carriers, which we addressed in Chapter 4. A significant attenuation in progesterone-induced proliferation was observed in 3D human breast organoids derived from preneoplastic $BRCA1^{mut/+}$ tissue following concomitant exposure to denosumab, a human-specific RANKL inhibitor. Importantly, this finding was confirmed *in vivo*, since breast cell proliferation was markedly reduced by short-term denosumab treatment in three *BRCA1*-mutation carriers participating in the BRCA-D pre-operative window study. Thus, RANKL blockade demonstrated efficacy in the human setting and almost completely abrogated proliferation in *BRCA1*-mutant breast epithelium during the preneoplastic phase. We are currently validating these findings in new BRCA-D study participants, and extending the analysis to include colony-forming and NF-κB reporter assays and gene-expression profiling. These experiments will provide additional insights into the biological consequences of RANKL inhibition in *BRCA1*-mutation carriers.

Through *in vivo* preclinical studies designed to recapitulate a prevention study in young *BRCA1*-mutation carriers, a significantly delayed tumour onset and reduced hyperplasia was observed in *MMTV-cre/*$Brca1^{fl/fl}$*/*$p53^{+/-}$ mice treated with either the RANKL inhibitor OPG-Fc or a neutralising anti-RANKL antibody during the preneoplastic phase. The efficacy of RANKL blockade was comparable to the delay in mammary tumorigenesis demonstrated in mice that underwent an

oophorectomy. These findings, coupled with the attenuation in proliferation observed in human *BRCA1*$^{mut/+}$ tissue, lend support to the 'repurposing' of denosumab as a novel, targeted prevention strategy for *BRCA1*-mutation carriers. Denosumab binds with high affinity and specificity to primate RANKL, and does not inhibit any other TNF family member such as TNFα or TRAIL (Kostenuik et al., 2009). It has a long circulating half-life, with an ability to suppress bone resorption in postmenopausal subjects for up to 6 months after a single subcutaneous injection (McClung et al., 2006). Furthermore, denosumab has been received by thousands of patients both in clinical trials and in routine practice, albeit mainly postmenopausal women. Low dose therapy has a well documented safely profile and serious adverse events are uncommon (for example Thomas et al., 2010). Osteonecrosis of the jaw and atypical fractures have emerged as rare but serious side effects, although this has typically been observed in cancer patients who receive prolonged high dose therapy for bone metastasis. It would however be imperative to establish whether denosumab has a favourable safety profile in young, premenopausal women. Our findings encourage the initiation of a large randomised international clinical trial to assess the true potential and safety of denosumab as a preventive therapy (either delaying or preventing breast cancer) in *BRCA1*-mutation carriers.

It is likely that denosumab therapy will be most effective when initiated at a younger age, allowing less time for the accumulation of DNA lesions and damage-induced NF-κB activity, which could persist in the absence of RANK signalling. The treatment period could be between 5 – 10 years, however, clinical studies are required to determine the optimal timing and duration of therapy. Clinical trials will also be important to determine whether denosumab treatment has any carry-over benefit, as been observed with tamoxifen therapy, whereby the effects of five years of treatment have been shown to persist for at least an additional 5 years (Peto, 1996).

It is possible that denosumab will have broader applicability for other women at increased genetic risk, including *BRCA2*-mutation carriers or women with a strong family history of breast cancer with no identifiable germline mutation. In support of this, we observed a modest attenuation in cell proliferation in 3D breast organoids

isolated from WT patients, suggesting that RANKL blockade may be beneficial for reducing cell proliferation within the breast epithelium irrespective of *BRCA1*-mutation status. It will also be important to ascertain whether post-menopausal *BRCA1*-mutation carriers could benefit from RANKL blockade, since this would substantially increase the number of women who could benefit from this prevention strategy. The marked decline in progesterone levels at the onset of menopause suggests that the resulting decrease in RANKL production may render denosumab therapy ineffective. However, the concurrent reduction in oestrogen at menopause would also lead to a reduction in OPG levels since oestrogen is a key regulator of *OPG* expression (Hofbauer, 1999). As OPG is the decoy receptor for RANKL, this could result in even low levels of RANKL being capable of inducing a biological effect. This is the basis for the use of denosumab to treat osteoporosis in postmenopausal women, since declining oestrogen levels alter the OPG/RANKL ratio in the bone microenvironment and increase bone resorption (Cummings et al., 2009). To address these questions, we plan to perform NF-κB reporter assays and colony-forming assays on $RANK^+$ cells isolated from $BRCA2^{mut/+}$ breast tissue, postmenopausal $BRCA1^{mut/+}$ breast tissue and prophylactic breast tissue obtained from high risk women, to determine whether perturbed RANKL/NF-κB signalling is a feature of these cells. Importantly, the BRCA-D window study is currently also recruiting *BRCA2*-mutation carriers, women with a strong family history and postmenopausal *BRCA1*-mutation carriers, which will provide crucial insights into broader utility of denosumab therapy.

6.1.3 RANKL and immune checkpoints as therapeutic targets for the treatment of *BRCA1*-mutated breast tumours

In Chapter 5, novel therapies or drug combinations for the treatment of *BRCA1*-mutated breast tumours were investigated. *BRCA1*-mutated human breast tumours were found to be significantly enriched for the expression of RANK compared to WT breast tumours or tumours from *BRCA2*-mutation carriers. This finding is compatible with previous observations that RANK is expressed in high grade, proliferative tumours that lack hormone receptor expression (Palafox et al., 2012; Pfitzner et al., 2014; Santini et al., 2011), all salient features of *BRCA1*-mutated tumours. It is also consistent with the prominent RANK expression observed in

MMTV-cre/Brca1$^{fl/fl}$*/p53*$^{+/-}$ mouse mammary tumours, detailed in Chapter 4. Thus, perhaps in addition to driving tumour initiation in *BRCA1*-mutated breast epithelium, the RANKL signalling axis may have a role in facilitating tumour progression. The combination of RANKL blockade and docetaxel significantly attenuated the growth of RANK^{+} PDX tumours *in vivo* and improved host survival. This is consistent with findings from a mouse model of prostate cancer bone metastasis, whereby RANKL inhibition plus docetaxel improved survival and reduced tumour burden (Miller et al., 2008). The synergistic relationship between RANKL inhibition and docetaxel chemotherapy has important therapeutic implications. *BRCA1*-mutated breast tumours typically show a poor response to taxane-based chemotherapy in the clinic (Byrski et al., 2008), therefore the concurrent use of denosumab could enhance the sensitivity of *BRCA1*-deficient cancer cells to docetaxel and augment treatment efficacy. Future work could involve identifying other chemotherapeutics that synergise with denosumab, and the exploration of potentially useful combinations in clinical studies. Importantly, given the favourable safety profile of denosumab, its inclusion in current treatment regimes for *BRCA1*-mutation carriers is unlikely to cause a significant increase in toxicity.

Notably, RANKL blockade could also impact on the burden of metastasis in *BRCA1*-mutation carriers or potentially other breast cancer patients with RANK^{+} tumours. RANK overexpression in *BRCA1*-mutated breast cancer cell lines stimulated their migration *in vitro* and increased the frequency and size of lung metastasis following tail vein injection *in vivo* (Palafox et al., 2012). Furthermore, *in vivo* neutralisation of RANKL led to a marked reduction in the burden of bone metastases in a RANK-expressing mouse melanoma model (Jones et al., 2006) and pulmonary metastasis in the *MMTV-Neu* mouse mammary tumour model (Gonzalez-Suarez et al., 2010; Tan et al., 2011). Since *MMTV-cre/Brca1*$^{fl/fl}$*/p53*$^{+/-}$ mice do not undergo spontaneous metastasis, and the *BRCA1*-mutant PDX models 110 and 303 are poorly metastatic, examining the effect of RANKL blockade on metastasis progression was not examined in this thesis. This question could be addressed in future studies by screening a large number of PDX models to identify additional RANK^{+} *BRCA1*-mutated tumours that have metastatic potential. Furthermore, insights may be provided from a randomised phase III clinical study that is underway (the D-CARE study, NCT01077154). The aim of this study

involving 4,509 women is to assess whether denosumab can prevent disease recurrence in bone or other sites when it is given as adjuvant therapy for early stage breast cancer. The results will determine whether RANKL blockade could prevent metastasis in breast cancer patients with early stage disease, particularly if information regarding the *BRCA1*-mutation status of participants is provided.

The efficacy of checkpoint blockade for the treatment of *BRCA1*-mutated breast cancers was also explored in Chapter 5. Immune checkpoint inhibitors have emerged as a powerful new cancer therapy and have changed the treatment landscape for a range of tumour types, particularly those with high mutational loads such as melanoma. However, only modest results have so far been observed in breast cancer, where tumours are rarely hypermutated (Alexandrov et al., 2013). In this chapter, we report that dual anti-PD1 and anti-CTLA4 therapy, when combined with cisplatin, profoundly attenuated the growth of *MMTV-cre/Brca1*$^{fl/fl}$*/p53*$^{+/-}$ mammary tumours *in vivo*, and markedly improved host survival. Analysis of tumour-infiltrating lymphocyte composition following short-term treatment revealed an augmented endogenous anti-tumour immunity in *MMTV-cre/Brca1*$^{fl/fl}$*/p53*$^{+/-}$ mice receiving combination therapy. Together these findings provide a strong rationale for further investigation of immunotherapy for the treatment of *BRCA1*-mutated breast cancers in the clinic. Two recent clinical trials have demonstrated efficacy of either anti-PD1 or anti-PDL1 antibodies in patients with TNBC, however, the reported response rate were only 20% (Emens et al., 2015; Nanda et al., 2015). We speculate that clinical trials of patients carrying germline *BRCA1*-mutations could lead to an improvement in tumour response rates. In addition, in contrast to chemotherapy which often elicits transient responses, clinical trials of checkpoint blockade indicate a prolonged response and survival in a proportion of patients, long after completion of a short-course of therapy (Hodi et al., 2010). This suggests that checkpoint blockade may re-educate the immune system to keep tumours in check after treatment completion. Therefore the inclusion of checkpoint inhibitors along with conventional chemotherapy for the treatment of *BRCA1*-mutation carriers may not only enhance treatment efficacy but has the potential for producing a more durable response.

It is possible that a combinatorial strategy involving RANKL inhibition and checkpoint blockade could deliver a superior response. Recently, remarkable synergy between denosumab and anti-CTLA4 therapy was reported in a patient with rapidly advancing metastatic melanoma (Smyth et al., 2016). The patient had aggressive and symptomatic bone metastasis and thus was receiving denosumab for palliation in conjunction with anti-CTLA4 therapy to reduce tumour burden. The patient had a dramatic response to combination therapy, and a positron emission tomography (PET) scan taken at 62 weeks post-treatment revealed no evidence of residual melanoma. In a preclinical melanoma model, lymphocytes (natural killer cells and T cells) were demonstrated to be responsible for the anti-tumour activity of dual-therapy (Smyth et al., 2016). Furthermore, RANKL blockade in an alternative mouse melanoma model has been shown to enhance endogenous anti-tumour immunity by transiently inhibiting negative selection in the thymus, allowing the persistence of tumour antigen-specific T cells (Khan et al., 2014). This led to a reduction in tumour burden and increased host survival in response to tumour challenge. Based on these studies we speculate that RANKL inhibition, in addition to directly attenuating the growth of *BRCA1*-mutant breast cancer cells, could rescue tumour-specific T cells from thymic deletion and lead to an enhanced anti-cancer immune response when used in conjunction with checkpoint blockade and chemotherapy. Thus, triple therapy (RANKL blockade, chemotherapy and checkpoint inhibitors) could lead to a superior response compared to one or two agents. The efficacy and safety of this approach would need to be evaluated in preclinical and clinical studies. For instance, tumour growth and treatment toxicity could be assessed in the *MMTV-cre/Brca1*$^{fl/fl}$*/p53*$^{+/-}$ mouse model following treatment with cisplatin, anti-PD1 and anti-CTLA4 in the presence or absence of OPG-Fc.

6.2 Conclusions

Women who harbour germline *BRCA1* mutations have an approximately 65% lifetime risk of developing breast cancer (Antoniou et al., 2003). The focus of research efforts for *BRCA1*-mutated breast cancer is currently two-pronged. Firstly, the identification of a non-invasive breast cancer prevention therapy remains a pressing area of need, since there are currently no effective options available for

BRCA1-mutation carriers to reduce their risk besides a prophylactic mastectomy. Secondly, due to the aggressive clinical behaviour of *BRCA1*-mutated breast tumours, lack of targeted treatments and a high rate of relapse, the discovery of novel molecular targets for therapy is a key focus for the field. The objectives of this thesis were to address both research questions, and our key findings are summarised in Figure 6.1. We have identified RANKL inhibition as a potential breast cancer prevention strategy for *BRCA1*-mutation carriers, and this is currently being investigated in a pilot clinical trial and will likely lead to the initiation of an international prevention study in the next 1 – 2 years. We have also reported two new strategies for the treatment of established *BRCA1*-mutated breast cancers, providing proof-of-principle findings that warrant further investigation. Together, these findings provide important insights into the molecular mechanisms governing oncogenesis and tumour progression in *BRCA1*-mutation carriers and offer novel strategies for cancer prevention and treatment. If confirmed in clinical trials, these therapies could have a significant impact on the lives of *BRCA1*-mutation carriers and possibly other women at high risk of developing breast cancer.

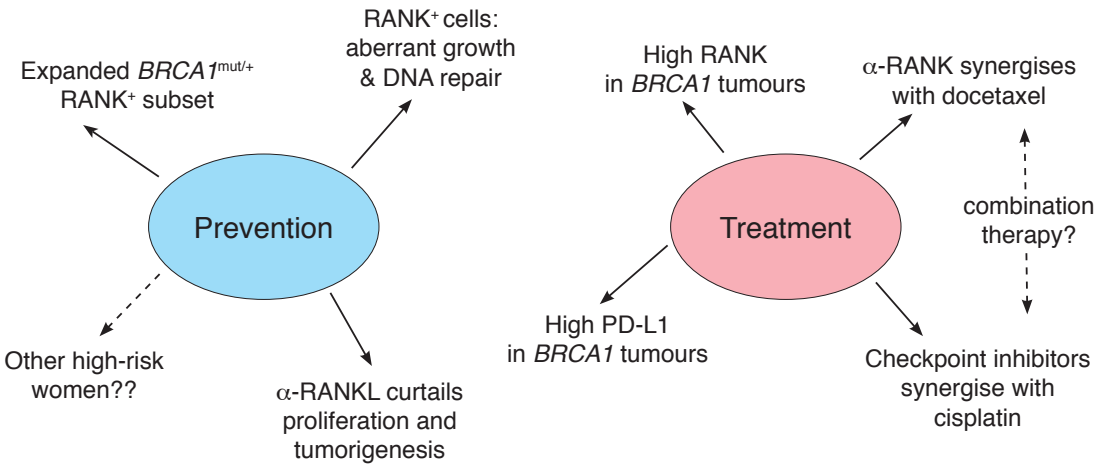

Figure 6.1: Overview of key findings presented in this thesis.
RANKL blockade via denosumab may be an effective breast cancer prevention therapy for *BRCA1*-mutation carriers. For the treatment of *BRCA1*-mutated breast tumours, both RANKL and immune checkpoints represent promising new molecular targets when used in conjunction with conventional therapies.

Bibliography

Al Sayed, A. D., El Weshi, A. N., Tulbah, A. M., Rahal, M. M. and Ezzat, A. A. (2006). Metaplastic carcinoma of the breast clinical presentation, treatment results and prognostic factors. *Acta Oncologica* **45**, 188-195.

Alexandrov, L. B., Nik-Zainal, S., Wedge, D. C., Aparicio, S. A., Behjati, S., Biankin, A. V., Bignell, G. R., Bolli, N., Borg, A., Borresen-Dale, A. L., et al. (2013). Signatures of mutational processes in human cancer. *Nature* **500**, 415-421.

Anderson, D. M., Maraskovsky, E., Billingsley, W. L., Dougall, W. C., Tometsko, M. E., Roux, E. R., Teepe, M. C., DuBose, R. F., Cosman, D. and Galibert, L. (1997). A homologue of the TNF receptor and its ligand enhance T-cell growth and dendritic-cell function. *Nature* **390**, 175-179.

Anderson, S. F., Schlegel, B. P., Nakajima, T., Wolpin, E. S. and Parvin, J. D. (1998). BRCA1 protein is linked to the RNA polymerase II holoenzyme complex via RNA helicase A. *Nature Genetics* **19**, 254-256.

Antoniou, A., Pharoah, P. D., Narod, S., Risch, H. A., Eyfjord, J. E., Hopper, J. L., Loman, N., Olsson, H., Johannsson, O., Borg, A., et al. (2003). Average risks of breast and ovarian cancer associated with BRCA1 or BRCA2 mutations detected in case Series unselected for family history: a combined analysis of 22 studies. *American Journal of Human Genetics* **72**, 1117-1130.

Antoniou, A. C., Cunningham, A. P., Peto, J., Evans, D. G., Lalloo, F., Narod, S. A., Risch, H. A., Eyfjord, J. E., Hopper, J. L., Southey, M. C., et al. (2008). The BOADICEA model of genetic susceptibility to breast and ovarian cancers: updates and extensions. *British Journal of Cancer* **98**, 1457-1466.

Aparicio, S., Hidalgo, M. and Kung, A. L. (2015). Examining the utility of patient-derived xenograft mouse models. *Nature Reviews Cancer* **15**, 311-316.

Arendt, L. M., Keller, P. J., Skibinski, A., Goncalves, K., Naber, S. P., Buchsbaum, R. J., Gilmore, H., Come, S. E. and Kuperwasser, C. (2014). Anatomical localization of progenitor cells in human breast tissue reveals enrichment of uncommitted cells within immature lobules. *Breast Cancer Research* **16**, 453.

Arendt, L. M. and Kuperwasser, C. (2015). Form and function: how estrogen and progesterone regulate the mammary epithelial hierarchy. *Journal of Mammary Gland Biology and Neoplasia* **20**, 9-25.

Asselin-Labat, M. L., Sutherland, K. D., Barker, H., Thomas, R., Shackleton, M., Forrest, N. C., Hartley, L., Robb, L., Grosveld, F. G., van der Wees, J., et al. (2007). Gata-3 is an essential regulator of mammary-gland morphogenesis and luminal-cell differentiation. *Nature Cell Biology* **9**, 201-209.

Asselin-Labat, M. L., Sutherland, K. D., Vaillant, F., Gyorki, D. E., Wu, D., Holroyd, S., Breslin, K., Ward, T., Shi, W., Bath, M. L., et al. (2011). Gata-3 negatively regulates the tumor-initiating capacity of mammary luminal progenitor cells and targets the putative tumor suppressor caspase-14. *Molecular and Cellular Biology* **31**, 4609-4622.

Asselin-Labat, M. L., Vaillant, F., Sheridan, J. M., Pal, B., Wu, D., Simpson, E. R., Yasuda, H., Smyth, G. K., Martin, T. J., Lindeman, G. J., et al. (2010). Control of mammary stem cell function by steroid hormone signalling. *Nature* **465**, 798-802.

Audeh, M. W., Carmichael, J., Penson, R. T., Friedlander, M., Powell, B., Bell-McGuinn, K. M., Scott, C., Weitzel, J. N., Oaknin, A., Loman, N., et al. (2010). Oral poly(ADP-ribose) polymerase inhibitor olaparib in patients with BRCA1 or BRCA2 mutations and recurrent ovarian cancer: a proof-of-concept trial. *Lancet* **376**, 245-251.

Azim, H. A., Jr., Peccatori, F. A., Brohee, S., Branstetter, D., Loi, S., Viale, G., Piccart, M., Dougall, W. C., Pruneri, G. and Sotiriou, C. (2015). RANK-ligand (RANKL) expression in young breast cancer patients and during pregnancy. *Breast Cancer Research* **17**, 24.

Bachelier, R., Xu, X., Li, C., Qiao, W., Furth, P. A., Lubet, R. A. and Deng, C. X. (2005). Effect of bilateral oophorectomy on mammary tumor formation in BRCA1 mutant mice. *Oncology Reports* **14**, 1117-1120.

Bancroft, E. K., Page, E. C., Castro, E., Lilja, H., Vickers, A., Sjoberg, D., Assel, M., Foster, C. S., Mitchell, G. and Drew, K. (2014). Targeted prostate cancer screening in BRCA1 and BRCA2 mutation carriers: results from the initial screening round of the IMPACT study. *European Urology* **66**, 489-499.

Barker, N., Ridgway, R. A., van Es, J. H., van de Wetering, M., Begthel, H., van den Born, M., Danenberg, E., Clarke, A. R., Sansom, O. J. and Clevers, H. (2009). Crypt stem cells as the cells-of-origin of intestinal cancer. *Nature* **457**, 608-611.

Basu, G. D., Ghazalpour, A., Gatalica, Z., Anderson, K. S., McCullough, A. E., Spetzer, D. B. and Pockaj, B. A. (2014). Expression of novel immunotherapeutic targets in triple-negative breast cancer. In *ASCO Annual Meeting Proceedings*, pp. 1001.

Baud, V. and Karin, M. (2009). Is NF-kappaB a good target for cancer therapy? Hopes and pitfalls. *Nature Reviews Drug Discovery* **8**, 33-40.

Baulieu, E.-E. (1989). Contragestion and other clinical applications of RU 486, an antiprogesterone at the receptor. *Science* **245**, 1351-1357.

Beato, M., Herrlich, P. and Schutz, G. (1995). Steroid hormone receptors: many actors in search of a plot. *Cell* **83**, 851-857.

Beatson, G. (1896). On the treatment of inoperable cases of carcinoma of the mamma: suggestions for a new method of treatment, with illustrative cases. *The Lancet* **148**, 162-165.

Beleut, M., Rajaram, R. D., Caikovski, M., Ayyanan, A., Germano, D., Choi, Y., Schneider, P. and Brisken, C. (2010). Two distinct mechanisms underlie progesterone-induced proliferation in the mammary gland. *Proceedings of the National Academy of Sciences of the United States of America* **107**, 2989-2994.

Bellacosa, A., Godwin, A. K., Peri, S., Devarajan, K., Caretti, E., Vanderveer, L., Bove, B., Slater, C., Zhou, Y., Daly, M., et al. (2010). Altered gene expression in morphologically normal epithelial cells from heterozygous carriers of BRCA1 or BRCA2 mutations. *Cancer Prevention Research* **3**, 48-61.

Beral, V. (2003). Breast cancer and hormone-replacement therapy in the Million Women Study. *Lancet* **362**, 419-427.

Bernardo, G. M., Lozada, K. L., Miedler, J. D., Harburg, G., Hewitt, S. C., Mosley, J. D., Godwin, A. K., Korach, K. S., Visvader, J. E., Kaestner, K. H., et al. (2010). FOXA1 is an essential determinant of ERalpha expression and mammary ductal morphogenesis. *Development* **137**, 2045-2054.

Bhattacharyya, A., Ear, U. S., Koller, B. H., Weichselbaum, R. R. and Bishop, D. K. (2000). The breast cancer susceptibility gene BRCA1 is required for subnuclear assembly of Rad51 and survival following treatment with the DNA cross-linking agent cisplatin. *The Journal of Biological Chemistry* **275**, 23899-23903.

Bianchini, G., Balko, J. M., Mayer, I. A., Sanders, M. E. and Gianni, L. (2016). Triple-negative breast cancer: challenges and opportunities of a heterogeneous disease. *Nature Reviews Clinical Oncology*. Epub ahead of print.

Blank, C., Brown, I., Peterson, A. C., Spiotto, M., Iwai, Y., Honjo, T. and Gajewski, T. F. (2004). PD-L1/B7H-1 inhibits the effector phase of tumor rejection by T cell receptor (TCR) transgenic CD8+ T cells. *Cancer Research* **64**, 1140-1145.

Bocchinfuso, W. P., Hively, W. P., Couse, J. F., Varmus, H. E. and Korach, K. S. (1999). A mouse mammary tumor virus-Wnt-1 transgene induces mammary gland hyperplasia and tumorigenesis in mice lacking estrogen receptor-alpha. *Cancer Research* **59**, 1869-1876.

Bochar, D. A., Wang, L., Beniya, H., Kinev, A., Xue, Y., Lane, W. S., Wang, W., Kashanchi, F. and Shiekhattar, R. (2000). BRCA1 is associated with a human SWI/SNF-related complex: linking chromatin remodeling to breast cancer. *Cell* **102**, 257-265.

Bonifaci, N., Palafox, M., Pellegrini, P., Osorio, A., Benitez, J., Peterlongo, P., Manoukian, S., Peissel, B., Zaffaroni, D., Roversi, G., et al. (2011). Evidence for a link between TNFRSF11A and risk of breast cancer. *Breast Cancer Research and Treatment* **129**, 947-954.

Boras-Granic, K., Dann, P. and Wysolmerski, J. J. (2014). Embryonic cells contribute directly to the quiescent stem cell population in the adult mouse mammary gland. *Breast Cancer Research : BCR* **16**, 487.

Borras, M., Hardy, L., Lempereur, F., el Khissiin, A. H., Legros, N., Gol-Winkler, R. and Leclercq, G. (1994). Estradiol-induced down-regulation of estrogen receptor. Effect of various modulators of protein synthesis and expression. *The Journal of Steroid Biochemistry and Molecular Biology* **48**, 325-336.

Bossen, C., Ingold, K., Tardivel, A., Bodmer, J. L., Gaide, O., Hertig, S., Ambrose, C., Tschopp, J. and Schneider, P. (2006). Interactions of tumor necrosis factor (TNF) and TNF receptor family members in the mouse and human. *The Journal of Biological Chemistry* **281**, 13964-13971.

Brekelmans, C. T., Seynaeve, C., Bartels, C. C., Tilanus-Linthorst, M. M., Meijers-Heijboer, E. J., Crepin, C. M., van Geel, A. A., Menke, M., Verhoog, L. C., van den Ouweland, A., et al. (2001). Effectiveness of breast cancer surveillance in BRCA1/2 gene mutation carriers and women with high familial risk. *Journal of Clinical Oncology* **19**, 924-930.

Brisken, C. (2002). Hormonal control of alveolar development and its implications for breast carcinogenesis. *Journal of Mammary Gland Biology and Neoplasia* **7**, 39-48.

Brisken, C. (2013). Progesterone signalling in breast cancer: a neglected hormone coming into the limelight. *Nature Reviews Cancer* **13**, 385-396.

Brisken, C., Ayyannan, A., Nguyen, C., Heineman, A., Reinhardt, F., Tan, J., Dey, S. K., Dotto, G. P. and Weinberg, R. A. (2002). IGF-2 is a mediator of prolactin-induced morphogenesis in the breast. *Developmental Cell* **3**, 877-887.

Brisken, C., Heineman, A., Chavarria, T., Elenbaas, B., Tan, J., Dey, S. K., McMahon, J. A., McMahon, A. P. and Weinberg, R. A. (2000). Essential function of Wnt-4 in mammary gland development downstream of progesterone signaling. *Genes & Development* **14**, 650-654.

Brisken, C., Kaur, S., Chavarria, T. E., Binart, N., Sutherland, R. L., Weinberg, R. A., Kelly, P. A. and Ormandy, C. J. (1999). Prolactin controls mammary gland development via direct and indirect mechanisms. *Developmental Biology* **210**, 96-106.

Brisken, C. and O'Malley, B. (2010). Hormone action in the mammary gland. *Cold Spring Harbor Perspectives in Biology* **2**, a003178.

Brisken, C., Park, S., Vass, T., Lydon, J. P., O'Malley, B. W. and Weinberg, R. A. (1998). A paracrine role for the epithelial progesterone receptor in mammary gland development. *Proceedings of the National Academy of Sciences of the United States of America* **95**, 5076-5081.

Broca, P. (1866). *Traité des tumeurs*: P. Asselin.

Brodie, S. G., Xu, X., Qiao, W., Li, W. M., Cao, L. and Deng, C. X. (2001). Multiple genetic changes are associated with mammary tumorigenesis in Brca1 conditional knockout mice. *Oncogene* **20**, 7514-7523.

Bulun, S. E., Lin, Z., Imir, G., Amin, S., Demura, M., Yilmaz, B., Martin, R., Utsunomiya, H., Thung, S., Gurates, B., et al. (2005). Regulation of aromatase expression in estrogen-responsive breast and uterine disease: from bench to treatment. *Pharmacological Reviews* **57**, 359-383.

Byrski, T., Gronwald, J., Huzarski, T., Grzybowska, E., Budryk, M., Stawicka, M., Mierzwa, T., Szwiec, M., Wisniowski, R., Siolek, M., et al. (2010). Pathologic complete response rates in young women with BRCA1-positive breast cancers after neoadjuvant chemotherapy. *Journal of Clinical Oncology* **28**, 375-379.

Byrski, T., Gronwald, J., Huzarski, T., Grzybowska, E., Budryk, M., Stawicka, M., Mierzwa, T., Szwiec, M., Wisniowski, R., Siolek, M., et al. (2008). Response to neo-adjuvant chemotherapy in women with BRCA1-positive breast cancers. *Breast Cancer Research and Treatment* **108**, 289-296.

Byrski, T., Huzarski, T., Dent, R., Gronwald, J., Zuziak, D., Cybulski, C., Kladny, J., Gorski, B., Lubinski, J. and Narod, S. A. (2009). Response to neoadjuvant therapy with cisplatin in BRCA1-positive breast cancer patients. *Breast Cancer Research and Treatment* **115**, 359-363.

Byrski, T., Huzarski, T., Dent, R., Marczyk, E., Jasiowka, M., Gronwald, J., Jakubowicz, J., Cybulski, C., Wisniowski, R., Godlewski, D., et al. (2014). Pathologic complete response to neoadjuvant cisplatin in BRCA1-positive breast cancer patients. *Breast Cancer Research and Treatment* **147**, 401-405.

Caestecker, K. W. and Van de Walle, G. R. (2013). The role of BRCA1 in DNA double-strand repair: past and present. *Experimental Cell Research* **319**, 575-587.

Cao, Y., Bonizzi, G., Seagroves, T. N., Greten, F. R., Johnson, R., Schmidt, E. V. and Karin, M. (2001). IKKalpha provides an essential link between RANK signaling and cyclin D1 expression during mammary gland development. *Cell* **107**, 763-775.

Cao, Y., Luo, J. L. and Karin, M. (2007). IkappaB kinase alpha kinase activity is required for self-renewal of ErbB2/Her2-transformed mammary tumor-initiating cells. *Proceedings of the National Academy of Sciences of the United States of America* **104**, 15852-15857.

Carey, L. A., Dees, E. C., Sawyer, L., Gatti, L., Moore, D. T., Collichio, F., Ollila, D. W., Sartor, C. I., Graham, M. L. and Perou, C. M. (2007). The triple negative paradox: primary tumor chemosensitivity of breast cancer subtypes. *Clinical Cancer Research* **13**, 2329-2334.

Catteau, A., Harris, W. H., Xu, C. F. and Solomon, E. (1999). Methylation of the BRCA1 promoter region in sporadic breast and ovarian cancer: correlation with disease characteristics. *Oncogene* **18**, 1957-1965.

Cawthon, R. M. (2009). Telomere length measurement by a novel monochrome multiplex quantitative PCR method. *Nucleic Acids Research* **37**, e21.

Celeste, A., Petersen, S., Romanienko, P. J., Fernandez-Capetillo, O., Chen, H. T., Sedelnikova, O. A., Reina-San-Martin, B., Coppola, V., Meffre, E. and Difilippantonio, M. J. (2002). Genomic instability in mice lacking histone H2AX. *Science* **296**, 922-927.

Chabalier, C., Lamare, C., Racca, C., Privat, M., Valette, A. and Larminat, F. (2006). BRCA1 downregulation leads to premature inactivation of spindle checkpoint and confers paclitaxel resistance. *Cell Cycle* **5**, 1001-1007.

Cheang, M. C., Chia, S. K., Voduc, D., Gao, D., Leung, S., Snider, J., Watson, M., Davies, S., Bernard, P. S., Parker, J. S., et al. (2009). Ki67 index, HER2 status, and prognosis of patients with luminal B breast cancer. *Journal of the National Cancer Institute* **101**, 736-750.

Cheang, M. C., Martin, M., Nielsen, T. O., Prat, A., Voduc, D., Rodriguez-Lescure, A., Ruiz, A., Chia, S., Shepherd, L., Ruiz-Borrego, M., et al. (2015). Defining breast cancer intrinsic subtypes by quantitative receptor expression. *The Oncologist* **20**, 474-482.

Chen, D. S. and Mellman, I. (2013). Oncology meets immunology: the cancer-immunity cycle. *Immunity* **39**, 1-10.

Chen, L. and Flies, D. B. (2013). Molecular mechanisms of T cell co-stimulation and co-inhibition. *Nature Reviews Immunology* **13**, 227-242.

Chen, S. and Parmigiani, G. (2007). Meta-analysis of BRCA1 and BRCA2 penetrance. *Journal of Clinical Oncology* **25**, 1329-1333.

Chepko, G. and Smith, G. H. (1997). Three division-competent, structurally-distinct cell populations contribute to murine mammary epithelial renewal. *Tissue & Cell* **29**, 239-253.

Cheung, A. M., Elia, A., Tsao, M. S., Done, S., Wagner, K. U., Hennighausen, L., Hakem, R. and Mak, T. W. (2004). Brca2 deficiency does not impair mammary epithelium development but promotes mammary adenocarcinoma formation in p53(+/-) mutant mice. *Cancer Research* **64**, 1959-1965.

Chlebowski, R. T., Anderson, G. L., Gass, M., Lane, D. S., Aragaki, A. K., Kuller, L. H., Manson, J. E., Stefanick, M. L., Ockene, J., Sarto, G. E., et al. (2010). Estrogen plus progestin and breast cancer incidence and mortality in postmenopausal women. *Journal of the American Medical Association* **304**, 1684-1692.

Ciarloni, L., Mallepell, S. and Brisken, C. (2007). Amphiregulin is an essential mediator of estrogen receptor alpha function in mammary gland development. *Proceedings of the National Academy of Sciences of the United States of America* **104**, 5455-5460.

Ciruelos Gil, E. M. (2014). Targeting the PI3K/AKT/mTOR pathway in estrogen receptor-positive breast cancer. *Cancer Treatment Reviews* **40**, 862-871.

Clarke, R. B., Howell, A., Potten, C. S. and Anderson, E. (1997). Dissociation between steroid receptor expression and cell proliferation in the human breast. *Cancer Research* **57**, 4987-4991.

Clevers, H. and Nusse, R. (2012). Wnt/beta-catenin signaling and disease. *Cell* **149**, 1192-1205.

Colditz, G. A., Rosner, B. A., Chen, W. Y., Holmes, M. D. and Hankinson, S. E. (2004). Risk factors for breast cancer according to estrogen and progesterone receptor status. *Journal of the National Cancer Institute* **96**, 218-228.

Collaborative Group on Hormonal Factors in Breast Cancer (1997). Breast cancer and hormone replacement therapy: collaborative reanalysis of data from 51 epidemiological studies of 52,705 women with breast cancer and 108,411 women without breast cancer. *Lancet* **350**, 1047-1059.

Cortez, D., Wang, Y., Qin, J. and Elledge, S. J. (1999). Requirement of ATM-dependent phosphorylation of brca1 in the DNA damage response to double-strand breaks. *Science* **286**, 1162-1166.

Couch, F. J., Nathanson, K. L. and Offit, K. (2014). Two decades after BRCA: setting paradigms in personalized cancer care and prevention. *Science* **343**, 1466-1470.

Crowder, R. J., Phommaly, C., Tao, Y., Hoog, J., Luo, J., Perou, C. M., Parker, J. S., Miller, M. A., Huntsman, D. G., Lin, L., et al. (2009). PIK3CA and PIK3CB inhibition produce synthetic lethality when combined with estrogen deprivation in estrogen receptor-positive breast cancer. *Cancer Research* **69**, 3955-3962.

Cui, Y., Riedlinger, G., Miyoshi, K., Tang, W., Li, C., Deng, C. X., Robinson, G. W. and Hennighausen, L. (2004). Inactivation of Stat5 in mouse mammary epithelium during pregnancy reveals distinct functions in cell proliferation, survival, and differentiation. *Molecular and Cellular Biology* **24**, 8037-8047.

Cummings, S. R., San Martin, J., McClung, M. R., Siris, E. S., Eastell, R., Reid, I. R., Delmas, P., Zoog, H. B., Austin, M., Wang, A., et al. (2009). Denosumab for prevention of fractures in postmenopausal women with osteoporosis. *The New England Journal of Medicine* **361**, 756-765.

Dabydeen, S. A. and Furth, P. A. (2014). Genetically engineered ERalpha-positive breast cancer mouse models. *Endocrine-Related Cancer* **21**, R195-208.

Daniel, C. W., De Ome, K. B., Young, J. T., Blair, P. B. and Faulkin, L. J., Jr. (1968). The in vivo life span of normal and preneoplastic mouse mammary glands: a serial transplantation study. *Proceedings of the National Academy of Sciences of the United States of America* **61**, 53-60.

Daniel, C. W., Silberstein, G. B. and Strickland, P. (1987). Direct action of 17 beta-estradiol on mouse mammary ducts analyzed by sustained release implants and steroid autoradiography. *Cancer Research* **47**, 6052-6057.

Daniel, C. W. and Smith, G. H. (1999). The mammary gland: a model for development. *Journal of Mammary Gland Biology and Neoplasia* **4**, 3-8.

de Lau, W., Peng, W. C., Gros, P. and Clevers, H. (2014). The R-spondin/Lgr5/Rnf43 module: regulator of Wnt signal strength. *Genes & Development* **28**, 305-316.

Deng, C. X. (2006). BRCA1: cell cycle checkpoint, genetic instability, DNA damage response and cancer evolution. *Nucleic Acids Research* **34**, 1416-1426.

Dent, R., Trudeau, M., Pritchard, K. I., Hanna, W. M., Kahn, H. K., Sawka, C. A., Lickley, L. A., Rawlinson, E., Sun, P. and Narod, S. A. (2007). Triple-negative breast cancer: clinical features and patterns of recurrence. *Clinical cancer research* **13**, 4429-4434.

DeOme, K. B., Faulkin, L. J., Jr., Bern, H. A. and Blair, P. B. (1959). Development of mammary tumors from hyperplastic alveolar nodules transplanted into gland-free mammary fat pads of female C3H mice. *Cancer Research* **19**, 515-520.

DeRose, Y. S., Wang, G., Lin, Y.-C., Bernard, P. S., Buys, S. S., Ebbert, M. T., Factor, R., Matsen, C., Milash, B. A. and Nelson, E. (2011). Tumor grafts derived from women with breast cancer authentically reflect tumor pathology, growth, metastasis and disease outcomes. *Nature Medicine* **17**, 1514-1520.

Dieci, M. V., Mathieu, M. C., Guarneri, V., Conte, P., Delaloge, S., Andre, F. and Goubar, A. (2015). Prognostic and predictive value of tumor-infiltrating lymphocytes in two phase III randomized adjuvant breast cancer trials. *Annals of Oncology* **26**, 1698-1704.

Djonov, V., Andres, A. C. and Ziemiecki, A. (2001). Vascular remodelling during the normal and malignant life cycle of the mammary gland. *Microscopy Research and Technique* **52**, 182-189.

Domchek, S. M., Friebel, T. M., Neuhausen, S. L., Wagner, T., Evans, G., Isaacs, C., Garber, J. E., Daly, M. B., Eeles, R., Matloff, E., et al. (2006). Mortality after bilateral salpingo-oophorectomy in BRCA1 and BRCA2 mutation carriers: a prospective cohort study. *The Lancet Oncology* **7**, 223-229.

Domchek, S. M., Friebel, T. M., Singer, C. F., Evans, D. G., Lynch, H. T., Isaacs, C., Garber, J. E., Neuhausen, S. L., Matloff, E., Eeles, R., et al. (2010). Association of risk-reducing surgery in BRCA1 or BRCA2 mutation carriers with cancer risk and mortality. *Journal of the American Medical Association* **304**, 967-975.

Dong, H., Strome, S. E., Salomao, D. R., Tamura, H., Hirano, F., Flies, D. B., Roche, P. C., Lu, J., Zhu, G., Tamada, K., et al. (2002). Tumor-associated B7-H1 promotes T-cell apoptosis: a potential mechanism of immune evasion. *Nature Medicine* **8**, 793-800.

dos Santos, C. O., Rebbeck, C., Rozhkova, E., Valentine, A., Samuels, A., Kadiri, L. R., Osten, P., Harris, E. Y., Uren, P. J., Smith, A. D., et al. (2013). Molecular hierarchy of mammary differentiation yields refined markers of mammary stem cells. *Proceedings of the National Academy of Sciences of the United States of America* **110**, 7123-7130.

Drost, R. and Jonkers, J. (2014). Opportunities and hurdles in the treatment of BRCA1-related breast cancer. *Oncogene* **33**, 3753-3763.

Drost, R. M. and Jonkers, J. (2009). Preclinical mouse models for BRCA1-associated breast cancer. *British Journal of Cancer* **101**, 1651-1657.

Dutta, J., Fan, Y., Gupta, N., Fan, G. and Gelinas, C. (2006). Current insights into the regulation of programmed cell death by NF-kappaB. *Oncogene* **25**, 6800-6816.

Early Breast Cancer Trialists' Collaborative Group. (2005). Effects of chemotherapy and hormonal therapy for early breast cancer on recurrence and 15-year survival: an overview of the randomised trials. *Lancet* **365**, 1687-1717.

Easton, D., Ford, D. and Peto, J. (1993). Inherited susceptibility to breast cancer. *Cancer Surveys* **18**, 95-113.

Eirew, P., Kannan, N., Knapp, D. J., Vaillant, F., Emerman, J. T., Lindeman, G. J., Visvader, J. E. and Eaves, C. J. (2012). Aldehyde dehydrogenase activity is a biomarker of primitive normal human mammary luminal cells. *Stem Cells* **30**, 344-348.

Eirew, P., Steif, A., Khattra, J., Ha, G., Yap, D., Farahani, H., Gelmon, K., Chia, S., Mar, C. and Wan, A. (2015). Dynamics of genomic clones in breast cancer patient xenografts at single-cell resolution. *Nature* **518**, 422-426.

Eirew, P., Stingl, J., Raouf, A., Turashvili, G., Aparicio, S., Emerman, J. T. and Eaves, C. J. (2008). A method for quantifying normal human mammary epithelial stem cells with in vivo regenerative ability. *Nature Medicine* **14**, 1384-1389.

Eisen, A., Lubinski, J., Klijn, J., Moller, P., Lynch, H. T., Offit, K., Weber, B., Rebbeck, T., Neuhausen, S. L., Ghadirian, P., et al. (2005). Breast cancer risk following bilateral oophorectomy in BRCA1 and BRCA2 mutation carriers: an international case-control study. *Journal of Clinical Oncology* **23**, 7491-7496.

Eisenhauer, E. A. and Vermorken, J. B. (1998). The taxoids. Comparative clinical pharmacology and therapeutic potential. *Drugs* **55**, 5-30.

Ellis, L. M. and Fidler, I. J. (2010). Finding the tumor copycat. Therapy fails, patients don't. *Nature Medicine* **16**, 974-975.

Ellis, M. J. and Perou, C. M. (2013). The genomic landscape of breast cancer as a therapeutic roadmap. *Cancer Discovery* **3**, 27-34.

Emens, L. A., Braiteh, F. S., Cassier, P., DeLord, J.-P., Eder, J. P., Shen, X., Xiao, Y., Wang, Y., Hegde, P. S. and Chen, D. S. (2015). Abstract PD1-6: inhibition of PD-L1 by mpdl3280a leads to clinical activity in patients with metastatic triple-negative breast cancer. *Cancer Research* **75**, PD1-6-PD1-6.

Esteller, M., Silva, J. M., Dominguez, G., Bonilla, F., Matias-Guiu, X., Lerma, E., Bussaglia, E., Prat, J., Harkes, I. C., Repasky, E. A., et al. (2000). Promoter hypermethylation and BRCA1 inactivation in sporadic breast and ovarian tumors. *Journal of the National Cancer Institute* **92**, 564-569.

Evans, D. G. and Howell, A. (2004). Are BRCA1- and BRCA2-related breast cancers associated with increased mortality? *Breast Cancer Research* **6**, E7.

Evers, B. and Jonkers, J. (2006). Mouse models of BRCA1 and BRCA2 deficiency: past lessons, current understanding and future prospects. *Oncogene* **25**, 5885-5897.

Fan, C., Oh, D. S., Wessels, L., Weigelt, B., Nuyten, D. S., Nobel, A. B., van't Veer, L. J. and Perou, C. M. (2006). Concordance among gene-expression-based predictors for breast cancer. *The New England Journal of Medicine* **355**, 560-569.

Fantl, V., Stamp, G., Andrews, A., Rosewell, I. and Dickson, C. (1995). Mice lacking cyclin D1 are small and show defects in eye and mammary gland development. *Genes & Development* **9**, 2364-2372.

Farhat, G. N., Walker, R., Buist, D. S., Onega, T. and Kerlikowske, K. (2010). Changes in invasive breast cancer and ductal carcinoma in situ rates in relation to the decline in hormone therapy use. *Journal of Clinical Oncology* **28**, 5140-5146.

Farmer, H., McCabe, N., Lord, C. J., Tutt, A. N., Johnson, D. A., Richardson, T. B., Santarosa, M., Dillon, K. J., Hickson, I. and Knights, C. (2005). Targeting the DNA repair defect in BRCA mutant cells as a therapeutic strategy. *Nature* **434**, 917-921.

Fata, J. E., Kong, Y. Y., Li, J., Sasaki, T., Irie-Sasaki, J., Moorehead, R. A., Elliott, R., Scully, S., Voura, E. B., Lacey, D. L., et al. (2000). The osteoclast differentiation factor osteoprotegerin-ligand is essential for mammary gland development. *Cell* **103**, 41-50.

Faulkin, L. J., Jr. and Deome, K. B. (1960). Regulation of growth and spacing of gland elements in the mammary fat pad of the C3H mouse. *Journal of the National Cancer Institute* **24**, 953-969.

Fernandez-Valdivia, R., Mukherjee, A., Ying, Y., Li, J., Paquet, M., DeMayo, F. J. and Lydon, J. P. (2009). The RANKL signaling axis is sufficient to elicit ductal side-branching and alveologenesis in the mammary gland of the virgin mouse. *Developmental Biology* **328**, 127-139.

Finn, R. S., Aleshin, A. and Slamon, D. J. (2016). Targeting the cyclin-dependent kinases (CDK) 4/6 in estrogen receptor-positive breast cancers. *Breast Cancer Research* **18**, 17.

FitzGerald, M. G., MacDonald, D. J., Krainer, M., Hoover, I., O'Neil, E., Unsal, H., Silva-Arrieto, S., Finkelstein, D. M., Beer-Romero, P., Englert, C., et al. (1996). Germ-line BRCA1 mutations in Jewish and non-Jewish women with early-onset breast cancer. *The New England Journal of Medicine* **334**, 143-149.

Ford, D., Easton, D., Stratton, M., Narod, S., Goldgar, D., Devilee, P., Bishop, D., Weber, B., Lenoir, G. and Chang-Claude, J. (1998). Genetic heterogeneity and penetrance analysis of the BRCA1 and BRCA2 genes in breast cancer families. *The American Journal of Human Genetics* **62**, 676-689.

Forster, C., Makela, S., Warri, A., Kietz, S., Becker, D., Hultenby, K., Warner, M. and Gustafsson, J. A. (2002). Involvement of estrogen receptor beta in terminal differentiation of mammary gland epithelium. *Proceedings of the National Academy of Sciences of the United States of America* **99**, 15578-15583.

Foulkes, W. D. (2004). BRCA1 functions as a breast stem cell regulator. *Journal of Medical Genetics* **41**, 1-5.

Foulkes, W. D., Stefansson, I. M., Chappuis, P. O., Begin, L. R., Goffin, J. R., Wong, N., Trudel, M. and Akslen, L. A. (2003). Germline BRCA1 mutations and a basal epithelial phenotype in breast cancer. *Journal of the National Cancer Institute* **95**, 1482-1485.

Fritz, M.A and Speroff, L. (2012). *Clinical Gynecologic Endocrinology and Infertility* (8 edn): Lippincott Williams & Wilkins, 2012.

Fu, N. Y., Rios, A. C., Pal, B., Soetanto, R., Lun, A. T., Liu, K., Beck, T., Best, S. A., Vaillant, F., Bouillet, P., et al. (2015). EGF-mediated induction of Mcl-1 at the switch to lactation is essential for alveolar cell survival. *Nature Cell Biology* **17**, 365-375.

Gallego, M. I., Binart, N., Robinson, G. W., Okagaki, R., Coschigano, K. T., Perry, J., Kopchick, J. J., Oka, T., Kelly, P. A. and Hennighausen, L. (2001). Prolactin, growth hormone, and epidermal growth factor activate Stat5 in different compartments of mammary tissue and exert different and overlapping developmental effects. *Developmental Biology* **229**, 163-175.

García-García, C., Ibrahim, Y. H., Serra, V., Calvo, M. T., Guzmán, M., Grueso, J., Aura, C., Pérez, J., Jessen, K. and Liu, Y. (2012). Dual mTORC1/2 and HER2 blockade results in antitumor activity in preclinical models of breast cancer resistant to anti-HER2 therapy. *Clinical Cancer Research* **18**, 2603-2612.

Gelmon, K. A., Tischkowitz, M., Mackay, H., Swenerton, K., Robidoux, A., Tonkin, K., Hirte, H., Huntsman, D., Clemons, M., Gilks, B., et al. (2011). Olaparib in patients with recurrent high-grade serous or poorly differentiated ovarian carcinoma or triple-negative breast cancer: a phase 2, multicentre, open-label, non-randomised study. *The Lancet Oncology* **12**, 852-861.

Gillet, J. P., Calcagno, A. M., Varma, S., Marino, M., Green, L. J., Vora, M. I., Patel, C., Orina, J. N., Eliseeva, T. A., Singal, V., et al. (2011). Redefining the relevance of established cancer cell lines to the study of mechanisms of clinical anti-cancer drug resistance. *Proceedings of the National Academy of Sciences of the United States of America* **108**, 18708-18713.

Ginestier, C., Hur, M. H., Charafe-Jauffret, E., Monville, F., Dutcher, J., Brown, M., Jacquemier, J., Viens, P., Kleer, C. G., Liu, S., et al. (2007). ALDH1 is a marker of normal and malignant human mammary stem cells and a predictor of poor clinical outcome. *Cell Stem Cell* **1**, 555-567.

Gonzalez-Suarez, E., Branstetter, D., Armstrong, A., Dinh, H., Blumberg, H. and Dougall, W. C. (2007). RANK overexpression in transgenic mice with mouse mammary tumor virus promoter-controlled RANK increases proliferation and impairs alveolar differentiation in the mammary epithelia and disrupts lumen formation in cultured epithelial acini. *Molecular and Cellular Biology* **27**, 1442-1454.

Gonzalez-Suarez, E., Jacob, A. P., Jones, J., Miller, R., Roudier-Meyer, M. P., Erwert, R., Pinkas, J., Branstetter, D. and Dougall, W. C. (2010). RANK ligand mediates progestin-induced mammary epithelial proliferation and carcinogenesis. *Nature* **468**, 103-107.

Gorrini, C., Baniasadi, P. S., Harris, I. S., Silvester, J., Inoue, S., Snow, B., Joshi, P. A., Wakeham, A., Molyneux, S. D., Martin, B., et al. (2013). BRCA1 interacts with Nrf2 to regulate antioxidant signaling and cell survival. *The Journal of Experimental Medicine* **210**, 1529-1544.

Gorrini, C., Gang, B. P., Bassi, C., Wakeham, A., Baniasadi, S. P., Hao, Z., Li, W. Y., Cescon, D. W., Li, Y. T., Molyneux, S., et al. (2014). Estrogen controls the survival of BRCA1-deficient cells via a PI3K-NRF2-regulated pathway. *Proceedings of the National Academy of Sciences of the United States of America* **111**, 4472-4477.

Gouilleux, F., Wakao, H., Mundt, M. and Groner, B. (1994). Prolactin induces phosphorylation of Tyr694 of Stat5 (MGF), a prerequisite for DNA binding and induction of transcription. *The EMBO journal* **13**, 4361-4369.

Gowen, L. C., Johnson, B. L., Latour, A. M., Sulik, K. K. and Koller, B. H. (1996). Brca1 deficiency results in early embryonic lethality characterized by neuroepithelial abnormalities. *Nature Genetics* **12**, 191-194.

Graham, J. D., Mote, P. A., Salagame, U., van Dijk, J. H., Balleine, R. L., Huschtscha, L. I., Reddel, R. R. and Clarke, C. L. (2009). DNA replication licensing and progenitor numbers are increased by progesterone in normal human breast. *Endocrinology* **150**, 3318-3326.

Greenblatt, M. S., Chappuis, P. O., Bond, J. P., Hamel, N. and Foulkes, W. D. (2001). TP53 mutations in breast cancer associated with BRCA1 or BRCA2 germ-line mutations: distinctive spectrum and structural distribution. *Cancer Research* **61**, 4092-4097.

Grimm, S. L., Seagroves, T. N., Kabotyanski, E. B., Hovey, R. C., Vonderhaar, B. K., Lydon, J. P., Miyoshi, K., Hennighausen, L., Ormandy, C. J., Lee, A. V., et al. (2002). Disruption of steroid and prolactin receptor patterning in the mammary gland correlates with a block in lobuloalveolar development. *Molecular Endocrinology* **16**, 2675-2691.

Gurney, A., Axelrod, F., Bond, C. J., Cain, J., Chartier, C., Donigan, L., Fischer, M., Chaudhari, A., Ji, M. and Kapoun, A. M. (2012). Wnt pathway inhibition via the targeting of Frizzled receptors results in decreased growth and tumorigenicity of human tumors. *Proceedings of the National Academy of Sciences* **109**, 11717-11722.

Guy, C. T., Cardiff, R. D. and Muller, W. J. (1992a). Induction of mammary tumors by expression of polyomavirus middle T oncogene: a transgenic mouse model for metastatic disease. *Molecular and Cellular Biology* **12**, 954-961.

Guy, C. T., Webster, M. A., Schaller, M., Parsons, T. J., Cardiff, R. D. and Muller, W. J. (1992b). Expression of the neu protooncogene in the mammary epithelium of transgenic mice induces metastatic disease. *Proceedings of the National Academy of Sciences of the United States of America* **89**, 10578-10582.

Hahn, S. A., Greenhalf, B., Ellis, I., Sina-Frey, M., Rieder, H., Korte, B., Gerdes, B., Kress, R., Ziegler, A. and Raeburn, J. A. (2003). BRCA2 germline mutations in familial pancreatic carcinoma. *Journal of the National Cancer Institute* **95**, 214-221.

Hall, J. M., Lee, M. K., Newman, B., Morrow, J. E., Anderson, L. A., Huey, B. and King, M. C. (1990). Linkage of early-onset familial breast cancer to chromosome 17q21. *Science* **250**, 1684-1689.

Hashizume, R., Fukuda, M., Maeda, I., Nishikawa, H., Oyake, D., Yabuki, Y., Ogata, H. and Ohta, T. (2001). The RING heterodimer BRCA1-BARD1 is a ubiquitin ligase inactivated by a breast cancer-derived mutation. *The Journal of Biological Chemistry* **276**, 14537-14540.

Hayden, M. S. and Ghosh, S. (2008). Shared principles in NF-kappaB signaling. *Cell* **132**, 344-362.

Heemskerk-Gerritsen, B. A., Seynaeve, C., van Asperen, C. J., Ausems, M. G., Collee, J. M., van Doorn, H. C., Gomez Garcia, E. B., Kets, C. M., van Leeuwen, F. E., Meijers-Heijboer, H. E., et al. (2015). Breast cancer risk after salpingo-oophorectomy in healthy BRCA1/2 mutation carriers: revisiting the evidence for risk reduction. *Journal of the National Cancer Institute* **107**.

Hennessy, B. T., Krishnamurthy, S., Giordano, S., Buchholz, T. A., Kau, S. W., Duan, Z., Valero, V. and Hortobagyi, G. N. (2005). Squamous cell carcinoma of the breast. *Journal of Clinical Oncology* **23**, 7827-7835.

Hens, J. R. and Wysolmerski, J. J. (2005). Key stages of mammary gland development: molecular mechanisms involved in the formation of the embryonic mammary gland. *Breast Cancer Research* **7**, 220-224.

Herschkowitz, J. I., Simin, K., Weigman, V. J., Mikaelian, I., Usary, J., Hu, Z., Rasmussen, K. E., Jones, L. P., Assefnia, S., Chandrasekharan, S., et al. (2007). Identification of conserved gene expression features between murine mammary carcinoma models and human breast tumors. *Genome Biology* **8**, R76.

Hidalgo, M., Amant, F., Biankin, A. V., Budinska, E., Byrne, A. T., Caldas, C., Clarke, R. B., de Jong, S., Jonkers, J., Maelandsmo, G. M., et al. (2014). Patient-derived xenograft models: an emerging platform for translational cancer research. *Cancer Discovery* **4**, 998-1013.

Hodi, F. S., O'Day, S. J., McDermott, D. F., Weber, R. W., Sosman, J. A., Haanen, J. B., Gonzalez, R., Robert, C., Schadendorf, D., Hassel, J. C., et al. (2010). Improved survival with ipilimumab in patients with metastatic melanoma. *The New England Journal of Medicine* **363**, 711-723.

Hofbauer, L. C. (1999). Osteoprotegerin ligand and osteoprotegerin: novel implications for osteoclast biology and bone metabolism. *European Journal of Endocrinology* **141**, 195-210.

Hofseth, L. J., Raafat, A. M., Osuch, J. R., Pathak, D. R., Slomski, C. A. and Haslam, S. Z. (1999). Hormone Replacement Therapy with Estrogen or Estrogen plus Medroxyprogesterone Acetate Is Associated with Increased Epithelial Proliferation in the Normal Postmenopausal Breast. *The Journal of Clinical Endocrinology & Metabolism* **84**, 4559-4565.

Honrado, E., Osorio, A., Palacios, J. and Benitez, J. (2006). Pathology and gene expression of hereditary breast tumors associated with BRCA1, BRCA2 and CHEK2 gene mutations. *Oncogene* **25**, 5837-5845.

Hoshino, K. (1962). Morphogenesis and growth potentiality of mammary glands in mice. I. Transplantability and growth potentiality of mammary tissue of virgin mice. *Journal of the National Cancer Institute* **29**, 835-851.

Hoshino, K. (1964). Regeneration and growth of quantitatively transplanted mammary glands of normal female mice. *The Anatomical Record* **150**, 221-235.

Hovey, R. C., McFadden, T. B. and Akers, R. M. (1999). Regulation of mammary gland growth and morphogenesis by the mammary fat pad: a species comparison. *Journal of Mammary Gland Biology and Neoplasia* **4**, 53-68.

Howard, B. A. and Gusterson, B. A. (2000). Human breast development. *Journal of Mammary Gland Biology and Neoplasia* **5**, 119-137.

Howlett, N. G., Taniguchi, T., Olson, S., Cox, B., Waisfisz, Q., de Die-Smulders, C., Persky, N., Grompe, M., Joenje, H. and Pals, G. (2002). Biallelic inactivation of BRCA2 in Fanconi anemia. *Science* **297**, 606-609.

Hu, H., Wang, J., Gupta, A., Shidfar, A., Branstetter, D., Lee, O., Ivancic, D., Sullivan, M., Chatterton, R. T., Jr., Dougall, W. C., et al. (2014). RANKL expression in normal and malignant breast tissue responds to progesterone and is up-regulated during the luteal phase. *Breast Cancer Research and Treatment* **146**, 515-523.

Hudziak, R. M., Lewis, G. D., Winget, M., Fendly, B. M., Shepard, H. M. and Ullrich, A. (1989). p185HER2 monoclonal antibody has antiproliferative effects in vitro and sensitizes human breast tumor cells to tumor necrosis factor. *Molecular and Cellular Biology* **9**, 1165-1172.

Huen, M. S., Sy, S. M. and Chen, J. (2010). BRCA1 and its toolbox for the maintenance of genome integrity. *Nature Reviews Molecular Cell Biology* **11**, 138-148.

Hugo, W., Zaretsky, J. M., Sun, L., Song, C., Moreno, B. H., Hu-Lieskovan, S., Berent-Maoz, B., Pang, J., Chmielowski, B., Cherry, G., et al. (2016). Genomic and Transcriptomic Features of Response to Anti-PD-1 Therapy in Metastatic Melanoma. *Cell* **165**, 35-44.

Hulka, B. S. (1997). Epidemiologic analysis of breast and gynecologic cancers. *Progress in Clinical and Biological Research* **396**, 17-29.

Humphreys, R. C., Krajewska, M., Krnacik, S., Jaeger, R., Weiher, H., Krajewski, S., Reed, J. C. and Rosen, J. M. (1996). Apoptosis in the terminal endbud of the murine mammary gland: a mechanism of ductal morphogenesis. *Development* **122**, 4013-4022.

Hutchinson, J. N. and Muller, W. J. (2000). Transgenic mouse models of human breast cancer. *Oncogene* **19**, 6130-6137.

Iwai, Y., Ishida, M., Tanaka, Y., Okazaki, T., Honjo, T. and Minato, N. (2002). Involvement of PD-L1 on tumor cells in the escape from host immune system and tumor immunotherapy by PD-L1 blockade. *Proceedings of the National Academy of Sciences of the United States of America* **99**, 12293-12297.

Jacks, T., Remington, L., Williams, B. O., Schmitt, E. M., Halachmi, S., Bronson, R. T. and Weinberg, R. A. (1994). Tumor spectrum analysis in p53-mutant mice. *Current Biology* **4**, 1-7.

Jernstrom, H., Lerman, C., Ghadirian, P., Lynch, H. T., Weber, B., Garber, J., Daly, M., Olopade, O. I., Foulkes, W. D., Warner, E., et al. (1999). Pregnancy and risk of early breast cancer in carriers of BRCA1 and BRCA2. *Lancet* **354**, 1846-1850.

Johannesdottir, G., Gudmundsson, J., Bergthorsson, J. T., Arason, A., Agnarsson, B. A., Eiriksdottir, G., Johannsson, O. T., Borg, A., Ingvarsson, S., Easton, D. F., et al. (1996). High prevalence of the 999del5 mutation in icelandic breast and ovarian cancer patients. *Cancer Research* **56**, 3663-3665.

Johnson, J. I., Decker, S., Zaharevitz, D., Rubinstein, L. V., Venditti, J. M., Schepartz, S., Kalyandrug, S., Christian, M., Arbuck, S., Hollingshead, M., et al. (2001). Relationships between drug activity in NCI preclinical in vitro and in vivo models and early clinical trials. *British Journal of Cancer* **84**, 1424-1431.

Jones, D. H., Nakashima, T., Sanchez, O. H., Kozieradzki, I., Komarova, S. V., Sarosi, I., Morony, S., Rubin, E., Sarao, R., Hojilla, C. V., et al. (2006). Regulation of cancer cell migration and bone metastasis by RANKL. *Nature* **440**, 692-696.

Jones, L. P., Li, M., Halama, E. D., Ma, Y., Lubet, R., Grubbs, C. J., Deng, C. X., Rosen, E. M. and Furth, P. A. (2005). Promotion of mammary cancer development by tamoxifen in a mouse model of Brca1-mutation-related breast cancer. *Oncogene* **24**, 3554-3562.

Jonkers, J., Meuwissen, R., van der Gulden, H., Peterse, H., van der Valk, M. and Berns, A. (2001). Synergistic tumor suppressor activity of BRCA2 and p53 in a conditional mouse model for breast cancer. *Nature Genetics* **29**, 418-425.

Joshi, P. A., Jackson, H. W., Beristain, A. G., Di Grappa, M. A., Mote, P. A., Clarke, C. L., Stingl, J., Waterhouse, P. D. and Khokha, R. (2010). Progesterone induces adult mammary stem cell expansion. *Nature* **465**, 803-807.

Joshi, P. A., Waterhouse, P. D., Kannan, N., Narala, S., Fang, H., Di Grappa, M. A., Jackson, H. W., Penninger, J. M., Eaves, C. and Khokha, R. (2015). RANK Signaling Amplifies WNT-Responsive Mammary Progenitors through R-SPONDIN1. *Stem Cell Reports* **5**, 31-44.

Kabos, P., Finlay-Schultz, J., Li, C., Kline, E., Finlayson, C., Wisell, J., Manuel, C. A., Edgerton, S. M., Harrell, J. C. and Elias, A. (2012). Patient-derived luminal breast cancer xenografts retain hormone receptor heterogeneity and help define unique estrogen-dependent gene signatures. *Breast Cancer Research and Treatment* **135**, 415-432.

Kang, T. H., Mao, C. P., Lee, S. Y., Chen, A., Lee, J. H., Kim, T. W., Alvarez, R. D., Roden, R. B., Pardoll, D., Hung, C. F., et al. (2013). Chemotherapy acts as an adjuvant to convert the tumor microenvironment into a highly permissive state for vaccination-induced antitumor immunity. *Cancer Research* **73**, 2493-2504.

Kannan, N., Huda, N., Tu, L., Droumeva, R., Aubert, G., Chavez, E., Brinkman, R. R., Lansdorp, P., Emerman, J., Abe, S., et al. (2013). The luminal progenitor compartment of the normal human mammary gland constitutes a unique site of telomere dysfunction. *Stem Cell Reports* **1**, 28-37.

Karin, M., Cao, Y., Greten, F. R. and Li, Z. W. (2002). NF-kappaB in cancer: from innocent bystander to major culprit. *Nature reviews. Cancer* **2**, 301-310.

Kass, L., Erler, J. T., Dembo, M. and Weaver, V. M. (2007). Mammary epithelial cell: influence of extracellular matrix composition and organization during development and tumorigenesis. *The International Journal of Biochemistry & Cell Biology* **39**, 1987-1994.

Kassam, F., Enright, K., Dent, R., Dranitsaris, G., Myers, J., Flynn, C., Fralick, M., Kumar, R. and Clemons, M. (2009). Survival outcomes for patients with metastatic triple-negative breast cancer: implications for clinical practice and trial design. *Clinical Breast Cancer* **9**, 29-33.

Katiyar, P., Ma, Y., Fan, S., Pestell, R. G., Furth, P. A. and Rosen, E. M. (2006). Regulation of progesterone receptor signaling by BRCA1 in mammary cancer. *Nuclear Receptor Signaling* **4**, e006.

Kauff, N. D., Domchek, S. M., Friebel, T. M., Robson, M. E., Lee, J., Garber, J. E., Isaacs, C., Evans, D. G., Lynch, H., Eeles, R. A., et al. (2008). Risk-reducing salpingo-oophorectomy for the prevention of BRCA1- and BRCA2-associated breast and gynecologic cancer: a multicenter, prospective study. *Journal of Clinical Oncology* **26**, 1331-1337.

Keller, P. J., Arendt, L. M., Skibinski, A., Logvinenko, T., Klebba, I., Dong, S., Smith, A. E., Prat, A., Perou, C. M., Gilmore, H., et al. (2012). Defining the cellular precursors to human breast cancer. *Proceedings of the National Academy of Sciences of the United States of America* **109**, 2772-2777.

Kenney, N. J., Smith, G. H., Rosenberg, K., Cutler, M. L. and Dickson, R. B. (1996). Induction of ductal morphogenesis and lobular hyperplasia by amphiregulin in the mouse mammary gland. *Cell Growth & Differentiation* **7**, 1769-1781.

Khan, I. S., Mouchess, M. L., Zhu, M. L., Conley, B., Fasano, K. J., Hou, Y., Fong, L., Su, M. A. and Anderson, M. S. (2014). Enhancement of an anti-tumor immune response by transient blockade of central T cell tolerance. *The Journal of Experimental Medicine* **211**, 761-768.

Khramtsov, A. I., Khramtsova, G. F., Tretiakova, M., Huo, D., Olopade, O. I. and Goss, K. H. (2010). Wnt/beta-catenin pathway activation is enriched in basal-like breast cancers and predicts poor outcome. *The American Journal of Pathology* **176**, 2911-2920.

Kiely, B. E., Jenkins, M. A., McKinley, J. M., Friedlander, M. L., Weideman, P., Milne, R. L., McLachlan, S. A., Hopper, J. L. and Phillips, K. A. (2010). Contralateral risk-reducing mastectomy in BRCA1 and BRCA2 mutation carriers and other high-risk women in the Kathleen Cuningham Foundation Consortium for Research into Familial Breast Cancer (kConFab). *Breast Cancer Research and Treatment* **120**, 715-723.

Kim, N. S., Kim, H. J., Koo, B. K., Kwon, M. C., Kim, Y. W., Cho, Y., Yokota, Y., Penninger, J. M. and Kong, Y. Y. (2006). Receptor activator of NF-kappaB ligand regulates the proliferation of mammary epithelial cells via Id2. *Molecular and Cellular Biology* **26**, 1002-1013.

Kim, N. S., Kim, H. T., Kwon, M. C., Choi, S. W., Kim, Y. Y., Yoon, K. J., Koo, B. K., Kong, M. P., Shin, J., Cho, Y., et al. (2011). Survival and differentiation of mammary epithelial cells in mammary gland development require nuclear retention of Id2 due to RANK signaling. *Molecular and Cellular Biology* **31**, 4775-4788.

Kim, Y. C., Clark, R. J., Pelegri, F. and Alexander, C. M. (2009). Wnt4 is not sufficient to induce lobuloalveolar mammary development. *BMC Developmental Biology* **9**, 55.

King, M. C., Wieand, S., Hale, K., Lee, M., Walsh, T., Owens, K., Tait, J., Ford, L., Dunn, B. K., Costantino, J., et al. (2001). Tamoxifen and breast cancer incidence among women with inherited mutations in BRCA1 and BRCA2: National Surgical Adjuvant Breast and Bowel Project (NSABP-P1) Breast Cancer Prevention Trial. *Journal of the American Medical Association* **286**, 2251-2256.

King, T. A., Gemignani, M. L., Li, W., Giri, D. D., Panageas, K. S., Bogomolniy, F., Arroyo, C., Olvera, N., Robson, M. E., Offit, K., et al. (2004). Increased progesterone receptor expression in benign epithelium of BRCA1-related breast cancers. *Cancer Research* **64**, 5051-5053.

King, T. A., Li, W., Brogi, E., Yee, C. J., Gemignani, M. L., Olvera, N., Levine, D. A., Norton, L., Robson, M. E., Offit, K., et al. (2007). Heterogenic loss of the wild-type BRCA allele in human breast tumorigenesis. *Annals of Surgical Oncology* **14**, 2510-2518.

Kleiman, F. E., Wu-Baer, F., Fonseca, D., Kaneko, S., Baer, R. and Manley, J. L. (2005). BRCA1/BARD1 inhibition of mRNA 3' processing involves targeted degradation of RNA polymerase II. *Genes & Development* **19**, 1227-1237.

Komatsu, M., Yoshimaru, T., Matsuo, T., Kiyotani, K., Miyoshi, Y., Tanahashi, T., Rokutan, K., Yamaguchi, R., Saito, A., Imoto, S., et al. (2013). Molecular features of triple negative breast cancer cells by genome-wide gene expression profiling analysis. *International Journal of Oncology* **42**, 478-506.

Konishi, H., Mohseni, M., Tamaki, A., Garay, J. P., Croessmann, S., Karnan, S., Ota, A., Wong, H. Y., Konishi, Y., Karakas, B., et al. (2011). Mutation of a single allele of the cancer susceptibility gene BRCA1 leads to genomic instability in human breast epithelial cells. *Proceedings of the National Academy of Sciences of the United States of America* **108**, 17773-17778.

Konishi, J., Yamazaki, K., Azuma, M., Kinoshita, I., Dosaka-Akita, H. and Nishimura, M. (2004). B7-H1 expression on non-small cell lung cancer cells and its relationship with tumor-infiltrating lymphocytes and their PD-1 expression. *Clinical Cancer Research* **10**, 5094-5100.

Korach, K. S., Couse, J. F., Curtis, S. W., Washburn, T. F., Lindzey, J., Kimbro, K. S., Eddy, E. M., Migliaccio, S., Snedeker, S. M., Lubahn, D. B., et al. (1996). Estrogen receptor gene disruption: molecular characterization and experimental and clinical phenotypes. *Recent Progress in Hormone Research* **51**, 159-186

Kordon, E. C. and Smith, G. H. (1998). An entire functional mammary gland may comprise the progeny from a single cell. *Development* **125**, 1921-1930.

Kostenuik, P. J., Nguyen, H. Q., McCabe, J., Warmington, K. S., Kurahara, C., Sun, N., Chen, C., Li, L., Cattley, R. C., Van, G., et al. (2009). Denosumab, a fully human monoclonal antibody to RANKL, inhibits bone resorption and increases BMD in knock-in mice that express chimeric (murine/human) RANKL. *Journal of Bone and Mineral Research* **24**, 182-195.

Kramer, J. L., Velazquez, I. A., Chen, B. E., Rosenberg, P. S., Struewing, J. P. and Greene, M. H. (2005). Prophylactic oophorectomy reduces breast cancer penetrance during prospective, long-term follow-up of BRCA1 mutation carriers. *Journal of Clinical Oncology* **23**, 8629-8635.

Kratochwil, K. (1969). Organ specificity in mesenchymal induction demonstrated in the embryonic development of the mammary gland of the mouse. *Developmental Biology* **20**, 46-71.

Kriege, M., Brekelmans, C. T., Boetes, C., Besnard, P. E., Zonderland, H. M., Obdeijn, I. M., Manoliu, R. A., Kok, T., Peterse, H., Tilanus-Linthorst, M. M., et al. (2004). Efficacy of MRI and mammography for breast-cancer screening in women with a familial or genetic predisposition. *The New England Journal of Medicine* **351**, 427-437.

Kuperwasser, C., Chavarria, T., Wu, M., Magrane, G., Gray, J. W., Carey, L., Richardson, A. and Weinberg, R. A. (2004). Reconstruction of functionally normal and malignant human breast tissues in mice. *Proceedings of the National Academy of Sciences of the United States of America* **101**, 4966-4971.

Kuperwasser, C., Hurlbut, G. D., Kittrell, F. S., Dickinson, E. S., Laucirica, R., Medina, D., Naber, S. P. and Jerry, D. J. (2000). Development of spontaneous mammary tumors in BALB/c p53 heterozygous mice. A model for Li-Fraumeni syndrome. *The American Journal of Pathology* **157**, 2151-2159.

Labovsky, V., Vallone, V. B., Martinez, L. M., Otaegui, J. and Chasseing, N. A. (2012). Expression of osteoprotegerin, receptor activator of nuclear factor kappa-B ligand, tumor necrosis factor-related apoptosis-inducing ligand, stromal cell-derived factor-1 and their receptors in epithelial metastatic breast cancer cell lines. *Cancer Cell International* **12**, 29.

Lacey, D. L., Timms, E., Tan, H. L., Kelley, M. J., Dunstan, C. R., Burgess, T., Elliott, R., Colombero, A., Elliott, G., Scully, S., et al. (1998). Osteoprotegerin ligand is a cytokine that regulates osteoclast differentiation and activation. *Cell* **93**, 165-176.

Ladoire, S., Arnould, L., Apetoh, L., Coudert, B., Martin, F., Chauffert, B., Fumoleau, P. and Ghiringhelli, F. (2008). Pathologic complete response to neoadjuvant chemotherapy of breast carcinoma is associated with the disappearance of tumor-infiltrating foxp3+ regulatory T cells. *Clinical Cancer Research* **14**, 2413-2420.

Ladoire, S., Mignot, G., Dabakuyo, S., Arnould, L., Apetoh, L., Rebe, C., Coudert, B., Martin, F., Bizollon, M. H., Vanoli, A., et al. (2011). In situ immune response after neoadjuvant chemotherapy for breast cancer predicts survival. *The Journal of Pathology* **224**, 389-400.

Lafarge, S., Sylvain, V., Ferrara, M. and Bignon, Y. J. (2001). Inhibition of BRCA1 leads to increased chemoresistance to microtubule-interfering agents, an effect that involves the JNK pathway. *Oncogene* **20**, 6597-6606.

Lafkas, D., Rodilla, V., Huyghe, M., Mourao, L., Kiaris, H. and Fre, S. (2013). Notch3 marks clonogenic mammary luminal progenitor cells in vivo. *The Journal of Cell Biology* **203**, 47-56.

Lakhani, S. R., Jacquemier, J., Sloane, J. P., Gusterson, B. A., Anderson, T. J., van de Vijver, M. J., Farid, L. M., Venter, D., Antoniou, A., Storfer-Isser, A., et al. (1998). Multifactorial analysis of differences between sporadic breast cancers and cancers involving BRCA1 and BRCA2 mutations. *Journal of the National Cancer Institute* **90**, 1138-1145.

Lakhani, S. R., Manek, S., Penault-Llorca, F., Flanagan, A., Arnout, L., Merrett, S., McGuffog, L., Steele, D., Devilee, P., Klijn, J. G., et al. (2004). Pathology of ovarian cancers in BRCA1 and BRCA2 carriers. *Clinical Cancer Research* **10**, 2473-2481.

Larkin, J., Chiarion-Sileni, V., Gonzalez, R., Grob, J. J., Cowey, C. L., Lao, C. D., Schadendorf, D., Dummer, R., Smylie, M., Rutkowski, P., et al. (2015). Combined Nivolumab and Ipilimumab or Monotherapy in Untreated Melanoma. *The New England Journal of Medicine* **373**, 23-34.

Larsen, M. J., Kruse, T. A., Tan, Q., Lænkholm, A.-V., Bak, M., Lykkesfeldt, A. E., Sørensen, K. P., Hansen, T. v. O., Ejlertsen, B. and Gerdes, A.-M. (2013). Classifications within molecular subtypes enables identification of BRCA1/BRCA2 mutation carriers by RNA tumor profiling. *PloS One* **8**, e64268.

Law, C. W., Chen, Y., Shi, W. and Smyth, G. K. (2014). voom: Precision weights unlock linear model analysis tools for RNA-seq read counts. *Genome Biology* **15**, R29.

Lee, H. J., Gallego-Ortega, D., Ledger, A., Schramek, D., Joshi, P., Szwarc, M. M., Cho, C., Lydon, J. P., Khokha, R., Penninger, J. M., et al. (2013). Progesterone drives mammary secretory differentiation via RankL-mediated induction of Elf5 in luminal progenitor cells. *Development* **140**, 1397-1401.

Lee, J.-H. and Paull, T. T. (2005). ATM activation by DNA double-strand breaks through the Mre11-Rad50-Nbs1 complex. *Science* **308**, 551-554.

Lehmann, B. D., Bauer, J. A., Schafer, J. M., Pendleton, C. S., Tang, L., Johnson, K. C., Chen, X., Balko, J. M., Gomez, H., Arteaga, C. L., et al. (2014). PIK3CA mutations in androgen receptor-positive triple negative breast cancer confer sensitivity to the combination of PI3K and androgen receptor inhibitors. *Breast Cancer Research* **16**, 406.

Li, F. P. and Fraumeni, J. F., Jr. (1969). Soft-tissue sarcomas, breast cancer, and other neoplasms. A familial syndrome? *Annals of Internal Medicine* **71**, 747-752.

Li, M., Liu, X., Robinson, G., Bar-Peled, U., Wagner, K. U., Young, W. S., Hennighausen, L. and Furth, P. A. (1997). Mammary-derived signals activate programmed cell death during the first stage of mammary gland involution. *Proceedings of the National Academy of Sciences of the United States of America* **94**, 3425-3430.

Li, S. and Rosen, J. M. (1995). Nuclear factor I and mammary gland factor (STAT5) play a critical role in regulating rat whey acidic protein gene expression in transgenic mice. *Molecular and Cellular Biology* **15**, 2063-2070.

Li, S., Shen, D., Shao, J., Crowder, R., Liu, W., Prat, A., He, X., Liu, S., Hoog, J., Lu, C., et al. (2013). Endocrine-therapy-resistant ESR1 variants revealed by genomic characterization of breast-cancer-derived xenografts. *Cell Reports* **4**, 1116-1130.

Li, Y., Hively, W. P. and Varmus, H. E. (2000). Use of MMTV-Wnt-1 transgenic mice for studying the genetic basis of breast cancer. *Oncogene* **19**, 1002-1009.

Liao, Y., Smyth, G. K. and Shi, W. (2013). The Subread aligner: fast, accurate and scalable read mapping by seed-and-vote. *Nucleic Acids Research* **41**, e108.

Liao, Y., Smyth, G. K. and Shi, W (2014). featureCounts: an efficient general purpose program for assigning sequence reads to genomic features. *Bioinformatics* **30**, 923-930.

Lim, E., Vaillant, F., Wu, D., Forrest, N. C., Pal, B., Hart, A. H., Asselin-Labat, M. L., Gyorki, D. E., Ward, T., Partanen, A., et al. (2009). Aberrant luminal progenitors as the candidate target population for basal tumor development in BRCA1 mutation carriers. *Nature Medicine* **15**, 907-913.

Lim, E., Wu, D., Pal, B., Bouras, T., Asselin-Labat, M. L., Vaillant, F., Yagita, H., Lindeman, G. J., Smyth, G. K. and Visvader, J. E. (2010). Transcriptome analyses of mouse and human mammary cell subpopulations reveal multiple conserved genes and pathways. *Breast Cancer Research* **12**, R21.

Lin, S. C., Lee, K. F., Nikitin, A. Y., Hilsenbeck, S. G., Cardiff, R. D., Li, A., Kang, K. W., Frank, S. A., Lee, W. H. and Lee, E. Y. (2004). Somatic mutation of p53 leads to estrogen receptor alpha-positive and -negative mouse mammary tumors with high frequency of metastasis. *Cancer Research* **64**, 3525-3532.

Lipton, A., Steger, G. G., Figueroa, J., Alvarado, C., Solal-Celigny, P., Body, J. J., de Boer, R., Berardi, R., Gascon, P., Tonkin, K. S., et al. (2007). Randomized active-controlled phase II study of denosumab efficacy and safety in patients with breast cancer-related bone metastases. *Journal of Clinical Oncology*

Liu, S., Ginestier, C., Charafe-Jauffret, E., Foco, H., Kleer, C. G., Merajver, S. D., Dontu, G. and Wicha, M. S. (2008). BRCA1 regulates human mammary stem/progenitor cell fate. *Proceedings of the National Academy of Sciences of the United States of America* **105**, 1680-1685.

Liu, X., Holstege, H., van der Gulden, H., Treur-Mulder, M., Zevenhoven, J., Velds, A., Kerkhoven, R. M., van Vliet, M. H., Wessels, L. F., Peterse, J. L., et al. (2007). Somatic loss of BRCA1 and p53 in mice induces mammary tumors with features of human BRCA1-mutated basal-like breast cancer. *Proceedings of the National Academy of Sciences of the United States of America* **104**, 12111-12116.

Liu, X., Robinson, G. W., Wagner, K. U., Garrett, L., Wynshaw-Boris, A. and Hennighausen, L. (1997). Stat5a is mandatory for adult mammary gland development and lactogenesis. *Genes & Development* **11**, 179-186.

Lord, C. J. and Ashworth, A. (2013). Mechanisms of resistance to therapies targeting BRCA-mutant cancers. *Nature Medicine* **19**, 1381-1388.

Lord, C. J. and Ashworth, A. (2016). BRCAness revisited. *Nature Reviews Cancer*.

Lu, P., Ewald, A. J., Martin, G. R. and Werb, Z. (2008). Genetic mosaic analysis reveals FGF receptor 2 function in terminal end buds during mammary gland branching morphogenesis. *Developmental Biology* **321**, 77-87.

Ludwig, T., Fisher, P., Murty, V. and Efstratiadis, A. (2001). Development of mammary adenocarcinomas by tissue-specific knockout of Brca2 in mice. *Oncogene* **20**, 3937-3948.

Luetteke, N. C., Qiu, T. H., Fenton, S. E., Troyer, K. L., Riedel, R. F., Chang, A. and Lee, D. C. (1999). Targeted inactivation of the EGF and amphiregulin genes reveals distinct roles for EGF receptor ligands in mouse mammary gland development. *Development* **126**, 2739-2750.

Lydon, J. P., DeMayo, F. J., Funk, C. R., Mani, S. K., Hughes, A. R., Montgomery, C. A., Jr., Shyamala, G., Conneely, O. M. and O'Malley, B. W. (1995). Mice lacking progesterone receptor exhibit pleiotropic reproductive abnormalities. *Genes & Development* **9**, 2266-2278.

Ma, C. X., Ellis, M. J., Petroni, G. R., Guo, Z., Cai, S.-r., Ryan, C. E., Lockhart, A. C., Naughton, M. J., Pluard, T. J. and Brenin, C. M. (2013). A phase II study of UCN-01 in combination with irinotecan in patients with metastatic triple negative breast cancer. *Breast Cancer Research and Treatment* **137**, 483-492.

Ma, Y., Katiyar, P., Jones, L. P., Fan, S., Zhang, Y., Furth, P. A. and Rosen, E. M. (2006). The breast cancer susceptibility gene BRCA1 regulates progesterone receptor signaling in mammary epithelial cells. *Molecular Endocrinology* **20**, 14-34.

Macias, H. and Hinck, L. (2012). Mammary gland development. *Wiley Interdisciplinary Reviews Developmental Biology* **1**, 533-557.

MacLachlan, T. K., Somasundaram, K., Sgagias, M., Shifman, Y., Muschel, R. J., Cowan, K. H. and El-Deiry, W. S. (2000). BRCA1 effects on the cell cycle and the DNA damage response are linked to altered gene expression. *The Journal of Biological Chemistry* **275**, 2777-2785.

Mahoney, K. M., Rennert, P. D. and Freeman, G. J. (2015). Combination cancer immunotherapy and new immunomodulatory targets. *Nature Reviews Drug Discovery* **14**, 561-584.

Makarem, M., Kannan, N., Nguyen, L. V., Knapp, D. J., Balani, S., Prater, M. D., Stingl, J., Raouf, A., Nemirovsky, O., Eirew, P., et al. (2013). Developmental changes in the in vitro activated regenerative activity of primitive mammary epithelial cells. *PLoS Biology* **11**, e1001630.

Mallepell, S., Krust, A., Chambon, P. and Brisken, C. (2006). Paracrine signaling through the epithelial estrogen receptor alpha is required for proliferation and morphogenesis in the mammary gland. *Proceedings of the National Academy of Sciences of the United States of America* **103**, 2196-2201.

Mann, G. J., Thorne, H., Balleine, R. L., Butow, P. N., Clarke, C. L., Edkins, E., Evans, G. M., Fereday, S., Haan, E., Gattas, M., et al. (2006). Analysis of cancer risk and BRCA1 and BRCA2 mutation prevalence in the kConFab familial breast cancer resource. *Breast Cancer Research* **8**, R12.

Marangoni, E., Vincent-Salomon, A., Auger, N., Degeorges, A., Assayag, F., de Cremoux, P., de Plater, L., Guyader, C., De Pinieux, G., Judde, J. G., et al. (2007). A new model of patient tumor-derived breast cancer xenografts for preclinical assays. *Clinical Cancer Research* **13**, 3989-3998.

Martins, F. C., De, S., Almendro, V., Gonen, M., Park, S. Y., Blum, J. L., Herlihy, W., Ethington, G., Schnitt, S. J., Tung, N., et al. (2012). Evolutionary pathways in BRCA1-associated breast tumors. *Cancer Discovery* **2**, 503-511.

Marzec, M., Zhang, Q., Goradia, A., Raghunath, P. N., Liu, X., Paessler, M., Wang, H. Y., Wysocka, M., Cheng, M., Ruggeri, B. A., et al. (2008). Oncogenic kinase NPM/ALK induces through STAT3 expression of immunosuppressive protein CD274 (PD-L1, B7-H1). *Proceedings of the National Academy of Sciences of the United States of America* **105**, 20852-20857.

Mavaddat, N., Antoniou, A. C., Easton, D. F. and Garcia-Closas, M. (2010). Genetic susceptibility to breast cancer. *Molecular Oncology* **4**, 174-191.

Mavaddat, N., Barrowdale, D., Andrulis, I. L., Domchek, S. M., Eccles, D., Nevanlinna, H., Ramus, S. J., Spurdle, A., Robson, M. and Sherman, M. (2012). Pathology of breast and ovarian cancers among BRCA1 and BRCA2 mutation carriers: results from the Consortium of Investigators of Modifiers of BRCA1/2 (CIMBA). *Cancer Epidemiology Biomarkers & Prevention* **21**, 134-147.

McCarthy, A., Savage, K., Gabriel, A., Naceur, C., Reis‐Filho, J. and Ashworth, A. (2007). A mouse model of basal‐like breast carcinoma with metaplastic elements. *The Journal of Pathology* **211**, 389-398.

McClung, M. R., Lewiecki, E. M., Cohen, S. B., Bolognese, M. A., Woodson, G. C., Moffett, A. H., Peacock, M., Miller, P. D., Lederman, S. N., Chesnut, C. H., et al. (2006). Denosumab in postmenopausal women with low bone mineral density. *The New England Journal of Medicine* **354**, 821-831.

Meijers-Heijboer, H., van Geel, B., van Putten, W. L., Henzen-Logmans, S. C., Seynaeve, C., Menke-Pluymers, M. B., Bartels, C. C., Verhoog, L. C., van den Ouweland, A. M., Niermeijer, M. F., et al. (2001). Breast cancer after prophylactic bilateral mastectomy in women with a BRCA1 or BRCA2 mutation. *The New England Journal of Medicine* **345**, 159-164.

Meiser, B., Butow, P., Price, M., Bennett, B., Berry, G. and Tucker, K. (2003). Attitudes to prophylactic surgery and chemoprevention in Australian women at increased risk for breast cancer. *Journal of Women's Health (2002)* **12**, 769-778.

Mellman, I., Coukos, G. and Dranoff, G. (2011). Cancer immunotherapy comes of age. *Nature* **480**, 480-489.

Meng, X., Huang, Z., Teng, F., Xing, L. and Yu, J. (2015). Predictive biomarkers in PD-1/PD-L1 checkpoint blockade immunotherapy. *Cancer Treatment Reviews* **41**, 868-876.

Meyer, S., Tischkowitz, M., Chandler, K., Gillespie, A., Birch, J. M. and Evans, D. G. (2014). Fanconi anaemia, BRCA2 mutations and childhood cancer: a developmental perspective from clinical and epidemiological observations with implications for genetic counselling. *Journal of Medical Genetics* **51**, 71-75.

Michalak, E. M., Nacerddine, K., Pietersen, A., Beuger, V., Pawlitzky, I., Cornelissen-Steijger, P., Wientjens, E., Tanger, E., Seibler, J., van Lohuizen, M., et al. (2013). Polycomb group gene Ezh2 regulates mammary gland morphogenesis and maintains the luminal progenitor pool. *Stem Cells* **31**, 1910-1920.

Miki, Y., Swensen, J., Shattuck-Eidens, D., Futreal, P. A., Harshman, K., Tavtigian, S., Liu, Q., Cochran, C., Bennett, L. M., Ding, W., et al. (1994). A strong candidate for the breast and ovarian cancer susceptibility gene BRCA1. *Science* **266**, 66-71.

Miller, R. E., Roudier, M., Jones, J., Armstrong, A., Canon, J. and Dougall, W. C. (2008). RANK ligand inhibition plus docetaxel improves survival and reduces tumor burden in a murine model of prostate cancer bone metastasis. *Molecular Cancer Therapeutics* **7**, 2160-2169.

Minotti, G., Menna, P., Salvatorelli, E., Cairo, G. and Gianni, L. (2004). Anthracyclines: molecular advances and pharmacologic developments in antitumor activity and cardiotoxicity. *Pharmacological Reviews* **56**, 185-229.

Miyoshi, K., Shillingford, J. M., Smith, G. H., Grimm, S. L., Wagner, K. U., Oka, T., Rosen, J. M., Robinson, G. W. and Hennighausen, L. (2001). Signal transducer and activator of transcription (Stat) 5 controls the proliferation and differentiation of mammary alveolar epithelium. *The Journal of Cell Biology* **155**, 531-542.

Moiseyenko, V. M., Dolmatov, G. D., Moiseyenko, F. V., Ivantsov, A. O., Volkov, N. M., Chubenko, V. A., Abduloeva, N., Bogdanov, A. A., Sokolenko, A. P. and Imyanitov, E. N. (2015). High efficacy of cisplatin neoadjuvant therapy in a prospective series of patients carrying BRCA1 germ-line mutation. *Medical Oncology* **32**, 89.

Molyneux, G., Geyer, F. C., Magnay, F. A., McCarthy, A., Kendrick, H., Natrajan, R., Mackay, A., Grigoriadis, A., Tutt, A., Ashworth, A., et al. (2010). BRCA1 basal-like breast cancers originate from luminal epithelial progenitors and not from basal stem cells. *Cell Stem Cell* **7**, 403-417.

Mombaerts, P., Iacomini, J., Johnson, R. S., Herrup, K., Tonegawa, S. and Papaioannou, V. E. (1992). RAG-1-deficient mice have no mature B and T lymphocytes. *Cell* **68**, 869-877.

Monteiro, A. N. (2003). BRCA1: the enigma of tissue-specific tumor development. *Trends in Genetics* **19**, 312-315.

Mori, S., Nishikawa, S. I. and Yokota, Y. (2000). Lactation defect in mice lacking the helix-loop-helix inhibitor Id2. *The EMBO Journal* **19**, 5772-5781.

Moynahan, M. E. (2002). The cancer connection: BRCA1 and BRCA2 tumor suppression in mice and humans. *Oncogene* **21**, 8994-9007.

Moynahan, M. E., Cui, T. Y. and Jasin, M. (2001). Homology-directed dna repair, mitomycin-c resistance, and chromosome stability is restored with correction of a Brca1 mutation. *Cancer Research* **61**, 4842-4850.

Moynahan, M. E. and Jasin, M. (2010). Mitotic homologous recombination maintains genomic stability and suppresses tumorigenesis. *Nature Reviews Molecular Cell Biology* **11**, 196-207.

Mukherjee, A., Soyal, S. M., Li, J., Ying, Y., He, B., DeMayo, F. J. and Lydon, J. P. (2010). Targeting RANKL to a specific subset of murine mammary epithelial cells induces ordered branching morphogenesis and alveologenesis in the absence of progesterone receptor expression. *Federation of American Societies for Experimental Biology Journal* **24**, 4408-4419.

Mulac-Jericevic, B., Lydon, J. P., DeMayo, F. J. and Conneely, O. M. (2003). Defective mammary gland morphogenesis in mice lacking the progesterone receptor B isoform. *Proceedings of the National Academy of Sciences of the United States of America* **100**, 9744-9749.

Mulac-Jericevic, B., Mullinax, R. A., DeMayo, F. J., Lydon, J. P. and Conneely, O. M. (2000). Subgroup of reproductive functions of progesterone mediated by progesterone receptor-B isoform. *Science* **289**, 1751-1754.

Murphy, K. M., Brune, K. A., Griffin, C., Sollenberger, J. E., Petersen, G. M., Bansal, R., Hruban, R. H. and Kern, S. E. (2002). Evaluation of Candidate Genes MAP2K4, MADH4, ACVR1B, and BRCA2 in Familial Pancreatic Cancer Deleterious BRCA2 Mutations in 17%. *Cancer Research* **62**, 3789-3793.

Nakagawa, M., Bando, Y., Nagao, T., Morimoto, M., Takai, C., Ohnishi, T., Honda, J., Moriya, T., Izumi, K., Takahashi, M., et al. (2011). Expression of p53, Ki-67, E-cadherin, N-cadherin and TOP2A in triple-negative breast cancer. *Anticancer Research* **31**, 2389-2393.

Nanda, R., Chow, L. Q., Dees, E. C., Berger, R., Gupta, S., Geva, R., Pusztai, L., Dolled-Filhart, M., Emancipator, K. and Gonzalez, E. J. (2015). Abstract S1-09: a phase Ib study of pembrolizumab (MK-3475) in patients with advanced triple-negative breast cancer. *Cancer Cesearch* **75**, S1-09-S01-09.

Narod, S. A. (2001). Hormonal prevention of hereditary breast cancer. *Annals of the New York Academy of Sciences* **952**, 36-43.

Narod, S. A. and Foulkes, W. D. (2004). BRCA1 and BRCA2: 1994 and beyond. *Nature Reviews Cancer* **4**, 665-676.

Nelson, H. D., Smith, M. E., Griffin, J. C. and Fu, R. (2013). Use of medications to reduce risk for primary breast cancer: a systematic review for the U.S. Preventive Services Task Force. *Annals of Internal Medicine* **158**, 604-614.

Nielsen, T. O., Parker, J. S., Leung, S., Voduc, D., Ebbert, M., Vickery, T., Davies, S. R., Snider, J., Stijleman, I. J., Reed, J., et al. (2010). A comparison of PAM50 intrinsic subtyping with immunohistochemistry and clinical prognostic factors in tamoxifen-treated estrogen receptor-positive breast cancer. *Clinical Cancer Research* **16**, 5222-5232.

Nik-Zainal, S., Davies, H., Staaf, J., Ramakrishna, M., Glodzik, D., Zou, X., Martincorena, I., Alexandrov, L. B., Martin, S. and Wedge, D. C. (2016). Landscape of somatic mutations in 560 breast cancer whole-genome sequences. *Nature* **534**, 47-54.

Nitiss, J. L. (2009). DNA topoisomerase II and its growing repertoire of biological functions. *Nature Reviews Cancer* **9**, 327-337.

Nolan, E., Vaillant, F., Branstetter, D., Pal, B., Giner, G., Whitehead, L., Lok, S.W., Mann, G.B., kConFab, Rohrbach, K., et al. (2016). RANK ligand as a potential target for breast cancer prevention in *BRCA1* mutation carriers. *Nature Medicine* **22**, 933-939

Nugoli, M., Chuchana, P., Vendrell, J., Orsetti, B., Ursule, L., Nguyen, C., Birnbaum, D., Douzery, E. J., Cohen, P. and Theillet, C. (2003). Genetic variability in MCF-7 sublines: evidence of rapid genomic and RNA expression profile modifications. *BMC Cancer* **3**, 13.

Nusse, R. and Varmus, H. E. (1982). Many tumors induced by the mouse mammary tumor virus contain a provirus integrated in the same region of the host genome. *Cell* **31**, 99-109.

Oakes, S. R., Naylor, M. J., Asselin-Labat, M. L., Blazek, K. D., Gardiner-Garden, M., Hilton, H. N., Kazlauskas, M., Pritchard, M. A., Chodosh, L. A., Pfeffer, P. L., et al. (2008). The Ets transcription factor Elf5 specifies mammary alveolar cell fate. *Genes & Development* **22**, 581-586.

Obr, A. E., Grimm, S. L., Bishop, K. A., Pike, J. W., Lydon, J. P. and Edwards, D. P. (2013). Progesterone receptor and Stat5 signaling cross talk through RANKL in mammary epithelial cells. *Molecular Endocrinology* **27**, 1808-1824.

Oddoux, C., Struewing, J. P., Clayton, C. M., Neuhausen, S., Brody, L. C., Kaback, M., Haas, B., Norton, L., Borgen, P., Jhanwar, S., et al. (1996). The carrier frequency of the BRCA2 6174delT mutation among Ashkenazi Jewish individuals is approximately 1%. *Nature Genetics* **14**, 188-190.

Ormandy, C. J., Camus, A., Barra, J., Damotte, D., Lucas, B., Buteau, H., Edery, M., Brousse, N., Babinet, C., Binart, N., et al. (1997). Null mutation of the prolactin receptor gene produces multiple reproductive defects in the mouse. *Genes & Development* **11**, 167-178.

Ormandy, C. J., Naylor, M., Harris, J., Robertson, F., Horseman, N. D., Lindeman, G. J., Visvader, J. and Kelly, P. A. (2003). Investigation of the transcriptional changes underlying functional defects in the mammary glands of prolactin receptor knockout mice. *Recent Progress in Hormone Research* **58**, 297-323.

Page, D., Anderson, T. and Sakamoto, G. (1987). Infiltrating carcinoma: major histological types. *Diagnostic Histopathology of the Breast* **1**, 193-235.

Pal, B., Bouras, T., Shi, W., Vaillant, F., Sheridan, J. M., Fu, N., Breslin, K., Jiang, K., Ritchie, M. E., Young, M., et al. (2013). Global changes in the mammary epigenome are induced by hormonal cues and coordinated by Ezh2. *Cell Reports* **3**, 411-426.

Palafox, M., Ferrer, I., Pellegrini, P., Vila, S., Hernandez-Ortega, S., Urruticoechea, A., Climent, F., Soler, M. T., Munoz, P., Vinals, F., et al. (2012). RANK induces epithelial-mesenchymal transition and stemness in human mammary epithelial cells and promotes tumorigenesis and metastasis. *Cancer Research* **72**, 2879-2888.

Pardoll, D. M. (2012). The blockade of immune checkpoints in cancer immunotherapy. *Nature Reviews Cancer* **12**, 252-264.

Park, J. H., Lin, M. L., Nishidate, T., Nakamura, Y. and Katagiri, T. (2006). PDZ-binding kinase/T-LAK cell-originated protein kinase, a putative cancer/testis antigen with an oncogenic activity in breast cancer. *Cancer Research* **66**, 9186-9195.

Parker, J. S., Mullins, M., Cheang, M. C., Leung, S., Voduc, D., Vickery, T., Davies, S., Fauron, C., He, X., Hu, Z., et al. (2009a). Supervised risk predictor of breast cancer based on intrinsic subtypes. *Journal of Clinical Oncology* **27**, 1160-1167.

Parker, W. H., Broder, M. S., Chang, E., Feskanich, D., Farquhar, C., Liu, Z., Shoupe, D., Berek, J. S., Hankinson, S. and Manson, J. E. (2009b). Ovarian conservation at the time of hysterectomy and long-term health outcomes in the nurses' health study. *Obstetrics and Gynecology* **113**, 1027-1037.

Parmar, H. and Cunha, G. R. (2004). Epithelial-stromal interactions in the mouse and human mammary gland in vivo. *Endocrine-Related Cancer* **11**, 437-458.

Parsa, A. T., Waldron, J. S., Panner, A., Crane, C. A., Parney, I. F., Barry, J. J., Cachola, K. E., Murray, J. C., Tihan, T., Jensen, M. C., et al. (2007). Loss of tumor suppressor PTEN function increases B7-H1 expression and immunoresistance in glioma. *Nature Medicine* **13**, 84-88.

Pathania, S., Bade, S., Le Guillou, M., Burke, K., Reed, R., Bowman-Colin, C., Su, Y., Ting, D. T., Polyak, K., Richardson, A. L., et al. (2014). BRCA1 haploinsufficiency for replication stress suppression in primary cells. *Nature Communications* **5**, 5496.

Perou, C. M., Sorlie, T., Eisen, M. B., van de Rijn, M., Jeffrey, S. S., Rees, C. A., Pollack, J. R., Ross, D. T., Johnsen, H., Akslen, L. A., et al. (2000). Molecular portraits of human breast tumours. *Nature* **406**, 747-752.

Peto, J. (2002). Breast cancer susceptibility-A new look at an old model. *Cancer Cell* **1**, 411-412.

Peto, J., Collins, N., Barfoot, R., Seal, S., Warren, W., Rahman, N., Easton, D. F., Evans, C., Deacon, J. and Stratton, M. R. (1999). Prevalence of BRCA1 and BRCA2 gene mutations in patients with early-onset breast cancer. *Journal of the National Cancer Institute* **91**, 943-949.

Peto, R. (1996). Five years of tamoxifen--or more? *Journal of the National Cancer Institute* **88**, 1791-1793.

Pfefferle, A. D., Herschkowitz, J. I., Usary, J., Harrell, J. C., Spike, B. T., Adams, J. R., Torres-Arzayus, M. I., Brown, M., Egan, S. E., Wahl, G. M., et al. (2013). Transcriptomic classification of genetically engineered mouse models of breast cancer identifies human subtype counterparts. *Genome Biology* **14**, R125.

Pfitzner, B. M., Branstetter, D., Loibl, S., Denkert, C., Lederer, B., Schmitt, W. D., Dombrowski, F., Werner, M., Rudiger, T., Dougall, W. C., et al. (2014). RANK expression as a prognostic and predictive marker in breast cancer. *Breast Cancer Research and Treatment* **145**, 307-315.

Pharoah, P. D., Antoniou, A. C., Easton, D. F. and Ponder, B. A. (2008). Polygenes, risk prediction, and targeted prevention of breast cancer. *New England Journal of Medicine* **358**, 2796-2803.

Phillips, K. A., Jenkins, M. A., Lindeman, G. J., McLachlan, S. A., McKinley, J. M., Weideman, P. C., Hopper, J. L. and Friedlander, M. L. (2006). Risk-reducing surgery, screening and chemoprevention practices of BRCA1 and BRCA2 mutation carriers: a prospective cohort study. *Clinical Genetics* **70**, 198-206.

Phillips, K. A. and Lindeman, G. J. (2014). Breast cancer prevention for BRCA1 and BRCA2 mutation carriers: is there a role for tamoxifen? *Future Oncology* **10**, 499-502.

Phillips, K. A., Milne, R. L., Rookus, M. A., Daly, M. B., Antoniou, A. C., Peock, S., Frost, D., Easton, D. F., Ellis, S., Friedlander, M. L., et al. (2013). Tamoxifen and risk of contralateral breast cancer for BRCA1 and BRCA2 mutation carriers. *Journal of Clinical Oncology* **31**, 3091-3099.

Piccart-Gebhart, M. J., Procter, M., Leyland-Jones, B., Goldhirsch, A., Untch, M., Smith, I., Gianni, L., Baselga, J., Bell, R., Jackisch, C., et al. (2005). Trastuzumab after adjuvant chemotherapy in HER2-positive breast cancer. *The New England Journal of Medicine* **353**, 1659-1672.

Pike, M. C., Spicer, D. V., Dahmoush, L. and Press, M. F. (1993). Estrogens, progestogens, normal breast cell proliferation, and breast cancer risk. *Epidemiologic Reviews* **15**, 17-35.

Polyak, K. and Kalluri, R. (2010). The role of the microenvironment in mammary gland development and cancer. *Cold Spring Harbor Perspectives in Biology* **2**, a003244.

Poole, A. J., Li, Y., Kim, Y., Lin, S. C., Lee, W. H. and Lee, E. Y. (2006). Prevention of Brca1-mediated mammary tumorigenesis in mice by a progesterone antagonist. *Science* **314**, 1467-1470.

Prat, A., Parker, J. S., Karginova, O., Fan, C., Livasy, C., Herschkowitz, J. I., He, X. and Perou, C. M. (2010). Phenotypic and molecular characterization of the claudin-low intrinsic subtype of breast cancer. *Breast Cancer Research* **12**, R68.

Prat, A. and Perou, C. M. (2011). Deconstructing the molecular portraits of breast cancer. *Molecular Oncology* **5**, 5-23.

Pratt, M. A., Tibbo, E., Robertson, S. J., Jansson, D., Hurst, K., Perez-Iratxeta, C., Lau, R. and Niu, M. Y. (2009). The canonical NF-kappaB pathway is required for formation of luminal mammary neoplasias and is activated in the mammary progenitor population. *Oncogene* **28**, 2710-2722.

Proia, T. A., Keller, P. J., Gupta, P. B., Klebba, I., Jones, A. D., Sedic, M., Gilmore, H., Tung, N., Naber, S. P., Schnitt, S., et al. (2011). Genetic predisposition directs breast cancer phenotype by dictating progenitor cell fate. *Cell Stem Cell* **8**, 149-163.

Propper, A. Y. (1978). Wandering epithelial cells in the rabbit embryo milk line. A preliminary scanning electron microscope study. *Developmental Biology* **67**, 225-231.

Qiu, P., Simonds, E. F., Bendall, S. C., Gibbs, K. D., Jr., Bruggner, R. V., Linderman, M. D., Sachs, K., Nolan, G. P. and Plevritis, S. K. (2011). Extracting a cellular hierarchy from high-dimensional cytometry data with SPADE. *Nature Biotechnology* **29**, 886-891.

Quinn, J. E., Kennedy, R. D., Mullan, P. B., Gilmore, P. M., Carty, M., Johnston, P. G. and Harkin, D. P. (2003). BRCA1 functions as a differential modulator of chemotherapy-induced apoptosis. *Cancer Research* **63**, 6221-6228.

Rahman, N. and Stratton, M. R. (1998). The genetics of breast cancer susceptibility. *Annual Review of Genetics* **32**, 95-121.

Rebbeck, T. R., Friebel, T., Lynch, H. T., Neuhausen, S. L., van't Veer, L., Garber, J. E., Evans, G. R., Narod, S. A., Isaacs, C. and Matloff, E. (2004). Bilateral prophylactic mastectomy reduces breast cancer risk in BRCA1 and BRCA2 mutation carriers: the PROSE Study Group. *Journal of Clinical Oncology* **22**, 1055-1062.

Rebbeck, T. R., Levin, A. M., Eisen, A., Snyder, C., Watson, P., Cannon-Albright, L., Isaacs, C., Olopade, O., Garber, J. E., Godwin, A. K., et al. (1999). Breast cancer risk after bilateral prophylactic oophorectomy in BRCA1 mutation carriers. *Journal of the National Cancer Institute* **91**, 1475-1479.

Rebbeck, T. R., Lynch, H. T., Neuhausen, S. L., Narod, S. A., Van't Veer, L., Garber, J. E., Evans, G., Isaacs, C., Daly, M. B., Matloff, E., et al. (2002). Prophylactic oophorectomy in carriers of BRCA1 or BRCA2 mutations. *The New England Journal of Medicine* **346**, 1616-1622.

Regan, J. L., Kendrick, H., Magnay, F. A., Vafaizadeh, V., Groner, B. and Smalley, M. J. (2012). c-Kit is required for growth and survival of the cells of origin of Brca1-mutation-associated breast cancer. *Oncogene* **31**, 869-883.

Reis-Filho, J. S. and Lakhani, S. R. (2008). Breast cancer special types: why bother? *The Journal of Pathology* **216**, 394-398.

Rice, J. C., Ozcelik, H., Maxeiner, P., Andrulis, I. and Futscher, B. W. (2000). Methylation of the BRCA1 promoter is associated with decreased BRCA1 mRNA levels in clinical breast cancer specimens. *Carcinogenesis* **21**, 1761-1765.

Ringold, G. M., Shank, P. R., Varmus, H. E., Ring, J. and Yamamoto, K. R. (1979). Integration and transcription of mouse mammary tumor virus DNA in rat hepatoma cells. *Proceedings of the National Academy of Sciences of the United States of America* **76**, 665-669.

Rios, A. C., Fu, N. Y., Jamieson, P. R., Pal, B., Whitehead, L., Nicholas, K. R., Lindeman, G. J. and Visvader, J. E. (2016). Essential role for a novel population of binucleated mammary epithelial cells in lactation. *Nature Communications* **7**, 11400.

Rios, A. C., Fu, N. Y., Lindeman, G. J. and Visvader, J. E. (2014). In situ identification of bipotent stem cells in the mammary gland. *Nature* **506**, 322-327.

Risch, H. A., McLaughlin, J. R., Cole, D. E., Rosen, B., Bradley, L., Kwan, E., Jack, E., Vesprini, D. J., Kuperstein, G., Abrahamson, J. L., et al. (2001). Prevalence and penetrance of germline BRCA1 and BRCA2 mutations in a population series of 649 women with ovarian cancer. *American Journal of Human Genetics* **68**, 700-710.

Ritchie, M. E., Phipson, B., Wu, D., Hu, Y., Law, C. W., Shi, W. and Smyth, G. K. (2015). limma powers differential expression analyses for RNA-sequencing and microarray studies. *Nucleic Acids Research* **43**, e47.

Rizkallah, R., Batsomboon, P., Dudley, G. B. and Hurt, M. M. (2015). Identification of the oncogenic kinase TOPK/PBK as a master mitotic regulator of C2H2 zinc finger proteins. *Oncotarget* **6**, 1446-1461.

Roa, B. B., Boyd, A. A., Volcik, K. and Richards, C. S. (1996). Ashkenazi Jewish population frequencies for common mutations in BRCA1 and BRCA2. *Nature Genetics* **14**, 185-187.

Roberts, P. J., Bisi, J. E., Strum, J. C., Combest, A. J., Darr, D. B., Usary, J. E., Zamboni, W. C., Wong, K. K., Perou, C. M. and Sharpless, N. E. (2012). Multiple roles of cyclin-dependent kinase 4/6 inhibitors in cancer therapy. *Journal of the National Cancer Institute* **104**, 476-487.

Robinson, M. D., McCarthy, D. J. and Smyth, G. K. (2010). edgeR: a Bioconductor package for differential expression analysis of digital gene expression data. *Bioinformatics* **26**, 139-140.

Robinson, M. D. and Oshlack, A. (2010). A scaling normalization method for differential expression analysis of RNA-seq data. *Genome Biology* **11**, R25.

Robson, M. and Offit, K. (2007). Management of an inherited predisposition to breast cancer. *New England Journal of Medicine* **357**, 154-162.

Robson, M. E., Boyd, J., Borgen, P. I. and Cody, H. S., 3rd (2001). Hereditary breast cancer. *Current Problems in Surgery* **38**, 387-480.

Rodilla, V., Dasti, A., Huyghe, M., Lafkas, D., Laurent, C., Reyal, F. and Fre, S. (2015). Luminal progenitors restrict their lineage potential during mammary gland development. *PLoS Biology* **13**, e1002069.

Romanelli, A., Clark, A., Assayag, F., Chateau-Joubert, S., Poupon, M. F., Servely, J. L., Fontaine, J. J., Liu, X., Spooner, E., Goodstal, S., et al. (2012). Inhibiting aurora kinases reduces tumor growth and suppresses tumor recurrence after chemotherapy in patient-derived triple-negative breast cancer xenografts. *Molecular Cancer Therapeutics* **11**, 2693-2703.

Romond, E. H., Perez, E. A., Bryant, J., Suman, V. J., Geyer, C. E., Jr., Davidson, N. E., Tan-Chiu, E., Martino, S., Paik, S., Kaufman, P. A., et al. (2005). Trastuzumab plus adjuvant chemotherapy for operable HER2-positive breast cancer. *The New England Journal of Medicine* **353**, 1673-1684.

Rosen, E. M. (2013). BRCA1 in the DNA damage response and at telomeres. *Frontiers in Genetics* **4**, 85.

Rosen, E.M. and Pishvaian, M.J. (2014). Targeting the BRCA1/2 tumor suppressors. *Current Drug Targets* **15**, 17-31.

Roskelley, C. D., Desprez, P. Y. and Bissell, M. J. (1994). Extracellular matrix-dependent tissue-specific gene expression in mammary epithelial cells requires both physical and biochemical signal transduction. *Proceedings of the National Academy of Sciences of the United States of America* **91**, 12378-12382.

Rossouw, J. E., Anderson, G. L., Prentice, R. L., LaCroix, A. Z., Kooperberg, C., Stefanick, M. L., Jackson, R. D., Beresford, S. A., Howard, B. V., Johnson, K. C., et al. (2002). Risks and benefits of estrogen plus progestin in healthy postmenopausal women: principal results From the Women's Health Initiative randomized controlled trial. *Journal of the American Medical Association* **288**, 321-333.

Rottenberg, S., Jaspers, J. E., Kersbergen, A., van der Burg, E., Nygren, A. O., Zander, S. A., Derksen, P. W., de Bruin, M., Zevenhoven, J., Lau, A., et al. (2008). High sensitivity of BRCA1-deficient mammary tumors to the PARP inhibitor AZD2281 alone and in combination with platinum drugs. *Proceedings of the National Academy of Sciences of the United States of America* **105**, 17079-17084.

Rottenberg, S., Nygren, A. O., Pajic, M., van Leeuwen, F. W., van der Heijden, I., van de Wetering, K., Liu, X., de Visser, K. E., Gilhuijs, K. G., van Tellingen, O., et al. (2007). Selective induction of chemotherapy resistance of mammary tumors in a conditional mouse model for hereditary breast cancer. *Proceedings of the National Academy of Sciences of the United States of America* **104**, 12117-12122.

Rottenberg, S., Vollebergh, M. A., de Hoon, B., de Ronde, J., Schouten, P. C., Kersbergen, A., Zander, S. A., Pajic, M., Jaspers, J. E., Jonkers, M., et al. (2012). Impact of intertumoral heterogeneity on predicting chemotherapy response of BRCA1-deficient mammary tumors. *Cancer Research* **72**, 2350-2361.

Rouzier, R., Perou, C. M., Symmans, W. F., Ibrahim, N., Cristofanilli, M., Anderson, K., Hess, K. R., Stec, J., Ayers, M., Wagner, P., et al. (2005). Breast cancer molecular subtypes respond differently to preoperative chemotherapy. *Clinical Cancer Research* **11**, 5678-5685.

Roy, R., Chun, J. and Powell, S. N. (2012). BRCA1 and BRCA2: different roles in a common pathway of genome protection. *Nature Reviews Cancer* **12**, 68-78.

Rudolph, P., Olsson, H., Bonatz, G., Ratjen, V., Bolte, H., Baldetorp, B., Ferno, M., Parwaresch, R. and Alm, P. (1999). Correlation between p53, c-erbB-2, and topoisomerase II alpha expression, DNA ploidy, hormonal receptor status and proliferation in 356 node-negative breast carcinomas: prognostic implications. *The Journal of Pathology* **187**, 207-216.

Russo, J., Ao, X., Grill, C. and Russo, I. H. (1999). Pattern of distribution of cells positive for estrogen receptor alpha and progesterone receptor in relation to proliferating cells in the mammary gland. *Breast Cancer Research and Treatment* **53**, 217-227.

Russo, J., Gusterson, B. A., Rogers, A. E., Russo, I. H., Wellings, S. R. and van Zwieten, M. J. (1990). Comparative study of human and rat mammary tumorigenesis. *Laboratory Investigation; a journal of technical methods and pathology* **62**, 244-278.

Russo, J., Rivera, R. and Russo, I. H. (1992). Influence of age and parity on the development of the human breast. *Breast Cancer Research and Treatment* **23**, 211-218.

Russo, J and Russo, I.H. (1987). Development of the human mammary gland. In: Neville MC, Daniel C, eds. *The Mammary Gland.* 67 – 93. New York: Plenum Press.

Sakakura, T., Nishizuka, Y. and Dawe, C. J. (1976). Mesenchyme-dependent morphogenesis and epithelium-specific cytodifferentiation in mouse mammary gland. *Science* **194**, 1439-1441.

Sakakura, T., Suzuki, Y. and Shiurba, R. (2013). Mammary stroma in development and carcinogenesis. *Journal of Mammary Gland Biology and Neoplasia* **18**, 189-197.

Sanchez, C. G., Ma, C. X., Crowder, R. J., Guintoli, T., Phommaly, C., Gao, F., Lin, L. and Ellis, M. J. (2011). Preclinical modeling of combined phosphatidylinositol-3-kinase inhibition with endocrine therapy for estrogen receptor-positive breast cancer. *Breast Cancer Research* **13**, R21.

Santini, D., Schiavon, G., Vincenzi, B., Gaeta, L., Pantano, F., Russo, A., Ortega, C., Porta, C., Galluzzo, S., Armento, G., et al. (2011). Receptor activator of NF-kB (RANK) expression in primary tumors associates with bone metastasis occurrence in breast cancer patients. *PloS One* **6**, e19234.

Sau, A., Lau, R., Cabrita, M. A., Nolan, E., Crooks, P. A., Visvader, J. E. and Pratt, M. A. (2016). Persistent Activation of NF-kappaB in BRCA1-Deficient Mammary Progenitors Drives Aberrant Proliferation and Accumulation of DNA Damage. *Cell Stem Cell* **19**, 52-65.

Savage, K. I., Matchett, K. B., Barros, E. M., Cooper, K. M., Irwin, G. W., Gorski, J. J., Orr, K. S., Vohhodina, J., Kavanagh, J. N., Madden, A. F., et al. (2014). BRCA1 deficiency exacerbates estrogen-induced DNA damage and genomic instability. *Cancer Research* **74**, 2773-2784.

Savas, P., Salgado, R., Denkert, C., Sotiriou, C., Darcy, P. K., Smyth, M. J. and Loi, S. (2016). Clinical relevance of host immunity in breast cancer: from TILs to the clinic. *Nature Reviews Clinical Oncology* **13**, 228-241.

Schepers, A. G., Snippert, H. J., Stange, D. E., van den Born, M., van Es, J. H., van de Wetering, M. and Clevers, H. (2012). Lineage tracing reveals Lgr5+ stem cell activity in mouse intestinal adenomas. *Science* **337**, 730-735.

Schindler, C. and Darnell, J. E., Jr. (1995). Transcriptional responses to polypeptide ligands: the JAK-STAT pathway. *Annual Review of Biochemistry* **64**, 621-651.

Schramek, D., Leibbrandt, A., Sigl, V., Kenner, L., Pospisilik, J. A., Lee, H. J., Hanada, R., Joshi, P. A., Aliprantis, A., Glimcher, L., et al. (2010). Osteoclast differentiation factor RANKL controls development of progestin-driven mammary cancer. *Nature* **468**, 98-102.

Schramek, D., Sigl, V. and Penninger, J. M. (2011). RANKL and RANK in sex hormone-induced breast cancer and breast cancer metastasis. *Trends in Endocrinology and Metabolism* **22**, 188-194.

Scully, R., Chen, J., Plug, A., Xiao, Y., Weaver, D., Feunteun, J., Ashley, T. and Livingston, D. M. (1997). Association of BRCA1 with Rad51 in mitotic and meiotic cells. *Cell* **88**, 265-275.

Seagroves, T. N., Lydon, J. P., Hovey, R. C., Vonderhaar, B. K. and Rosen, J. M. (2000). C/EBPbeta (CCAAT/enhancer binding protein) controls cell fate determination during mammary gland development. *Molecular Endocrinology* **14**, 359-368.

Sedic, M., Skibinski, A., Brown, N., Gallardo, M., Mulligan, P., Martinez, P., Keller, P. J., Glover, E., Richardson, A. L., Cowan, J., et al. (2015). Haploinsufficiency for BRCA1 leads to cell-type-specific genomic instability and premature senescence. *Nature Communications* **6**, 7505.

Shackleton, M., Vaillant, F., Simpson, K. J., Stingl, J., Smyth, G. K., Asselin-Labat, M. L., Wu, L., Lindeman, G. J. and Visvader, J. E. (2006). Generation of a functional mammary gland from a single stem cell. *Nature* **439**, 84-88.

Shafee, N., Smith, C. R., Wei, S., Kim, Y., Mills, G. B., Hortobagyi, G. N., Stanbridge, E. J. and Lee, E. Y. (2008). Cancer stem cells contribute to cisplatin resistance in Brca1/p53-mediated mouse mammary tumors. *Cancer Research* **68**, 3243-3250.

Shakya, R., Szabolcs, M., McCarthy, E., Ospina, E., Basso, K., Nandula, S., Murty, V., Baer, R. and Ludwig, T. (2008). The basal-like mammary carcinomas induced by Brca1 or Bard1 inactivation implicate the BRCA1/BARD1 heterodimer in tumor suppression. *Proceedings of the National Academy of Sciences of the United States of America* **105**, 7040-7045.

Shao, C., Stambrook, P. J. and Tischfield, J. A. (2001). Mitotic recombination is suppressed by chromosomal divergence in hybrids of distantly related mouse strains. *Nature Genetics* **28**, 169-172.

Sharpless, N. E. and Depinho, R. A. (2006). The mighty mouse: genetically engineered mouse models in cancer drug development. *Nature Reviews Drug Discovery* **5**, 741-754.

Shehata, M., Teschendorff, A., Sharp, G., Novcic, N., Russell, I. A., Avril, S., Prater, M., Eirew, P., Caldas, C., Watson, C. J., et al. (2012). Phenotypic and functional characterisation of the luminal cell hierarchy of the mammary gland. *Breast Cancer Research* **14**, R134.

Shuen, A. Y. and Foulkes, W. D. (2011). Inherited mutations in breast cancer genes—risk and response. *Journal of Mammary Gland Biology and Neoplasia* **16**, 3-15.

Shultz, L. D., Lyons, B. L., Burzenski, L. M., Gott, B., Chen, X., Chaleff, S., Kotb, M., Gillies, S. D., King, M., Mangada, J., et al. (2005). Human lymphoid and myeloid cell development in NOD/LtSz-scid IL2R gamma null mice engrafted with mobilized human hemopoietic stem cells. *Journal of Immunology* **174**, 6477-6489.

Sicinski, P., Donaher, J. L., Parker, S. B., Li, T., Fazeli, A., Gardner, H., Haslam, S. Z., Bronson, R. T., Elledge, S. J. and Weinberg, R. A. (1995). Cyclin D1 provides a link between development and oncogenesis in the retina and breast. *Cell* **82**, 621-630.

Siegel, R. L., Miller, K. D. and Jemal, A. (2015). Cancer statistics, 2015. *CA: A Cancer Journal for Clinicians* **65**, 5-29.

Sigl, V., Owusu-Boaitey, K., Joshi, P. A., Kavirayani, A., Wirnsberger, G., Novatchkova, M., Kozieradzki, I., Schramek, D., Edokobi, N., Hersl, J., et al. (2016). RANKL/RANK control Brca1 mutation-driven mammary tumors. *Cell Research* **26**, 761-774.

Silver, D. P., Richardson, A. L., Eklund, A. C., Wang, Z. C., Szallasi, Z., Li, Q., Juul, N., Leong, C. O., Calogrias, D., Buraimoh, A., et al. (2010). Efficacy of neoadjuvant Cisplatin in triple-negative breast cancer. *Journal of Clinical Oncology* **28**, 1145-1153.

Simpson, E. R., Mahendroo, M. S., Means, G. D., Kilgore, M. W., Hinshelwood, M. M., Graham-Lorence, S., Amarneh, B., Ito, Y., Fisher, C. R., Michael, M. D., et al. (1994). Aromatase cytochrome P450, the enzyme responsible for estrogen biosynthesis. *Endocrine Reviews* **15**, 342-355.

Slamon, D. J., Clark, G. M., Wong, S. G., Levin, W. J., Ullrich, A. and McGuire, W. L. (1987). Human breast cancer: correlation of relapse and survival with amplification of the HER-2/neu oncogene. *Science* **235**, 177-182.

Sleeman, K. E., Kendrick, H., Ashworth, A., Isacke, C. M. and Smalley, M. J. (2006). CD24 staining of mouse mammary gland cells defines luminal epithelial, myoepithelial/basal and non-epithelial cells. *Breast Cancer Research* **8**, R7.

Sleeman, K. E., Kendrick, H., Robertson, D., Isacke, C. M., Ashworth, A. and Smalley, M. J. (2007). Dissociation of estrogen receptor expression and in vivo stem cell activity in the mammary gland. *The Journal of Cell Biology* **176**, 19-26.

Smith, G. H. (2005). Label-retaining epithelial cells in mouse mammary gland divide asymmetrically and retain their template DNA strands. *Development* **132**, 681-687.

Smith, G. H. and Medina, D. (1988). A morphologically distinct candidate for an epithelial stem cell in mouse mammary gland. *Journal of Cell Science* **90 (Pt 1)**, 173-183.

Smyth, G. K. (2004). Linear models and empirical bayes methods for assessing differential expression in microarray experiments. *Statistical Applications in Genetics and Molecular Biology* **3**, Article3.

Smyth, M. J., Yagita, H. and McArthur, G. A. (2016). Combination Anti-CTLA-4 and Anti-RANKL in Metastatic Melanoma. *Journal of Clinical Oncology* **34**, e104-106.

Snyder, A., Makarov, V., Merghoub, T., Yuan, J., Zaretsky, J. M., Desrichard, A., Walsh, L. A., Postow, M. A., Wong, P., Ho, T. S., et al. (2014). Genetic basis for clinical response to CTLA-4 blockade in melanoma. *The New England Journal of Medicine* **371**, 2189-2199.

Somasundaram, K., Zhang, H., Zeng, Y. X., Houvras, Y., Peng, Y., Zhang, H., Wu, G. S., Licht, J. D., Weber, B. L. and El-Deiry, W. S. (1997). Arrest of the cell cycle by the tumour-suppressor BRCA1 requires the CDK-inhibitor p21WAF1/CiP1. *Nature* **389**, 187-190.

Sorlie, T., Perou, C. M., Tibshirani, R., Aas, T., Geisler, S., Johnsen, H., Hastie, T., Eisen, M. B., van de Rijn, M., Jeffrey, S. S., et al. (2001). Gene expression patterns of breast carcinomas distinguish tumor subclasses with clinical implications. *Proceedings of the National Academy of Sciences of the United States of America* **98**, 10869-10874.

Sotiriou, C., Neo, S. Y., McShane, L. M., Korn, E. L., Long, P. M., Jazaeri, A., Martiat, P., Fox, S. B., Harris, A. L. and Liu, E. T. (2003). Breast cancer classification and prognosis based on gene expression profiles from a population-based study. *Proceedings of the National Academy of Sciences of the United States of America* **100**, 10393-10398.

Spike, B. T., Engle, D. D., Lin, J. C., Cheung, S. K., La, J. and Wahl, G. M. (2012). A mammary stem cell population identified and characterized in late embryogenesis reveals similarities to human breast cancer. *Cell Stem Cell* **10**, 183-197.

Spranger, S., Spaapen, R. M., Zha, Y., Williams, J., Meng, Y., Ha, T. T. and Gajewski, T. F. (2013). Up-regulation of PD-L1, IDO, and T(regs) in the melanoma tumor microenvironment is driven by CD8(+) T cells. *Science Translational Medicine* **5**, 200ra116.

Srivastava, S., Matsuda, M., Hou, Z., Bailey, J. P., Kitazawa, R., Herbst, M. P. and Horseman, N. D. (2003). Receptor activator of NF-kappaB ligand induction via Jak2 and Stat5a in mammary epithelial cells. *The Journal of Biological Chemistry* **278**, 46171-46178.

Sternlicht, M. D., Kouros-Mehr, H., Lu, P. and Werb, Z. (2006). Hormonal and local control of mammary branching morphogenesis. *Differentiation* **74**, 365-381.

Stingl, J., Eaves, C. J., Zandieh, I. and Emerman, J. T. (2001). Characterization of bipotent mammary epithelial progenitor cells in normal adult human breast tissue. *Breast Cancer Research and Treatment* **67**, 93-109.

Stingl, J., Eirew, P., Ricketson, I., Shackleton, M., Vaillant, F., Choi, D., Li, H. I. and Eaves, C. J. (2006). Purification and unique properties of mammary epithelial stem cells. *Nature* **439**, 993-997.

Strickland, K. C., Howitt, B. E., Shukla, S. A., Rodig, S., Ritterhouse, L. L., Liu, J. F., Garber, J. E., Chowdhury, D., Wu, C. J., D'Andrea, A. D., et al. (2016). Association and prognostic significance of BRCA1/2-mutation status with neoantigen load, number of tumor-infiltrating lymphocytes and expression of PD-1/PD-L1 in high grade serous ovarian cancer. *Oncotarget* **7**, 13587-13598.

Struewing, J. P., Abeliovich, D., Peretz, T., Avishai, N., Kaback, M. M., Collins, F. S. and Brody, L. C. (1995). The carrier frequency of the BRCA1 185delAG mutation is approximately 1 percent in Ashkenazi Jewish individuals. *Nature Genetics* **11**, 198-200.

Sum, E. Y., Shackleton, M., Hahm, K., Thomas, R. M., O'Reilly, L. A., Wagner, K. U., Lindeman, G. J. and Visvader, J. E. (2005). Loss of the LIM domain protein Lmo4 in the mammary gland during pregnancy impedes lobuloalveolar development. *Oncogene* **24**, 4820-4828.

Sung, P. and Klein, H. (2006). Mechanism of homologous recombination: mediators and helicases take on regulatory functions. *Nature Reviews Molecular Cell Biology* **7**, 739-750.

Tan, D. S., Marchio, C., Jones, R. L., Savage, K., Smith, I. E., Dowsett, M. and Reis-Filho, J. S. (2008). Triple negative breast cancer: molecular profiling and prognostic impact in adjuvant anthracycline-treated patients. *Breast Cancer Research and Treatment* **111**, 27-44.

Tan, W., Zhang, W., Strasner, A., Grivennikov, S., Cheng, J. Q., Hoffman, R. M. and Karin, M. (2011). Tumour-infiltrating regulatory T cells stimulate mammary cancer metastasis through RANKL-RANK signalling. *Nature* **470**, 548-553.

Tanos, T., Sflomos, G., Echeverria, P. C., Ayyanan, A., Gutierrez, M., Delaloye, J. F., Raffoul, W., Fiche, M., Dougall, W., Schneider, P., et al. (2013). Progesterone/RANKL is a major regulatory axis in the human breast. *Science Translational Medicine* **5**, 182ra155.

Tassone, P., Tagliaferri, P., Perricelli, A., Blotta, S., Quaresima, B., Martelli, M. L., Goel, A., Barbieri, V., Costanzo, F., Boland, C. R., et al. (2003). BRCA1 expression modulates chemosensitivity of BRCA1-defective HCC1937 human breast cancer cells. *British Journal of Cancer* **88**, 1285-1291.

The Cancer Genome Atlas Network (2012). Comprehensive molecular portraits of human breast tumours. *Nature* **490**, 61-70.

Thomas, D., Carriere, P. and Jacobs, I. (2010). Safety of denosumab in giant-cell tumour of bone. *The Lancet Oncology* **11**, 815.

Thomas, R. J., Guise, T. A., Yin, J. J., Elliott, J., Horwood, N. J., Martin, T. J. and Gillespie, M. T. (1999). Breast cancer cells interact with osteoblasts to support osteoclast formation. *Endocrinology* **140**, 4451-4458.

Tibbetts, R. S., Cortez, D., Brumbaugh, K. M., Scully, R., Livingston, D., Elledge, S. J. and Abraham, R. T. (2000). Functional interactions between BRCA1 and the checkpoint kinase ATR during genotoxic stress. *Genes & Development* **14**, 2989-3002.

Tirkkonen, M., Johannsson, O., Agnarsson, B. A., Olsson, H., Ingvarsson, S., Karhu, R., Tanner, M., Isola, J., Barkardottir, R. B., Borg, A., et al. (1997). Distinct somatic genetic changes associated with tumor progression in carriers of BRCA1 and BRCA2 germ-line mutations. *Cancer Research* **57**, 1222-1227.

To, C., Kim, E. H., Royce, D. B., Williams, C. R., Collins, R. M., Risingsong, R., Sporn, M. B. and Liby, K. T. (2014). The PARP inhibitors, veliparib and olaparib, are effective chemopreventive agents for delaying mammary tumor development in BRCA1-deficient mice. *Cancer Prevention Research* **7**, 698-707.

Topalian, S. L., Drake, C. G. and Pardoll, D. M. (2015). Immune checkpoint blockade: a common denominator approach to cancer therapy. *Cancer Cell* **27**, 450-461.

Trott, J. F., Vonderhaar, B. K. and Hovey, R. C. (2008). Historical perspectives of prolactin and growth hormone as mammogens, lactogens and galactagogues--agog for the future! *Journal of Mammary Gland Biology and Neoplasia* **13**, 3-11.

Truneh, A., Sharma, S., Silverman, C., Khandekar, S., Reddy, M. P., Deen, K. C., McLaughlin, M. M., Srinivasula, S. M., Livi, G. P., Marshall, L. A., et al. (2000). Temperature-sensitive differential affinity of TRAIL for its receptors. DR5 is the highest affinity receptor. *The Journal of Biological Chemistry* **275**, 23319-23325.

Tsai, M. J. and O'Malley, B. W. (1994). Molecular mechanisms of action of steroid/thyroid receptor superfamily members. *Annual Review of Biochemistry* **63**, 451-486.

Tsai, Y. C., Lu, Y., Nichols, P. W., Zlotnikov, G., Jones, P. A. and Smith, H. S. (1996). Contiguous patches of normal human mammary epithelium derived from a single stem cell: implications for breast carcinogenesis. *Cancer Research* **56**, 402-404.

Tsukamoto, A. S., Grosschedl, R., Guzman, R. C., Parslow, T. and Varmus, H. E. (1988). Expression of the int-1 gene in transgenic mice is associated with mammary gland hyperplasia and adenocarcinomas in male and female mice. *Cell* **55**, 619-625.

Turner, N., Tutt, A. and Ashworth, A. (2004). Hallmarks of 'BRCAness' in sporadic cancers. *Nature Reviews Cancer* **4**, 814-819.

Tutt, A. and Ashworth, A. (2002). The relationship between the roles of BRCA genes in DNA repair and cancer predisposition. *Trends in Molecular Medicine* **8**, 571-576.

Tutt, A., Robson, M., Garber, J. E., Domchek, S. M., Audeh, M. W., Weitzel, J. N., Friedlander, M., Arun, B., Loman, N., Schmutzler, R. K., et al. (2010). Oral poly(ADP-ribose) polymerase inhibitor olaparib in patients with BRCA1 or BRCA2 mutations and advanced breast cancer: a proof-of-concept trial. *Lancet* **376**, 235-244.

Vaillant, F., Asselin-Labat, M. L., Shackleton, M., Forrest, N. C., Lindeman, G. J. and Visvader, J. E. (2008). The mammary progenitor marker CD61/beta3 integrin identifies cancer stem cells in mouse models of mammary tumorigenesis. *Cancer Research* **68**, 7711-7717.

Vaillant, F., Merino, D., Lee, L., Breslin, K., Pal, B., Ritchie, M. E., Smyth, G. K., Christie, M., Phillipson, L. J., Burns, C. J., et al. (2013). Targeting BCL-2 with the BH3 mimetic ABT-199 in estrogen receptor-positive breast cancer. *Cancer Cell* **24**, 120-129.

Van Allen, E. M., Miao, D., Schilling, B., Shukla, S. A., Blank, C., Zimmer, L., Sucker, A., Hillen, U., Geukes Foppen, M. H., Goldinger, S. M., et al. (2015). Genomic correlates of response to CTLA-4 blockade in metastatic melanoma. *Science* **350**, 207-211.

Van Keymeulen, A., Rocha, A. S., Ousset, M., Beck, B., Bouvencourt, G., Rock, J., Sharma, N., Dekoninck, S. and Blanpain, C. (2011). Distinct stem cells contribute to mammary gland development and maintenance. *Nature* **479**, 189-193.

Villadsen, R., Fridriksdottir, A. J., Ronnov-Jessen, L., Gudjonsson, T., Rank, F., LaBarge, M. A., Bissell, M. J. and Petersen, O. W. (2007). Evidence for a stem cell hierarchy in the adult human breast. *The Journal of Cell Biology* **177**, 87-101.

Visvader, J. E. (2009). Keeping abreast of the mammary epithelial hierarchy and breast tumorigenesis. *Genes & Development* **23**, 2563-2577.

Visvader (2011). Cells of origin in cancer. *Nature* **469**, 314-322.

Visvader, J. E. and Lindeman, G. J. (2003). Transcriptional regulators in mammary gland development and cancer. *The International journal of Biochemistry & Cell Biology* **35**, 1034-1051.

Visvader, J. E. and Stingl, J. (2014). Mammary stem cells and the differentiation hierarchy: current status and perspectives. *Genes & Development* **28**, 1143-1158.

Vogel, C. L., Cobleigh, M. A., Tripathy, D., Gutheil, J. C., Harris, L. N., Fehrenbacher, L., Slamon, D. J., Murphy, M., Novotny, W. F., Burchmore, M., et al. (2002). Efficacy and safety of trastuzumab as a single agent in first-line treatment of HER2-overexpressing metastatic breast cancer. *Journal of Clinical Oncology* **20**, 719-726.

Vonderhaar, B. K. (1999). Prolactin involvement in breast cancer. *Endocrine-Related Cancer* **6**, 389-404.

Waddell, N., Arnold, J., Cocciardi, S., Da Silva, L., Marsh, A., Riley, J., Johnstone, C. N., Orloff, M., Assie, G. and Eng, C. (2010). Subtypes of familial breast tumours revealed by expression and copy number profiling. *Breast Cancer Research and Treatment* **123**, 661-677.

Wagner, K. U., Boulanger, C. A., Henry, M. D., Sgagias, M., Hennighausen, L. and Smith, G. H. (2002). An adjunct mammary epithelial cell population in parous females: its role in functional adaptation and tissue renewal. *Development* **129**, 1377-1386.

Wagner, K. U., Krempler, A., Triplett, A. A., Qi, Y., George, N. M., Zhu, J. and Rui, H. (2004). Impaired alveologenesis and maintenance of secretory mammary epithelial cells in Jak2 conditional knockout mice. *Molecular and Cellular Biology* **24**, 5510-5520.

Wagner, K. U., Wall, R. J., St-Onge, L., Gruss, P., Wynshaw-Boris, A., Garrett, L., Li, M., Furth, P. A. and Hennighausen, L. (1997). Cre-mediated gene deletion in the mammary gland. *Nucleic Acids Research* **25**, 4323-4330.

Wang, D., Cai, C., Dong, X., Yu, Q. C., Zhang, X. O., Yang, L. and Zeng, Y. A. (2015). Identification of multipotent mammary stem cells by protein C receptor expression. *Nature* **517**, 81-84.

Wang, I. C., Chen, Y. J., Hughes, D., Petrovic, V., Major, M. L., Park, H. J., Tan, Y., Ackerson, T. and Costa, R. H. (2005). Forkhead box M1 regulates the transcriptional network of genes essential for mitotic progression and genes encoding the SCF (Skp2-Cks1) ubiquitin ligase. *Molecular and Cellular Biology* **25**, 10875-10894.

Wang, S., Counterman, L. J. and Haslam, S. Z. (1990). Progesterone action in normal mouse mammary gland. *Endocrinology* **127**, 2183-2189.

Watson, C. J. and Khaled, W. T. (2008). Mammary development in the embryo and adult: a journey of morphogenesis and commitment. *Development* **135**, 995-1003.

Whittle, J. R., Lewis, M. T., Lindeman, G. J. and Visvader, J. E. (2015). Patient-derived xenograft models of breast cancer and their predictive power. *Breast Cancer Research* **17**, 17.

Widschwendter, M., Burnell, M., Fraser, L., Rosenthal, A. N., Philpott, S., Reisel, D., Dubeau, L., Cline, M., Pan, Y., Yi, P. C., et al. (2015). Osteoprotegerin (OPG), The Endogenous Inhibitor of Receptor Activator of NF-kappaB Ligand (RANKL), is Dysregulated in BRCA Mutation Carriers. *EBioMedicine* **2**, 1331-1339.

Widschwendter, M., Rosenthal, A. N., Philpott, S., Rizzuto, I., Fraser, L., Hayward, J., Intermaggio, M. P., Edlund, C. K., Ramus, S. J., Gayther, S. A., et al. (2013). The sex hormone system in carriers of BRCA1/2 mutations: a case-control study. *The Lancet Oncology* **14**, 1226-1232.

Williams, J. M. and Daniel, C. W. (1983). Mammary ductal elongation: differentiation of myoepithelium and basal lamina during branching morphogenesis. *Developmental Biology* **97**, 274-290.

Wong, A. K., Pero, R., Ormonde, P. A., Tavtigian, S. V. and Bartel, P. L. (1997). RAD51 interacts with the evolutionarily conserved BRC motifs in the human breast cancer susceptibility gene brca2. *Journal of Biological Chemistry* **272**, 31941-31944.

Wood, C. E., Branstetter, D., Jacob, A. P., Cline, J. M., Register, T. C., Rohrbach, K., Huang, L. Y., Borgerink, H. and Dougall, W. C. (2013). Progestin effects on cell proliferation pathways in the postmenopausal mammary gland. *Breast Cancer Research* **15**, R62.

Wooster, R., Bignell, G., Lancaster, J., Swift, S., Seal, S., Mangion, J., Collins, N., Gregory, S., Gumbs, C. and Micklem, G. (1995). Identification of the breast cancer susceptibility gene BRCA2. *Nature* **378**, 789-792.

Wooster, R., Neuhausen, S. L., Mangion, J., Quirk, Y., Ford, D., Collins, N., Nguyen, K., Seal, S., Tran, T., Averill, D., et al. (1994). Localization of a breast cancer susceptibility gene, BRCA2, to chromosome 13q12-13. *Science* **265**, 2088-2090.

Wu, D., Lim, E., Vaillant, F., Asselin-Labat, M. L., Visvader, J. E. and Smyth, G. K. (2010). ROAST: rotation gene set tests for complex microarray experiments. *Bioinformatics* **26**, 2176-2182.

Wu, L. C., Wang, Z. W., Tsan, J. T., Spillman, M. A., Phung, A., Xu, X. L., Yang, M. C., Hwang, L. Y., Bowcock, A. M. and Baer, R. (1996). Identification of a RING protein that can interact in vivo with the BRCA1 gene product. *Nature Genetics* **14**, 430-440.

Xia, B., Sheng, Q., Nakanishi, K., Ohashi, A., Wu, J., Christ, N., Liu, X., Jasin, M., Couch, F. J. and Livingston, D. M. (2006). Control of BRCA2 cellular and clinical functions by a nuclear partner, PALB2. *Molecular Cell* **22**, 719-729.

Xu, L., Zhao, Y., Chen, Z., Wang, Y., Chen, L. and Wang, S. (2015). Tamoxifen and risk of contralateral breast cancer among women with inherited mutations in BRCA1 and BRCA2: a meta-analysis. *Breast Cancer* **22**, 327-334.

Xu, S., Li, S., Guo, Z., Luo, J., Ellis, M. J. and Ma, C. X. (2013). Combined targeting of mTOR and AKT is an effective strategy for basal-like breast cancer in patient-derived xenograft models. *Molecular Cancer Therapeutics* **12**, 1665-1675.

Xu, X., Wagner, K. U., Larson, D., Weaver, Z., Li, C., Ried, T., Hennighausen, L., Wynshaw-Boris, A. and Deng, C. X. (1999). Conditional mutation of Brca1 in mammary epithelial cells results in blunted ductal morphogenesis and tumour formation. *Nature Genetics* **22**, 37-43.

Yarden, R. I. and Brody, L. C. (1999). BRCA1 interacts with components of the histone deacetylase complex. *Proceedings of the National Academy of Sciences of the United States of America* **96**, 4983-4988.

Yasuda, H., Shima, N., Nakagawa, N., Yamaguchi, K., Kinosaki, M., Mochizuki, S., Tomoyasu, A., Yano, K., Goto, M., Murakami, A., et al. (1998). Osteoclast differentiation factor is a ligand for osteoprotegerin/osteoclastogenesis-inhibitory factor and is identical to TRANCE/RANKL. *Proceedings of the National Academy of Sciences of the United States of America* **95**, 3597-3602.

Yoshida, K. and Miki, Y. (2004). Role of BRCA1 and BRCA2 as regulators of DNA repair, transcription, and cell cycle in response to DNA damage. *Cancer Science* **95**, 866-871.

Yu, X., Chini, C. C., He, M., Mer, G. and Chen, J. (2003). The BRCT domain is a phospho-protein binding domain. *Science* **302**, 639-642.

Yu, X., Fu, S., Lai, M., Baer, R. and Chen, J. (2006). BRCA1 ubiquitinates its phosphorylation-dependent binding partner CtIP. *Genes & Development* **20**, 1721-1726.

Zander, S. A., Kersbergen, A., van der Burg, E., de Water, N., van Tellingen, O., Gunnarsdottir, S., Jaspers, J. E., Pajic, M., Nygren, A. O., Jonkers, J., et al. (2010). Sensitivity and acquired resistance of BRCA1;p53-deficient mouse mammary tumors to the topoisomerase I inhibitor topotecan. *Cancer Research* **70**, 1700-1710.

Zeppernick, F., Meinhold-Heerlein, I. and Shih Ie, M. (2015). Precursors of ovarian cancer in the fallopian tube: serous tubal intraepithelial carcinoma--an update. *The Journal of Obstetrics and Gynaecology Research* **41**, 6-11.

Zhang, F., Ma, J., Wu, J., Ye, L., Cai, H., Xia, B. and Yu, X. (2009). PALB2 links BRCA1 and BRCA2 in the DNA-damage response. *Current Biology* **19**, 524-529.

Zhang, X., Claerhout, S., Prat, A., Dobrolecki, L. E., Petrovic, I., Lai, Q., Landis, M. D., Wiechmann, L., Schiff, R., Giuliano, M., et al. (2013). A renewable tissue resource of phenotypically stable, biologically and ethnically diverse, patient-derived human breast cancer xenograft models. *Cancer Research* **73**, 4885-4897.

Zitvogel, L., Apetoh, L., Ghiringhelli, F. and Kroemer, G. (2008). Immunological aspects of cancer chemotherapy. *Nature reviews Immunology* **8**, 59-73.